THE PHASE-SPACE DYNAMICS OF SYSTEMS OF SPIKING NEURONS

BY ARUNAVA BANERJEE

A dissertation submitted to the

Graduate School—New Brunswick

Rutgers, The State University of New Jersey

in partial fulfillment of the requirements

for the degree of

Doctor of Philosophy

Graduate Program in Computer Science

Written under the direction of

Prof. Haym Hirsh

and approved by

_____

_____

_____

_____

New Brunswick, New Jersey

January, 2001

ABSTRACT OF THE DISSERTATION

The Phase-Space Dynamics of Systems of Spiking Neurons

by Arunava Banerjee

Dissertation Director: Prof. Haym Hirsh

This thesis investigates the dynamics of systems of neurons in the brain. It considers two questions: (1) Are there *coherent* spatiotemporal structures in the dynamics of neuronal systems that can denote *discrete computational states*, and (2) If such structures exist, what restrictions do the dynamics of the system at the physical level impose on the dynamics of the system at the corresponding abstracted computational level.

These problems are addressed by way of an investigation of the phase-space dynamics of a general model of local systems of biological neurons.

An abstract physical system is constructed based on a limited set of realistic assumptions about the biological neuron. The system, in consequence, accommodates a wide range of neuronal models.

Appropriate instantiations of the system are used to simulate the dynamics of a typical column in the neocortex. The results demonstrate that the dynamical behavior of the system is akin to that observed in neurophysiological experiments.

Formal analysis of local properties of flows reveals contraction, expansion, and folding in different sections of the phase-space. A stochastic process is formulated in order to determine

the salient properties of the dynamics of a generic column in the neocortex. The process is analyzed and the criterion for the dynamics of the system to be *sensitive to initial conditions* is identified. Based on physiological parameters, it is then deduced that periodic orbits in the region of the phase-space corresponding to "normal operational conditions" in the neocortex are almost surely (with probability 1) *unstable*, those in the region corresponding to "seizure-like conditions" in the neocortex are almost surely *stable*, and trajectories in the region of the phase-space corresponding to "normal operational conditions" in the neocortex are almost surely *sensitive to initial conditions*.

Next, a procedure is introduced that isolates from the phase-space all basic sets, complex sets, and attractors incrementally.

Based on the two sets of results, it is concluded that *chaotic attractors* that are potentially *anisotropic* play a central role in the dynamics of such systems. Finally, the ramifications of this result with regard to the computational nature of neocortical neuronal systems are discussed.

Acknowledgements

I would like to thank my wife, Jyoti, for her enduring patience, my mother for her effort to instill in me her structure and discipline, my father for infecting me with his lofty ideas, and my sister for her unreserved love and affection.

I would also like to thank Prof. Haym Hirsh for his encouragement and for the confidence he bestowed upon me as I pursued my interests.

Finally, I would like to thank Prof. Peter Rowat and Prof. Eduardo Sontag for their insightful comments on the biological and mathematical aspects of this thesis.

Table of Contents

List of Figures

Chapter 1

Introduction

It is in the nature of human-kind to strive towards a better understanding of the world it inhabits. The past two thousand five hundred years of documented human history is compelling testament to this veritable obsession. One merely need consider one's own daily existence to appreciate the extent of the progress made. Our grasp and subsequent application of some of the fundamental principles underlying nature has allowed us to communicate via electromagnetic waves, predict storms, and travel by air, to cite but a few examples. If there is one phenomenon, however, that continues to elude our understanding, it is the human *mind*.

1.1 History

Evidence of a scientific approach to the question of the nature of the mind can be found as early as the 5th century BC. Several physicians, among them Alcmaeon of Crotona (535-500 BC), Anaxagoras of Clazomenae (500-428 BC), Hippocrates of Cos (460-379 BC), and Herophilus of Alexandria (335-280 BC) are known to have practiced dissections of the human and the vertebrate brains. Alcmaeon is also recognized as being among the first to have proposed the brain as the central organ of thought. Aristotle (384-323 BC) laid what is now regarded as the foundations of comparative anatomy. He also conjectured that the mind and the body were merely two aspects of the same entity, the mind being one of the body's functions. His views were further developed by Galen (131-201 AD) who founded the science of nervous system physiology. Galen recognized that nerves originate in the brain and the spinal cord, and not in the heart as Aristotle had maintained. His pioneering spinal dissection studies shed light on the function of the nervous system. This golden age of enquiry was, however, short lived. The knowledge accumulated during this period was lost in the dark ages, when the mind came to be considered more a transcendent entity than a phenomenon, its study consequently relegated to religion.

Science remained out of favor until the beginning of the Renaissance. In 1543 Andreas Vesalius published *De Humani Corporis Fabrica* that helped correct numerous misconceptions about the human anatomy that had prevailed for fifteen hundred years. The 1641 publication of René Descartes' *Meditationes de Prima Philosophia: In quibus Dei existentia, & animae humanae à corpore distinctio demonstratur* replaced the Platonic conception of a tripartite soul with that of a unitary mind (*res cogitans*) distinct from the body. Descartes considered the body and the soul to be ontologically separate but interacting entities.

The mechanistic approach to the human mind was once again taken up in earnest during the 19th century. Between 1810 and 1819 Franz Joseph Gall published *Anatomie et physiologie du systême nerveux en général* wherein he propounded the Phrenological Doctrine.[1] Functional localization gained empirical support with Paul Broca's identification of the seat of the faculty of articular speech in the human brain (Broca, 1861) and Gustav Fritsch's and Eduard Hitzig's identification of the motor cortex in dogs and monkeys (Fritsch & Hitzig, 1870).

The first half of the 20th century saw a flurry of activity that included Brodmann's account of the cytoarchitectural map of cortical areas (Brodmann, 1909), Cajal's histological investigations corroborating the Neuron Doctrine[2] (Cajal, 1909, 1910), Sherrington's treatise on reflex and the function of neurons in the brain and spinal chord (Sherrington, 1906), Adrian's recording of the electrical activity of single nerve cells (Adrian & Zotterman, 1926; Adrian & Bronk, 1928), and Berger's recording of the electroencephalogram of man (Berger, 1929). Subsequent work by Loewi, Dale, and Katz on the nature of chemical transmission of impulses across neurons (Loewi, 1921; Dale, 1914, 1935; Fatt & Katz, 1951, 1953; Katz & Miledi, 1967), and by Eccles, Hodgkin, and Huxley on the biophysics of nerve impulse generation and conduction (Eccles, 1936, 1937a-b, 1957; Hodgkin & Huxley, 1952a-d) led to a detailed understanding of the biophysical basis of the activity of a single neuron.

---

[1] The Phrenological Doctrine holds that the mind can be divided into separate faculties, each of which is discretely localized in the brain. Furthermore, the prominence of any such faculty should appear as a cranial prominence of the appropriate area in the brain.

[2] The Neuron Doctrine holds that the neuron is the anatomical, physiological, genetic and metabolic unit of the nervous system. It is an extension of Cell Theory enunciated in 1838-1839 by Matthias Jacob Schleiden and Theodor Schwann to nervous tissue. In contrast, the Reticular theory, a widely held view during this period (that included such renowned neuroscientists as Camillo Golgi), asserted that the nervous system consisted of a *diffuse* nerve network formed by the anastomosing branches of nerve cell processes, with the cell somata having mostly a nourishing role (for review, refer to Shepherd, 1991; Jones, 1994).

These developments, while significant in their own right, did not substantially advance the understanding of the principles underlying the activity of the greater system, the brain. The reasons were primarily twofold. First, *computation* as a formal concept had just begun to be investigated (Post, 1936; Turing, 1936, 1937; Kleene, 1936a-b), and second, it was realized that understanding the dynamics of a system of interacting neurons was a problem quite distinct from that of understanding the dynamics of a single neuron.

Rashevsky, McCulloch, and Pitts were the first to investigate the properties of systems of interconnected neuron-like elements (Rashevsky, 1938; McCulloch & Pitts, 1943). Although their research was based on a highly simplified model of the biological neuron, the threshold gate,[3] they were the first to demonstrate that the computational power of a network could greatly exceed that of its constituent elements. Feedforward networks constructed of a slightly more general element, the sigmoidal gate,[4] gained in popularity after several researchers introduced learning into such systems via local link-strength updates (Rosenblatt, 1958; Bryson & Ho, 1969; Werbos, 1974; Parker, 1985; Rumelhart, Hinton & Williams, 1986). Likewise, recurrent networks of symmetrically coupled sigmoidal gates gained in popularity after Hopfield demonstrated that such networks could be trained to remember patterns and retrieve them upon presentation of appropriate cues (Hopfield, 1982).

Our understanding of the computational nature of such systems has grown steadily since then (Amit, Gutfreund & Sompolinsky, 1987; Hornik, Stinhcombe & White, 1989; Siegelmann & Sontag, 1992; Omlin & Giles, 1996, and the references therein). The extent to which some of these results apply to systems of neurons in the brain, however, remains uncertain, primarily because the models of the neurons as well as those of the networks used in such studies do not sufficiently resemble their biological counterparts.

The past decade has been witness to several theories advanced to explain the observed behavioral properties of large fields of neurons in the brain (Nunez, 1989; Wright, 1990; Freeman,

---

[3]The threshold gate computes the function $H(\sum w_i x_i - T)$ where $x_i \in \{0, 1\}$ are binary inputs to the gate, $w_i \in \{-1, 1\}$ are weights assigned to the input lines, T is the threshold, and $H(\cdot)$ is the Heaviside step function ($H(x) = 1$ if $x \geq 0$ and $H(x) = 0$ if $x < 0$).

[4]The weights w_i are generalized to assume real values, and the Heaviside step function is replaced with a smooth sigmoid function.

1991). In general, these models do not adopt the neuron as their basic functional unit; for example, Freeman's model uses the K0, KI, KII, and KIII configurations of neurons[5] as its basic units, and Wright's model 'lumps' small cortical areas into single functional units. Moreover, some of these models are founded on presupposed functional properties of the macroscopic phenomenon under investigation; for example, both Wright's and Nunez's models assume that the global wavelike processes revealed in EEG recordings satisfy linear dynamics. These reasons account, in part, for the controversies that surround these theories.

The search for coherent structures in the dynamics of neuronal systems has also seen a surge of activity in recent times (Basar, 1990; Krüger, 1991a; Aertsen & Braitenberg, 1992; Bower & Beeman, 1995). Armed with faster and more powerful computers, scientists are replicating salient patterns of activity observed in neuronal systems in phenomena as diverse as motor behavior in animals and oscillatory activity in the cortex. The models of the neurons as well as those of the networks are considerably more realistic in these cases. There is an emphasis on simulation and it is hoped that analytic insight will be forthcoming from such experimentation.

1.2 Objectives

The research presented in this thesis shares the broad objectives of the diverse endeavors mentioned in the previous section: to unravel the dynamical and computational properties of systems of neurons in the brain. A detailed account of the goals of our research, however, requires that a proper terminology be established and explicated. We begin by clarifying what we intend by the phrase *discrete computational state*.

There are no serious disagreements in the scientific community regarding the position that the *physical states* of the brain are causally implicated in cognition, and that the intrinsic nature of these states plays a significant role in controlling behavior. It is only when the issue of whether or not these states bear *representational content* is broached, that we encounter divergent views. Anti-representationalists, for example, contend that these physical states are merely

[5] We quote Leslie Kay, "…Briefly, a K0 set represents a population of similar neurons, such as the mitral and tufted cells in the OB (Olfactory Bulb), or the granule cells in the OB. A KI set is two populations of neurons interconnected with feedback. A KII set is two (or more) interconnected KI sets with feedback; in the model this would refer to the representation of the OB (Olfactory Bulb) or the AON (Anterior Olfactory Nucleus) or the PPC (PrePyriform Complex). A KIII set is the whole thing connected with feedback delays (emphasis on the delays)…"

the reflection of the organism's acquired skills at performing the task at hand, that is, the activation of traces of an indefinite number of occasions where similar situations have been encountered (Dreyfus & Dreyfus, 1988). (See also related perspectives in (Merleau-Ponty, 1942) where it is maintained that the organism and the physical world are tightly coupled, and in (Heidegger, 1927) where the duality between subject and object is denied.)

Even within the Representationalist camp (those who adhere to the view that the brain states have semantic content in the sense that they "stand for" or encode objects, events, states of affair, etc., in the world) there are serious differences of opinion. The Classical school of cognitive architecture with its foundations in the *Physical Symbol System hypothesis* (Newell & Simon, 1976), has steadfastly rejected the tenets of the Connectionist school, arguing that the latter is not committed to a language of thought (Fodor & Pylyshyn, 1988).

Our sole concern in this thesis is the physical *nature* of these brain states as constrained by the anatomy and the physiology of the brain. Our use of the phrase "discrete computational states" therefore conforms with the notion of symbolic states or tokens as used in Computer Science—states that mark a discrete computational process regardless of representational content, if any, and not the related notion of "symbols" as used in the Cognitive Sciences—the physical embodiment of semantic units.

While there have been several proposals regarding the realization of such states in the processes of the brain, such as Hebbian Cell Assemblies (Hebb, 1949) and Reverberating Synfire Chains (Abeles, 1982, 1990), such theories have not been entirely satisfactory. The characterization of a Hebbian Cell Assembly, for example, lacks specificity since the notion of a "consistent firing pattern" has no definitive interpretation. Reverberating Synfire Chains, on the other hand, though well defined, lack causal justification; the formation of stable cycles (recurrence of firing patterns of groups of neurons) with periods extending over hundreds of milliseconds has not been formally established.

We believe that such drawbacks can be remedied by taking into consideration the physical constraints imposed by the system. The objective of our research has therefore been to answer two crucial questions:

1. Are there *coherent* spatiotemporal structures in the dynamics of neuronal systems that can

denote discrete computational states?

2. If such structures exist, what restrictions do the dynamics of the system at the physical level impose on the dynamics of the system at the corresponding abstracted computational level?

The results presented in this thesis constitute a step towards the resolution of these queries. Our approach is characterized by our position on two significant methodological issues. First, we take a conservative bottom-up approach to the problem, that is, we adopt the biological neuron as our basic functional unit. We believe that by not assuming a 'lumped' unit with presupposed functional characteristics, we not only detract from controversy, but also add to the well-foundedness of the theory. Second, we believe that answers to the above questions can be obtained primarily through a *formal analysis* of the phase-space dynamics of an abstract system whose dynamical behavior matches, sufficiently, that of the biological system.

From a purely conceptual perspective, the content of this thesis may be regarded as an exercise in demonstrating that certain seemingly innocuous assumptions about the dynamics of an individual neuron have rather significant and stringent implications for the dynamics of a system of neurons. From a more material perspective, this thesis may be viewed as an attempt at quantifying the nature of the representation of information in the brain. In this case, the core constitution of the model of the individual neuron takes prominence, for, the extent to which the results of the thesis foretell Nature is conditioned by the extent to which the model of the neuron captures the salient characteristics of the biological neuron. With this in mind, we have included a chapter that summarizes the biophysical basis of the activity of a biological neuron. The chapter is intended to equip the reader lacking a background in the neurosciences with sufficient information so as to be able to evaluate the model.

1.3 Organization of the Thesis

We have taken an unconventional two-pass approach to presenting the contents of this thesis. The substance of the thesis is first presented in an informal vein in Chapter 2. This chapter is intended both for the casual reader who is interested primarily in the general claims of the thesis, as well as the scrupulous reader, for whom the chapter affords a framework for the material

that follows. The subsequent chapters, with the exception of Chapters 3 and 5 which contain background material, offer a detailed and comprehensive account of the thesis.

In Chapter 3, we present a summary description of the biophysical basis of the activity of a neuron. In keeping with the objectives outlined in the previous section, we then construct a model of a biological neuron in Chapter 4 that is, on the one hand, sufficiently realistic so that conclusions drawn from the investigation of a system derived from the model may be applied with reasonable confidence to the target system, the brain, and on the other, sufficiently simple so that any system derived from the model may be investigated through analytical means. The model is based on a general set of characteristics of a biological neuron, which we set forth in some detail at the beginning of the chapter.

In Chapter 5, we present a brief tutorial on the subject of manifold theory, a rudimentary knowledge of which is essential to the comprehension of the material that follows. We also present a novel approach to defining certain concepts in dynamical systems analysis that allows us to construct new structures relevant to our system in Chapter 9.

In Chapter 6, we formulate an abstract dynamical system that models *systems* of biological neurons. The abstract system is based on the model of the neuron presented in Chapter 4. The chapter begins with a formal description of the phase-space of the system. It then describes the geometric structure immanent in the phase-space, and concludes with a description of the velocity field that overlays the phase-space.

Chapter 7 is devoted to a numerical investigation of the system. Simulation results are presented for several instantiations of the abstract system, each modeling a typical column in the neocortex to a different degree of accuracy. The results demonstrate that the dynamics of the abstract system is generally consistent with that observed in neurophysiological experiments. They also highlight certain dynamical properties that are robust across the instantiations.

In Chapter 8, we analyze the local properties of flows in the phase-space of the abstract dynamical system. A measure analysis reveals contraction, expansion, and folding in different sections of the phase-space. In order to identify the salient properties of the dynamics of a generic column in the neocortex, we model its dynamics as a stochastic process. The process is analyzed and the criterion for the dynamics of the system to be sensitive to initial conditions is derived through an appropriate application of a local cross-section analysis. The salient qualitative

characteristics of the system are then deduced based on physiological and anatomical parameters. The results not only explain the simulation results obtained in Chapter 7, but also make predictions that are borne out by further experimentation.

In Chapter 9, we first define the novel concept of a complex set. We then introduce a procedure that isolates from the phase-space all basic sets, complex sets, and attractors incrementally. Based on the results presented in this and the preceding chapter, we conclude that the *coherent* structures sought after in the questions posed earlier, are almost surely *chaotic attractors* that are potentially *anisotropic*.

Finally, in Chapter 10 we examine the impact of this result on the dynamics of the system at the abstracted computational level, and discuss directions for future research.

Chapter 2

Summary of Results

The neuron, in and of itself, is a remarkably complex device. Action potentials (also known as spikes) arrive at the various synapses located on the cell body (soma) and the multitudinous dendrites of a neuron. The effects of the spikes then propagate towards the axon hillock of the neuron. The integration of the effects of the various spikes arriving at temporally and spatially removed locations on the neuron is a complex nonlinear process. Weak nonlinearities are engendered, among other causes, by branch points on dendrites, while strong nonlinearities are engendered by the precipitation of local action potentials on the dendrites of the neuron. When the potential at the axon hillock exceeds the threshold of the neuron, the neuron emits an action potential which then travels down its axon to influence other neurons in like manner. A more detailed account of the biophysics underlying these processes is presented in Chapter 3.

Not only does one have to contend with the realization that the neuron is by no standard an elementary device, but also that the brain contains on the order of 3×10^{10} of these units. The salient nature of the dynamics of the brain, which evidently impacts the manner in which it represents and manipulates information, is therefore an issue of profound difficulty. There is, nevertheless, no denying that the issue begs to be addressed, for it underlies almost all problems in the fields of human vision, language acquisition and use, olfaction, motor control, attention, planning, decision making, etc.

The traditional approaches to understanding the nature of this dynamics can, by and large, be classified into two groups. In the first approach, the model of the individual neuron is simplified to an extent that formal analysis becomes feasible. Analysis of feed-forward and recurrent networks of hard and soft threshold gates and integrate-and-fire neurons fall within this category. The second approach maintains a more realistic view of the neuron, but in the process is compelled to draw conclusions based on the results of simulation experiments. Compartmental

approaches to modeling individual and groups of interconnected neurons fall within this category. There is also a third category of hybrid approaches, where higher level models of small groups of neurons (based on experimental observations) are used to model and formally analyze the dynamics of larger groups of neurons. Models based on the Wilson Cowan oscillator (Wilson & Cowan, 1972, 1973), and Freeman's KI, KII, and KIII configurations of neurons (Freeman, 1991) are prototypical examples of approaches that fall within this category.

Our approach to the problem can be classified under the first group. Although we do present results from simulation experiments in Chapter 7, our principal intent is to deduce the qualitative characteristics of the dynamics of systems of neurons through formal analysis. As alluded to in the previous chapter, the model of the individual neuron constitutes the weakest link in such an approach. We describe our model informally in the next section and again in a formal setting in Chapters 4 and 6.

In the remainder of this section, we aim to acquaint the reader with the observed *generic* dynamics of systems of neurons at the global (hundreds of thousands of neurons) as well as the local (individual neuron) scales.

The dynamics of the brain observed at the global scale is illustrated in Figure 2.1. The left column in the figure presents an EEG record of a young healthy human subject with eyes open over an 8 sec epoch.[1] The data was accumulated at a sampling rate of 128 Hz, cast through a band-pass filter (0.1 Hz to 30 Hz, 12 dB/octave roll-off), and digitized by an 8-bit digitizer. The standard international $10-20$ system of electrode placement on the scalp was utilized, resulting in 19 simultaneous EEG measurements. The right column in the figure presents the corresponding power spectrum charts.

For the reader not acquainted with EEG records, we quote Wright (1997):

> "The dendrites of cortical pyramidal neurones generate local field potentials (LFP) during processing of cognitive information (John et al., 1969; Mitzdorf, 1988; Gevins et al., 1983; Picton and Hillyard, 1988). Summed at a point on the cortical surface these LFP form the ECoG., and when recorded via the scalp, the electroencephalogram (EEG)…"

[1] This data is presented with permission from Prof. Dennis Duke and Dr. Krishna Nayak at SCRI, Florida State University.

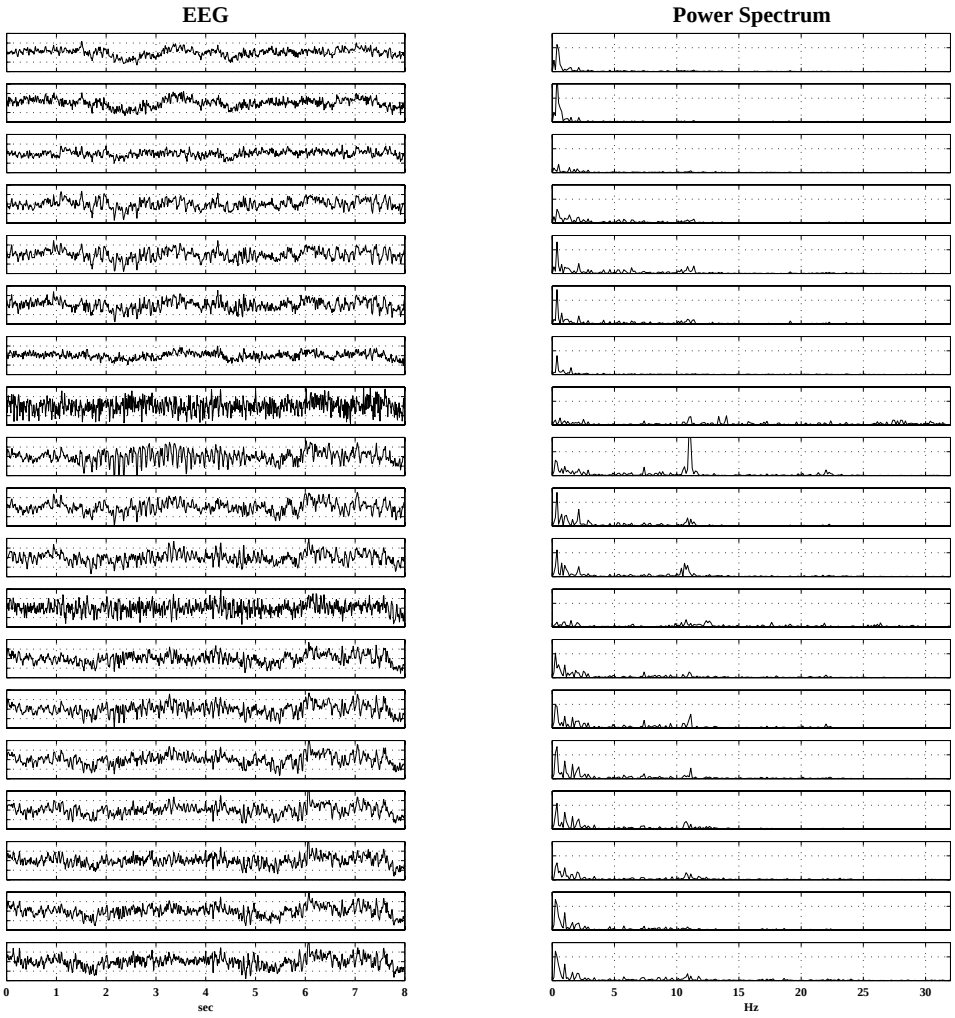

Figure 2.1: EEG records and corresponding power spectrums of a young healthy human subject with eyes open over an 8 sec epoch.

The temporal records appear noisy and the power spectrums have a "1/f" noise envelope with intermediate peaks at certain frequencies. These are generic properties of EEG records.

The dynamics of the brain observed at the local scale is illustrated in Figure 2.2. The left column in the figure presents several spike trains recorded from a direction selective neuron in area V1 of a macaque monkey.[2] The stimulus was a sinusoidal grating oriented orthogonal to the cell's axis of preferred motion. For a 30 sec period, the grating moved according to a random walk along the cell's axis of preferred motion. The graphs present successive inter-spike interval (ISI) times beginning with the onset of the first video frame for ten independent trials. The right

[2]This data is presented with permission from Prof. Wyeth Bair at CNS, New York University.

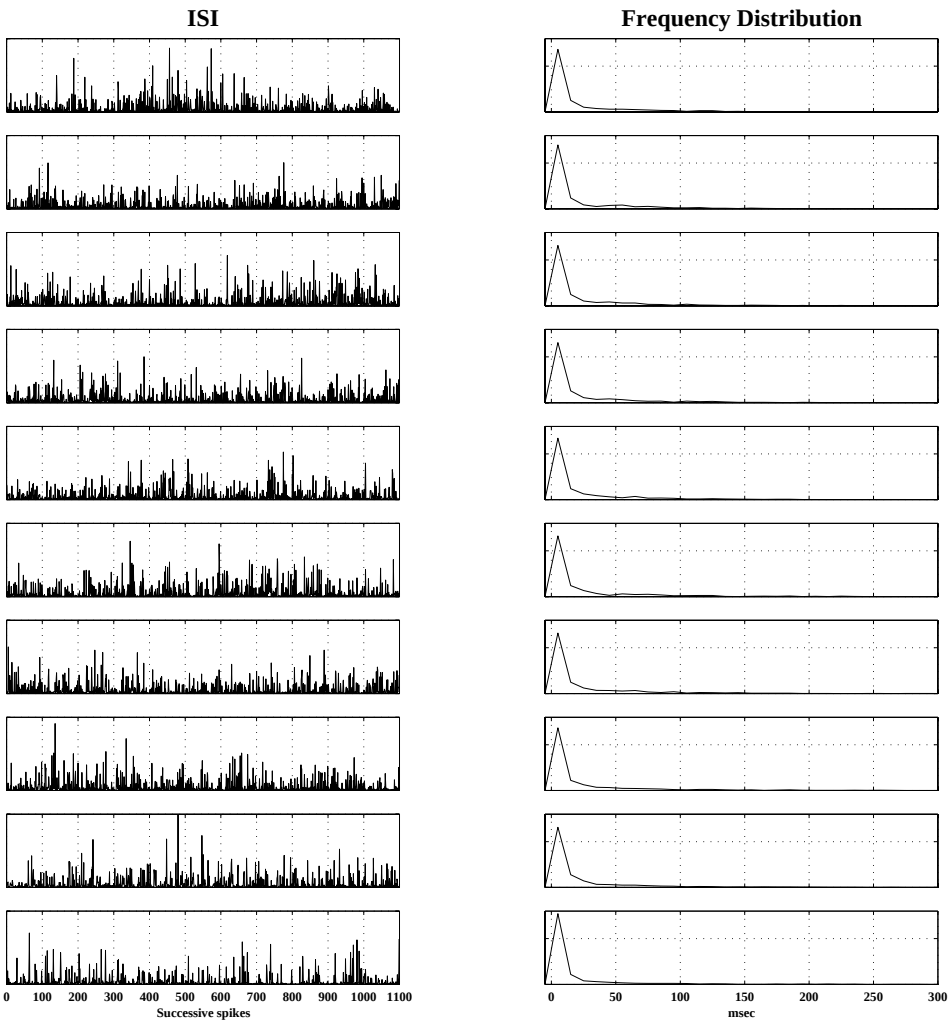

Figure 2.2: ISI records and corresponding frequency distributions of a direction selective neuron in area V1 of a macaque monkey.

column in the figure presents the corresponding frequency distributions.

The temporal records are aperiodic and the frequency distributions suggest that they could be generated from a Poisson process. These are generic properties of ISI records.[3]

We now proceed to informally describe the results of this thesis. The title of each section contains the chapter of the thesis that it corresponds to in parenthesis. A note of caution before we begin: The material presented in this chapter should be considered more a motivation

[3]The perceptive reader may be troubled by the possibility of the aperiodicity in the spike trains arising entirely from the randomness in the stimulus. That this is not the case has been documented in numerous other experiments with more regular stimuli. The aperiodic nature of the spike trains is an intrinsic feature of the activity of neurons in most regions of the brain.

for than an elucidation of the contents of the upcoming chapters. Informal descriptions, by nature, lack rigor and therefore leave open the possibility of misinterpretation. In the face of any ambiguity, the reader should defer to the more formal treatment in the upcoming chapters.

2.1 Model of the Neuron (Chapter 4)

As was described at the beginning of this chapter, at the highest level of abstraction, a biological neuron is a device that transforms a series of incoming (afferent) spikes at its various synapses, and in certain cases intrinsic signals, into a series of outgoing (efferent) spikes on its axon. At the heart of this transformation lies the quantity $P^*(\cdot)$, the membrane potential at the soma of the neuron. Effects of the afferent as well as those of the efferent spikes of the neuron interact nonlinearly to generate this potential. The series of efferent spikes generated by the neuron coincide with the times at which this potential reaches the threshold, $\mathcal{T}$, of the neuron. All realistic models of the neuron proposed to date attempt to model the precise manner in which this potential is generated.

We take a different approach to the problem. We simply assume that there exists an implicit function $P^*(\vec{x}_1, \vec{x}_2, ..., \vec{x}_m; \vec{x}_0)$ that yields the *current* membrane potential at the soma of the neuron. The subscripts $i = 1, ..., m$ represent the synapses on the neuron, and each $\vec{x}_i = \langle x_i^1, x_i^2, ..., x_i^j, ... \rangle$ is a *denumerable* sequence of variables that represent, for spikes arriving at synapse i since infinite past, the time lapsed since their arrivals. $\vec{x}_0$ is a sequence of variables that represent, in like manner, the time lapsed since the generation of spikes at the soma of the neuron. For example, $\vec{x}_5 = \langle 17.4, 4.5, 69.1, 36.0, 83.7, ... \rangle$ conveys that at synapse #5 of the neuron, a spike arrived 17.4 msec ago, one arrived 4.5 msec ago, one 69.1 msec ago, one 36.0 msec ago, one 83.7 msec ago, and so forth. We have, in this example, intentionally left the times of arrival of the spikes unsorted. Note that this would then imply that $P^*(\cdot)$ is symmetric with respect to the set of variables in each $\vec{x}_i$, since $\langle 17.4, 4.5, 69.1, 36.0, 83.7, ... \rangle$ and $\langle 4.5, 17.4, 36.0, 69.1, 83.7, ... \rangle$ denote the same set of arrival times of spikes.

Most of Chapter 4 is an exercise in demonstrating that based on a well recognized set of characteristics of the biological neuron, a time bound can be computed such that all spikes that arrived prior to that time bound (and all spikes that were generated by the neuron prior to that

bound) can be discounted in the computation of the current membrane potential at the soma of the neuron. For example, if calculations based on physiological and anatomical parameters resulted in a bound of 500 msec, the assertion would be that if a spike arrived at any synapse 500 or more msec ago (or was generated by the neuron 500 or more msec ago), its impact on the current membrane potential would be so negligible that it could be discounted. Finally, since spikes can not be generated arbitrarily close in time (another well recognized feature of the biological neuron, known as refractoriness, that prevents spikes from being generated within an absolute refractory period after the generation of a spike), this would imply that there can be, at any time, only finitely many spikes that have an impact on $P^*(\cdot)$. In our example, if the absolute refractory period of the neuron in question and of all neurons presynaptic to it were 1 msec, then of the spikes generated by the neuron at most 500 could be effective[4] at any time, and of the spikes arriving at each synapse at most 500 (per synapse) could be effective at any time.

The import, in essence, is that $P^*(\cdot)$ can be suitably redefined over a *finite dimensional* domain (that corresponds to a maximal set of effective spikes) without incurring any loss of information. The resulting function is labeled $P(\cdot)$.

2.2 Abstract Dynamical System for a System of Neurons (Chapter 6)

How do we represent the state of a system of neurons assuming that we possess absolute knowledge about the potential functions ($P_i(\cdot)$'s) of the constituent neurons? From a dynamical systems perspective, what then is the nature of the phase-space and the velocity field that overlays this space? These are the issues addressed in Chapter 6.

We begin with the first question. Figure 2.3 presents a schematic diagram of a toy system consisting of two neurons (and two inputs) and is intended to supplement the description below.

For the moment, we disregard the case where the system receives external input. We first note that a record of the temporal locations of all afferent spikes into neurons in a system is potentially redundant since multiple neurons in the system might receive spikes from a common neuron. As a first step, we therefore execute a conceptual shift in focus from afferent spikes to efferent spikes. We now observe that if for each neuron in the system, we maintain a log

[4] An effective spike refers to a spike that currently has an effect on the membrane potential at the soma of the neuron.

of the times at which the neuron generated spikes in the past (each entry in the log reporting how long ago from the present the neuron generated a given spike), then the set of logs yield a complete description of the state of the system. This follows from the fact that not only do the logs specify the location of all spikes that are still situated on the axons of the neurons, but also, in conjunction with the potential functions, they specify the current states of the somas of all neurons.

Based on the time bounds (for each neuron in the system) derived in the previous section and information regarding the time it takes a spike to reach a synapse from its inception at a given soma, we can compute a new bound such that all spikes that were generated in the system before this bound are currently ineffective. Returning to our example, if 500 msec was the longest a spike could remain effective on any neuron, and if 5 msec was the longest it took a spike to arrive at a synapse from its inception at a soma, then any spike that was generated in the system more than 505 msec ago is currently ineffective. Since ineffective spikes can be disregarded, and each neuron has an absolute refractory period, it would suffice to maintain a log of finite length (in our example, a length of 505 msec$/1$ msec$= 505$).

The state of the system can now be described by a list of logs of real numbers. Each log has a fixed number of entries, and the value of each entry is bounded from above by a fixed quantity. In our example, each neuron would be assigned a 505-tuple of reals whose elements would have values less than 505 msec. The membrane potential at the soma of each neuron in the system can be computed based on these logs and the potential functions (which, along with other information, contain the connectivity data).

We have assumed thus far that the recurrent system receives no external input. External input, however, can be easily modeled by introducing additional neurons whose spike patterns mimic the input. The state of the system is therefore completely specified by the list of logs.

At this juncture an assay at specifying the phase-space for the entire system would yield a closed hypercube in Euclidean space, $[0.0, 505.0]^{505\times\{\#\text{ of neurons in the system}\}}$ in our example. However, this formulation of the phase-space suffers from two forms of redundancies. We shall articulate both using our example. First, 505 was computed as an upper bound on the number of effective spikes that a neuron can possess at any time. It is conceivable that there will be times at which a neuron will have spiked fewer than 505 times in the past 505 msec. Under

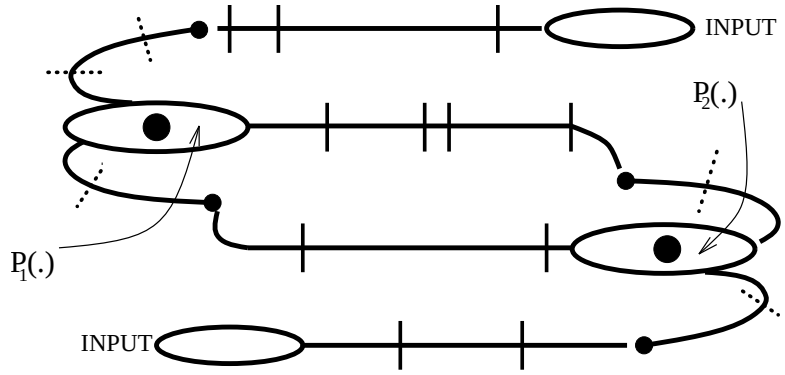

Figure 2.3: A schematic diagram of a system of neurons. The input neurons are placeholders for the external input. Spikes on the axon are depicted as solid lines. Those on the dendrites are depicted as broken lines, for, having been converted into graded potentials, their existence is only abstract (point objects indicating the time of arrival of the spike).

such conditions, where should the remaining elements in its 505-tuple be set? To answer this question, we consider the dynamics of the system. When an element in the tuple is assigned to a spike its value is set at 0 msec. Then, as time passes, its value grows until the bound of 505 msec is reached, at which time the spike turns ineffective. When the element is assigned to a new spike at a later time, its value is reset to 0 msec.[5] In essence, not only is one of the two values 0.0 and 505.0 redundant, but also, this representation gives rise to discontinuities in the dynamics. The resolution lies in identifying the value 0.0 with the value 505.0.

Second, whereas a tuple is an ordered list of elements, our true objective lies in representing an unordered list of times (which element of a tuple represents a given spike is immaterial). For example, whereas $\langle 17.4, 4.5, 69.1, 36.0, 83.7\rangle$ and $\langle 4.5, 17.4, 36.0, 69.1, 83.7\rangle$ are two distinct 5-tuples, they denote the same set of spike generations. This redundancy also adversely impacts the description of the dynamics of the system. For example, if a neuron, on the brink of spiking, was in the state $\langle 4.5, 505.0, 36.0, 69.1, 505.0\rangle$, which of the two elements set at 505.0 would we reset to 0.0?

In Section 6.2, a phase-space is constructed that resolves both issues. In two successive transformations a real number (how long ago the spike was generated) is converted into a complex number of unit modulus (so that the terminal points, 0.0 and 505.0 in our example, meet),

[5]Note that since a neuron, in its lifetime, will fire many more times than the number of variables assigned to it, variables will necessarily have to be reused. The number of variables assigned to a neuron has, however, been computed in a manner such that there will always exist at least one variable with value set at 505 msec when the time comes for a variable to be reassigned to a new spike.

and then this ordered set of complex numbers is converted into an unordered set by recording instead the coefficients of the complex polynomial whose roots lie at these values. The new phase-space is then shown to be a compact manifold with boundaries. Various other features of the phase-space are also explicated.

In Section 6.3 a crucial topological issue is addressed. To illustrate using our example: what should be considered a neighborhood of the state $\langle 4.5, 17.4, 0.0, 0.0, 0.0\rangle$ of a neuron? Should it be (for some $\epsilon > 0$) $\langle 4.5 \pm \epsilon, 17.4 \pm \epsilon, 0.0 \pm \epsilon, 0.0 \pm \epsilon, 0.0 \pm \epsilon\rangle$ or $\langle 4.5 \pm \epsilon, 17.4 \pm \epsilon, 0.0, 0.0, 0.0\rangle$. This issue has significant implications for the accurate identification of attractors in the phase-space of the system. Since an element set at 0.0 is merely an artifact of the representation, the second choice is appropriate. Translating this intuition onto the new phase-space is the subject of Section 6.3.

Finally, in Section 6.4, the velocity field that overlays the phase-space is defined. The dynamics of the abstract system is elementary when characterized over the initial phase-space described above. For each tuple (corresponding to a distinct neuron in the system), all non-zero elements grow at a constant rate until the upper bound (505.0 in our example) is reached, at which time its value is reset to 0.0. When neuron i is on the brink of spiking (the trajectory in the phase-space impinges on the surface $P_i(\cdot) = \mathcal{T}$), exactly one of the elements in the ith tuple that is set at 0.0 is set to grow. The section transplants this dynamics appropriately onto the new phase-space.

2.3 Simulation Experiments (Chapter 7)

The primary objective of Chapter 7 is to familiarize the reader with the generic dynamics of the abstract dynamical system formulated in Chapters 4 and 6. Questions such as how the dynamics of the system compares with the generic dynamics of systems of neurons in the brain (described earlier in this chapter) are addressed through the application of simulation experiments.

The target unit in the brain to which the system is compared is a *column* in the *neocortex*. The choice is based on several reasons. First, there stands the issue of tractability; the computational resources required to simulate a column lies barely within the reach of modern workstations. Although simulation results are presented for systems comprising 10^3 model neurons

(in comparison, a typical column contains on the order of 10^5 neurons), a limited set of experiments with larger systems (10^4 model neurons) were also conducted. These experiments did not reveal any significant differences with regard to the generic dynamics of the system, instead the qualitative aspects of the dynamics became more pronounced.

Second, in neocortical columns, the distribution of the various classes of neurons, the location of synapses on their somas and dendrites, the patterns of connectivity between them, etc., can be described statistically. Finally, the qualitative features of the dynamics of generic neocortical columns are well documented.

Simulation results for several instantiations of the abstract system, with varying degrees of physiological and anatomical accuracy (starting from $P(\cdot)$ being a unimodal piecewise linear function to it being a complex parameterized function reported in (MacGregor & Lewis, 1977) fitted to realistic response functions) are presented.

The results demonstrate a substantial match between the dynamics of the abstract system and that of generic neocortical columns. A significant outcome of the experiments is the emergence of three distinct classes of qualitative behavior: quiescence, intense periodic activity resembling a state of seizure, and chaotic activity in the realm associated with "normal operational conditions" in the neocortex.

2.4 Local Analysis (Chapter 8)

Chapter 8 is devoted to the study of local properties of trajectories in the phase-space of the abstract dynamical system.

The phase-space (which is a compact manifold with boundaries as described in Section 2.2) is first endowed with a Riemannian metric in Section 8.1. The definition of a differentiable manifold does not stipulate an inner product on the tangent space at a point. The Riemannian metric, by specifying this inner product, institutes the notion of a distance between points in the phase-space, a notion that is indispensable to the analysis of local properties of trajectories.

Although the initial formulation of the phase-space suffered several drawbacks, the corresponding velocity field was inordinately simple. The Riemannian metric is defined such that this simplicity is preserved. To elaborate, the metric causes the phase-space to appear *locally*

like the initial formulation of the phase-space; if point p in the phase-space corresponds to the point $\langle 17.4, 4.5, 69.1, 36.0, 83.7\rangle$ in the initial formulation, then (for $\epsilon \to 0$) vectors directed to the point corresponding to $\langle 17.4+\epsilon, 4.5, 69.1, 36.0, 83.7\rangle$, or to $\langle 17.4, 4.5+\epsilon, 69.1, 36.0, 83.7\rangle$, or to $\langle 17.4, 4.5, 69.1+\epsilon, 36.0, 83.7\rangle$, etc., are mutually orthogonal. This arrangement yields an excellent blend of global consistency and local simplicity.

It is then demonstrated that with regard to this metric, the velocity field is not only measure preserving but also shape preserving over the short intervals during which neither any neuron in the system spikes (labeled the *birth* of a spike) nor any spike in the system turns ineffective (labeled the *death* of a spike). What transpires in the neighborhood of a trajectory in the event of the birth of a spike or that of the death of a spike is considered in Sections 8.2 and 8.3.

In Section 8.2, a perturbation analysis is conducted on trajectories around the events of the birth and the death of a spike. To illustrate using an example, if the current state of a 2-neuron system is specified by the pair of 5-tuples $\langle 17.4, 4.5, 69.1, 0.0, 0.0\rangle$, $\langle 36.0, 83.7, 0.0, 0.0, 0.0\rangle$, and the second neuron is on the brink of spiking, then the state of the system 1 msec later will be specified by the pair $\langle 18.4, 5.5, 70.1, 0.0, 0.0\rangle$, $\langle 37.0, 84.7, 1.0, 0.0, 0.0\rangle$. The question addressed by the perturbation analysis is: What would the perturbation be after the 1 msec interval had we begun from the infinitesimally removed state $\langle 17.4+\epsilon_1^1, 4.5+\epsilon_1^2, 69.1+\epsilon_1^3, 0.0, 0.0\rangle$, $\langle 36.0+\epsilon_2^1, 83.7+\epsilon_2^2, 0.0, 0.0, 0.0\rangle$, where the ϵ_i^j's are the components of an initial perturbation? It is apparent that not only would all spikes maintain their initial perturbations, but also that the new spike would undergo a perturbation (denoted here by ϵ_2^3). It is demonstrated that $\epsilon_2^3 = \alpha_1^1\epsilon_1^1 + \alpha_1^2\epsilon_1^2 + \alpha_1^3\epsilon_1^3 + \alpha_2^1\epsilon_2^1 + \alpha_2^2\epsilon_2^2$, where the α_i^j's are the *normalized gradients* of the potential function of the second neuron—$P_2(\cdot)$—with respect to the various spikes, computed at the instant of the birth of the spike. The same question, with the intermediate event set as the death of a spike, is addressed in like manner.

In Section 8.3, the results of Section 8.2 are applied to demonstrate that an infinitesimal hypercube of phase-space around a trajectory expands in the event of the birth of a spike and contracts in the event of the death of a spike. This is a rather straightforward consequence of the fact that at the birth of a spike a component perturbation is gained, and at the death of a spike a component perturbation is lost. It is also shown that folding of phase-space can occur across a series of births and deaths of spikes. Folding is a phenomenon that befalls systems with bounded

phase-spaces that are expansive in at least one direction. In such cases, sections of the phase-space can not expand unfettered. The expansion of the section is therefore accompanied by a folding so that it may fit back into the phase-space.

Section 8.4 considers the effect of a series of births and deaths of spikes on a trajectory. Just as in traditional stability analysis, the relationship between an initial perturbation and a final perturbation, both of which lie on transverse sections through the trajectory under consideration, is examined as a function of increasing time.

We consider here an example that, even though acutely simplistic, illustrates the general import of the result presented in the section. The system is specified by three spikes. When all 3 spikes are active, the impending event is that of the death of the oldest spike, and when 2 spikes are active, it is that of the birth of a spike. In other words, the dynamics is an alternating sequence of birth and death of spikes, the system switching between 2 and 3 effective spikes in the phase-space. Note that at the birth of a spike, there are 2 effective spikes in the system that can be referenced by their respective ages (young vs. old). The equation describing the perturbation on the new spike (at its birth) is given by $\epsilon_{\text{new}} = \alpha_1 \epsilon_{\text{old}} + \alpha_2 \epsilon_{\text{young}}$.

We consider two cases, $(\alpha_1 = 0.95, \alpha_2 = 0.05)$ and $(\alpha_1 = 1.05, \alpha_2 = -0.05)$. Note that in both cases, the α_i's are fixed. Moreover, the α_i's sum to 1 in recognition of the constraint that they be normalized. Since the initial perturbation must lie on a transverse section through the trajectory, it must take the form $\langle \epsilon, -\epsilon \rangle$. The final perturbation must, likewise, be adjusted along its trajectory to lie on the same plane. Figure 2.4 presents the temporal evolution of the adjusted final perturbations for the two cases. The initial perturbation is $\sqrt{(\epsilon)^2 + (-\epsilon)^2} = \sqrt{2}\epsilon$ in both cases.

In the first case $(\alpha_1 = 0.95, \alpha_2 = 0.05)$ the perturbation decays exponentially, whereas in the second $(\alpha_1 = 1.05, \alpha_2 = -0.05)$ it rises exponentially. In other words, the trajectory in the first case is insensitive to initial conditions, and in the second is sensitive to initial conditions. What feature of the α_i's makes this determination? Section 8.4 answers this question in a probabilistic framework.

Section 8.5 applies the result of Section 8.4 to the dynamics of systems of neurons (a column in the neocortex) in the brain. Based on physiological and anatomical parameters it is deduced that trajectories in the region of the phase-space corresponding to "normal operational

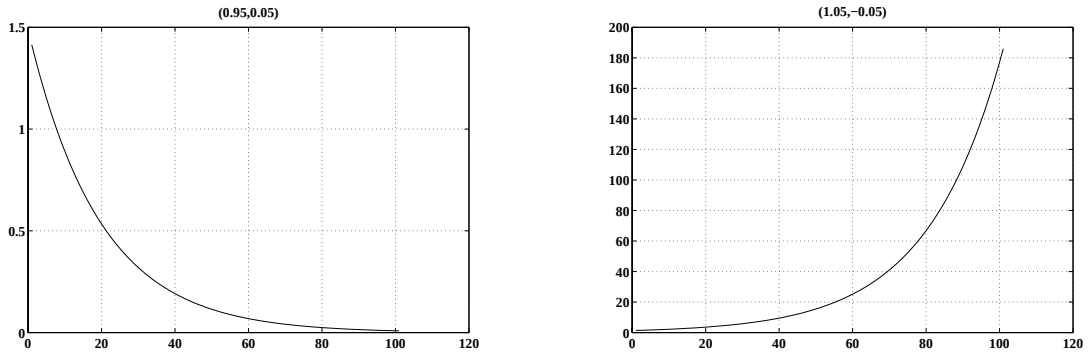

Figure 2.4: Temporal evolution of the adjusted final perturbation for a simple 3 spike system. Two cases are shown: $(\alpha_1 = 0.95, \alpha_2 = 0.05)$ and $(\alpha_1 = 1.05, \alpha_2 = -0.05)$.

conditions" in the neocortex are almost surely (with probability 1) sensitive to initial conditions and those in the region of the phase-space corresponding to "seizure-like conditions" are almost surely insensitive to initial conditions.

2.5 Global Analysis (Chapter 9)

Chapter 9 is devoted to a global analysis of the phase-space dynamics of the abstract system.

Section 9.1 reviews the definitions of wandering points, nonwandering points, and basic sets that were introduced in Chapter 5, Section 3. A wandering point (also referred to as a transient point) in the phase-space of an abstract system is a point such that the system, initiated anywhere in a neighborhood of the point returns to the neighborhood at most finitely many times (the existence of at least one such neighborhood is guaranteed). A nonwandering point is a point that is not wandering. A basic set is a concept that was instituted to identify coherent sets (such as isolated fixed points and periodic orbits) as distinct from the remainder of the phase-space, but matured substantially with the discovery of chaos. The definitions used in all cases are variations of the classical definitions of these concepts, and reduce to them when the iterated map is a homeomorphism. The fact that our system is not even continuous therefore plays a significant role in the further development of these concepts. The existence of discontinuities in the dynamics of the system spawns a new concept, that of a complex set. It is shown that a complex set that is also an attractor, is potentially *anisotropic* (under noise-free conditions, a trajectory visits only part of the set, depending upon its point of entry into the basin of attraction of the

set).

Section 9.2 presents a revision of the phase-space of the abstract system so as to yield a discrete dynamical system. The revision underscores the discontinuities that are inherent in the dynamics of the system.

Finally in Section 9.3, a traditional method geared to recover basic sets is augmented to recover complex sets and attractors from the phase-space of the revised abstract dynamical system.

2.6 Summary

In this chapter, we have informally described the core results of the thesis. In the upcoming chapters we recount these results in formal detail.

Chapter 3

Background: The Biophysics of Neuronal Activity

In this chapter, we present a brief description of the biophysics that underlies the activity of a biological neuron. A basic understanding of this material should facilitate any evaluation of the strengths and weaknesses of the model of the neuron that we propose in Chapter 4. Familiarity with this material is, however, not a prerequisite to the comprehension of the contents of the thesis.

3.1 The Brain: Basic Features

The brain is an exceptionally complex organ. It can be regarded at various levels of organization and detail. From a functional perspective, the brain can be partitioned into (i) the cerebral cortex, responsible for all higher order functions, (ii) the thalamus, which acts as a processing gateway to all information bound for and departing the cerebral cortex, and (iii) the perithalamic structures comprising the hypothalamus, the reticular formation, the nigrostriate formation, the cerebellum, the hippocampus, and the colliculus, each performing peripheral tasks essential to the proper functioning of the system as a whole.

At the highest level of abstraction, the brain is a device that is composed of numerous copies (approximately 3×10^{10} in the human brain) of a lone functional unit, the *neuron* (or the *nerve cell*).[1] This outlook, however, changes drastically when the brain is viewed at a more concrete level. Physiological and anatomical investigations have established that neurons in the brain come in an overwhelming variety of shapes, forms, and functional types. Furthermore, there is extensive evidence both of structure and the lack thereof in the layout of connections between

[1]The other category of cell known as the *glial* (or *neuroglial*) *cell* outnumbers the neuron eight or nine times to one, and is believed to serve as a structural and metabolic support element, a role played by connective tissue elsewhere in the body.

individual neurons (Braitenberg & Schüz, 1991; Schüz, 1992; Shepherd, 1998).

Notwithstanding the great variety of neurons present in the various structures enumerated above, and significant variations in cytoarchitecture both between and within each structure, the basic principles that govern the operation of their constituent neurons are substantially the same. This fortuitous finding has led to the formulation of the *model neuron*, a construction that embodies the general characteristics of the majority of the neurons.

3.2 Morphology of the Biological Neuron

A model neuron can be partitioned into four morphological regions: the soma, the dendrites, the axon, and the presynaptic terminals. The *soma* or the *cell body* contains the organelles (subcellular components) necessary for cellular function. The soma gives rise to the *axon*, a tubular process that in most instances extends over a considerable distance. For example, the axons of pyramidal neurons in layers 2/3 of the cortex extend to distances of 100 μm to 400 μm. At the distal end the axon divides into fine branches (axonal arborization) that have specialized terminal regions called *presynaptic (axonal) terminals*. Terminals convey information regarding the activity of the neuron by contacting *dendrites* that are receptive surfaces of other neurons. Dendrites typically consist of arborizing processes, that is, processes that divide repeatedly to form a treelike structure, that extend from the soma. The point of contact between two neurons is labeled a *synapse*. It is formed by the presynaptic terminal of one cell (the presynaptic neuron) and the receptive surface on the dendrite of the other (the postsynaptic neuron). Figure 3.1 displays a schematic diagram of a pair of model neurons and their various morphological regions.

Electrical signals known as *action potentials*[2] travel down the axon and arrive at presynaptic terminals, whereupon they are transmitted to the dendrite of the postsynaptic neuron through a chemically mediated process. The electrical signal in the dendrite then spreads to the soma (the impulse has by now lost its localized form) where it is integrated with signals arriving from other such presynaptic neurons, and in certain cases signals generated intrinsically. When the potential at the soma exceeds the *threshold* of the neuron, the soma generates an action potential that travels down its axon.

[2] Also known as *spikes*, each such nerve impulse is a roughly triangular solitary wave of amplitude 100 mV that lasts approximately 1 msec.

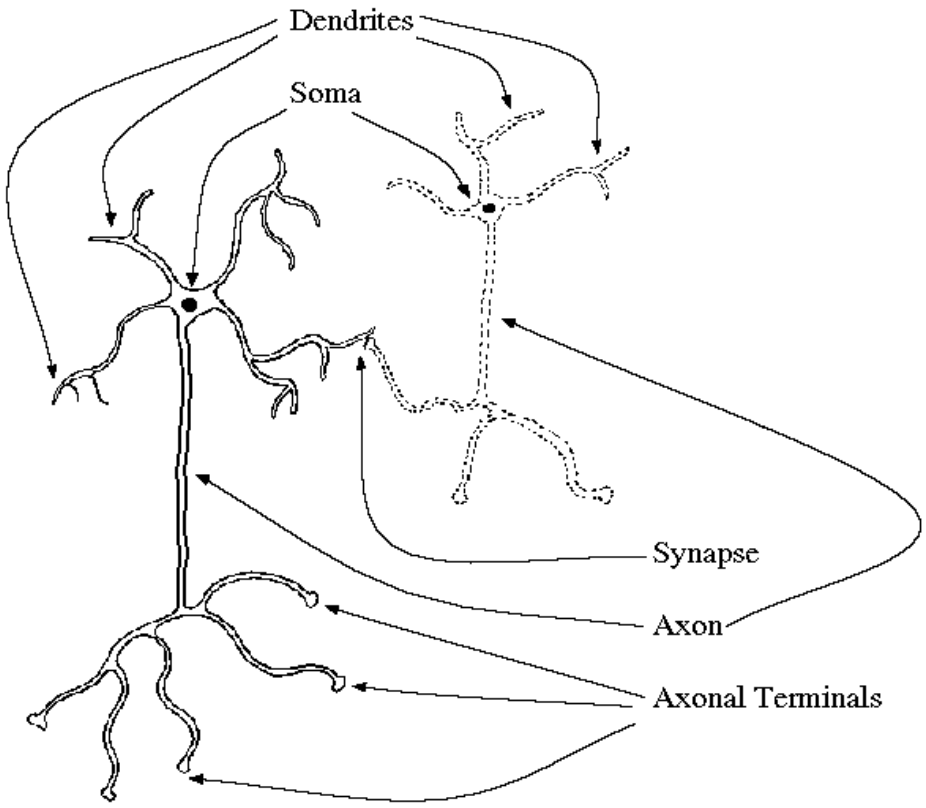

Figure 3.1: Schematic diagram of a pair of model neurons.

From a systems perspective, a neuron transforms multiple series of input action potentials arriving at its various afferent (incoming) synapses and in addition, in certain cases intrinsic signals, into a series of output action potentials on its axon. It is this view of the neuron that we adopt in the upcoming chapters.

In order to build a *viable* model of the biological neuron, we impose several formal constraints on the noted transformation, constraints that we enumerate in Chapter 4. Evaluating the veridicality of the constraints, however, requires a basic understanding of the functioning of the neuron. In the remainder of this chapter we therefore shed light on the nature of this transformation by describing briefly the biophysics that underlies the various stages of the process described above. Readers who desire a more comprehensive exposition of the material should consult (Kandel, 1976; Cronin, 1987; Tuckwell, 1988; Koch, 1998; Zigmond et al., 1999).

3.3 The Membrane Potential

The cell membrane of a typical neuron ranges in thickness between 30 and 50 Å and consists of two layers of phospholipid molecules. This insulating bilipid membrane is interspersed with membrane spanning protein molecules with water filled pores that act as *ionic channels*, that is, conduits through which ions can pass. At its resting state a neuron maintains a potential difference across its cell membrane, the inside of the cell being negative in relation to the outside. This potential difference, known as the *membrane potential*, ranges between -40 and -70 mV (with the mode at -60 mV) depending upon the organism as well as the classification of the neuron (Bernstein, 1902; Hodgkin & Huxley, 1939; Curtis & Cole, 1942).

The potential difference is derived primarily from an unequal distribution of K^+ and Na^+ ions across the cell membrane. The membrane is selectively permeable and allows ions to diffuse through the specific and sparsely distributed ionic channels at rates determined by the permeability of the membrane to the particular ion, the electrical gradient across the membrane, and the concentration gradient of the ion across the membrane. The membrane maintains numerous electrogenic[3] $Na^+ - K^+$ pumps (also known as Na^+, K^+-ATPase) that actively transport Na^+ ions out of the cell and K^+ ions into the cell. It is primarily the effect of these pumps and the differential permeability of the membrane to Na^+ and K^+ ions at resting state that results in the membrane potential.

Due to the concentration gradient generated by the pumps, K^+ ions diffuse across the membrane. This is, however, not accompanied by the entry of an equal quantity of positive charge (borne by cations such as Na^+) into the cell or the exit of negative charge (borne by anions such as Cl^- and other organic anions) out of the cell, the permeability of the membrane to these ions being very low at resting state. There is therefore a buildup of electrical charge across the membrane. At steady state, there is a net balance between flow of charge into the cell (Na^+ ions drawn in due to the equilibrium potential difference and its concentration gradient across the membrane) and flow of charge out of the cell (K^+ and Cl^- ions driven out for like reasons). The equilibrium potential difference is given by the solution to the Goldman-Hodgkin-Katz equation

[3]Three Na^+ ions are expelled for every two K^+ ions drawn into the cell. This unequal transport of ions leads to a hyperpolarizing potential, and the pump is therefore electrogenic.

(Goldman, 1943)

$$V_m = \frac{RT}{F} ln \frac{P_{\text{K}}[\text{K}^+]_o + P_{\text{Na}}[\text{Na}^+]_o + P_{\text{Cl}}[\text{Cl}^-]_i}{P_{\text{K}}[\text{K}^+]_i + P_{\text{Na}}[\text{Na}^+]_i + P_{\text{Cl}}[\text{Cl}^-]_o} \tag{3.1}$$

where R is the gas constant, T the absolute temperature, F the Faraday constant, $[\cdot]_o$'s and $[\cdot]_i$'s the concentrations of the ions outside and inside the cell respectively, and $P_{\cdot}$'s the permeability of the membrane to the ions.

3.4 Passive Conductance of Synaptic Potential across Dendrites

Synaptic potentials, generated by the arrival of action potentials at synapses, are conducted passively over the dendrites to the soma. This passive conductance is generally modeled using cable theory (Rall, 1960).

The dendrite is modeled as a uniform cylindrical core conductor with length much larger than diameter. Membrane properties such as resistivity and capacitance are assumed to be uniform. The gradient of the membrane potential v_m along the axis of the cable can then be expressed as

$$\frac{\partial v_m}{\partial x} = -ri \quad \text{and as a result} \quad \frac{\partial^2 v_m}{\partial x^2} = -r\frac{\partial i}{\partial x}, \tag{3.2}$$

where x represents the distance along the axis of the cable, i the current flowing along the axis, and $r = (r_i + r_o)$ the compound resistance per unit length of the cable (r_i is the intracellular and r_o the extracellular resistance per unit length). If there is no current injected by an intracellular electrode, and i_m is the membrane current density per unit length of the cylinder (current flowing perpendicular to the axis of the cable), then

$$i_m = -\frac{\partial i}{\partial x}. \tag{3.3}$$

Equations 3.2 and 3.3, when combined, yield

$$\frac{\partial^2 v_m}{\partial x^2} = r i_m. \tag{3.4}$$

Finally, a unit length of the membrane is modeled as an equivalent circuit (Figure 3.2) consisting of two components connected in parallel. The first is the membrane capacitance, and the second is a compound component that consists of the membrane resistance and a cell (modeling the resting potential) connected in series. This results in the equation

$$i_m = c_m \frac{\partial v_m}{\partial t} + \frac{v_m}{r_m} \quad \text{or} \quad i_m = c_m \frac{\partial v_m}{\partial t} + g_m v_m, \tag{3.5}$$

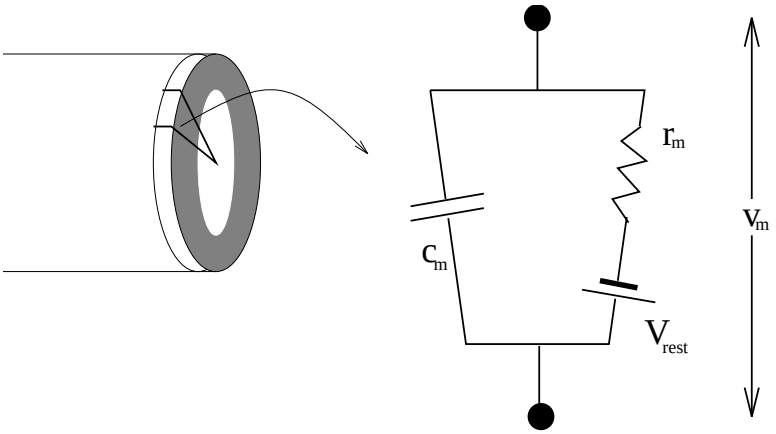

Figure 3.2: Schematic diagram of the equivalent circuit for a passive membrane.

where c_m is the membrane capacitance per unit length, and $g_m = \frac{1}{r_m}$ is the membrane conductance per unit length. The partial differential equations 3.4 and 3.5 together form the basis of cable theory. The equations have been solved for various boundary conditions. One such solution (MacGregor & Lewis, 1977) uses the Laplace transform method to yield

$$v_m(x,s) = v(0,s)\cosh[\sqrt{rg_m + rc_m s}\, x] - \sqrt{\frac{r}{g_m + c_m s}} i(0,s)\sinh[\sqrt{rg_m + rc_m s}\, x], \quad (3.6)$$

$$i(x,s) = i(0,s)\cosh[\sqrt{rg_m + rc_m s}\, x] - \sqrt{\frac{g_m + c_m s}{r}} v(0,s)\sinh[\sqrt{rg_m + rc_m s}\, x]. \quad (3.7)$$

Assuming a short circuit at the soma, that is, $v_m(l,s) = 0$, a synaptic impulse at the near end, that is, $i(0,s) = I_{syn}(s) = Q$, and a semi-infinite dendrite ($l \to \infty$) so that higher order terms in the solution may be disregarded, one arrives at the solutions,

$$i(x,t) = [\frac{Q\sqrt{rc_m x^2}}{2\sqrt{\pi t^3}}] e^{-rc_m x^2/4t} e^{-(g_m/c_m)t}, \quad (3.8)$$

$$v_m(x,t) = [\frac{Qr}{\sqrt{rc_m x^2 \pi t}}] e^{-rc_m x^2/4t} e^{-(g_m/c_m)t}. \quad (3.9)$$

The membrane potential at the soma is computed by integrating the impact of the PSP's (postsynaptic potentials) generated by the arrival of spikes at the various synapses on the dendritic tree. An advantage of using cable theory to model subthreshold response at the soma is that the equations are linear. In other words, if V_1 is the solution to the equation $V_t = V_{xx} - V + I_1$, with initial value $v_1(x)$ (I_1 is introduced as injected current density at $\langle x,t \rangle$), and V_2 is the solution to the equation $V_t = V_{xx} - V + I_2$, with initial value $v_2(x)$ and the same boundary

conditions, then the solution to $V_t = V_{xx} - V + I_1 + I_2$, with initial value $v_1(x) + v_2(x)$ and the same boundary conditions is $V(x,t) = V_1(x,t) + V_2(x,t)$.

While spatiotemporal integration of PSP's on a single dendritic branch is linear (the consequence of the linearity of cable theory), spatiotemporal integration of PSP's on an entire dendritic tree is in general not so. It has, however, been shown in (Walsh & Tuckwell, 1985) that if all dendritic terminals are at the same distance from the origin, and at all branch points on the dendritic tree $\text{diameter}^{3/2}_{\text{parent-cylinder}} = \sum \text{diameter}^{3/2}_{\text{daughter-cylinder}}$, then the entire dendritic tree can be mapped onto a single nerve cylinder, in which case integration of PSP's over the entire dendritic tree becomes linear.

Dendritic trees do not, in general, satisfy the above criterion. Passive conductance of synaptic potential across structurally complex dendritic trees is therefore computed using compartmental modeling. The main assumption in the compartmental approach is that small pieces of the neuron can be treated as isopotential elements. The continuous structure of the neuron is approximated by a linked assembly of discrete elements (compartments), and the resulting coupled partial differential equations are solved numerically.

In order to determine how reasonable the boundary conditions are that lead to the closed form solution of (MacGregor & Lewis, 1977), we compared it to simulations of subthreshold response in a neuron to synaptic inputs on an implementation of the compartmental approach, NEURON v2.0 (Hines, 1993).[4] We constructed a toy neuron with the soma and axon modeled as a single compartment and six dendritic branches connected irregularly to form a tree of depth two. Synaptic inputs were applied at various locations on the dendrites and the responses at the soma were noted. Figure 3.3 displays the result of one such experiment. As seen in the figure, we found a good fit between the simulation results and the closed form solution (with parameters set at optimal values).

We also tested the results of linear summation of PSP's against simulations on the toy neuron described above (the toy neuron violated the assumptions delineated in (Walsh & Tuckwell, 1985)) and found an agreeable fit. Figure 3.4 displays the result of one such experiment.

[4]NEURON, like GENESIS, is a neuronal simulation software that, given a compartmental model of a neuron, simulates its dynamics by solving numerically a coupled set of the Hodgkin-Huxley equations for each compartment. It is a freeware and is available at "http://neuron.duke.edu/".

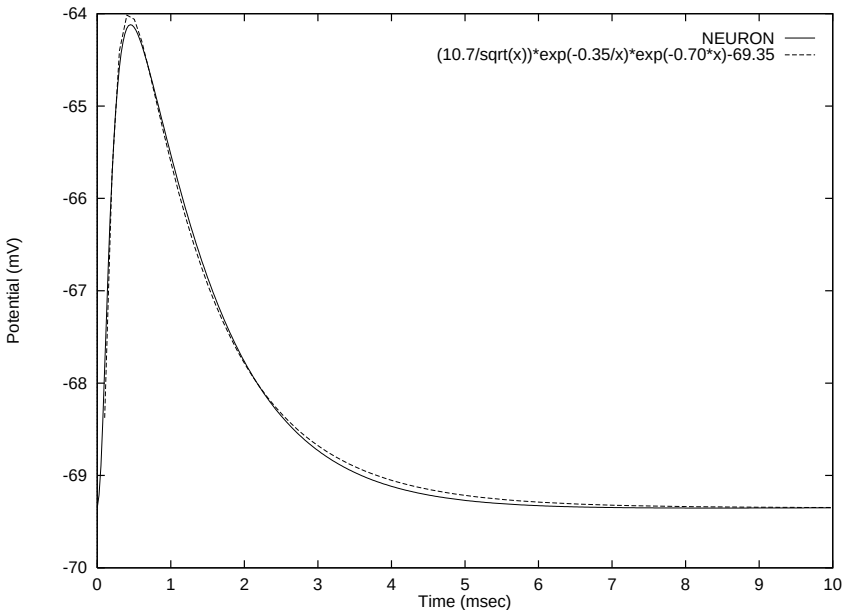

Figure 3.3: Comparison of PSP traces: Simulation on NEURON v2.0 versus Closed form solution.

The results of the simulation experiments that are presented in Chapter 7 are based on a model of a neuron, the membrane potential of which is computed as a linear summation of the above noted closed form solution to passive conductance of potential across individual dendrites. It should, however, be noted that the model of the neuron that we formulate and analyze in this thesis is not so constrained. The potential in the simulation experiments is computed as a linear summation for reasons of tractability. Moreover, as will become clear in Chapters 8 and 9, this issue does not play a significant role in the determination of the generic qualitative dynamics of systems of neurons.

3.5 Generation and Conduction of Action Potentials

If the cell membrane is depolarized (the membrane potential is driven towards 0 mV by injecting a current) by a critical amount, it generates a large but brief (≈ 1 msec) active response known as an *action potential* or *spike*. The membrane potential at which the action potential is triggered varies from -55 to -45 mV (depending on the morphological class of the neuron) and is called the *threshold*. The action potential is generated in an all-or-none fashion; increase in current strength (to depolarize the membrane) above the threshold does not increase the amplitude of

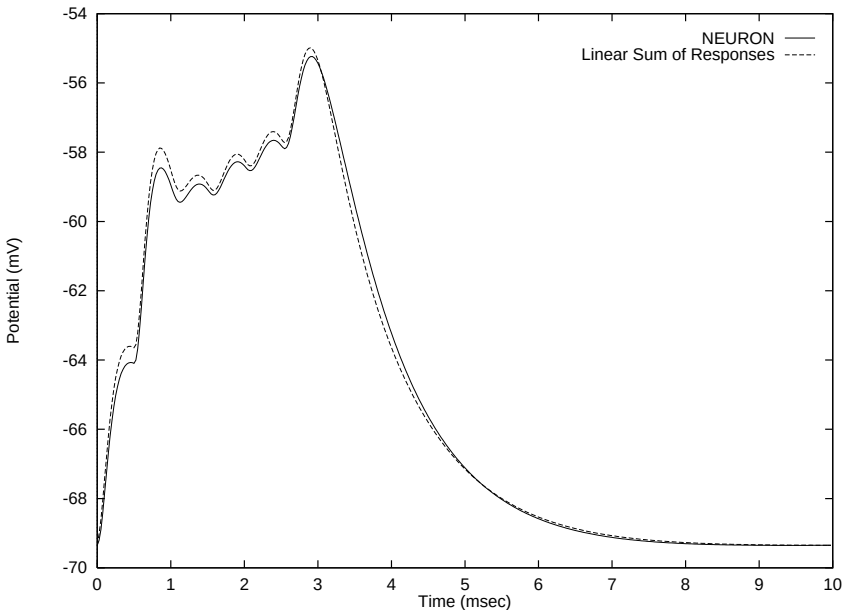

Figure 3.4: Comparison of PSP integration: Simulation on NEURON v2.0 versus Linear summation of individual solutions.

the action potential or change its shape (Adrian & Zotterman, 1926). The action potential not only eliminates the resting potential (at ≈ -60 mV) but actually reverses the membrane potential for an instant, raising it to approximately $+55$ mV. Upon reaching this peak, the potential rapidly repolarizes to a value below the resting potential in a process referred to as *afterhyperpolarization.* Following afterhyperpolarization, the potential gradually (over several msec) decays to the resting level. Unlike the passive conductance of PSP's described in the previous section, the action potential is conducted without any loss of amplitude.

The generation of an action potential is the result of a dramatic, albeit transient, increase in the ionic conductance of the membrane (an approximately forty-fold increase resulting from the activation of voltage sensitive ionic channels). The initial increase in the ionic conductance during the action potential is due to a sudden reversal in the permeability characteristics of the membrane; it temporarily becomes more permeable to Na^+ ions than to K^+ ions. Depolarization of the membrane increases Na^+ permeability, producing an influx of Na^+ ions into the cell and causing further depolarization, which increases Na^+ permeability even more. This catastrophic event, known as Na^+ current *activation*, eventually reverses the membrane potential.

The sudden reversal of the membrane potential is, however, transient. The progressive depolarization described above shuts off the Na^+ permeability in due course, a process labeled

sodium current *inactivation*. This is accompanied by an increase in the already high K^+ permeability, a process labeled *delayed rectification*. Na^+ current inactivation and delayed rectification together result in the afterhyperpolarization of the membrane potential. At this point the repolarization of the membrane potential leads to the *deactivation* of the K^+ and Na^+ channels and the membrane potential gradually returns to its resting level. The removal of the depolarization also leads to the *deinactivation* of the Na^+ channels and the membrane is ready for the next action potential.

Immediately following an action potential there is a time interval of approximately 1 msec during which no stimulus, however strong, can elicit a second action potential. This is called the *absolute refractory period*, and is largely mediated by the inactivation of the sodium channels. After the absolute refractory period there is a *relative refractory period* during which an action potential can be evoked only by a stimulus of much larger amplitude than the normal threshold value, a condition that results from the persistence of the outward K^+ current.

The above process is modeled by replacing the partial differential equation 3.5 derived in the previous section to model passive conductance of potential across dendrites, by the more general equation

$$i_m = c_m \frac{\partial v_m}{\partial t} + g_{\text{Na}}(v_m - V_{\text{Na}}) + g_{\text{K}}(v_m - V_{\text{K}}) + g_{\text{L}}(v_m - V_{\text{L}}), \tag{3.10}$$

where $g_.$'s are the voltage sensitive membrane conductances for the respective ions and $V_.$'s their respective equilibrium potentials (L denotes leakage and is a variable that represents Cl^- and all other organic ions lumped together). Furthermore, the relation between the various conductances and the membrane potential is modeled based on empirical data. One such set of equations (Hodgkin & Huxley, 1952a-d; Hodgkin, Huxley & Katz, 1952),

$$i_m = c_m \frac{\partial v_m}{\partial t} + \bar{g}_{\text{Na}} m^3 h (v_m - V_{\text{Na}}) + \bar{g}_{\text{K}} n^4 (v_m - V_{\text{K}}) + \bar{g}_{\text{L}}(v_m - V_{\text{L}}), \tag{3.11}$$

$$\frac{dm}{dt} = \alpha_m(1 - m) - \beta_m m, \tag{3.12}$$

$$\frac{dh}{dt} = \alpha_h(1 - h) - \beta_h h, \tag{3.13}$$

$$\frac{dn}{dt} = \alpha_n(1 - n) - \beta_n n, \tag{3.14}$$

called the Hodgkin-Huxley equations, agrees well with physiological data. $\alpha_m, \beta_m, \alpha_h, \beta_h, \alpha_n$ and β_n are functions of v_m given as

$$\alpha_m = \frac{0.1(v_m + 25)}{e^{\frac{v_m+25}{10}} - 1}, \qquad \beta_m = 4e^{\frac{v_m}{18}}, \tag{3.15}$$

$$\alpha_h = 0.07e^{\frac{v_m}{20}}, \qquad \beta_h = \frac{1}{e^{\frac{v_m+30}{10}} + 1}, \tag{3.16}$$

$$\alpha_n = \frac{0.01(v_m + 10)}{e^{\frac{v_m+10}{10}} - 1}, \qquad \beta_m = 0.125e^{\frac{v_m}{80}}. \tag{3.17}$$

There have been several attempts to reduce the complexity of these equations while maintaining their qualitative properties (Fitzhugh, 1961; Nagumo, Arimoto & Yoshizawa, 1962). The prospect of a closed form solution to the above process, however, remains bleak.

3.6 Beyond the Basic Model

The true electrophysiology of neurons in the central nervous system (CNS) is substantially more complex than the basic electrophysiology elucidated in the previous sections. The variations in the electrophysiology of morphologically distinct classes of neurons in the CNS allows them to operate in different firing modes. Several of these modes have been cataloged and their electrophysiological basis identified.

The simplest mode of behavior (manifest by the model described in the previous sections) is called “regular-firing” and is characterized by the generation of action potentials one at a time. Motor neurons in the brainstem and the spinal cord are examples of neurons that lie in this category. Such neurons also exhibit a brand of linearity of behavior: the longer the depolarization of their somas, the longer their discharge, and the more intense the depolarization, the higher the frequency of their discharge.

A slight modification of this basic behavior is characterized by neurons that, upon sustained depolarization of their somas, generate spike trains that exhibit a marked decay in spike frequency over time, a process known as *spike frequency adaptation*. Examples of cells that discharge in this manner are cortical and hippocampal pyramidal neurons (McCormick et al., 1985; Connors & Gutnick, 1990). The basis for this behavior has been identified to be the activation of a slow K^+ afterhyperpolarization current that builds up over several action potentials.

A third category of behavior is characterized by an intrinsic propensity to generate bursts of spikes instead of single action potentials. Thalamic relay neurons, some pyramidal and stellate cells, and neurons in the inferior olive spike in this manner (Connors & Gutnick, 1990). The clusters of action potentials are generated by the activation of specialized Ca^{2+} currents that, by virtue of their slow kinetics, allow the membrane potential to remain depolarized for sufficiently long periods of time so as to generate several regular $Na^{+} - K^{+}$-dependent action potentials.

Yet another category of behavior is characterized by relatively short duration (< 1 msec) action potentials that discharge at relatively high frequencies ($> 300\ Hz$). Inhibitory interneurons in the cortex, the thalamus, and the hippocampus display this kind of behavior (Connors & Gutnick, 1990).

Finally, there is a class of neurons called *pacemaker* neurons that spontaneously generate relatively low frequency ($1 - 10\ Hz$) spike trains. These neurons innervate wide regions of the brain and appear to set the "state" of the entire local network.

It is now well recognized that these diverse behaviors are the result of the wide variety of ionic channels that are present in the neurons in addition to the basic Na^{+} and K^{+} channels described in the previous sections. Some of these channels activate and rapidly inactivate, whereas others do not inactivate. Some are fast acting while others display very slow (> 1000 msec) kinetics. Some are directly activated by variations in the membrane potential while others require second messengers for activation.

Several of these ionic channels have been identified, and the search and classification of others remains an integral part of ongoing research in the field.

3.7 Synaptic Transmission

The effects of an action potential arriving at a presynaptic terminal is transferred to the postsynaptic neuron through a chemically mediated process. Currents for excitatory (encouraging the neuron to spike) and inhibitory (discouraging the neuron to spike) synaptic actions are generated in the postsynaptic neuron via changes in membrane conductance (Fatt & Katz, 1951, 1953). The biophysical processes involved in several aspects of synaptic transmission are not yet completely understood, and the phenomenon continues to inspire intense research.

Synaptic transmission is fairly rapid (synaptic delays range from 0.3 to 0.5 msec). The nervous system achieves such speeds by confining transmitter molecules to *synaptic vesicles* (rather than leaving them free floating in the plasma) that are docked in specialized sites along the presynaptic membrane called *active zones*.

The depolarization that results from the arrival of an action potential at a synaptic terminal leads to the activation of Ca^{2+} channels that are strategically co-located with the synaptic vesicles in the active zones. The opening of the Ca^{2+} channels causes an intense rise in Ca^{2+} ion concentration in the immediate vicinity of the channels, thus creating Ca^{2+} rich fields known as *microdomains*.

The intense rise in Ca^{2+} ion concentration triggers the fusion of the synaptic vesicles with the plasma membrane (a process known as *exocytosis* that is believed to be mediated by several calcium-binding proteins) which results in the transmitter molecules being released into the *synaptic cleft*. The released transmitter molecules drift across the cleft and bind with receptors on the postsynaptic membrane. This leads to opening/closing of various chemically gated Na^+ and K^+ channels on the postsynaptic membrane giving rise to a postsynaptic current (PSC). The resultant effect can be one of an excitatory postsynaptic potential or one of an inhibitory postsynaptic potential.

It was discovered around fifty years ago that the release of synaptic vesicles from their respective sites in the presynaptic terminal takes place in a stochastic manner (Fatt & Katz, 1951). This led to the postulation of the *quantal hypothesis* (del Castillo & Katz, 1954), according to which neurotransmitter molecules are released from single presynaptic terminals in quantal packets corresponding to synaptic vesicles, and the strength of a synaptic transmission is the product of three parameters: *Strength* $= pnq$, where p is the probability of triggering quantal release during a presynaptic action potential, n is the number of readily releasable quanta available (which depends upon the number of release sites in the presynaptic terminal), and q is the response (which can be excitatory or inhibitory) of the postsynaptic neuron to a single quantum of neurotransmitter.

Excitatory postsynaptic potentials (EPSP's) are generated by a sudden increase in g_{Na} often accompanied by an increase in g_{K}. These increases are simultaneous and not sequential.

Moreover, the increase in g_{Na} is not voltage dependent as in the case of action potentials. Because g_{Na} and g_{K} increase simultaneously, the EPSP is a compound potential that lies midway between E_{Na} ($+55$ mV) and E_{K} (-75 mV). In other words, an excitatory synaptic action drives the membrane potential from its resting value (-60 mV) past the threshold (-45 mV) to a value of approximately -10 mV (that is, about 50 mV above resting potential).

Inhibitory postsynaptic potentials (IPSP's) are generated by sudden increases in g_{K} and g_{Cl}. IPSP's inhibit neurons from firing in two different ways. First, by increasing the conductance to Cl^-, synaptic inhibition increases the overall conductance of the membrane. Any EPSP generated by a postsynaptic current is subsequently lowered. This process is labeled *shunting* or *short circuiting*. Second, inhibitory synaptic action due to increased conductance usually hyperpolarizes the membrane, moving it further away from threshold.

3.8 The Neuron-Synapse Ensemble: Should it be Modeled as a Deterministic or a Stochastic Unit?

Modeling any physical system entails making choices. The first decision that confronts our undertaking is whether the neuron-synapse ensemble ought to be modeled as a stochastic or a deterministic unit.[5] We have elected to pursue a deterministic model. In the remainder of this section we present the reasons that led to this choice.

Whether the neuron-synapse ensemble should be modeled as a stochastic or a deterministic unit is an issue that is closely related to the question of the reliability of the nervous system. There is now mounting evidence that the mammalian (as well as others) nervous system is highly reliable. For example, responses to the arrival of *single* photons in retinal receptor cells have been shown to be highly reproducible (Baylor, Lamb & Yau, 1979; Baylor, Nunn & Schnapf, 1984). Based on data pertaining to the spontaneous noise in these cells, it has been demonstrated that the limits to the reliability of night vision are set by the photoreceptor cells, that is, little additional noise is introduced by subsequent neuronal processing (Barlow, 1988; Donner, 1989; Bialek & Owen, 1990; Rieke, Owen & Bialek, 1991). Similar results have been reported for spatial discrimination (Parker & Hawken, 1985) and somatosensory tasks (Valbo, 1995).

[5] At issue is whether a fixed input into a neuron should produce a fixed output, or a variable output based on some probability distribution.

The neuron-synapse ensemble has traditionally been modeled as a stochastic unit for the simple reason that repeated presentation of the same sensory stimulus elicits variable response. This apparent noise can, however, be the result of the ineluctable noise in the stimulus itself, as well as information feedback from systems that are not driven by the same stimulus, for example, when recording from the primary and secondary sensory cortex (these areas are of the order of four synapses removed from the sensory receptors). A second reason for the choice has been the apparent stochastic nature of spike train recordings from neurons in the cortex. However, as shall be demonstrated in Chapter 7, such recordings can also be elicited from a deterministic system.

If the neuron-synapse ensemble is indeed an unreliable unit (a case that warrants the use of a stochastic model for the unit), there are two possible courses that the nervous system can adopt in order to maintain reliability: (i) reduce the noise-induced variance in the signal by choosing the number of times the neuron spikes in a relatively large time window as the relevant variable (rate coding), or (ii) reduce the variance by choosing the instantaneous spike rate averaged over a large population of neurons as the relevant variable (population coding).

In order for rate coding to be a viable scheme, modulations in the signal must be slow compared to the average spiking rate of the neuron. It has, however, been shown that not only do modulations in natural signals occur over time scales comparable to typical interspike intervals (ISI's) recorded in the cortex, but also that behavioral decisions are made over the same time scale (for example, sonar detection by bats (Simmons, 1989; Dear, Simmons & Fritz, 1993), bat evasion by moths (Roeder, 1963), preattentive discrimination by monkeys and cats (Knierem & van Essen, 1992; Reid, Soodak & Shapley, 1991), and tactile discrimination by rats (Fee & Kleinfeld, 1994).).

Population coding, on the other hand, can reduce the noise induced variance in the signal significantly only if the activity of the ensemble of neurons from which the average spiking rate is computed, is uncorrelated. There is, however, strong evidence that this is not the case (Zohary, Shadlen & Newsome, 1994). Although there exist more robust schemes (such as maximum likelihood estimates) that can extract the appropriate variable under such conditions, they are based on the availability of the entire joint probability distribution of the spike rates of the neurons. Over the time scales under consideration, these schemes approach temporal coding

(where spike times are relevant).

It is now widely held that cortical neurons are quite reliable. Experimental results have demonstrated that cortical neurons are capable of extraordinary precision (to within ≈ 1 msec) when transforming injected currents into spike trains (Mainen & Sejnowski, 1995). Propagation of action potentials on axons has likewise been shown to be relatively noise-free (Lass & Abeles, 1975).

Noise and transmission failure at synapses is, however, a hotly debated issue. Some in the field have reported that excitatory synapses in the cerebral cortex and the hippocampus are extremely unreliable; the value of p (from the equation *Strength* $= pnq$) in response to a single spike has been estimated at 10% or lower (Rosenmund, Clements & Westbrook, 1993; Hessler, Shirke & Malinow, 1993; Allen & Stevens, 1994; Stevens & Wang, 1994, 1995; Dobrunz & Stevens, 1997), whereas others have reported that synapses in the same areas are quite reliable (p is estimated upwards of 80%) (Thomson, Deuchars & West, 1993; Markram, Lübke, Frotscher, Roth & Sakmann, 1997; Larkman, Jack & Stratford, 1997). In an attempt to explain this disparity Hardingham & Larkman (1998) have demonstrated that quantal transmitter release is temperature dependent in cortical synapses, and that experiments performed at room temperature could lead to an exaggerated impression of their unreliability.

Finally, the notion that spike timing across an ensemble of cells plays an important role in encoding various aspects of a stimulus is gaining support from experiments in a variety of systems such as locust olfaction, electric fish electrosensation, cat and monkey vision, audition and olfaction (Chung, Raymond & Lettvin, 1970; Freeman, 1975; Strehler & Lestienne, 1986; Abeles, 1990; Richmond, Optican & Spitzer, 1990; Krüger, 1991b; Bialek, Rieke, de Ruyter van Steveninck & Warland, 1991; Bialek & Rieke, 1992; Bair, Koch, Newsome & Britten, 1994; Singer & Gray, 1995; Bair & Koch, 1996; Decharms & Merzenich, 1996; Laurent, 1996; Wehr & Laurent, 1996; Gabbiani, Metzner, Wessel & Koch, 1996; Lisman, 1997).

The apparent contradiction between evidence of unreliable synaptic transmission and that of reliable spike trains may be the outcome of short term synaptic plasticity. That the strength of synapses change in a history dependent manner during short term plasticity is well documented (Magleby, 1987; Zucker, 1989; Fisher, Fischer & Carew, 1997; Dobrunz & Stevens, 1997; Markram & Tsodyks, 1996; Tsodyks & Markram, 1997; Abbott, Varela, Sen & Nelson,

1997; Varela, Sen, Gibson, Fost, Abbott & Nelson, 1997; Zador & Dobrunz, 1997). Since most central synapses have very few release sites (n ranges from 1 to 5 (Raastad, Storm & Andersen, 1992; Gulyas, Miles, Sik, Toth, Tamamaki & Freund, 1993; Bolshakov & Siegelbaum, 1995; Schikorski & Stevens, 1997)), it is conceivable that in order to achieve a rapid and wide range of efficacy, synapses modulate transmission in a deterministic history dependent manner.

Since the temporal sequence of ISI's is abstracted away in a stochastic model, there is little hope that such a model would shed light on all aspects of information processing in a neuronal system. Second, while thermodynamic noise in the guise of random miniature postsynaptic potentials do exist, their mean amplitude is at least an order of magnitude smaller than the mean amplitude of the postsynaptic potential elicited by the arrival of a spike at a synapse. The impact of such noise on the dynamics of the system is best identified by contrasting the dynamics of a noise-free model to that of a model augmented with the appropriate noise. We have therefore chosen to investigate a deterministic model for the neuron.

3.9 Summary

The neuron constitutes the basic building block of the nervous system. In this chapter, we have briefly described the biophysical processes that underlie the dynamics of a neuron, including the generation of the membrane potential, the passive conduction of synaptic input across the dendritic arborization, the generation of the action potential and the transmission of the action potential across a synapse.

While we do not deny that the neuron-synapse ensemble, like any other physical device, must admit some noise, we have argued that in the light of the evidence supporting the relevance of spike timing in information representation and transmission, it is logical to begin with the analysis of a deterministic system.

Chapter 4

Model of the Neuron

In the previous chapter we presented a brief description of the biophysics that underlies the dynamics of a neuron, and argued in favor of a deterministic model for the neuron-synapse ensemble. In this chapter we formulate an abstract, deterministic model for the biological neuron. Our objective is to construct a model that is sufficiently realistic while keeping it amenable to formal analysis. We begin by enumerating the set of assumptions on which the model is based.

4.1 Assumptions

Our model of the biological neuron is based on the following four observations.

(1) The biological neuron, like any other physical device, is a finite precision machine—the depolarization at the soma that elicits an action potential is of a finite range ($\mathcal{T} \pm \epsilon$) and not a precise value ($\mathcal{T}$).

(2) The effect of a synaptic impulse (that results from the arrival of an afferent spike) at the soma has the characteristic form of an abrupt increase or decrease in potential followed by a longer *exponential-like* decay toward the resting level.

(3) The postspike elevation of the threshold that may be modeled as the inhibitory effect of an efferent spike also decays after a while at an *exponential* rate, and

(4) The inter-spike intervals (ISI's) of any given neuron is *bounded from below* by its absolute refractory period, r, that is, no two spikes originate closer than r in time.

Based on these, we construct our model of the neuron as follows. (Figure 4.1 is provided as a visual aid to complement the formal presentation below. The various aspects of the diagram are explained in the caption.)

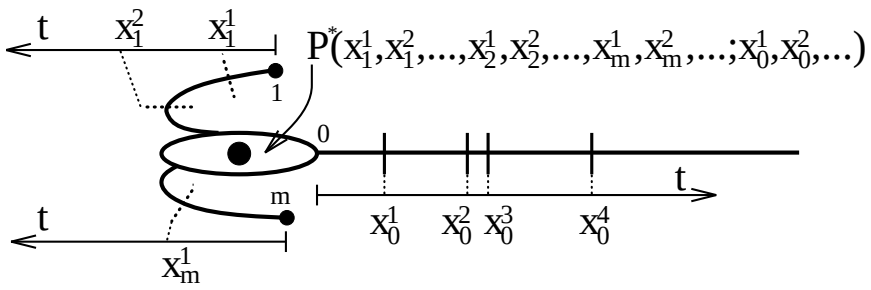

Figure 4.1: Schematic diagram of a neuron that depicts the soma, axon, and two synapses on as many dendrites. The axes by the synapses and the axon denote time (with respective origins set at *present* and the direction of the arrows indicating *past*). Spikes on the axon are depicted as solid lines. Those on the dendrites are depicted as broken lines, for, having been converted into graded potentials, their existence is only abstract (point objects indicating the time of arrival of the spike).

4.2 The Model

(i) **Spikes**: Spikes are the sole bearers of information. They are identical except for their spatiotemporal location.

Spikes are defined as point objects. Although action potentials are not instantaneous, they can always be assigned occurance times, which may, for example, be the time at which the membrane potential at the soma reached the threshold $\mathcal{T}$.

(ii) **Membrane Potential**: For any given neuron we assume an *implicit, C^∞, everywhere bounded* function $P^*(\vec{x}_1, \vec{x}_2, ..., \vec{x}_m; \vec{x}_0)$ that yields the *current* membrane potential at its soma.

The subscripts $i = 1, ..., m$ in the parameters defining the domain of the function represent the afferent synapses, and $\vec{x}_i = \langle x_i^1, x_i^2, ..., x_i^j, ...\rangle$ is a *denumerable* sequence of variables that represent, for spikes arriving at synapse i since infinite past, the time lapsed since their arrivals. In other words, each x_i^j for $i = 1, ..., m$ reports the time interval between the present and the time of arrival of a distinct spike at synapse i. Finally, $\vec{x}_0$ is a denumerable sequence of variables that represent, in like manner, the time lapsed since the departure of individual spikes generated at the soma of the neuron.

To repeat an example introduced in Chapter 2, $\vec{x}_5 = \langle 17.4, 4.5, 69.1, 36.0, 83.7, ...\rangle$ conveys that at synapse #5 of the neuron, a spike arrived 17.4 msec ago, one arrived 4.5 msec

ago, one 69.1 msec ago, one 36.0 msec ago, one 83.7 msec ago, and so forth.

$P^*: \mathbb{R}^\infty \rightarrow \mathbb{R}$ accounts for the entire spatiotemporal aspect of the neuron's response to spikes. All information regarding the strength of afferent synapses, their location on the dendrites, and their modulation of one another's effects at the soma is implicitly contained within $P^*(\cdot)$. So is the exact nature of the postspike hyperpolarization that gives rise to both the absolute and the relative refractory periods.

In order for it to be well-defined, either the domain of $P^*(\cdot)$ should be restricted to $0 \leq x_i^1 \leq x_i^2 \leq ...$ for all i, or $P^*(\cdot)$ should be constrained to be symmetric with respect to $x_i^1, x_i^2, ...$ for all i.

(iii) **Effectiveness of a Spike**: After the effect of a spike at the soma of a biological neuron has decayed below $\frac{\epsilon}{C(m+1)}$, where ϵ is the range of error of the threshold, $C > 1$ an appropriate constant (defined below), and m the number of afferent synapses on the cell, its effectiveness on the neuron expires.

This inference is based on the observations that (a) the biological neuron is a finite precision machine, (b) the total effect of a set of spikes on the soma is almost linear in their individual effects when such effects are small ($\approx \frac{\epsilon}{C(m+1)}$), and (c) owing to the exponential nature of the decay of the effects of afferent as well as efferent spikes and the existence of a refractory period, a quantity $\mu < 1$ can be computed such that the residual effect of the afferent spikes that have arrived at a synapse, whose effects on the soma have decayed below $\frac{\epsilon}{C(m+1)}$ (and that of the efferent spikes of the neuron satisfying the same constraint) is bounded from above by the infinite series $\frac{\epsilon}{C(m+1)}(1 + \mu + \mu^2 + ... + \mu^k + ...)$. Setting $C > \frac{1}{1-\mu}$ then guarantees that each such residual is less than $\frac{\epsilon}{(m+1)}$.

This argument, in essence, demonstrates that the period of effectiveness of a spike since its impact at a given afferent synapse or departure after being generated at the soma is *bounded from above*.[1]

We model this feature by imposing the following restrictions on P^*.

[1]This does not necessarily imply that the neuron has a bounded memory of events. Information can be transfered from input spikes to output spikes during the input spikes' period of effectiveness.

1. $\forall i = 0, ..., m$ and $\forall j$, $\exists \tau_i$ such that $\forall t \geq \tau_i$ $\frac{\partial P^*}{\partial x_i^j} \mid_{x_i^j = t} = 0$ irrespective of the values assigned to the other variables.
2. $\forall i = 0, ..., m$ and $\forall j$, $\forall t \leq 0$ $\frac{\partial P^*}{\partial x_i^j} \mid_{x_i^j = t} = 0$ irrespective of the values assigned to the other variables.
3. $\forall i = 0, ..., m$ and $\forall j$, $P^*(\cdot) \mid_{x_i^j = 0} = P^*(\cdot) \mid_{x_i^j = \tau_i}$ all other variables held constant at any values.
4. If $\forall i = 0, ..., m$ and $\forall j$ $x_i^j = 0$ or τ_i, then $P^*(\cdot) = 0$.

The first criterion enforces that the sensitivity of $P^*(\cdot)$ to spike x_i^j expires after time τ_i. It therefore follows that if for every i there exists an n_i such that $j > n_i \Rightarrow a_i^j \geq \tau_i$, then $P^*(\vec{a}_1, \vec{a}_2, ..., \vec{a}_m; \vec{a}_0) = P^*(\vec{a}'_1, \vec{a}'_2, ..., \vec{a}'_m; \vec{a}'_0)$ where each $\vec{a}'_i$ is derived from the corresponding $\vec{a}_i$ by setting all values after index n_i to τ_i.

The second criterion results from $P^*(\cdot)$ being C^∞ and $\frac{\partial P^*}{\partial x_i^j} \mid_{x_i^j < 0} = 0$ (a spike that has not yet arrived at an afferent synapse can have no effect on the membrane potential, and likewise, a spike that has not yet been generated at the soma can not elicit a postspike hyperpolarization).

The third criterion enforces that all else being equal, the membrane potential at the soma is the same whether an afferent spike has just arrived or its effectiveness has just expired, and in the case of an efferent spike whether it has just been generated or its inhibitory effect on the soma has just expired.

The fourth criterion enforces that the resting state of the soma is set at 0.

Note that the time bound of 500 msec introduced in an example in Chapter 2 corresponds to the quantity $\max_{i=0}^{m}\{\tau_i\}$ here.

(iv) **Finite dimensionality**: The function characterizing the membrane potential can, as a result, be defined over a finite dimensional space.

This is based on the observation that at any afferent synapse $i = 1, ..., m$, spikes arrive at intervals bounded from below by r_i (the absolute refractory period of the neuron presynaptic to i), and for $i = 0$ spikes are generated at the soma of the neuron at intervals

bounded from below by r_0 (the absolute refractory period of the neuron in question). Consequently, at most $n_i = \lceil \tau_i / r_i \rceil$ variables can have values less than τ_i.

Based on (iii) above, we can define,

$$P(x_1^1, ..., x_1^{n_1}, x_2^1, ..., x_2^{n_2}, ..., x_m^1, ..., x_m^{n_m}; x_0^1, ..., x_0^{n_0}) =$$
$$P^*(\langle x_1^1, ..., x_1^{n_1}, \tau_1, \tau_1, ...\rangle, \langle x_2^1, ..., x_2^{n_2}, \tau_2, \tau_2, ...\rangle, ...,$$
$$\langle x_m^1, ..., x_m^{n_m}, \tau_m, \tau_m, ...\rangle; \langle x_0^1, ..., x_0^{n_0}, \tau_0, \tau_0, ...\rangle) \quad (4.1)$$

and use $P(\cdot)$ instead of $P^*(\cdot)$ to represent the current membrane potential.

We must mention here that the definition of P^* assumes that spikes have been arriving at each synapse and have been leaving the soma since time $t = -\infty$. If the number of spikes on any synapse or the number of efferent spikes is finite over the time $(-\infty, 0)$, a denumerable set of dummy variables can be introduced to extend the function's domain to $\mathbb{R}^\infty$. For any such dummy variable x, $\frac{\partial P^*}{\partial x}$=0 is consistent with the constraints imposed on P^*.

(v) **Threshold and Refractoriness**: A simple model is assumed for the generation of a spike at a soma, that is, a spike is generated when $P(\cdot) = \mathcal{T}$ and $\frac{dP(\cdot)}{dt} \geq 0$.

Since $P(\cdot)$ is C^∞, the postspike hyperpolarization can not be instantaneous. $P(\cdot) = \mathcal{T}$ is crossed twice—once when the spike is generated and once when the inhibitory effect of the spike comes into play. The second constraint $\frac{dP(\cdot)}{dt} = \sum_{i,j} \frac{\partial P(\cdot)}{\partial x_i^j} \frac{dx_i^j}{dt} \geq 0$ ensures that the neuron does not spike during the membrane potential's downward journey.

$\mathcal{T}$ is assumed to be a constant. It should, however, be noted that a more general criterion of the form $P(\cdot) = \mathcal{T}(\cdot)$, where $\mathcal{T}$ is a function rather than a constant, can be transformed into the form $P(\cdot) = \mathcal{T}$ if the parameters of $\mathcal{T}(\cdot)$ are a subset of those of $P(\cdot)$.

The above model of the neuron does not insist on a specific membrane potential function, only that the particular function possess certain qualitative properties. By retaining this level of generality, we can pose questions that are more basic, such as to what extent are the dynamics of a neuronal system affected if the potential function $P(\cdot)$ is replaced by any arbitrary function that is unimodal with respect to all variables, and at the same time satisfies all the constraints

(items (ii), (iii), and (v) above). Furthermore, making a model more specific by resorting to explicit functions is a much easier task than making it more general.

4.3 Evaluating the Model

In order to assess the scope of the model introduced in the previous section, we reexamine the biophysical processes that underlie the dynamics of a biological neuron. These processes can, with a few exceptions, be classified under two mutually interacting classes: synaptic transmission and postsynaptic processes. We explore each class separately.

Synaptic modulations can, in general, be categorized as short-term or long-term. Long-term variations in the strength of synapses, which would translate into evolving potential functions, are not modeled in our framework. As was noted in Chapter 3, the biophysical processes that induce such changes are not yet completely understood, and the phenomenon continues to inspire intense research. With regard to short-term changes (including those that lead to transmission failure), however, the model is more robust. If future research determines that such changes are in fact a deterministic function of a bounded history of the pre- and postsynaptic activity of the neuron, then such changes are already accounted for in our model.

Postsynaptic effects of spikes are mediated by the activation of ionic currents. In Chapter 3 we described how synaptic potentials are passively conducted across dendrites. Since the process does not induce changes in the properties of ionic channels, the sole equilibrium state of the membrane is its resting state. Such a system has a fading memory of synaptic events, and can be modeled in our framework.

We also noted that the diverse behavior of the physiologically distinct classes of neurons in the brain is the outcome of the assortment of ionic channels that pervade the membranes of such neurons. Whereas some of these ionic channels are activating and self-inactivating, others are noninactivating. The corresponding currents produced are therefore either transient or persistent, for example, the Na^+ current ($I_{Na,t}$) underlying action potential generation is transient whereas the K^+ current (I_K) underlying the same process is persistent. Individual ionic channels that generate transient currents, as well as groups of ionic channels that operate in tandem to first destabilize and then return the membrane to its previous state of equilibrium, can be

modeled in our framework. Hence, neurons that on depolarization are subject to the generation of dendritic spikes, can be modeled in our framework. Likewise, rhythmically bursting neurons whose mode of activity is engendered by the activation of low-threshold Ca^{2+} currents can be modeled in our framework because the Ca^{2+} currents are self-inactivating. There are however other persistent currents, such as $I_{\text{Na,p}}$ that give rise to plateau potentials, that can not be modeled in our framework. This is so because membranes with such channels have multiple equilibrium states and therefore it becomes possible, in principle, for a spike to have an everlasting effect on the membrane potential.

Another dimension along which our model remains some distance from an accurate depiction of the biological neuron concerns diffuse processes. There are several non-localized processes in the brain, such as the influence of neuromodulators (molecules that are widely distributed in the system and spread into neurons to affect their internal processes over extended periods of time) that cannot be modeled in our framework. We can only hope that not much is lost in terms of the salient behavior of the system at our leaving out such details.

4.4 Summary

A biological neuron is a device that transforms multiple series of action potentials arriving at its various afferent synapses into a series of action potentials on its axon. At the heart of this transformation lies the quantity P^*, the membrane potential at the soma of the neuron. Effects of the afferent spikes that have arrived at the various synapses of the neuron, as well as those of the efferent spikes that have departed since being generated at its soma, interact nonlinearly to generate this potential. The efferent spikes generated by the neuron coincide with the times at which this potential reaches the threshold of the neuron.

It was demonstrated in this chapter, based on a set of realistic assumptions about the biological neuron, that it can reasonably be assumed that the individual effects of afferent as well as efferent spikes on the membrane potential at the soma of a neuron decay to 0 within a *bounded* period of time. It follows from the existence of the absolute refractory period of a neuron that at any given moment in time, there are at most a bounded number of most recent spikes (afferent as well as efferent) that are effective on the membrane potential at the soma of the neuron.

A function $P(\cdot)$ over a finite dimensional space (the axes representing the finite set of recent afferent as well as efferent spikes mentioned above) that satisfies a set of assumptions that embody characteristics of the membrane potential at the soma of a biological neuron is used to model the neuron. The temporal sequence of spikes generated by the neuron is derived by identifying the times at which $P(\cdot) = \mathcal{T}$ and $\frac{dP(\cdot)}{dt} \geq 0$, where $\mathcal{T}$ represents the threshold of the neuron.

Chapter 5

Background: Manifold Theory and Dynamical Systems Analysis

In Chapter 6, we construct an abstract dynamical system that models *systems* of biological neurons. The system is based on the model of the neuron delineated in the previous chapter. Following the presentation of results of simulation experiments in Chapter 7, we analyze the dynamics of the system in Chapters 8 and 9. In order to characterize the system formally and analyze its dynamics, we employ the vocabulary of real analysis, manifold theory, and dynamical systems analysis (the system is formulated as a dynamical system on a manifold).

In this chapter, we present primers on basic topology, manifold theory, and dynamical systems analysis. The material presented here is intended to ease comprehension of the chapters that follow. For a more extensive exposition, the reader should consult (Boothby, 1986) on Riemannian geometry and (Arrowsmith & Place, 1990) on dynamical systems analysis.

Whereas the sections on topology and manifold theory are drawn from standard bodies of work, the section on dynamical systems analysis features variations on standard definitions. A non-standard definition of a *basic set* is proposed that facilitates the extension of several concepts to dynamical systems defined by discontinuous maps.

5.1 Basic Topology

We conduct a rapid survey of several basic concepts in topology in this section. Our objective is to familiarize the reader with those concepts that are applied in the upcoming chapters. The material presented here is not intended to serve as an introduction to the subject of topology.

5.1.1 Metric Spaces

Definition 5.1.1 *A set $\mathbb{X}$ of elements referred to as* points*, is called a* metric space *if for every two points p and q in $\mathbb{X}$ there exists an associated real number $d(p, q)$ called the* distance *from*

p to q that satisfies the following properties.

1. $\forall p, q$ *if* $p \neq q$ *then* $d(p, q) > 0$, *and* $\forall p\ d(p, p) = 0$.

2. $\forall p, q\ d(p, q) = d(q, p)$.

3. $\forall p, q, r\ d(p, q) \leq d(p, r) + d(r, q)$.

The function $d(\cdot, \cdot)$ is called the metric.

The most common example of a metric space is $\mathbb{R}^n$ (the set of all n-tuples of reals) with distance between $\mathbf{x} = \langle x_1, ..., x_n \rangle$ and $\mathbf{y} = \langle y_1, ..., y_n \rangle$ defined as $\sqrt{\sum_{i=1}^{n}(x_i - y_i)^2}$.

Definition 5.1.2 *An* ϵ-neighborhood *(for some $\epsilon > 0$) of a point p in $\mathbb{X}$ is the set $U_\epsilon(p)$ of all points q in $\mathbb{X}$ that satisfy $d(p, q) < \epsilon$.*

The open ball, $B_\epsilon(\langle x_1, ..., x_n \rangle) = \{\langle y_1, ..., y_n \rangle \mid \sqrt{\sum_{i=1}^{n}(x_i - y_i)^2} < \epsilon\}$, is an example of an ϵ-neighborhood in $\mathbb{R}^n$.

Definition 5.1.3 *A point p is said to be a* limit-point *of a set E in $\mathbb{X}$ if every ϵ-neighborhood of p contains a point $q \neq p$ such that $q \in E$.*

Definition 5.1.4 *A point p is said to be an* interior-point *of a set E in $\mathbb{X}$ if there exists $U_\epsilon(p)$, an ϵ-neighborhood of p, such that $U_\epsilon(p) \subset E$.*

Definition 5.1.5 *A set E is said to be* closed *in (or relative to) $\mathbb{X}$ if every limit-point of E belongs to E.*

Definition 5.1.6 *A set E is said to be* open *in (or relative to) $\mathbb{X}$ if every point of E is an interior-point of E.*

It follows that the empty set $\emptyset$ and the entire set $\mathbb{X}$ are both open and closed relative to $\mathbb{X}$. The *segment* $(0, 1) \subset \mathbb{R}$, consisting of all points between but not including 0 and 1, is an example of a set that is open relative to $\mathbb{R}$, and the *interval* $[0, 1] \subset \mathbb{R}$, consisting of all points between and including 0 and 1, is an example of a set that is closed relative to $\mathbb{R}$.

Theorem 5.1.1 *A set E is open in $\mathbb{X}$ if and only if its complement $E^c = \mathbb{X}\backslash E$ is closed in $\mathbb{X}$. Moreover, the union of any* arbitrary *family of open sets in $\mathbb{X}$ is open in $\mathbb{X}$, and the intersection of any* finite *family of open sets in $\mathbb{X}$ is open in $\mathbb{X}$.*

Theorem 5.1.2 *Every ϵ-neighborhood is an open set. It is therefore also known as an* open neighborhood.

5.1.2 Topological Spaces

One may alternatively begin with the fundamental notion of an open set without reference to any metric. The resultant space, although weaker than a metric space, does admit the notion of continuity. An open neighborhood of a point that was hitherto defined by the metric becomes a derived concept in this formulation.

Definition 5.1.7 *A set $\mathbb{X}$ of elements referred to as* points*, is called a* topological space *if there exists an associated system $\mathcal{O}$ of subsets of $\mathbb{X}$ that satisfy the following properties.*

1. *Both $\emptyset$ and $\mathbb{X}$ belong to $\mathcal{O}$.*
2. *The union of any arbitrary family of sets in $\mathcal{O}$ belongs to $\mathcal{O}$.*
3. *The intersection of any finite family of sets in $\mathcal{O}$ belongs to $\mathcal{O}$.*

$\mathcal{O}$ is then said to define a topology *on $\mathbb{X}$, and the sets in $\mathcal{O}$ are called the* open sets *of the topology.*

Definition 5.1.8 *Given any point p in a topological space $\mathbb{X}$, every open set of $\mathbb{X}$ that contains p is called an* open neighborhood *of p.*

Definition 5.1.9 *Given any metric space, the (open) ϵ-neighborhoods of points in the space generate a topology on the space. This topology is said to be* induced by the given metric.

Definition 5.1.10 *Let $\mathbb{X}$ be a topological space (topologized by the system $\mathcal{O}$ of subsets of $\mathbb{X}$) and $\mathbb{Y}$ be a subset of $\mathbb{X}$. A topology can then be defined on $\mathbb{Y}$ as the system $\tilde{\mathcal{O}}$ of subsets of $\mathbb{Y}$ defined as $\tilde{U} \in \tilde{\mathcal{O}}$ if and only if there exists a $U \in \mathcal{O}$ such that $\tilde{U} = U \cap \mathbb{Y}$. $\mathbb{Y}$ is then called a* subspace *of $\mathbb{X}$ and its topology is referred to as the* subspace topology.

Definition 5.1.11 *Let $\mathbb{X}$ be a topological space and $\sim$ an* equivalence *relation on $\mathbb{X}$. Let $[p]$ denote the equivalence class of points $[p] = \{q \in \mathbb{X} \mid q \sim p\}$. Let $\mathbb{X}/\sim$ denote the set of all equivalence classes of points, and $\pi : \mathbb{X} \to \mathbb{X}/\sim$ denote the natural mapping $\pi(p) = [p]$. The topology on $\mathbb{X}/\sim$ in which $U \subset \mathbb{X}/\sim$ is deemed open if and only if $\pi^{-1}(U)$ is open in $\mathbb{X}$, is then referred to as the* standard quotient topology *on $\mathbb{X}/\sim$.*

5.1.3 Compact Spaces

Definition 5.1.12 *Given any set E in a topological space $\mathbb{X}$, an* open cover *of E is a collection $\{U_\alpha\}$ of open subsets of $\mathbb{X}$ such that $E \subset \bigcup_\alpha U_\alpha$.*

Definition 5.1.13 *A set K in a topological space $\mathbb{X}$ is said to be* compact *if every open cover of K contains a* finite *subcover, that is, given any open cover $\{U_\alpha\}$ of K, there exist finitely many indices $\alpha_1, ..., \alpha_n$ such that $K \subset \bigcup_{i=1}^{n} U_{\alpha_i}$.*

Theorem 5.1.3 *Let $K \subset \mathbb{Y} \subset \mathbb{X}$, and $\mathbb{Y}$ be regarded as a subspace of $\mathbb{X}$. Then K is compact relative to $\mathbb{Y}$ if and only if K is compact relative to $\mathbb{X}$.*

Definition 5.1.14 *Given any set E in a metric space $\mathbb{X}$, E is said to be* bounded *if there exists a real number m and a point $q \in \mathbb{X}$ such that for any $p \in E$, $d(p, q) < m$.*

Theorem 5.1.4 (Heine-Borel) *Let K be a closed and bounded subset of $\mathbb{R}^n$. Then K is compact.*

5.1.4 Continuity

Definition 5.1.15 *Let $\mathbb{X}$ and $\mathbb{Y}$ be topological spaces and $f : \mathbb{X} \to \mathbb{Y}$ be a mapping. Then f is said to be* continuous *if the inverse image $V = f^{-1}(U)$ of any open set U in $\mathbb{Y}$, is open in $\mathbb{X}$.*

Definition 5.1.16 *Let $\mathbb{X}$ and $\mathbb{Y}$ be topological spaces and $f : \mathbb{X} \to \mathbb{Y}$ be a bijective (one-to-one and onto) mapping. Then f is said to be a* homeomorphism *if both f and f^{-1} are continuous.*

Definition 5.1.17 *Let $\mathbb{X}$ be a set, $\mathbb{Y}$ a topological space, and $f : \mathbb{X} \to \mathbb{Y}$ a mapping. Then $\mathbb{X}$ can be topologized by defining $V \subset \mathbb{X}$ as open in $\mathbb{X}$ if and only if $V = f^{-1}(U)$ for some open set*

U in $\mathbb{Y}$. This coarsest topology on $\mathbb{X}$ under which f is continuous is called the topology induced *by the mapping f.*

It follows that the subspace topology of $\mathbb{Y} \subset \mathbb{X}$ is the topology induced by the identity mapping, $f : \mathbb{Y} \to \mathbb{X}$, $f(p) = p$.

5.2 Manifold Theory

The content of this section is organized in order of spaces with successively richer structure. We begin with topological manifolds that support the notion of continuity, proceed to differentiable manifolds that support the notion of tangent vectors, and conclude with Riemannian manifolds that support operations such as integration and differentiation of vector fields.

5.2.1 Topological Manifolds

Definition 5.2.1 *An n-*dimensional topological manifold $\mathbb{M}$ *is a topological space that satisfies the following properties.*

1. $\mathbb{M}$ *is Hausdorff, that is, $\forall p, q \in \mathbb{M}$ such that $p \neq q$, there exist open neighborhoods U of p and V of q such that $U \cap V = \emptyset$.*

2. $\mathbb{M}$ *is locally Euclidean of dimension n, that is, $\forall p \in \mathbb{M}$, there exists an open neighborhood U of p such that U is* homeomorphic *to an open set in $\mathbb{R}^n$.*

   The dimensionality of the manifold, n, is represented as dim$(\mathbb{M})$. Each pair $\langle U, \phi \rangle$, where U is an open set in $\mathbb{M}$ and ϕ is a homeomorphism of U onto an open set in $\mathbb{R}^n$, is called a coordinate neighborhood *or a* chart. *The local coordinates of any $p \in U$ is given by $x_1, ..., x_n$, where $\phi(p) = \langle x_1, ..., x_n \rangle$.*

3. $\mathbb{M}$ *is second countable, that is, there exists a countable system of open sets, known as a basis, such that every open set in $\mathbb{M}$ is the countable union of some sets in the basis.*

5.2.2 Differentiable Manifolds

Whereas $\mathbb{R}^n$ was introduced in Section 5.1.1 as a metric space, it can also be viewed as a vector space with the choice of a basis, such as the set of vectors $\mathbf{e_1} = \langle 1, 0, ..., 0 \rangle$,...,$\mathbf{e_n} = \langle 0, ..., 0, 1 \rangle$,

or even as an Euclidean space with the choice of an inner product, such as $(\mathbf{x}, \mathbf{y}) = \sum_{i=1}^{n} x_i y_i$, which incidentally makes $\{\mathbf{e_1}, ..., \mathbf{e_n}\}$ orthonormal. Although the definition of a topological manifold requires $\mathbb{M}$ to be locally Euclidean, $\mathbb{R}^n$ here is regarded merely as a metric space. The following definition of a differentiable manifold employs the vector space structure of $\mathbb{R}^n$.

Definition 5.2.2 *A* differentiable *(or* smooth *or C^∞)* structure *on a topological manifold $\mathbb{M}$ is a family of coordinate neighborhoods, $\mathcal{U} = \{U_\alpha, \phi_\alpha\}$, such that*

1. *$\mathcal{U}$ covers $\mathbb{M}$, that is, $\mathbb{M} \subset \bigcup_\alpha U_\alpha$.*

2. *For any α, β, the coordinate neighborhoods $\langle U_\alpha, \phi_\alpha \rangle$ and $\langle U_\beta, \phi_\beta \rangle$ are C^∞-compatible, that is, the functions $\phi_\alpha \circ \phi_\beta^{-1}$ and $\phi_\beta \circ \phi_\alpha^{-1}$ are* diffeomorphisms *(homeomorphisms and both the functions and their inverses are C^∞) between the open subsets $\phi_\alpha(U_\alpha \cap U_\beta)$ and $\phi_\beta(U_\alpha \cap U_\beta)$.*

3. *Any coordinate neighborhood $\langle V, \psi \rangle$ that is C^∞-compatible with every $\langle U_\alpha, \phi_\alpha \rangle \in \mathcal{U}$ is itself in $\mathcal{U}$.*

Definition 5.2.3 *A* differentiable *(or* smooth *or C^∞)* manifold *is a topological manifold endowed with a C^∞ structure.*

Definition 5.2.4 *Let W be an open set in a C^∞ manifold $\mathbb{M}$. A function $f : W \to \mathbb{R}$ is said to be a C^∞* function *if for every coordinate neighborhood $\langle U, \phi \rangle$ that satisfies $U \cap W \neq \emptyset$, $f \circ \phi^{-1}$ is a C^∞ function from $\phi(U \cap W) \subset \mathbb{R}^n$ to $\mathbb{R}$. Likewise, $F : \mathbb{M} \to \mathbb{N}$ is said to be a C^∞ mapping from a C^∞ manifold $\mathbb{M}$ to a C^∞ manifold $\mathbb{N}$ if for every coordinate neighborhoods $\langle U, \phi \rangle$ of $\mathbb{M}$ and $\langle V, \psi \rangle$ of $\mathbb{N}$, $\psi \circ F \circ \phi^{-1} : \phi(U) \to \psi(V)$ is C^∞.*

With the introduction of a C^∞ structure on $\mathbb{M}$, a tangent vector at a point $p \in \mathbb{M}$ can be defined as a function from $C^\infty(p)$, the collection of all functions that are C^∞ in an open neighborhood of p, to $\mathbb{R}$. Intuitively, given any function f that is C^∞ at p, the mapping $X_p^* : C^\infty(p) \to \mathbb{R}$ that corresponds to the vector X_p, reports the directional derivative $\triangle f$ of f in the direction of X_p (X_p not necessarily an unit vector).[1] The mapping must therefore satisfy the constraints,

[1]The motivation behind representing vectors in this manner lies in the existence of the dual vector space $\mathbf{V}^*$ (whose elements, known as covectors, are the set of all linear functions from $\mathbf{V}$ to $\mathbb{R}$) of any vector space $\mathbf{V}$, and

$X_p^*(\alpha f + \beta g) = \alpha X_p^* f + \beta X_p^* g$ and $X_p^*(fg) = f(p)X_p^* g + g(p)X_p^* f$ where $\alpha, \beta \in \mathbb{R}$ and $f, g \in C^\infty(p)$.

Based on this formulation, the vector $X_{\hat{p}} = \sum_{i=1}^n \alpha_i \mathbf{e}_i$ at any point $\hat{p} \in \mathbb{R}^n$ can be written as $X_{\hat{p}}^* = \sum_{i=1}^n \alpha_i (\partial/\partial x_i)$, since $\mathbb{R}^n$ is also a manifold. Given any coordinate neighborhood $\langle U, \phi \rangle$ of $\mathbb{M}$, each vector $\mathbf{e}_i = (\partial/\partial x_i)$ at $\hat{p} \in \phi(U) \subset \mathbb{R}^n$ is now bound to the vector $\mathbf{E}_i = \phi_*^{-1}(\partial/\partial x_i)$ (defined as $(\phi_*^{-1}(\partial/\partial x_i))f = \partial/\partial x_i (f \circ \phi^{-1})$) at $p \in \mathbb{M}$ where $p = \phi^{-1}(\hat{p})$.

Definition 5.2.5 *The* tangent bundle *of a C^∞ manifold $\mathbb{M}$ is the collection of all tangent vectors to points of $\mathbb{M}$, including the zero vector at each point, and is denoted by $T(\mathbb{M}) = \bigcup_{p \in \mathbb{M}} T_p(\mathbb{M})$.*

We now introduce the notion of a submanifold. Although there are several varieties of submanifolds, all of them possess a basic feature: a submanifold $\mathbb{N}$ of a C^∞ manifold $\mathbb{M}$ is a subset which is itself a C^∞ manifold. In the following paragraphs, we define three types of submanifolds: immersions, imbeddings, and regular submanifolds.

Definition 5.2.6 *The* rank *of a mapping $F : \mathbb{N} \to \mathbb{M}$ at $p \in \mathbb{N}$ is defined as the rank of the Jacobian of $\psi \circ F \circ \phi^{-1}$ at $\phi(p)$, where $\langle U, \phi \rangle$ and $\langle V, \psi \rangle$ are coordinate neighborhoods of $\mathbb{N}$ and $\mathbb{M}$ satisfying $p \in U$ and $F(p) \in V$.*

Definition 5.2.7 *A C^∞ mapping $F : \mathbb{N} \to \mathbb{M}$ is called an* immersion *if at all points of $\mathbb{N}$, rank$(F) = n = dim(\mathbb{N})$. If F is one-to-one then F establishes a topology and a C^∞ structure on $F(\mathbb{N}) \subset \mathbb{M}$ that makes F a diffeomorphism. $F(\mathbb{N})$ with this C^∞ structure is called an* immersed submanifold.

Definition 5.2.8 *An* imbedding *is a one-to-one immersion $F : \mathbb{N} \to \mathbb{M}$ which is also a homeomorphism of $\mathbb{N}$ into $F(\mathbb{N})$ regarded as a subspace of $\mathbb{M}$.*

Definition 5.2.9 *A subspace $\mathbb{N}$ of a C^∞ manifold $\mathbb{M}$ is said to possess the* submanifold property *if each $p \in \mathbb{N}$ has a coordinate neighborhood $\langle U, \phi \rangle$ on $\mathbb{M}$ with local coordinates $x_1, ..., x_n$ such that $\phi(p) = \langle 0, ..., 0 \rangle$, $\phi(U) = C_\epsilon^n(0)$ (the open ϵ-cube around $\langle 0, ..., 0 \rangle$), and $\phi(U \cap \mathbb{N}) =$*

---

the natural isomorphism of $\mathbf{V}$ onto the dual of the dual $(\mathbf{V}^*)^*$ that maps $\mathbf{v} \in \mathbf{V}$ onto the linear functional on $\mathbf{V}^*$ whose value on any $\sigma \in \mathbf{V}^*$ is $\sigma(\mathbf{v})$. In other words, $\mathbf{v} \in \mathbf{V}$ is represented as its associated member in $(\mathbf{V}^*)^*$ that is a linear functional that maps linear functions onto reals.

$\{\mathbf{x} \in C_\epsilon^n(0) \mid x_{m+1} = ... = x_n = 0\}$. *Such a coordinate neighborhood is called the preferred coordinate neighborhood at* p.

Definition 5.2.10 *A* regular submanifold *of a* C^∞ *manifold* $\mathbb{M}$ *is any subspace* $\mathbb{N}$ *with the submanifold property and with a* C^∞ *structure that the corresponding preferred coordinate neighborhood determines on it.*

Theorem 5.2.1 *Let* $F : \mathbb{N} \to \mathbb{M}$ *be a one-to-one immersion and* $\mathbb{N}$ *be compact. Then* F *is an imbedding and* $F(\mathbb{N})$ *is a regular submanifold of* $\mathbb{M}$.

Finally, we introduce the standard notion of a C^∞ *manifold with boundary* and expand the definition to characterize a slightly more general object, a C^∞ *manifold with boundaries*. We begin by extending the definition of differentiability of functions to include those that are defined on subsets of $\mathbb{R}^n$ that are not necessarily open.

Definition 5.2.11 *A function* f *defined on a subset* E *of* $\mathbb{R}^n$ *is said to be* C^∞ *if* f *can be extended to a* C^∞ *function on an open subset* U *of* $\mathbb{R}^n$ *which contains* E.

Theorem 5.2.2 *Let the upper half-space* $\mathbb{H}^n = \{\langle x_1, ..., x_n\rangle \in \mathbb{R}^n \mid x_n \geq 0\}$ *and the positive space* $\mathbb{Q}^n = \{\langle x_1, ..., x_n\rangle \in \mathbb{R}^n \mid x_i \geq 0, i = 1, ..., n\}$ *be assigned the subspace topology of* $\mathbb{R}^n$. *Let* f *be a* C^∞ *function on* $\mathbb{H}^n$ *(*$\mathbb{Q}^n$*). Then the value of* $\partial f/\partial x_i$ *at any point of* $\mathbb{H}^n$ *(*$\mathbb{Q}^n$*) is independent of the extension chosen.*

We note that the notion of diffeomorphism applies immediately to relatively open subsets U and V of $\mathbb{H}^n$ ($\mathbb{Q}^n$); namely, U and V are diffeomorphic if there exists a bijection $F : U \to V$ such that F and F^{-1} are both C^∞. Moreover, it follows from the inverse function theorem that the diffeomorphism F, in the case of $\mathbb{H}^n$, maps interior points of U to interior points of V and boundary points of U to boundary points of V, and in the case of $\mathbb{Q}^n$, maps interior points of U to interior points of V and boundary points (in a boundary set of a given dimension) of U to boundary points (in a boundary set of the same dimension) of V. Finally, both F and F^{-1} can be extended to open sets U' and V' of $\mathbb{R}^n$ such that $U = U' \cap \mathbb{H}^n$ ($U = U' \cap \mathbb{Q}^n$) and $V = V' \cap \mathbb{H}^n$ ($V = V' \cap \mathbb{Q}^n$), and even though the extensions are neither unique nor necessarily the inverses of one another in the larger domains, it follows from the previous theorem that the Jacobians of F and F^{-1} are independent of the extensions.

Definition 5.2.12 *A C^∞* manifold with boundary *(*boundaries*) is a Hausdorff, second countable, topological space $\mathbb{M}$ with a C^∞ structure $\mathcal{U}$ in the following generalized sense: $\mathcal{U} = \{U_\alpha, \phi_\alpha\}$ consists of a family of open subsets U_α of $\mathbb{M}$ each with a homeomorphism ϕ_α onto an open subset of $\mathbb{H}^n$ ($\mathbb{Q}^n$) such that*

1. *$\mathcal{U}$ covers $\mathbb{M}$, that is, $\mathbb{M} \subset \bigcup_\alpha U_\alpha$.*
2. *For any α, β, if $\langle U_\alpha, \phi_\alpha\rangle$ and $\langle U_\beta, \phi_\beta\rangle$ are elements of $\mathcal{U}$, then $\phi_\alpha \circ \phi_\beta^{-1}$ and $\phi_\beta \circ \phi_\alpha^{-1}$ are diffeomorphisms of $\phi_\alpha(U_\alpha \cap U_\beta)$ and $\phi_\beta(U_\alpha \cap U_\beta)$, open subsets of $\mathbb{H}^n$ ($\mathbb{Q}^n$).*
3. *$\mathcal{U}$ is maximal with respect to properties 1. and 2.*

5.2.3 Riemannian Manifolds

Just as the vector space structure of $\mathbb{R}^n$ was employed to assign each point $p \in \mathbb{M}$ a tangent space $T_p(\mathbb{M})$, the Euclidean structure of $\mathbb{R}^n$ can be used to endow $T_p(\mathbb{M})$ with an inner product.

Definition 5.2.13 *Let $\mathbf{V}$ be a vector space over $\mathbb{R}$. A mapping $\Phi : \mathbf{V} \times \mathbf{V} \to \mathbb{R}$ is called a* bilinear form *on $\mathbf{V}$ if it is linear in each variable, that is, for $\alpha, \beta \in \mathbb{R}$ and $\mathbf{v}, \mathbf{v}_1, \mathbf{v}_2, \mathbf{w}, \mathbf{w}_1, \mathbf{w}_2 \in \mathbf{V}$, $\Phi(\alpha\mathbf{v}_1+\beta\mathbf{v}_2,\mathbf{w}) = \alpha\Phi(\mathbf{v}_1,\mathbf{w})+\beta\Phi(\mathbf{v}_2,\mathbf{w})$ and $\Phi(\mathbf{v}, \alpha\mathbf{w}_1+\beta\mathbf{w}_2) = \alpha\Phi(\mathbf{v},\mathbf{w}_1)+\beta\Phi(\mathbf{v},\mathbf{w}_2)$.*

Definition 5.2.14 *A bilinear form that is symmetric, that is, for all $\mathbf{v}, \mathbf{w} \in \mathbf{V}$, $\Phi(\mathbf{v},\mathbf{w}) = \Phi(\mathbf{w},\mathbf{v})$, and positive definite, that is, for all $\mathbf{v} \in \mathbf{V}$, $\Phi(\mathbf{v},\mathbf{v}) \geq 0$ and $\Phi(\mathbf{v},\mathbf{v}) = 0$ if and only if $\mathbf{v}$ is the 0 vector, is called an* inner product *on $\mathbf{V}$.*

Definition 5.2.15 *A field $\mathbf{\Phi}$ of bilinear forms on a C^∞ manifold $\mathbb{M}$ is a function that assigns to each $p \in \mathbb{M}$ a bilinear form $\mathbf{\Phi}_p$ on $T_p(\mathbb{M})$. Furthermore, the field is C^∞ if for every coordinate neighborhood $\langle V, \psi\rangle$, the functions $g_{ij} = \mathbf{\Phi}(\mathbf{E}_i, \mathbf{E}_j)$ defined by $\mathbf{\Phi}$ and the coordinate frames $\mathbf{E}_1, ..., \mathbf{E}_n$, is C^∞.*

Definition 5.2.16 *A C^∞ manifold $\mathbb{M}$ endowed with a C^∞ field $\mathbf{\Phi}$ of symmetric, positive definite, bilinear forms is called a* Riemannian manifold*, and $\mathbf{\Phi}$ the* Riemannian metric*.*

The n^2 functions $g_{ij} = \mathbf{\Phi}(\mathbf{E}_i, \mathbf{E}_j)$ on V are called the components of $\mathbf{\Phi}$ in the coordinate neighborhood $\langle V, \psi\rangle$, and are usually represented in matrix form.

Given a Riemannian metric $\mathbf{\Phi}$ on $\mathbb{M}$, one can now choose an *orthonormal basis*, $\mathbf{F}_1, ..., \mathbf{F}_n$, for $T_p(\mathbb{M})$ at any point $p \in \mathbb{M}$. By assuming that the hypercube spanned by the vectors $\mathbf{F}_i$ for $i = 1, ..., n$ is of unit volume, one can extend *integration* of functions to the domain of Riemannian manifolds. This follows from the observation that the volume of the parallelepiped spanned by the members of the coordinate frame, $\mathbf{E}_i = \sum_{j=1}^{n} a_{ij}\mathbf{F}_j$ for $i = 1, ..., n$, is given by the determinant of the matrix $[a_{ij}]$, which we denote by $|[a_{ij}]|$. Simple algebra then demonstrates that $|[a_{ij}]| = \sqrt{|[g_{ij}]|}$. As a consequence, the volume of the parallelepiped spanned by the vectors $\mathbf{E}_i$ for $i = 1, ..., n$ is uniquely determined by the Riemannian metric $\mathbf{\Phi}$.

Likewise, as is demonstrated next, one can now define differentiation of *vector fields* on Riemannian manifolds.

Definition 5.2.17 *Let $\mathcal{X}(\mathbb{M})$ denote the set of all C^∞ vector fields on a Riemannian manifold $\mathbb{M}$. A* Riemannian connection $\nabla : \mathcal{X}(\mathbb{M}) \times \mathcal{X}(\mathbb{M}) \rightarrow \mathcal{X}(\mathbb{M})$ *(denoted by $\nabla : (X, Y) \rightarrow \nabla_X Y$) is a mapping that satisfies the following properties for all $f, g \in C^\infty(\mathbb{M})$ and $X, X', Y, Y' \in \mathcal{X}(\mathbb{M})$.*

1. $\nabla_{fX+gX'}Y = f(\nabla_X Y) + g(\nabla_{X'} Y)$.
2. $\nabla_X(fY + gY') = (Xf)Y + f\nabla_X Y + (Xg)Y' + g\nabla_X Y'$.
3. $(XY - YX) = \nabla_X Y - \nabla_Y X$.
4. $X\mathbf{\Phi}(Y, Y') = \mathbf{\Phi}(\nabla_X Y, Y') + \mathbf{\Phi}(Y, \nabla_X Y')$.

Intuitively, $\nabla_X Y$ is the vector field that denotes the rate of change of the vector field Y in the direction of the vector field X. It follows from criteria 1 and 2 above that given any coordinate neighborhood $\langle U, \phi \rangle$ of $\mathbb{M}$, if the functions Γ_{ij}^k in the equation $\nabla_{\mathbf{E}_i}\mathbf{E}_j = \sum_{k=1}^{n} \Gamma_{ij}^k \mathbf{E}_k$ are specified, then so is $\nabla_X Y$ for any C^∞ vector fields $X = \sum b_i(u)\mathbf{E}_i$ and $Y = \sum a_i(u)\mathbf{E}_i$, since $\nabla_X Y = \sum_k (Xa_k + \sum_{i,j} \Gamma_{ij}^k a_j b_i)\mathbf{E}_k$. In other words, if the functions Γ_{ij}^k are uniquely determined on a Riemannian manifold, then so is the Riemannian connection.

Theorem 5.2.3 *The Riemannian connection ∇ on a Riemannian manifold $\mathbb{M}$ is uniquely determined. Given any coordinate neighborhood $\langle U, \phi \rangle$ of $\mathbb{M}$ the C^∞ function Γ_{ij}^k is defined as $\Gamma_{ij}^k = (1/2)\sum_s g^{ks}\{(\partial g_{si}/\partial x_j) - (\partial g_{ij}/\partial x_s) + (\partial g_{js}/\partial x_i)\}$ where g_{ij} denotes the $(i, j)th$ element of the matrix defining $\mathbf{\Phi}$, and g^{ks} the $(k, s)th$ element of the inverse of the matrix.*

Definition 5.2.18 *A vector field Y on a Riemannian manifold $\mathbb{M}$ is said to be* constant *or* parallel *if $\nabla_{X_p} Y = 0$ for all $p \in \mathbb{M}$ and $X_p \in T_p(\mathbb{M})$.*

Constant vector fields are of substantial significance in dynamical systems analysis because they represent the simplest form of dynamics where the measure and shape of any section of the manifold is preserved under its action.

5.3 Dynamical Systems

Any system that evolves over time (henceforth denoted by the variable t) is called a dynamical system. Such systems are classified into discrete and continuous dynamical systems based on whether the time variable is discrete ($t \in \mathbb{Z}$) or continuous ($t \in \mathbb{R}$).

Definition 5.3.1 *A* discrete dynamical system *is expressed as an iteration of a function*

$$\mathbf{x}_{t+1} = f(\mathbf{x}_t), \quad t \in \mathbb{Z},$$

and a continuous dynamical system *as a differential equation*

$$\frac{d\mathbf{x}}{dt} = V(\mathbf{x}), \quad t \in \mathbb{R}.$$

In both cases, $\mathbf{x} \in \mathbb{M}$ represents the state of the system, $\mathbb{M}$ being the *state-* (or *phase-*) *space*. In the case of a discrete dynamical system, $\mathbb{M}$ must at the least be a topological manifold, and in the case of a continuous dynamical system, a C^∞ manifold. $f(\cdot)$ is a function $f : \mathbb{M} \to \mathbb{M}$ and $V(\cdot)$ a velocity field $V : \mathbb{M} \to T(\mathbb{M})$. In general, f is assumed to be a homeomorphism of $\mathbb{M}$ onto itself and V a C^∞ vector field.

Given any C^∞ manifold $\mathbb{M}$ and a homeomorphism $f : \mathbb{M} \to \mathbb{M}$, the *orbit* (or *trajectory*) of $\mathbf{x}$ under f is defined as $\{f^t(\mathbf{x}) \mid t \in \mathbb{Z}\}$. Likewise, given any compact C^∞ manifold $\mathbb{M}$ and a C^∞ vector field $V : \mathbb{M} \to T(\mathbb{M})$, the orbit (or *flow*) through $\mathbf{x}$ under V is defined as $\{\phi(t, \mathbf{x}) \mid t \in \mathbb{R}\}$, where ϕ is the C^∞ mapping $\phi : \mathbb{R} \times \mathbb{M} \to \mathbb{M}$ that satisfies $\phi(0, \mathbf{x}) = \mathbf{x}$ and $\frac{d\phi(t,\mathbf{x})}{dt} = V(\phi(t, \mathbf{x}))$. Note that without the noted restriction on the function f ($\mathbb{M}$ and the field V), the orbit is not necessarily well-defined for $t \in \mathbb{Z}^-$ ($t \in \mathbb{R}$).

Since this thesis investigates the characteristics of a discrete dynamical system, we restrict all future discussions to discrete systems. The reader must however note that diffeomorphisms and C^∞ flows are intimately related, and should consult (Smale, 1967) for more on this topic.

We begin with the notion of *conjugacy* that allows us to recognize when two diffeomorphisms exhibit the same behavior.

Definition 5.3.2 *Two diffeomorphisms $f : \mathbb{M} \to \mathbb{M}$ and $f' : \mathbb{N} \to \mathbb{N}$ are said to be* topologically conjugate *if there exists a homeomorphism $h : \mathbb{M} \to \mathbb{N}$ such that $h \circ f = f' \circ h$. If h is also a diffeomorphism then f and f' are said to be C^∞* conjugate.

Definition 5.3.3 *A point $\mathbf{x}^* \in \mathbb{M}$ is said to be a* fixed point *of the dynamical system defined by f if $f^t(\mathbf{x}^*) = \mathbf{x}^*$ for all $t \in \mathbb{Z}$.*

Definition 5.3.4 *A point $\mathbf{x}^* \in \mathbb{M}$ is said to be a* periodic point *of the dynamical system defined by f if $f^t(\mathbf{x}^*) = \mathbf{x}^*$ for some $t \in \mathbb{Z}$. The smallest such t is called the* period *of the periodic orbit.*

Definition 5.3.5 *A fixed point $\mathbf{x}^*$ is said to be* stable *if for every open neighborhood U of $\mathbf{x}^*$ there exists an open neighborhood $V \subseteq U$ of $\mathbf{x}^*$ such that for every $\mathbf{x} \in V$, $f^t(\mathbf{x}) \in U$ for all $t \in \mathbb{Z}^+$.*

Furthermore, $\mathbf{x}^*$ is said to be asymptotically *stable if, in addition, there exists some open neighborhood U of $\mathbf{x}^*$ such that all points $\mathbf{x} \in U$ satisfy $\lim_{t\to\infty} f^t(\mathbf{x}) = \mathbf{x}^*$. Fixed points that are stable but not asymptotically stable are called* neutrally *stable.*

Definition 5.3.6 *A set $\mathcal{I} \subseteq \mathbb{M}$ is said to be* invariant *under a homeomorphism f if $f^t(\mathcal{I}) \subseteq \mathcal{I}$ for all $t \in \mathbb{Z}$. The set is said to be* positively *(*negatively*) invariant if the criterion holds only for $t \in \mathbb{Z}^+$ ($t \in \mathbb{Z}^-$).*

Definition 5.3.7 *A point $\mathbf{x}$ is labeled a* nonwandering *point of a homeomorphism f if given any open neighborhood U of $\mathbf{x}$ and any $t_{min} > 0$ ($t_{min} \in \mathbb{Z}$), there exists a $t > t_{min}$ ($t \in \mathbb{Z}$) such that $f^t(U) \cap U \neq \emptyset$. A point that is not nonwandering is labeled* wandering *or* transient.

The set of all nonwandering points is called the *nonwandering set* and is represented by Ω.

Definition 5.3.8 *A set $\Lambda \subseteq \mathbb{M}$ is labeled a* basic set *of a homeomorphism f if given any points $\mathbf{x}, \mathbf{y} \in \Lambda$, any open neighborhoods U of $\mathbf{x}$ and V of $\mathbf{y}$ and any $t_{min} > 0$ ($t_{min} \in \mathbb{Z}$), there exist $t_1, t_2, t_3, t_4 > t_{min}$ ($t_1, t_2, t_3, t_4 \in \mathbb{Z}$) such that $f^{t_1}(U) \cap U \neq \emptyset$, $f^{t_2}(U) \cap V \neq \emptyset$,*

$f^{t_3}(V) \cap U \neq \emptyset$, *and* $f^{t_4}(V) \cap V \neq \emptyset$, *and furthermore,* Λ *is a* maximal set *with regard to this property.*

We now demonstrate that if f is a homeomorphism, the above definition reduces to the standard definition of a basic set.

Theorem 5.3.1 *The set of all nonwandering points,* Ω*, is closed. Moreover, any basic set,* Λ*, (which is necessarily a subset of* Ω*) is closed.*

Proof:

Let $\mathbf{x}$ *be a limit point of* Ω*. Given any open neighborhood* U *of* $\mathbf{x}$*, there exists a point* $\mathbf{y}$ *and an open neighborhood* V *of* $\mathbf{y}$ *such that* $\mathbf{y} \in \Omega$ *and* $V \subset U$*. Given any* $t_{min} > 0$ *there exists a* $t > t_{min}$ *such that* $f^t(V) \cap V \neq \emptyset$*. Since* $V \subset U$*,* $f^t(U) \cap U \neq \emptyset$*, and therefore* $\mathbf{x} \in \Omega$*.*

Let $\mathbf{x}$ *be a limit point of a basic set* Λ*. Given any open neighborhood* U *of* $\mathbf{x}$*, there exists a point* $\mathbf{y}$ *and an open neighborhood* V *of* $\mathbf{y}$ *such that* $\mathbf{y} \in \Lambda$ *and* $V \subset U$*. Given any* $\mathbf{z} \in \Lambda$*, open neighborhood* W *of* $\mathbf{z}$*, and* $t_{min} > 0$*, there exist* $t_1, t_2, t_3, t_4 > t_{min}$ *such that* $f^{t_1}(V) \cap V \neq \emptyset$*,* $f^{t_2}(V) \cap W \neq \emptyset$*,* $f^{t_3}(W) \cap V \neq \emptyset$*, and* $f^{t_4}(W) \cap W \neq \emptyset$*. Since* $V \subset U$*, the constraints are also satisfied by* U*. Finally,* Λ *being maximal,* $\mathbf{x} \in \Lambda$*.*

Theorem 5.3.2 *Let* f *be a homeomorphism, and* $\mathbf{x}$ *and* $\mathbf{y}$ *points in* $\mathbb{M}$*. Then, if given any open neighborhoods* U *of* $\mathbf{x}$ *and* V *of* $\mathbf{y}$ *and any* $t_{min} > 0$ *(*$t_{min} \in \mathbb{Z}$*) there exists a* $t > t_{min}$ *(*$t \in \mathbb{Z}$*) such that* $f^t(U) \cap V \neq \emptyset$*, then there exist* $t', t'' > t_{min}$ *(*$t', t'' \in \mathbb{Z}$*) such that* $\mathbf{y} \in f^{t'}(U)$ *and* $f^{t''}(\mathbf{x}) \in V$*.*

Proof:

Given any open neighborhoods U *of* $\mathbf{x}$ *and* V *of* $\mathbf{y}$*, let* $t_{min} < t_1 < ... < t_k < t_{k+1} < ...$ *be the times at which* $f^{t_i}(U) \cap V \neq \emptyset$*. Let* $W = \bigcup_{i=1}^{\infty}(f^{t_i}(U) \cap V)$*. Then* W *is an open set. Let us also assume that* $\mathbf{y} \notin f^t(U)$ *for all* $t > t_{min}$*. Then* $\mathbf{y} \notin W$*, in which case, either there exists an open neighborhood* $V' \subset V$ *of* $\mathbf{y}$ *such that* $V' \cap W = \emptyset$*, or* $\mathbf{y} \in \overline{W}$*. If the first case is true, we obviously have a contradiction. If, on the other hand, the second case is true, the sequence* $f^{-t_1}(\mathbf{y}), ..., f^{-t_k}(\mathbf{y}), f^{-t_{k+1}}(\mathbf{y}), ...$ *approaches* $\overline{U}$ *in the limit. We can then always choose an open neighborhood* $U' \subset U$ *of* $\mathbf{x}$ *such that the limit does not approach* $\overline{U'}$*. Replacing* U *with* U' *reduces this to the first case.*

The proof of the second claim follows along the same lines.

We note that if f is a homeomorphism, membership in the same basic set is an equivalence relation on points in Ω. The relation is reflexive since $\forall U, V$ open neighborhoods of $\mathbf{x}$, $U \cap V$ is an open neighborhood of $\mathbf{x}$, symmetric by definition, and transitive as a consequence of the previous theorem and the fact that each Λ is maximal with regard to the relation. In other words, the system of basic sets comprise a partition of Ω.

Theorem 5.3.3 *Let Λ be a basic set of the homeomorphism f. Then, Λ is an invariant set.*

Proof:

We first prove that $\mathbf{x} \in \Lambda \Rightarrow f(\mathbf{x}) \in \Lambda$. Since f is a homeomorphism, given any open neighborhood U of $f(\mathbf{x})$, $f^{-1}(U)$ is an open neighborhood of $\mathbf{x}$. $f^t(f^{-1}(U)) \cap f^{-1}(U) \neq \emptyset$ implies that $f^t(U) \cap U \neq \emptyset$, $f^{t+1}(f^{-1}(U)) \cap U \neq \emptyset$, and $f^{t-1}(U) \cap f^{-1}(U) \neq \emptyset$. Therefore, $f(\mathbf{x})$ is a member of the same basic set.

The proof for $\mathbf{x} \in \Lambda \Rightarrow f^{-1}(\mathbf{x}) \in \Lambda$ follows along the same lines.

Finally, we consider the notion of an attractor. Informally, a basic set that attracts some neighborhood of points in the phase-space is called an attractor.

Definition 5.3.9 *A basic set Λ is labeled an* attractor *if there exists a* bounded *set U such that $\Lambda \subset int(U)$ the interior[2] of U, for every basic set $\Lambda' \neq \Lambda$, $\overline{U} \cap \Lambda' = \emptyset$, and U is positively invariant, that is, $f^t(U) \subseteq U$ for every $t \in \mathbb{Z}^+$. The largest such U is then called the* realm of attraction *of Λ.*

We now demonstrate that if f is a homeomorphism, the above definition reduces to the standard definition of an attractor.

Theorem 5.3.4 *Let Λ be an attractor of the homeomorphism f. Let U be a set that satisfies the criteria introduced in the definition above. Then,* $\lim_{t\to\infty} f^t(\overline{U}) = \Lambda$.

Proof:

We first introduce some standard notation. Given any sequence of sets $A_0, A_1, ...$ we define $\lim_t \sup A_t = \bigcap_{n=0}^{\infty} \bigcup_{t=n}^{\infty} A_t$ *and* $\lim_t \inf A_t = \bigcup_{n=0}^{\infty} \bigcap_{t=n}^{\infty} A_t$. *The sequence A_t is said to* converge *to A (written as $\lim_{t\to\infty} A_t = A$) if* $\lim_t \sup A_t = \lim_t \inf A_t = A$.

[2]Interior is defined as the set of all interior-points of the noted set.

A standard theorem in set theory states that increasing and decreasing monotone sequences of sets converge. Stated formally, if $A_0 \supseteq A_1 \supseteq ...$ *then* $\lim_{t\to\infty} A_t = A = \bigcap_{t=0}^{\infty} A_t$*, and likewise, if* $A_0 \subseteq A_1 \subseteq ...$ *then* $\lim_{t\to\infty} A_t = A = \bigcup_{t=0}^{\infty} A_t$*.*

We now proceed to prove the theorem.

Since f *is continuous,* $f(\overline{U}) \subseteq \overline{f(U)}$*. In addition, since* $f(U) \subseteq U$ *implies that* $\overline{f(U)} \subseteq \overline{U}$*, we have* $f(\overline{U}) \subseteq \overline{U}$*. Repeated application of* f *to both sides yields* $\overline{U} \supseteq f(\overline{U}) \supseteq f^2(\overline{U})$*.... Being monotone, based on the theorem stated earlier the sequence converges to* $\bigcap_{t=0}^{\infty} f^t(\overline{U})$*.*

Based on the assumptions in the definition, that $\overline{U}$ *is compact and that* f *is a homeomorphism, and* $f(\overline{U}) \subseteq \overline{U}$*, we arrive at the additional conclusion that* $\bigcap_{t=0}^{\infty} f^t(\overline{U})$ *is compact and invariant. That it is compact follows from it being a closed subset of a compact set. That it is invariant follows from* $f(\bigcap_{t=0}^{\infty} f^t(\overline{U})) = \bigcap_{t=1}^{\infty} f^t(\overline{U})$ *and* $f^{-1}(\bigcap_{t=0}^{\infty} f^t(\overline{U})) = \bigcap_{t=-1}^{\infty} f^t(\overline{U})$*.*

$\Lambda \subset int(U)$ *implies that* $\Lambda \subset \overline{U}$*. Since* Λ *is invariant, repeated application of* f *to both sides yields* $\Lambda \subseteq f^t(\overline{U})$ *for every* $t \in \mathbb{Z}^+$*. Hence,* $\Lambda \subseteq \bigcap_{t=0}^{\infty} f^t(\overline{U})$*.*

If $\Lambda \subsetneq \bigcap_{t=0}^{\infty} f^t(\overline{U})$*, then based on the criteria that* $\overline{U} \cap \Lambda' = \emptyset$ *for every basic set* $\Lambda' \neq \Lambda$ *and* $f(\overline{U}) \subseteq \overline{U}$*, we can conclude that any point* $p \in \bigcap_{t=0}^{\infty} f^t(\overline{U}) \backslash \Lambda$ *is a wandering point. Since* $\bigcap_{t=0}^{\infty} f^t(\overline{U})$ *is invariant, it must then contain the entire trajectory through* p*. Finally, since* $\bigcap_{t=0}^{\infty} f^t(\overline{U})$ *is compact, the sequence* $\{f^t(p)\}$ *must have a subsequence that converges to some point in* $\bigcap_{t=0}^{\infty} f^t(\overline{U})$*. This, however, implies that* p *is a nonwandering point. Hence,* $\Lambda = \bigcap_{t=0}^{\infty} f^t(\overline{U})$*.*

Attractors are the structures that are manifest in the dynamics of dissipative systems. The simplest kind of attractor is a stable fixed point or a stable periodic orbit. There is, however, a third kind of attractor known as a *chaotic* attractor, that we define next.

We must mention here that although the field of dynamical systems analysis has not yet completely settled on a standard definition of chaos, two themes recur: topological transitivity[3] and sensitive dependence on initial conditions. The definition of a chaotic attractor that we introduce next requires both criteria to be satisfied.

[3] A set is said to be topologically transitive if given any relatively open subsets U and V of the set, there exists a $t \in \mathbb{Z}^+$ such that $f^t(U) \cap V \neq \emptyset$.

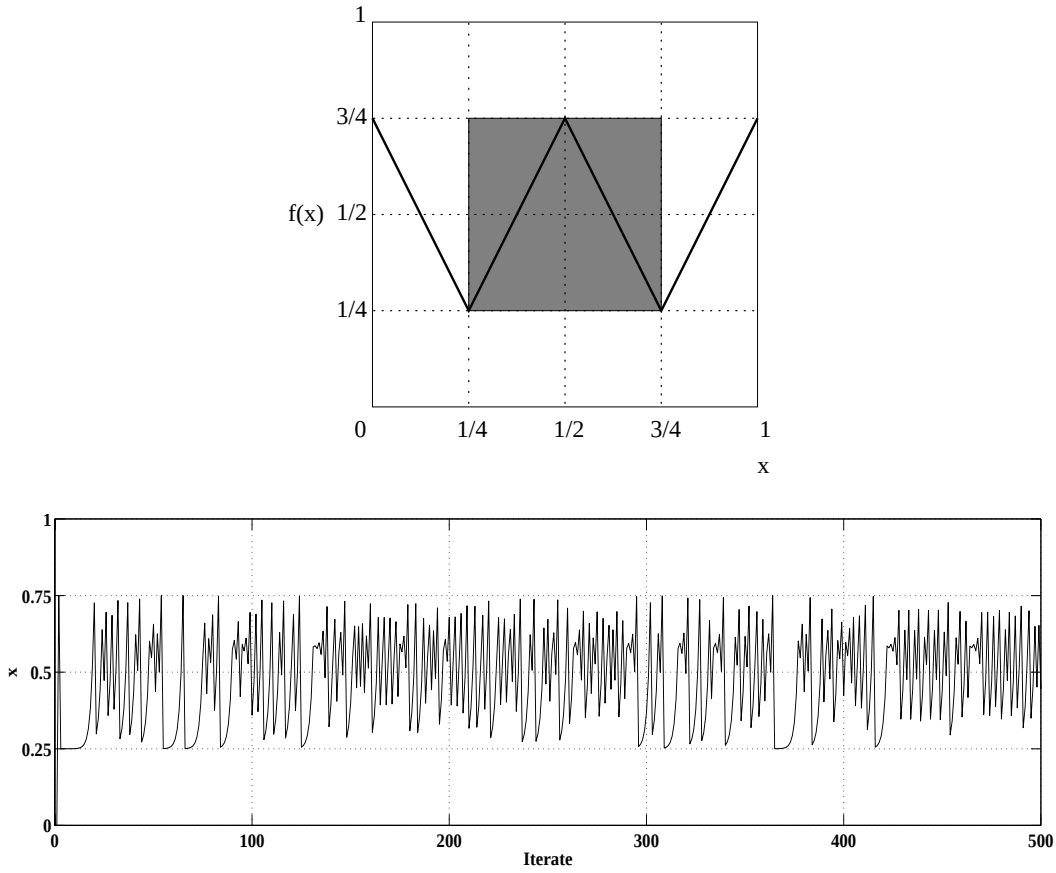

Figure 5.1: (a) A map $f : [0, 1] \to [\frac{1}{4}, \frac{3}{4}]$ that contains a chaotic attractor at $[\frac{1}{4}, \frac{3}{4}]$, and (b) Five hundred iterations of the point 0.000001 under the map.

Definition 5.3.10 *A map $f : U \to U$ has the property that its orbits depend* sensitively on initial conditions *if there exists an $\epsilon > 0$ such that for every $\mathbf{x} \in U$ and every open neighborhood V of $\mathbf{x}$, there is a point $\mathbf{y} \in V$ for which $|f^t(\mathbf{x}) - f^t(\mathbf{y})| > \epsilon$, for some $t \in \mathbb{Z}^+$.*

Definition 5.3.11 *An attractor Λ is said to be* chaotic *if the orbits of f in the realm of attraction U of Λ, depend sensitively on initial conditions.*

Figure 5.1(a) presents a mapping that displays a simple example of a chaotic attractor. The interval $[\frac{1}{4}, \frac{3}{4}]$ comprises the attractor and the interval $[0, 1]$ its realm of attraction. While $\frac{1}{4}$ and $\frac{7}{12}$ are both fixed points of the mapping, they are not basic sets since they do not satisfy the maximality criterion set forth in the definition of a basic set. That the intervals $[0, \frac{1}{4})$ and $(\frac{3}{4}, 1]$ are comprised of wandering points follows from the fact that the function maps $[0, \frac{1}{4})$ onto $(\frac{1}{4}, \frac{3}{4}]$ and $(\frac{3}{4}, 1]$ onto $[\frac{1}{4}, \frac{3}{4})$. In essence, any point in these regions is mapped to $[\frac{1}{4}, \frac{3}{4}]$ in a single

iteration of the function, never to return to its interval of origin.

The interval $[\frac{1}{4}, \frac{3}{4}]$, on the other hand, is comprised of nonwandering points. Not only does the function map $[\frac{1}{4}, \frac{3}{4}]$ onto itself, but any open set in the interval is stretched by a factor of two with every iteration of the function, and eventually covers the entire interval. This observation also proves that the entire interval $[\frac{1}{4}, \frac{3}{4}]$ comprises a single basic set and that trajectories in the region depend sensitively on initial conditions. Figure 5.1(b) presents five hundred iterations of the point 0.000001 under the map. The apparent randomness of the graph is the most distinctive feature of chaos.

Most of the results in this section assume that the map f that defines the dynamical system is a homeomorphism. In Chapter 9, we shall deduce the implications of it not being so. We will find that basic sets do not comprise a partition of the set of all nonwandering points. This observation will lead to the formulation of a new set, the complex set, that does. We will also demonstrate that a complex set that is a chaotic attractor is potentially *anisotropic* in nature in the sense that a trapped trajectory does not necessarily visit the entire complex set, and moreover, the section of the complex set visited by the trajectory depends on its point of entry.

5.4 Summary

Any system whose state changes with time is called a dynamical system. In this chapter, we have presented a brief review of dynamical systems analysis, emphasizing the role that manifolds play in it, forming the natural setting for the phase-spaces of such systems. The unconventional definition of a basic set presented in this chapter allows us to extend several concepts to dynamical systems that are defined by discontinuous maps.

We have also briefly reviewed basic concepts in topology and manifold theory. These concepts are used extensively in the upcoming chapters where an abstract dynamical system that models systems of biological neurons is formulated and its dynamics is analyzed.

Chapter 6

The Abstract Dynamical System: Phase-Space and Velocity Field

In Chapter 4, we presented a model of an individual neuron. In this chapter, we extend the model to accommodate a *system* of neurons. The eventual goal of the current enterprise is to construct an abstract dynamical system that, while instantiable to any particular neuronal system, can be analyzed in its generalized configuration.

This objective is accomplished through several stages of development. We begin by addressing in Section 6.1 issues pertaining to the framework of the conceived system; the specification of the temporal position of a spike in the system is standardized and the membrane potential function is reformulated accordingly. In Section 6.2, a well-founded representation of the state of a system of neurons is introduced, based on which the phase-space for the system is constructed. Section 6.3 is devoted to a careful development of the notion of the neighborhood of a state of the system. A new topology is introduced on the phase-space, the impact of which can be appreciated in Chapters 8 and 9. Section 6.4 completes the formulation of the dynamical system by specifying the velocity field that overlays the phase-space. Section 6.5 then describes the core components of the abstract dynamical system.

6.1 Standardization of Variables

The existence of two distinct sets of origins in relation to which the temporal positions of spikes are determined in the model of the individual neuron—synapses for spikes arriving from presynaptic neurons and the soma for spikes generated by the neuron—gives rise to complications in the further development of the model to accommodate a system of neurons.

We begin by revisiting these definitions with the intent to institute the measure of uniformity necessary for the construction of a phase-space for a system of neurons. Previously, x_i^j's for $i = 1, ..., m$ represented the time since the arrival of spikes at synapses, and for $i = 0$ the time

since the inception of spikes at the soma. We eliminate the asymmetry in the choice of origins of the two sets of variables by redefining $x_i^j \ \forall i, j$ to represent the time since the inception of the spike at the soma of the corresponding neuron. The subscript i in x_i^j is now set to refer to a neuron rather than a synapse. In addition to changes in $P(\cdot)$, this prompts a shift in focus from the postsynaptic to the presynaptic neuron.

Given a system of neurons, an upper bound on the number of effective, efferent spikes that a neuron can possess at any time is first computed as follows. Let $i = 1, ..., \mathcal{S}$ denote the set of all neurons in the system, $k_i = 1, ..., m_i$ the set of efferent synapses of neuron i (synapses to which neuron i is presynaptic), $\lambda_{k_i}^i$ the time it takes for a spike generated at the soma of neuron i to reach synapse k_i, $\tau_{k_i}^i$ (the superscript is introduced to denominate a synapse in the *system*) the interval over which a spike impinging on synapse k_i is effective on the corresponding postsynaptic neuron, and r_i the absolute refractory period of neuron i. Since its inception, the maximum time until which any spike can be effective on any corresponding postsynaptic neuron is then given by $\chi = \max_{i=1,k_i=1}^{\mathcal{S},m_i}\{\lambda_{k_i}^i + \tau_{k_i}^i\}$. Let ς denote the maximum time period over which any spike is effective on the neuron that generates it, and let $\Upsilon = \max\{\chi, \varsigma\}$. Then $n_i = \lceil \Upsilon / r_i \rceil$ provides an upper bound on the number of effective, efferent spikes that neuron i can possess at any time. Hence, for example, the time bound of 505 msec introduced in an example in Chapter 2 corresponds to the quantity Υ here. In the example, r_i was assumed to be 1 msec for each neuron i, and consequently n_i was set at 505 for each neuron in the system.

The requisite changes in $P(\cdot)$ are threefold. First, the number of variables associated with some synapses is increased so that all synapses actuated by neuron i are consistently assigned n_i variables. This is achieved by setting appropriately fewer variables in $P^*(\cdot)$ to $\tau_{k_i}^i$ in criterion (iv) of Chapter 4 Section 2. Next, $P(\cdot)$ is translated along all but one set of axes such that the former origin is now at $\langle \lambda_{k_{i_1}}^{i_1}, \lambda_{k_{i_1}}^{i_1}, ..., ..., \lambda_{k_{im}}^{i_m}, \lambda_{k_{im}}^{i_m}, ..., 0, 0, ... \rangle$, where $i_1, ..., i_m$ are the neurons presynaptic to the neuron in question (i_0) at synapses $k_{i_1}, ..., k_{i_m}$. $\frac{\partial P}{\partial x_{k_i}^j} \mid_{x_{k_i}^j = t} = 0$ for $0 \leq t \leq \lambda_{k_i}^i$ holds owing to the manner in which $P(\cdot)$ was previously defined. Finally, references to synapses in the variables are switched to references to appropriate neurons, and multiple variables referencing the same spike (occurs when a neuron makes multiple synapses on a postsynaptic neuron) are consolidated.

6.2 The Phase-Space

Our objective in this section is to formulate an appropriate *phase-space* for a system of neurons. We begin by identifying a suitable representation for the *state* of a system of neurons. The description of the phase-space is derived as a direct consequence of the representation.

While it is assumed in the following treatment that neurons do not receive external input, incorporating such is merely a matter of introducing additional neurons whose state descriptions are identical to that of the external input. We return to this issue in Chapter 10, where ramifications for the computational nature of systems of neurons in the brain are discussed in the light of the findings of this thesis.

6.2.1 Representation of the State of a System of Neurons

We first note that a record of the temporal locations of all afferent spikes into neurons in a system is potentially redundant since multiple neurons in the system might receive spikes from a common neuron. The issue is however resolved if we focus on efferent spikes rather than afferent spikes. The perspective developed in Section 6.1 leads to the immediate realization that the state of a system of neurons can be specified completely by enumerating, for all neurons $i = 1, ..., \mathcal{S}$, the temporal positions[1] of the n_i (or fewer) most recent spikes generated by neuron i within Υ time from the present. On the one hand, such a record specifies the exact location of all spikes that are still situated on the axons of respective neurons, and on the other, combined with the potential functions, it specifies the current state of the soma of all neurons.

This gives us the following initial representation of the state information contributed by each neuron toward the specification of the state of the system: at any given moment neuron i reports the n_i-tuple $\langle x_i^1, x_i^2, ..., x_i^{n_i} \rangle$, where each x_i^j denotes the time since the inception of a distinct member of the n_i most recent spikes generated at the soma of neuron i within Υ time from the present. Since n_i is merely an upper bound on the number of such spikes, it is conceivable that fewer than n_i spikes satisfy the criterion, in which case the remaining components in the n_i-tuple are set at Υ. From a dynamical perspective, this amounts to the value of a component growing

[1] How long ago the spike originated at the soma of the corresponding neuron is treated as the descriptor of its temporal position.

until Υ is reached, at which point the growth ceases. The phase-space for neuron i is then the closed n_i-cube $[0, \Upsilon]^{n_i} \subset \mathbb{R}^{n_i}$.

This representation of the state of a neuron is, however, fraught with redundancy. First, the *finite* description of the state of a neuron requires that a variable be reused to represent a new spike when the effectiveness of the old spike it represented terminates. Since a variable set at Υ (ineffective spike) is first set to 0 when assigned to a new spike, one of the two positions is redundant. The abstract equivalence of the positions then dictates that Υ be identified with 0.

Second, if $\mathbf{x} = \langle x_i^1, x_i^2, ..., x_i^{n_i} \rangle$ and $\mathbf{y} = \langle y_i^1, y_i^2, ..., y_i^{n_i} \rangle$ are two n_i-tuples that are a non-trivial permutation of one another ($\exists \sigma$, a permutation, such that $\forall j = 1, ..., n_i \; x_i^j = y_i^{\sigma(j)}$), then while $\mathbf{x}$ and $\mathbf{y}$ are two distinct points in $[0, \Upsilon]^{n_i}$, they represent the same state of the neuron (which variable represents a spike is immaterial). This stipulates that all permutations of an n_i-tuple be identified with the same state.

6.2.2 Formulation of the Phase-Space for a System of Neurons

Having identified the need for a more elaborate representation, we now propose a candidate solution and construct the associated phase-space. The phase-space is constructed as a differentiable manifold, the points of which satisfy both criteria enumerated in the previous section. The construction is divided into two stages. The first stage transforms the interval $[0, \Upsilon]$ into the unit circle S^1 (spikes now being represented as complex numbers of unit modulus), and the second computes a complex polynomial whose roots identically match this set of complex numbers. By retaining the coefficients of this polynomial to represent the state of the neuron, all order information is eliminated.

Stage 1

We impose on the manifold $\mathbb{R}$ the equivalence relation: $x \sim y$ if $(x - y) = a\Upsilon$, where $x, y \in \mathbb{R}$, and $a \in \mathbb{Z}$, and regard $\mathbb{R}/\sim$ with its standard quotient topology. The equivalence class mapping $\pi : \mathbb{R} \to \mathbb{R}/\sim$ can be identified with $\pi(t) = e^{\frac{2\pi i t}{\Upsilon}}$. π maps $\mathbb{R}/\sim$ onto $S^1 = \{z \in \mathbb{C} \mid |z| = 1\}$.

We therefore apply the transformation $\langle x^1, x^2, ..., x^n \rangle \to \langle e^{\frac{2\pi i x^1}{\Upsilon}}, e^{\frac{2\pi i x^2}{\Upsilon}}, ..., e^{\frac{2\pi i x^n}{\Upsilon}} \rangle$ to the initial formulation of the phase-space of a neuron. The new phase-space is $T^n = \prod_{i=1}^{n} S^1$, the

n-torus.

We assume hereafter that all variables x_i^j are normalized, that is, scaled from $[0, \Upsilon]$ to $[0, 2\pi]$. $P(\cdot)$ is also assumed to be modified to reflect the scaling of its domain.

Stage 2

That the set G=$\{\sigma \mid \sigma$ is a permutation of n elements$\}$ forms a *Group* motivates the approach that the *orbit space* T^n/G of the *action* of G on T^n be considered. G however, does not act *freely*[2] on T^n, and therefore the quotient topology of T^n/G does not inherit the locally Euclidean structure of T^n. Hence, we explicitly construct the space as a subset of the Euclidean space and endow it with the standard topology. While such a subset necessarily contains boundaries, the construction does shed light on the intrinsic structure of the space.

As noted earlier, we apply the transformation $\langle z_1, z_2, ..., z_n\rangle \rightarrow \langle a_n, a_{n-1}, ..., a_0\rangle$ where $a_n, a_{n-1}, ..., a_0 \in \mathbb{C}$ are the coefficients of $f(z) = a_n z^n + a_{n-1}z^{n-1} + ... + a_0$ whose roots lie at $z_1, z_2, ..., z_n \in \mathbb{C}$. Informally, this amounts to representing the quotient under reordering by elementary symmetric functions, a standard technique in algebra. The immediate question, then, is what are *necessary* and *sufficient* constraints on $\langle a_n, a_{n-1}, ..., a_0\rangle \in \mathbb{C}^{n+1}$ for all roots z_i of $f(z)$ to satisfy $|z_i| = 1$. We answer the question in two steps. First, we consider the case of distinct roots, and subsequently that of multiple roots.

Theorem 6.2.1 *Let $f(z) = a_n z^n + a_{n-1}z^{n-1} + ... + a_1 z + a_0$ be any complex polynomial of degree n.*

- *Let $f^*(z)$ be defined as $f^*(z) = z^n \bar{f}(1/z) = \bar{a}_0 z^n + \bar{a}_1 z^{n-1} + ... + \bar{a}_n$, where $\bar{a}_i$ represents the complex conjugate of a_i.*
- *Construct the sequence $\langle f_0(z), f_1(z), ..., f_{n-1}(z)\rangle$ as follows:*
  - *(i) $f_0(z) = f'(z)$ where $f'(z)$ is the derivative of $f(z)$, and*
  - *(ii) $f_{j+1}(z) = \bar{b}_0^{(j)} f_j(z) - b_{n-1-j}^{(j)} f_j^*(z)$ for $j = 0, 1, ..., n-2$, where $f_j(z)$ is represented as the polynomial $\sum_{k=0}^{n-1-j} b_k^{(j)} z^k$.*

In each polynomial $f_j(z)$, the constant term $b_0^{(j)}$ is a real number, which we denote by δ_j: $\delta_{j+1} = b_0^{(j+1)} = |b_0^{(j)}|^2 - |b_{n-1-j}^{(j)}|^2$ *for* $j = 0, 1, ..., n-2$.

[2] A Group G acts freely on a set X if for all x, $gx = x$ implies $g = e$.

Then, necessary *and* sufficient *conditions for all roots of* $f(z)$ *to be* distinct *and to lie on the unit circle,* $|z| = 1$*, assuming without loss of generalization that* $a_n = 1$*, are:*

$$|a_0| = 1, \ \textit{and} \ a_i = \bar{a}_{n-i} a_0 \ \textit{for} \ i = 1, 2, ..., n-1, \ \textit{and} \tag{6.1}$$

$$\delta_1 < 0 \ \textit{and} \ \delta_j > 0 \ \textit{for} \ j = 2, 3, ..., n-1. \tag{6.2}$$

Proof: *See Appendix A.*

Stated informally, equations (6.1) ensure that the degree of freedom reflected in the dimensionality of the initial space does not change as a result of the transformation. Of the coefficients $\langle a_{n-1}, a_{n-2}, ..., a_0 \rangle$ ($a_n = 1$ without loss of generalization), (i) a_0 has one degree of freedom ($|a_0| = 1$) and (ii) if n is odd, $\langle a_{\lceil n/2 \rceil - 1}, ..., a_1 \rangle$ can be derived from $\langle a_{n-1}, ..., a_{\lceil n/2 \rceil}; a_0 \rangle$ or (iii) if n is even, $a_{\lceil n/2 \rceil}$ has only one degree of freedom ($a_{\lceil n/2 \rceil} = \bar{a}_{\lceil n/2 \rceil} a_0$ implies that $\angle a_{\lceil n/2 \rceil} = (1/2)\angle a_0$) and $\langle a_{\lceil n/2 \rceil - 1}, ..., a_1 \rangle$ can be derived from $\langle a_{n-1}, ..., a_{\lceil n/2 \rceil + 1}; a_0 \rangle$. As a consequence, if n is odd, $\langle a_{n-1}, ..., a_{\lceil n/2 \rceil}; a_0 \rangle \in \mathbb{C}^{\lfloor n/2 \rfloor} \times S^1$ completely specifies the polynomial, and if n is even, $\langle a_{n-1}, ..., a_{\lceil n/2 \rceil + 1}; a_{\lceil n/2 \rceil}, a_0 \rangle \in \mathbb{C}^{\lfloor n/2 \rfloor - 1} \times \mathbb{M}^2$ does the same. $\mathbb{M}^2$ denotes the 2-dimensional Möbius band and we shall presently demonstrate that when n is even, $\langle a_{\lceil n/2 \rceil}, a_0 \rangle \in \mathbb{M}^2$.

$(1/2)\angle a_0$ has two solutions, θ and $(\theta + \pi)$, where $\theta \in [0, \pi)$. $\langle a_{\lceil n/2 \rceil}, a_0 \rangle$ is represented as $\langle \pm |a_{\lceil n/2 \rceil}|, \angle a_0 \rangle$, where $a_{\lceil n/2 \rceil}$'s choice between θ and $(\theta + \pi)$ is transferred to the sign of $|a_{\lceil n/2 \rceil}|$ (that is, positive $|a_{\lceil n/2 \rceil}|$ implies θ and negative $|a_{\lceil n/2 \rceil}|$ implies $(\theta + \pi)$). Topological constraints then require that any point satisfying $\langle \pm |a_{\lceil n/2 \rceil}|, \angle a_0 \rangle \equiv \langle \alpha, 0 \rangle$ be identified with the point satisfying $\langle \pm |a_{\lceil n/2 \rceil}|, \angle a_0 \rangle \equiv \langle -\alpha, 2\pi \rangle$.

Expressions (6.2) enforce $(n-1)$ additional constraints expressed as *strict* inequalities on C^∞ functions over the transformed space ($\mathbb{C}^{\lfloor n/2 \rfloor} \times S^1$ for odd n or $\mathbb{C}^{\lfloor n/2 \rfloor - 1} \times \mathbb{M}^2$ for even n). That the functions are C^∞ is evident from their being composed entirely of $+, -, \times$, and $\bar{}$ (the sum, difference, product and conjugate operators respectively).

We note immediately, based on continuity and strict inequality, that the resulting space is *open* in $\mathbb{C}^{\lfloor n/2 \rfloor} \times S^1$ (when n is odd) or $\mathbb{C}^{\lfloor n/2 \rfloor - 1} \times \mathbb{M}^2$ (when n is even). Moreover, since the space is the image of a connected set under a continuous mapping, it is *connected* as well. We denote the resultant space by $\mathbb{L}_n$.

We now consider the case wherein both distinct and multiple roots are allowed.

Theorem 6.2.2 *The transformed space corresponding to the polynomial $f(z)$ constrained to have all roots on $|z| = 1$ without the requirement that they be distinct, is the* closure *of $\mathbb{L}_n$ ($\overline{\mathbb{L}}_n$) in $\mathbb{C}^{\lfloor n/2 \rfloor} \times S^1$ for odd n, or in $\mathbb{C}^{\lfloor n/2 \rfloor - 1} \times \mathbb{M}^2$ for even n. Furthermore, the set $(\overline{\mathbb{L}}_n \backslash \mathbb{L}_n)$ lies on the boundary of $\overline{\mathbb{L}}_n$.*

Proof: *See Appendix A.*

The multidimensional boundary set $(\overline{\mathbb{L}}_n \backslash \mathbb{L}_n)$ can be partitioned, based on the multiplicity of corresponding roots, into connected sets of fixed dimensionality. Each such set is *diffeomorphic* to an appropriate manifold $\mathbb{L}_{n-1}, \mathbb{L}_{n-2}, ...,$ or $\mathbb{L}_0$ by way of the mapping that disregards all but one member of each multiple root. Finally, $\overline{\mathbb{L}}_n$ is bounded because $\forall i \; |a_i| \leq \binom{n}{i}$.

Corollary 6.2.1 *The transformed space is a* compact *manifold with* boundaries*; a subset of the same dimension of $\mathbb{C}^{\lfloor n/2 \rfloor} \times S^1$ if n is* odd *or of $\mathbb{C}^{\lfloor n/2 \rfloor - 1} \times \mathbb{M}^2$ if n is* even*.*

The nature of the spaces for dimensions $n = 1, 2, 3$ is best demonstrated in figures. For $n = 1$, the phase-space is the unit circle S^1, for $n = 2$, the Möbius band, and for $n = 3$, a solid torus whose cross-section is a concave triangle that revolves uniformly around its centroid as one travels around the torus. Figure 6.1 presents the phase-spaces for $n = 1$, 2 and 3.

Finally, the phase-space for the entire neuronal system is the Cartesian product of the phase-spaces of the individual neurons. We shall henceforth denote the phase-space of neuron i by ${}^i\overline{\mathbb{L}}_{n_i}$. The phase-space of the system is then $\prod_{i=1}^{\mathcal{S}} {}^i\overline{\mathbb{L}}_{n_i}$.

Having formulated the above representation for the state of a system of neurons, we must now consider the effect it has on the description of the membrane potential function. In Chapter 4, $P_i(x_1^1, ..., x_1^{n_1}, x_2^1, ..., x_2^{n_2}, ..., x_m^1, ..., x_m^{n_m}; x_i^1, ..., x_i^{n_i})$ was assumed to be C^∞ for all neurons i. In Appendix B we define a corresponding function $\widetilde{P}_i : {}^1\overline{\mathbb{L}}_{n_1} \times {}^2\overline{\mathbb{L}}_{n_2} \times ... \times {}^m\overline{\mathbb{L}}_{n_m} \times {}^i\overline{\mathbb{L}}_{n_i} \rightarrow \mathbb{R}$ on the transformed space, that is C^∞.

6.3 Geometric Structure of the Phase-Space: A Finer Topology

In the previous section we constructed the phase-space for an individual neuron as a fixed dimensional manifold, the fixed dimensionality derived from the existence of an upper bound on the number of effective, efferent spikes that the neuron can possess at any time. We also noted

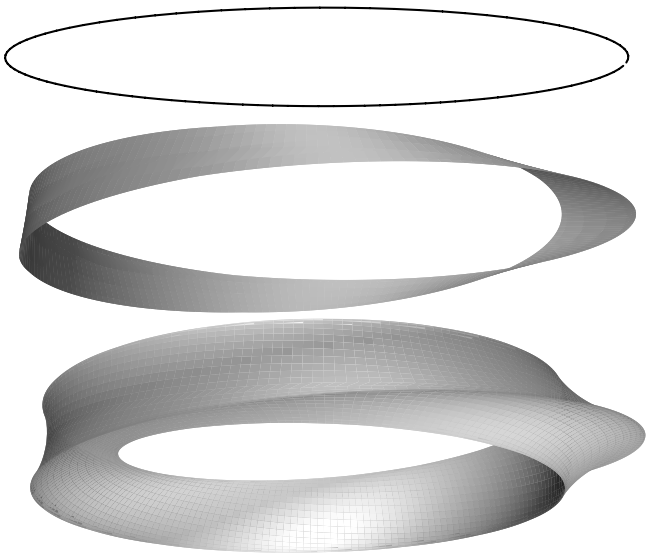

Figure 6.1: Phase-spaces for $n = 1, 2$ and 3. Note that the one-dimensional boundary of the Möbius band is a circle, and the two- and one-dimensional boundaries of the torus are a Möbius band and a circle, respectively.

that at certain times, the neuron might possess fewer effective spikes. It follows from the previous section that under such circumstances, the remaining variables are set at $e^{ix_i^j} = 1$. In this section, we examine the structure induced in the phase-space as a result of this feature.

Formally, we denote by $p \in \langle {}^1\overline{\mathbb{L}}_{n_1} \times {}^2\overline{\mathbb{L}}_{n_2} \times ... \times {}^{\mathcal{S}}\overline{\mathbb{L}}_{n_{\mathcal{S}}} \rangle$ a point in the phase-space and by $\langle p_1, p_2, ..., p_{\mathcal{S}} \rangle$ its projection on the corresponding individual spaces, that is, $p_i \in {}^i\overline{\mathbb{L}}_{n_i}$. For each neuron i, we denote the number of variables set at $e^{ix_i^j} = 1$ by σ_i. Such spikes we label as *dead* since their effectiveness on all neurons has expired. All other spikes we label as *live*.

To begin, we note that for any ${}^i\overline{\mathbb{L}}_{n_i}$, the subset of the space satisfying $\sigma_i \geq k$ lies within the subset of the space satisfying $\sigma_i \geq (k-1)$. In the previous section we established that the phase-space of a neuron with a sum total of k spikes is a *k-dimensional* compact manifold. We now relate (a) a phase-space A corresponding to k spikes to (b) the subset satisfying $\sigma \geq 1$ of a phase-space B corresponding to $(k+1)$ spikes. Equating the appropriate polynomials, $(z-1)[z^k + a_{k-1}z^{k-1} + ... + a_0] = z^{k+1} + b_k z^k + ... + b_0$, we arrive at

$$\begin{array}{ll} b_i = a_{i-1} - a_i & \text{for } i = 0, ..., k \quad \text{(assuming } a_{-1} = 0, a_k = 1), \quad \text{hence,} \\ a_{i-1} = \sum_{j=i}^{k} b_j + 1 & \text{for } i = 1, ..., k. \end{array} \tag{6.3}$$

That the mapping $\mathcal{F}_k : A \rightarrow B$, $\mathcal{F}_k(a_{k-1}, ..., a_{\lceil k/2 \rceil}; \angle a_0) = (b_k, ..., b_{\lceil (k+1)/2 \rceil}; \angle b_0)$,

is injective follows directly from equations (6.3). That the mapping is an immersion (that is, *rank*$(\mathcal{F}_k) = \dim(A) = k$ at all points) follows from the description of $(D\mathcal{F}_k)$, which when simplified results in the $(k+1 \times k)$ matrices (for even k and odd k respectively),

$$\begin{pmatrix} 1 & \cdots & 0 & 0 \\ \vdots & \ddots & \vdots & \vdots \\ 0 & \cdots & 1 & 0 \\ 0 & \cdots & 0 & \cos(\frac{\angle a_0}{2}) \\ 0 & \cdots & 0 & \sin(\frac{\angle a_0}{2}) \end{pmatrix} \text{ and } \begin{pmatrix} 1 & 0 & \cdots & 0 & 0 \\ 0 & 1 & \cdots & 0 & 0 \\ \vdots & \vdots & \ddots & \vdots & \vdots \\ 0 & 0 & \cdots & 1 & 0 \\ 0 & 0 & \cdots & 0 & 1 \\ |a_{\lceil \frac{k}{2} \rceil}| & 0 & \cdots & 2\sin(\frac{\angle a_0}{2}) & -2\cos(\frac{\angle a_0}{2}) \end{pmatrix}. \quad (6.4)$$

A being compact, $\mathcal{F}_k : A \to B$ is also an *imbedding*. Consequently, A is a homeomorphism onto its image, that is, the topology induced by A on $\mathcal{F}_k(A)$ is compatible with the subspace topology induced by B on $\mathcal{F}_k(A)$. Finally, repeated application of the argument for distinct values of k establishes that for all k, the subset of the space satisfying $\sigma \geq k$ is a *regular-submanifold* of the subset of the space satisfying $\sigma \geq (k-1)$.

Alternatively, the mapping from a space A corresponding to k spikes, to the subset satisfying $\sigma \geq (l-k)$ of a space B corresponding to l spikes, can be constructed directly by composing multiple $\mathcal{F}$'s. Not only does the mapping $\mathcal{F}_k^l = \mathcal{F}_{l-1} \circ \mathcal{F}_{l-2} \circ ... \circ \mathcal{F}_k$ map the space A into the space B, but it also maps relevant subspaces[3] of A into corresponding subspaces of B. Since $(D\mathcal{F}_k^l) = (D\mathcal{F}_{l-1}) * (D\mathcal{F}_{l-2}) * ... * (D\mathcal{F}_k)$, it follows from the arguments in the previous paragraph that $\mathcal{F}_k^l$ is an imbedding.

Figure 6.2 displays the subspaces satisfying $\sigma \geq 2$ (imbedding of a circle) and $\sigma \geq 1$ (imbedding of a Möbius band) located within the phase-space for $n = 3$. We shall henceforth denote by ${}^i\overline{\mathbb{L}}_{n_i}^j$ the subspace satisfying $\sigma_i \geq j$ for neuron i. Consequently, ${}^i\overline{\mathbb{L}}_{n_i} = {}^i\overline{\mathbb{L}}_{n_i}^0 \supset {}^i\overline{\mathbb{L}}_{n_i}^1 \supset ... \supset {}^i\overline{\mathbb{L}}_{n_i}^{n_i}$.

It must be noted that $\mathcal{F}_k^l : A \to B$ not only maps phase-spaces but also maps flows identically, a fact manifest in the following informal description of the dynamics of the system: If the state of the system at a given instant is such that neither any live spike is on the verge of death nor is any neuron on the verge of spiking, then all live spikes continue to age uniformly.

[3]Subspaces corresponding to at most $(k-1), (k-2), ..., 0$ live spikes.

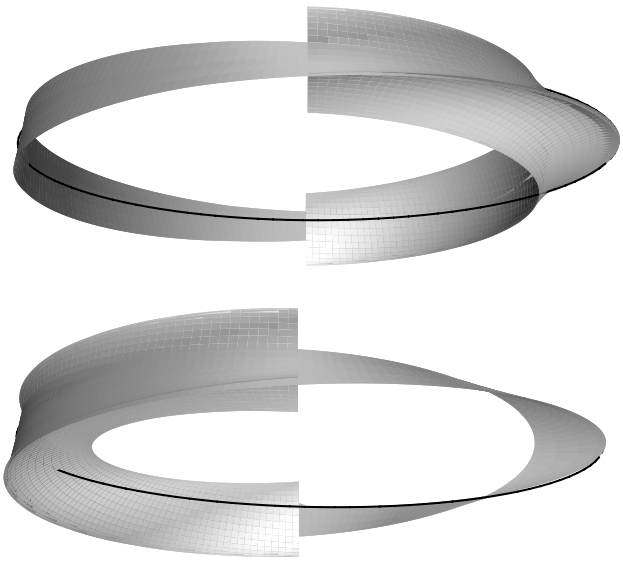

Figure 6.2: Subspaces $\sigma \geq 2$ and $\sigma \geq 1$ in the phase-space for $n = 3$. The torus is cut in half, and the circle and the Möbius band within each half are exposed separately.

If a spike is on the verge of death, it expires (stops aging). This occurs when the spike reaches $e^{ix_i^j} = 1$. If a neuron is on the verge of spiking, exactly one dead spike corresponding to that neuron is turned live.

Since all dead spikes remain stationary at $e^{ix_i^j} = 1$, they register as a constant factor in the dynamics of a neuron. This has the important ramification that the total number of spikes assigned to a neuron has little impact on its phase-space dynamics. $\mathcal{F}_k^l : A \to B$, in essence, constitutes a bridge between all flows that correspond to a given number of live spikes possessed by a neuron over a given interval of time. While the total number of spikes assigned to a neuron dictates the dimensionality of its entire phase-space, flows corresponding to a given number of live spikes lie on a fixed dimensional submanifold and are C^∞-*conjugate*[4] to each other.

We note that $\forall j \geq 1$ ${}^i\overline{\mathbb{L}}_{n_i}^j$ is a C^∞ hypersurface of dimension $(n_i - j)$ in ${}^i\overline{\mathbb{L}}_{n_i}$.[5] Moreover, since $\forall j \geq 2$ ${}^i\overline{\mathbb{L}}_{n_i}^j$ features a multiple root at e^{i0}, it lies on the boundary of ${}^i\overline{\mathbb{L}}_{n_i}$.

The submanifolds ${}^i\overline{\mathbb{L}}_{n_i}^j$ $(j = 1, ..., n_i)$ are not revealed in the topology of ${}^i\overline{\mathbb{L}}_{n_i}$ regarded (as

[4]Since $\mathcal{F}_k^l : A \to B$ is C^∞.

[5]$S \subset M$ is a k-dimensional C^p hypersurface in the m-dimensional manifold M if for every point $s \in S$ and coordinate neighborhood $\langle U, \phi \rangle$ of M such that $s \in U$, $\phi(U \cap S)$ is the *image* of an open set in $\mathbb{R}^k$ under an *injective* C^p mapping of rank k, $\varphi : \mathbb{R}^k \to \mathbb{R}^m$.

the case may be) as a subspace of $\mathbb{C}^{\lfloor n_i/2 \rfloor} \times S^1$ or of $\mathbb{C}^{\lfloor n_i/2 \rfloor - 1} \times \mathbb{M}^2$ (topologized by respective standard differentiable structures). We therefore assign ${}^i\overline{\mathbb{L}}_{n_i}$ the topology generated by the family of all *relatively* open subsets of ${}^i\overline{\mathbb{L}}^j_{n_i}$, $\forall j \geq 0$. This new, *strictly finer* topology better matches our intuitions regarding the set of states that should comprise the neighborhood of any given state of the system.

Previously, we defined a C^∞ function $\widetilde{P}_i(\cdot)$ that represented the potential at the soma of neuron i. We denote by P_i^S the subset of the space wherein $\widetilde{P}_i(\cdot) = \mathcal{T}$, and by P_i^I the subset wherein $d\widetilde{P}_i(\cdot)/dt \geq 0$ is also true. Trivially, $P_i^I \subseteq P_i^S$.

We now note that at all points satisfying $\widetilde{P}_i(\cdot) = \mathcal{T}$ there exists a direction x such that $\partial\widetilde{P}_i(\cdot)/\partial x \neq 0$.[6] It therefore follows from the implicit function theorem that P_i^S is a regular submanifold of codimension 1. Furthermore, P_i^I is a closed subset of P_i^S. This is based on the observation that $\widetilde{P}_i(\cdot)$ being C^∞, $d\widetilde{P}_i(\cdot)/dt$ along any direction d/dt is C^∞ on P_i^S.

To summarize, the phase space $\langle {}^1\overline{\mathbb{L}}_{n_1} \times {}^2\overline{\mathbb{L}}_{n_2} \times ... \times {}^{\mathcal{S}}\overline{\mathbb{L}}_{n_{\mathcal{S}}} \rangle$ contains (a) $\mathcal{S}$ C^∞ hypersurfaces P_i^I for $i = 1...\mathcal{S}$, and (b) for each ${}^i\overline{\mathbb{L}}_{n_i}$, C^∞ hypersurfaces ${}^i\overline{\mathbb{L}}^1_{n_i} \supset {}^i\overline{\mathbb{L}}^2_{n_i} \supset ... \supset {}^i\overline{\mathbb{L}}^{n_i}_{n_i}$ of successively lower dimensions.

6.4 The Velocity Field

In Section 6.2 we described the phase-space for a system of neurons, and in Section 6.3 we assigned it a particular topology. In order to complete the description of the abstract dynamical system, we must assign the phase-space a velocity field.

In this section we stipulate the velocity field, $\mathcal{V} : \prod_{i=1}^{\mathcal{S}} {}^i\overline{\mathbb{L}}_{n_i} \rightarrow \prod_{i=1}^{\mathcal{S}} T({}^i\overline{\mathbb{L}}_{n_i})$, which arises from the natural dynamics of the system. $T(\cdot)$ denotes the tangent bundle (appropriated from the ambient space $\mathbb{C}^{\lfloor n_i/2 \rfloor} \times S^1$ for odd n_i or $\mathbb{C}^{\lfloor n_i/2 \rfloor - 1} \times \mathbb{M}^2$ for even n_i).

We define two vector fields, $\mathcal{V}^1$ and $\mathcal{V}^2$. For the case in which no spike is on the verge of death and no neuron is on the verge of spiking, the velocity is specified by $\mathcal{V}^1$. Formally, $\mathcal{V}^1$ applies to all points $p \in \prod_{i=1}^{\mathcal{S}} ({}^i\overline{\mathbb{L}}^{\sigma_i}_{n_i} \backslash {}^i\overline{\mathbb{L}}^{\sigma_i+1}_{n_i})$ for all values of $\sigma_i \leq n_i$ that satisfy $\forall i = 1, ..., \mathcal{S}$ $p \notin P_i^I$. For the case in which a neuron is on the verge of spiking, the velocity is specified by $\mathcal{V}^2$.

[6] This is not the case when $\widetilde{P}_i(\cdot) = \mathcal{T}$ is a point. In all other cases there exist effective spikes that satisfy the criterion.

Formally, $\mathcal{V}^2$ applies to all points p that satisfy $\exists i$ such that $p \in P_i^I$. Since $\mathcal{V}^1$ is, by definition, a function of σ_i's for all $i = 1, ..., \mathcal{S}$, it accounts for the case in which a spike is on the verge of death.

It follows from the natural dynamics of the system that given point $p = \langle p_1, ..., p_{\mathcal{S}} \rangle$ in the phase-space, $\mathcal{V}^1(p) = \langle \mathcal{V}_1^1(p), ..., \mathcal{V}_{\mathcal{S}}^1(p) \rangle$ can be redefined as $\langle \mathcal{V}_1^1(p_1), ..., \mathcal{V}_{\mathcal{S}}^1(p_{\mathcal{S}}) \rangle$. That is, each component $\mathcal{V}_i^1$ of $\mathcal{V}^1$ is solely a function of $p_i \in {}^i\overline{\mathbb{L}}_{n_i}^{\sigma_i}$. This is also true for $\mathcal{V}^2$. Once it is determined which P_i^I's p lies on, each component $\mathcal{V}_i^2$ can be computed based solely on p_i.

We noted earlier that the differentiable structures of ${}^i\overline{\mathbb{L}}_{(n_i-\sigma_i)}^0$ and ${}^i\overline{\mathbb{L}}_{n_i}^{\sigma_i}$ are compatible by virtue of $\mathcal{F}_{(n_i-\sigma_i)}^{n_i}$ being an imbedding. We also noted that flows corresponding to $\mathcal{V}^1$ for k live spikes lie on a k-dimensional submanifold and are C^∞-*conjugate* to each other, $\mathcal{F}_k^l$ constituting the bridge between such flows. We therefore define $\mathcal{V}_i^1$ on $({}^i\overline{\mathbb{L}}_{(n_i-\sigma_i)}^0 \backslash {}^i\overline{\mathbb{L}}_{(n_i-\sigma_i)}^1)$. The corresponding velocity field on $({}^i\overline{\mathbb{L}}_{n_i}^{\sigma_i} \backslash {}^i\overline{\mathbb{L}}_{n_i}^{\sigma_i+1})$ is then defined as $\mathcal{F}_{(n_i-\sigma_i)_\star}^{n_i}(\mathcal{V}_i^1)$.[7]

Let p_i correspond to $z^{n_i-\sigma_i} + a_{n_i-\sigma_i-1} z^{n_i-\sigma_i-1} + ... + a_0 = \prod_{j=1}^{n_i-\sigma_i}(z - z_j)$. Since all roots rotate at constant speed, that is, $z_j = e^{i(\theta_j + \frac{2\pi t}{\Upsilon})}$, $dz_j/dt = \frac{2\pi i}{\Upsilon} z_j$. Simple algebra then demonstrates:

Theorem 6.4.1 *$\mathcal{V}_i^1$ for the C^∞-conjugate flows on $({}^i\overline{\mathbb{L}}_{(n_i-\sigma_i)}^0 \backslash {}^i\overline{\mathbb{L}}_{(n_i-\sigma_i)}^1)$ is given by*

$$\frac{da_{n_i-\sigma_i-k}}{dt} = \frac{2\pi}{\Upsilon} k\hat{\theta} \text{ for } k = 1, ..., \lfloor \frac{n_i - \sigma_i}{2} \rfloor \text{ and } k = n_i - \sigma_i \tag{6.5}$$

$$\frac{d|a_{\frac{n_i-\sigma_i}{2}}|}{dt} = 0 \text{ when } (n_i - \sigma_i) \text{ is even.} \tag{6.6}$$

$\hat{\theta}$ denotes the basis vector $\partial/\partial\theta$ on $\mathbb{C} \ni a_{n_i-\sigma_i-k}$ for any $k = 1, ..., \lfloor \frac{n_i-\sigma_i}{2} \rfloor$, represented as $\{\langle r, \theta \rangle \mid re^{i\theta} = a_{n_i-\sigma_i-k}\}$, on $S^1 \ni a_0$ represented as $\{\theta \mid \theta = \angle a_0\}$, and on $\mathbb{M}^2 \ni \langle a_{\frac{n_i-\sigma_i}{2}}, a_0 \rangle$ for even $(n_i - \sigma_i)$, represented as $\{\langle r, \theta \rangle \mid r = \pm|a_{\frac{n_i-\sigma_i}{2}}|, \theta = \angle a_0\}$.

Stated informally, each parameter revolves around its origin at uniform speed, the speed of successive parameters increasing in steps of $(2\pi/\Upsilon)$.

Turning our attention to $\mathcal{V}_i^2$, we note that $\mathcal{V}_i^2(p_i)$ can be obtained from $\mathcal{V}_i^1(p_i)$ by setting σ_i to $(\sigma_i - 1)$; $\mathcal{V}_i^2(p_i)$ for $p_i \in ({}^i\overline{\mathbb{L}}_{n_i}^{\sigma_i} \backslash {}^i\overline{\mathbb{L}}_{n_i}^{\sigma_i+1})$ is equivalent to $\mathcal{V}_i^1(p_i)$ on ${}^i\overline{\mathbb{L}}_{n_i}^{\sigma_i-1}$ *ignoring* the fact that p_i lies additionally on ${}^i\overline{\mathbb{L}}_{n_i}^{\sigma_i} \subset {}^i\overline{\mathbb{L}}_{n_i}^{\sigma_i-1}$.

[7] The reader should refer to Chapter 5 for questions regarding the mapping of vector fields from one C^∞ manifold to another.

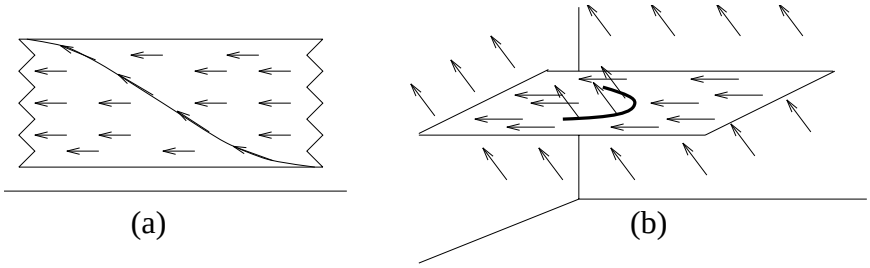

Figure 6.3: Schematic depiction of the velocity field $\mathcal{V}$.

We have defined $\mathcal{V} : \prod_{i=1}^{\mathcal{S}} {}^i\overline{\mathbb{L}}_{n_i} \rightarrow \prod_{i=1}^{\mathcal{S}} T({}^i\overline{\mathbb{L}}_{n_i})$ based on our absolute knowledge of flows in the phase-space. The utility of this construction is to be found in the assistance it renders in the analysis of local properties of flows (a topic that is pursued in Chapter 8). $\mathcal{V}$ is however *discontinuous*. It must therefore be confirmed that $\mathcal{V}$ does not generate inconsistencies in the model. We consider this problem next.

Both $\mathcal{V}_i^1$ and $\mathcal{V}_i^2$ are smooth on $({}^i\overline{\mathbb{L}}_{n_i}^{\sigma_i} \backslash {}^i\overline{\mathbb{L}}_{n_i}^{\sigma_i+1})$ for any σ_i. The only points where the projection of a trajectory $\Psi(x,t)$ on ${}^i\overline{\mathbb{L}}_{n_i}^{\sigma_i}$ is not differentiable (where, incidentally, it is not even continuous when regarded in the context of the new, finer topology) is therefore when it meets ${}^i\overline{\mathbb{L}}_{n_i}^{\sigma_i+1}$ or it meets P_i^I. This gives rise to the potential problem that $d\widetilde{P}_i(\cdot)/dt$ might not be computable on P_i^I, for whereas $\widetilde{P}_i(\cdot)$ is C^∞, one component of $d\Psi(x,t)/dt$ in ${}^i\overline{\mathbb{L}}_{n_i}^{\sigma_i}$—the velocity of the dead spike that just turned live—is undefined. However, one needs only to recall from Appendix B that for any spike x stationed at e^{i0}, $\partial P_i(\cdot)/\partial x = 0$ over an infinitesimal interval $(e^{i\delta} > e^{ix} > e^{i(2\pi-\delta)})$. The problem is therefore resolved trivially.

Figure 6.3 presents a schematic depiction of the velocity vector field $\mathcal{V}$ described above. Figure 6.3(a) displays $\mathcal{V}$ corresponding to a patch of ${}^i\overline{\mathbb{L}}_2^1$ within a patch of ${}^i\overline{\mathbb{L}}_2^0$, and Figure 6.3(b) displays $\mathcal{V}$ corresponding to a P_i^I lying on a patch of ${}^i\overline{\mathbb{L}}_3^1$ within ${}^i\overline{\mathbb{L}}_3^0$.

6.5 The Abstract Dynamical System

We are now in a position to define an abstract dynamical system without reference to neuronal systems. The phase-space of the system is given by $\prod_{i=1}^{\mathcal{S}} {}^i\overline{\mathbb{L}}_{n_i}$ (with the topology described in Section 6.3), which contains $\mathcal{S}$ C^∞ hypersurfaces P_i^I for $i = 1, ..., \mathcal{S}$. The velocity field $\mathcal{V}$ on the phase-space is as defined in the previous theorem.

In order for the system to be consistent, each hypersurface P_i^I must at the least satisfy two

additional constraints.

1. The criterion that any neuron i possess at most n_i live spikes can be enforced by the constraint: $\forall i = 1, ..., \mathcal{S},\ P_i^I \cap (\prod_{j=1}^{i-1} {}^j\overline{\mathbb{L}}_{n_j}^0 \times ({}^i\overline{\mathbb{L}}_{n_i}^0 \backslash {}^i\overline{\mathbb{L}}_{n_i}^1) \times \prod_{j=i+1}^{\mathcal{S}} {}^j\overline{\mathbb{L}}_{n_j}^0) = \emptyset$.

2. The criterion that multiple roots occur only at e^{i0} (when the spikes are dead) can be enforced by requiring the normal to the hypersurface $P_i^I \cap \prod_{j=1}^{\mathcal{S}} ({}^j\overline{\mathbb{L}}_{n_j}^{\sigma_j - 1} \backslash {}^j\overline{\mathbb{L}}_{n_j}^{\sigma_j + 1})$ at all locations on $P_i^I \cap \prod_{j=1}^{\mathcal{S}} ({}^j\overline{\mathbb{L}}_{n_j}^{\sigma_j} \backslash {}^j\overline{\mathbb{L}}_{n_j}^{\sigma_j + 1})$ not to be orthogonal to $\mathcal{V}^2$ for any values of i and $\sigma_j \leq n_j$.

Finally, since neurons that spike spontaneously are not modeled, one can additionally enforce the weaker constraint: $\forall i = 1, ..., \mathcal{S}$, $P_i^I \cap \prod_{j=1}^{\mathcal{S}} {}^j\overline{\mathbb{L}}_{n_j}^{n_j} = \emptyset$. It then follows that $\prod_{i=1}^{\mathcal{S}} {}^i\overline{\mathbb{L}}_{n_i}^{n_i}$, denoting the state of quiescence in the neuronal system, is the sole *fixed point* of the dynamical system.

6.6 Summary

In this chapter, we formulated an abstract dynamical system that models systems of biological neurons. The model was constructed by extending the model of a lone biological neuron described in Chapter 4.

We defined the phase-space of the system in Section 6.2, assigned it a particular topology in Section 6.3, and described the velocity field that overlays the phase-space in Section 6.4.

The phase-space of neuron i is represented by ${}^i\overline{\mathbb{L}}_{n_i}$ (the superscript i denotes the neuron and the subscript n_i the dimensionality of the space or equivalently the number of spikes assigned to the neuron). The phase-space for a system of $\mathcal{S}$ neurons is therefore given by $\prod_{i=1}^{\mathcal{S}} {}^i\overline{\mathbb{L}}_{n_i}$.

$\prod_{i=1}^{\mathcal{S}} {}^i\overline{\mathbb{L}}_{n_i}$ contains $\mathcal{S}$ C^∞ hypersurfaces P_i^I for $i = 1...\mathcal{S}$, each representing the class of states of the system that causes the corresponding neuron to spike. The specific instantiation of each hypersurface is determined by the connectivity between the neurons in the system, the strength of the synapses in the system, their modulation of one another's effects at the somas of individual neurons, and a host of other physiological and anatomical parameters.

Each ${}^i\overline{\mathbb{L}}_{n_i}$ contains n_i C^∞ hypersurfaces ${}^i\overline{\mathbb{L}}_{n_i}^1 \supset {}^i\overline{\mathbb{L}}_{n_i}^2 \supset ... \supset {}^i\overline{\mathbb{L}}_{n_i}^{n_i}$ of successively lower dimensions. These hypersurfaces denote the class of states of neuron i that correspond to at most $(n_i - 1)$ live spikes, at most $(n_i - 2)$ live spikes, and so forth.

This concludes the description of the abstract dynamical system. The remainder of the thesis investigates the salient characteristics of the dynamics of this system. In Chapter 7, we familiarize the reader with the generic dynamics of the system through numerous simulation experiments. We then formally analyze the dynamics of the system in Chapters 8 and 9.

Chapter 7

Model Simulation and Results

A model is worthwhile only to the extent to which it succeeds in emulating the salient behavior of the physical system it models. In this chapter, we therefore investigate by means of simulation the dynamical behavior of the model just described.

We have chosen as our target unit a typical *column* in the neocortex. These neuronal subsystems are ideally suited for our purpose because, on the one hand, their configurations (connectivity pattern, distribution of synapses, etc.) fit statistical distributions and, on the other, they exhibit distinctive patterns of *qualitative* dynamical behavior.

We must mention here that although the anatomy and physiology of the neocortical column has been thoroughly explored, the prodigious amount of information necessary to accurately model any particular neocortical column is neither available at present, nor is it expected to be available in the near future. Furthermore, it is not our intent to model any particular neocortical column. Our principal objective is to determine whether the qualitative aspects of the dynamics of appropriate instantiations of the system constructed in Chapter 6 match those of neocortical columns in the brain.

The nature of the results presented in this chapter is therefore more qualitative than quantitative. Any claims made regarding the capacity of the model at emulating a particular behavior should therefore be construed primarily as a *cautious* affirmation of the model.

Sections 7.1 and 7.2 describe the generic features of the anatomy, physiology, and the dynamics of neocortical columns. In Section 7.3, we describe several instantiations of the abstract dynamical system, each modeling a typical column in the neocortex to a different degree of accuracy. Section 7.4 describes the classes of data that are recorded from the simulation experiments, and Section 7.5 compares them to those reported from the real biological system.

7.1 General Features of the Anatomy and Physiology of Neocortical Columns

Extensive information is available about the anatomical and physiological composition of the neocortex (Braitenberg & Schüz, 1991; Shepherd, 1998). While not sharply defined everywhere, neocortical columns have a diameter of approximately 0.5 mm. Intracolumn connectivity is markedly denser than intercolumn connectivity. Whereas inhibitory connections play a prominent role within a column, intercolumn connections are distinctly excitatory. A column contains approximately 10^5 neurons. The number of synapses each neuron makes ranges between 10^3 and 10^4. The probability of a neuron's making multiple synapses on the dendrite of a postsynaptic neuron is fairly low (Braitenberg, 1978). The connectivity between neurons within a column (intracolumn as opposed to thalamic afferents), while having evolved to achieve a specific function, has been experimentally ascertained to *fit* a statistical distribution (Schüz, 1992). The location of afferent synapses on the collaterals of the neurons has similarly been shown to fit a statistical distribution (Braitenberg & Schüz, 1991).

Neurons in the neocortex can be divided into two main groups: the spiny and the smooth neurons. Spiny neurons can, in general, be subdivided into pyramidal and stellate cells, with pyramidal cells constituting by far the major morphological class. Diversity among smooth neurons is much higher (Peters & Regidor, 1981). Spiny cells receive only Type II (inhibitory) synapses on their somas and both Type I (excitatory) and Type II synapses on their dendrites. They are presynaptic to only Type I synapses. Smooth cells receive both Type I and Type II synapses on their somas and are, in general, presynaptic to Type II synapses (Peters & Proskauer, 1980). Approximately 80% of all neurons in the neocortex are spiny, and the rest are smooth. Both kinds contribute on average to the same number of synapses per neuron.

Axonal arborizations that make local connections range in length from 100 to 400 μm. The speed of propagation of a spike can be estimated at approximately 1 m/s based on the fact that axons within a column are unmyelinated. Synaptic delays range between 0.3 and 0.5 msec. Consequently, the time interval between the generation of a spike at an axon-hillock and its subsequent arrival across a synapse can be estimated to lie between 0.4 and 0.9 msec. Finally, anatomical investigations suggest that dendritic collaterals are seldom longer than three space constants.[1]

[1]The space constant is the distance over which response drops by a factor of e.

7.2 General Features of the Dynamics of Neocortical Columns

The past few decades have witnessed numerous investigations into the electrophysiological activity of the cortex. The majority of these studies fall under two categories. The first is the recording of action potentials (spikes), which reflect the output of single cortical neurons with a time resolution of milliseconds, and the second is the recording of the Electroencephalogram (EEG), a slow, continuous wave that reflects the activity of hundreds of thousands of neurons.[2]

An aspect shared universally among single neocortical neuron recordings is the apparent stochastic nature of the spike trains (Burns & Webb, 1976). A good measure of spike variability is given by the coefficient of variation (CV) of an ISI distribution.[3] Spike trains of cortical neurons have CV's ranging from 0.5 to 1.1, resembling a Poisson process for which CV$= 1$.

In the case of EEG recordings, the outputs are significantly more abstruse. Classical signal analysis has long considered EEG records as realizations of (often stationary) stochastic processes, and spectral analysis has been the conventional method for extracting the dominant frequencies of the rhythms (Érdi, 1996). Spectral charts of EEG records generally exhibit peak densities at frequencies of major cerebral rhythms, superimposed on a "1/f" spectral envelope.

Recently, some researchers have come to regard EEG records as the chaotic output of a nonlinear system (Basar, 1990), and have attempted to measure the dimensionality of its various components (Babloyantz, Salazar & Nicolis, 1985; Röschke & Basar, 1989). Unfortunately, the results remain varied and inconclusive.

7.3 Experimental Setup

We conducted simulation experiments to compare the dynamical characteristics of our model to the salient properties of the dynamics of neocortical columns.[4] The parameterized function $v(x,t) = \{\alpha Q/(x\sqrt{t})\}e^{-\beta x^2/t}e^{-\gamma t}$ was used to model the response to a spike at the soma of a

[2] In recent times, however, there has been a distinct shift towards Positron emission tomography (PET) and Functional magnetic resonance imaging (fMRI) studies of the brain.

[3] The CV is defined as the ratio of the standard deviation σ to the mean μ of a distribution.

[4] Instantiating the abstract dynamical system involves the choosing of an appropriate number of spikes to be assigned to each neuron and the associated specification of the hypersurfaces P_i^I for each neuron in the system. The nature of these hypersurfaces depends upon the connectivity of the neurons in the system, the location and strength of synapses, the lengths of the axonal collaterals of the neurons in the system, etc.

neuron (the reader should refer to Chapter 3 for a derivation of this equation). The total response at the soma was computed as the sum of the responses to individual spikes. The parameters α, β, and γ were set so as to fit response curves from NEURON v2.0 (Hines, 1993). Refractoriness was modeled by the function $ce^{-\delta t}$.[5]

Four separate sets of experiments were performed. The physiological accuracy of the model was enhanced with each successive set of experiments. In each case a neuronal system comprising 1000 neurons with each neuron connected *randomly* to 100 other neurons was modeled.[6]

Model I Eighty percent of all neurons in the system were randomly chosen to be excitatory (spiny) and the rest inhibitory (smooth). The strength of a synapse (Q) was chosen randomly from a uniform distribution over the range $[5.7, 15.7]$.[7] Values for the parameters α, β, and γ were chosen so as to model a synaptic response with an uncharacteristically short period of effectiveness ($\tau \approx 10$ msec) and were set at fixed values for the entire system. x in $v(x,t)$ was also set at a fixed value for the entire system. In other words, not only were all afferent synapses assumed to be located at the same distance from the soma, but they were also assumed to be generating identical (to a constant factor) responses. Excitatory and inhibitory neurons were constructed to be identical in all respects save the strength of *inhibitory* synapses, which was enhanced to six times the magnitude ($Q \times 6.0$). The lengths of the axonal collaterals and their variability were assumed to be uncharacteristically large; the time interval between the birth of a spike at a soma and its subsequent arrival across a synapse was randomly chosen to lie between 5 and 15 msec (uniformly distributed). The parameters c and δ in the function modeling refractoriness were set at appropriate values and held constant over the entire system. The threshold was established such that at least 10 excitatory spikes (and no inhibitory spikes) with *coincident* peak impact[8] were required to cause a neuron to fire and it was held constant over the entire system.

---

[5] Whereas in the abstract model, $P(\cdot)$ must necessarily be C^∞, such restrictions do not apply here because the function is, in any case, discretized in time for simulation.

[6] Simulating larger systems of neurons was found to be computationally intractable. Although we did run a few simulations with 10^4 neurons, the limited scope of the simulations did not warrant their inclusion in the text. We also ran experiments on systems with 100 and 500 neurons. The qualitative characteristics of the dynamics described here became more pronounced as the number of neurons in the system (and their connectivity) was increased.

[7] Although arbitrary, this range demonstrated a rich variety of dynamical behaviors with regard to the numerous instantiations of the model. Moreover, the reader should note that the threshold of the neuron was set based on this range, and therefore any model based on a scaled version of this range (with the threshold appropriately scaled) would exhibit identical behavior.

[8] The probability of 10 spikes' arriving in such a manner that their peak impacts on a soma coincide is very low.

The system was initialized with 5 live spikes per neuron chosen randomly over their respective lifetimes (approximately 200 spikes per second per neuron).

Model II The lengths of the axonal collaterals as well as their variability were modified to reflect realistic dimensions; the time interval between the birth of a spike at a soma and its subsequent arrival across a synapse was randomly chosen to lie in the aforementioned range of 0.4 to 0.9 msec. All other aspects of the model were left unchanged.

Model III The unrealistic assumption that all afferent synapses be located at the same distance from the soma and generate similar responses was eliminated. Instead, the locations of the synapses were chosen based on anatomical data (Bernander, Douglas & Koch 1992). On the spiny cells, inhibitory synapses were cast randomly to within a distance of 0.3 space constants from the soma, and excitatory synapses were cast randomly from a distance of 0.3 to 3.0 space constants from the soma. On smooth cells, both inhibitory and excitatory synapses were cast randomly between distances of 0.0 and 3.0 space constants from the soma. Since a synapse closer to the soma induced a more intense response, we were also able to eliminate the factitious assumption of inhibitory synapses' being six times stronger than excitatory synapses. Next, 50% of all excitatory synapses were randomly chosen to be of type non-NMDA (AMPA/kainate) and the rest of type NMDA.[9] Likewise, 50% of all inhibitory synapses were randomly chosen to be of type GABA_A and the rest of type GABA_B. The characteristic response of each kind of synapse was modeled after graphs reported in Bernander, Douglas & Koch (1992) using the parameterized potential function. Finally, the threshold for firing of a neuron was reduced to an uncharacteristically low value, and the system was initialized at a very sparsely active state (approximately 20 spikes per second per neuron).

Model IV a,b The threshold for firing of a neuron was returned to its characteristic value, and the system was initialized at a more realistic state. Two separate initializations, one with approximately 100 spikes per second per neuron and another with approximately 150 spikes per second per neuron, were considered.

It took on average 20 live spikes to cause a neuron to fire.

[9] While the voltage dependence of NMDA synapses can be modeled in this framework, for the sake of simplicity, the NMDA receptors were assumed to be relieved of the Mg^{2+} block at all times. In other words, they were set at peak conductance irrespective of the postsynaptic polarization.

7.4 Data Recorded

The dynamics of several random instantiations of the models was investigated. In each case neurons were assigned a maximum number of effective spikes ($n = \lceil \Upsilon / r \rceil$) based on upper (for Υ) and lower (for r) bounds computed from physiological parameters (Bernander, Douglas & Koch 1992). Each system was initialized randomly, and the ensuing dynamics was observed in the *absence* of external input. Two classes of data was recorded. The temporal evolution of the total number of *live* spikes registered by the entire system (a feature peculiar to the dynamical system under consideration) was recorded as an approximation to EEG data, and individual spike trains of 10 randomly chosen neurons from each system were recorded for comparison with real spike train recordings.

7.5 Results

The most significant outcome of the simulation experiments was the emergence of distinct patterns of *qualitative* dynamical behavior that were found to be robust across all models and their numerous instantiations. Three classes of behavior were encountered. Each randomly generated instantiation of the models possessed an intrinsic range of activity[10] over which the system displayed sustained chaotic behavior. This range was found to conform with what is generally held as "normal operational conditions" in the neocortex. If the system was initiated at an activity level below this range, the total number of live spikes dropped as the dynamics evolved, until the trivial fixed point of zero activity (the state of quiescence) was reached. In contrast, if the system was initiated at an activity level above this range, the total number of live spikes rose until each neuron spiked *periodically* at a rate determined primarily by its absolute refractory period. In other words, the system settled into a periodic orbit of intense regular activity resembling a state of seizure. Figure 7.1 displays the result of one such experiment (two of the three classes of behavior, intense periodic activity and sustained chaotic activity are shown), a result that is representative of the qualitative dynamics of all the systems that were investigated.

The span of the above-mentioned range was identified to be dependent on an assortment

[10]The corresponding region in the phase-space is not exactly quantifiable through numerical analysis because of the nature of chaos. Under conditions of relatively uniform activity, a range with soft bounds was, however, detected with respect to the average spike frequency.

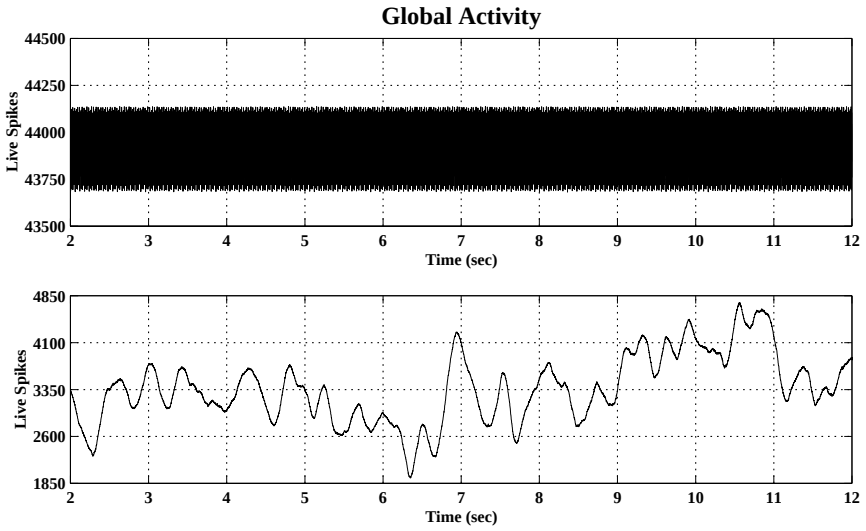

Figure 7.1: Time series (over the same interval) of the total number of live spikes from a representative system initiated at different levels of activity. Two of the three classes of behavior, intense periodic activity and sustained chaotic activity, are shown.

of parameters, most prominent among which were the proportion of inhibitory neurons in the system, their synaptic strengths, and their characteristic responses. Systems constructed from Models III and IV manifest wider spans for the noted range. A closer inspection of the dynamics revealed the almost guardian-like role that the pool of inhibitory neurons played to the volatile tendencies of the excitatory neuron population. Two factors were found critical in the determination of the noted span. The first was the magnitude of the bounds (a) the maximum level of aggregate excitatory activity that the inhibitory pool, when fully operative, could subdue, and (b) the minimum level of aggregate excitatory activity that could recuperate once the inhibitory pool ceased to inhibit, and the second was the gradient of the characteristic response of the inhibitory neuron population in the neighborhood of these bounds, that is, the speed with which the inhibitory population responded to subdue increased activity as well as the speed with which it ceased when activity was sparse.

Figures 7.2 and 7.3 report results from simulations of systems that were initialized at activity levels within the above-mentioned range. Figure 7.2 displays normalized time series data pertaining to the total number of live spikes from representative instantiations of each model. Also shown are the results of a power spectrum analysis corresponding to each of the time series. Although there is substantially more to an EEG record than the dynamics of 1000 model

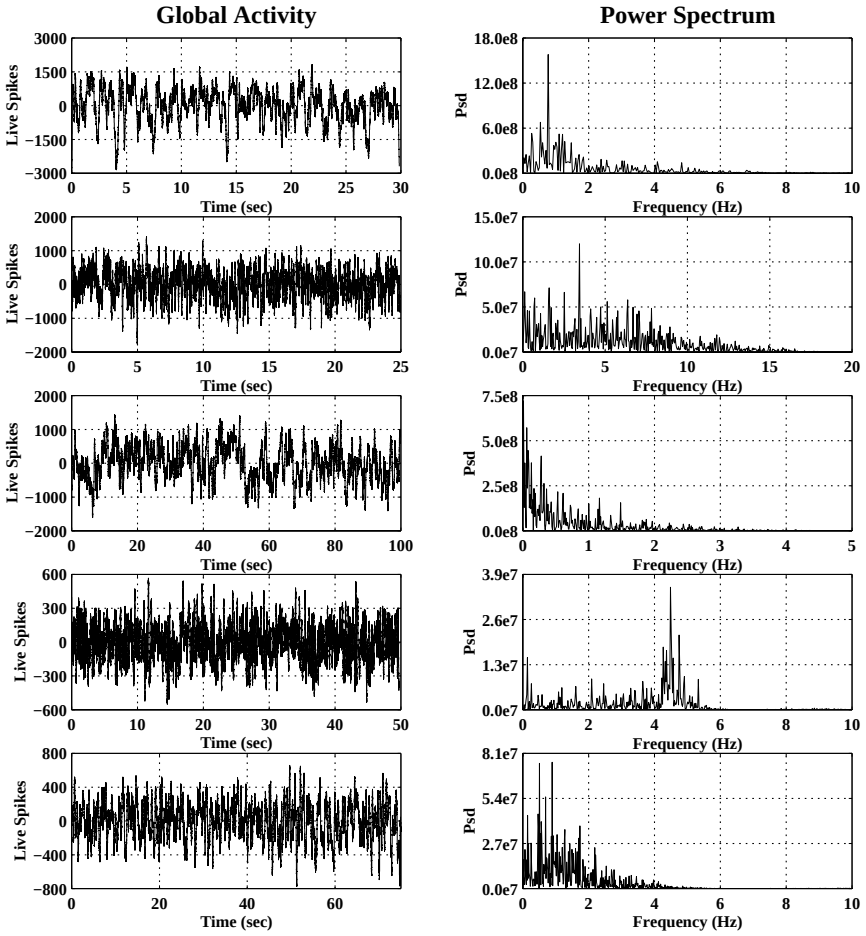

Figure 7.2: Normalized time series of total number of live spikes from instantiations of each model and corresponding Power Spectrums.

neurons, the presence of peak densities at specific frequencies and a "1/f" spectral envelope in each of the spectra supports the view that the abstract system does model the salient aspects of the dynamics of neocortical columns.[11] Furthermore, the absence of any stochastic component to the model[12] demonstrates that the standard features of the EEG spectrum do not necessarily imply that the underlying process is stochastic.

Of the 10 neurons from each system whose spike trains were recorded during simulation, we chose one whose behavior we identified as representative of the mean. Figure 7.3 displays the time series of ISI's of these neurons (one per model) and their corresponding frequency distributions. The spike trains are not only aperiodic, but their ISI distributions suggest that they

[11]The reader is referred to Chapter 2 for specimens of real EEG recordings and corresponding spectra.

[12]The neurons are deterministic, and the system does not receive external input.

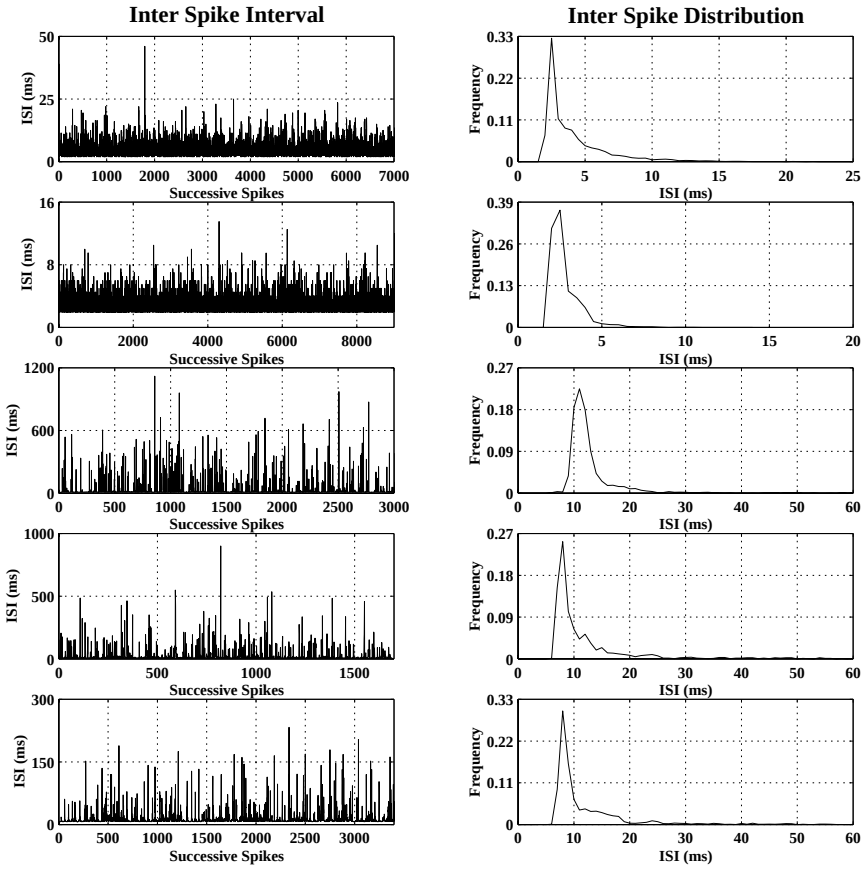

Figure 7.3: Interspike interval recordings of representative neurons from each model and corresponding frequency distributions.

could be generated from a Poisson process. We also computed the values of the CV's for the various spike trains. The results obtained were encouraging: values ranged from 0.063 to 2.921 with the majority falling around 1.21.[13] Neurons with higher rates of firing tended to have lower values of CV. The agreement between the qualitative aspects of the simulation data and that of real ISI recordings speaks additionally in favor of the viability of our model.

We conducted a second set of experiments to ascertain how predisposed the systems were to the chaotic behavior in the presence of *regulating external input*. Each system was augmented with 2 pacemaker neurons—an excitatory and an inhibitory—that spiked at regular intervals.[14] The topology of the system was modified such that of the 100 afferent synapses on each neuron,

[13] Softky & Koch (1993) report that the CV's for spike trains of fast-firing monkey visual cortex neurons lie between 0.5 and 1.1. As the results clearly indicate, our deterministic model can account for this range of data.

[14] The two pacemaker cells spiked every seventeenth time step, generating the simplest form of periodic input.

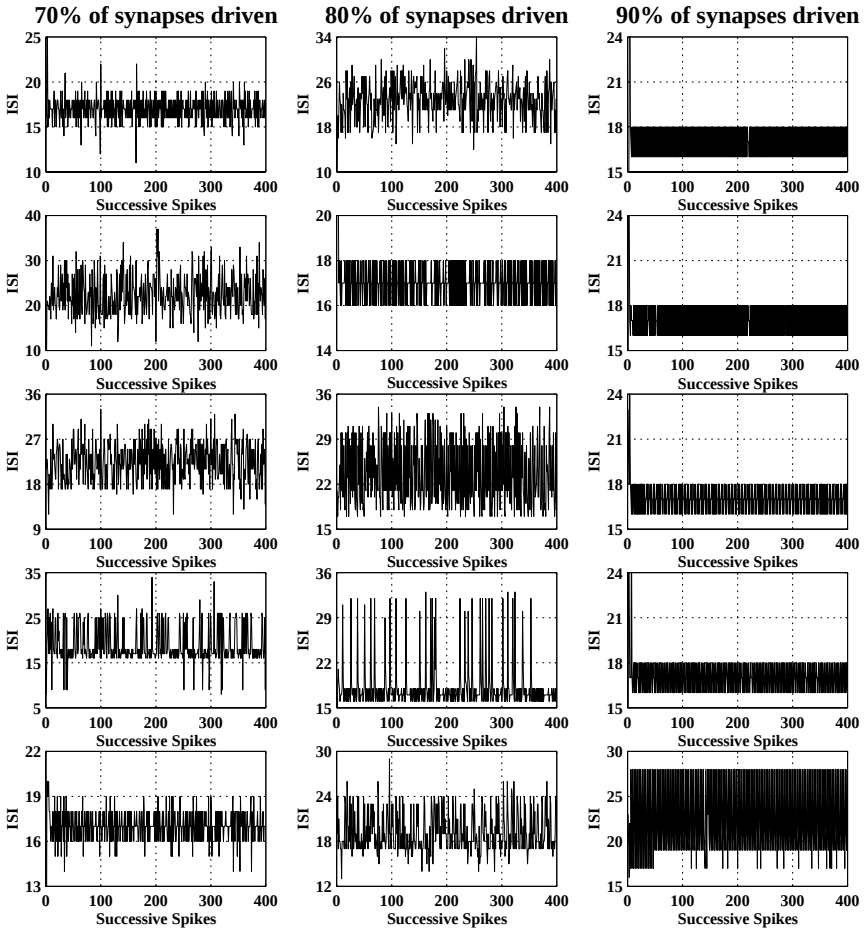

Figure 7.4: Interspike interval recordings of five representative neurons each, from three systems with 70%, 80%, and 90% of the synapses on neurons driven by two pacemaker cells, are shown.

s received their input from one of the 2 pacemaker cells chosen randomly, and the remaining $(100-s)$ received their input from other neurons in the system. s was increased with successive experiments until the system was found to settle into a periodic orbit. Figure 7.4 depicts the ISI's of 5 representative neurons each, from systems with s set at 70, 80, and 90. The discovery that the system did not quite settle into a periodic orbit even when 90% of all synapses were driven by periodic spikes bears witness to the system's propensity for chaotic behavior.

Finally, experiments were conducted to determine whether the systems were sensitive to initial conditions, a feature closely associated with chaotic behavior. Each system was initialized at two proximal points in state-space, and the resulting dynamics was recorded. Respective trajectories were found either to diverge strongly or become coincident. Figure 7.5 depicts the

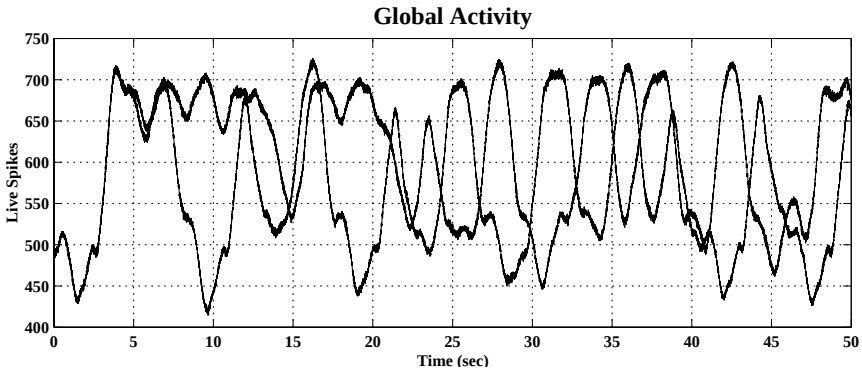

Figure 7.5: Two trajectories that diverge from very close initial conditions.

temporal evolution of the total number of live spikes registered by two identical systems of 100 neurons that were initialized with approximately five live spikes per neuron, chosen randomly over respective lifetimes. The initialization of the two systems was identical except for one spike (chosen randomly) in the second system, which was perturbed by 1 msec. As the figure demonstrates, the trajectories diverged strongly.[15]

The results presented in this chapter are substantially more qualitative than quantitative. The goal of the simulation experiments was not to emulate the dynamics of any *specific* neocortical column. The data necessary to accomplish such a feat are not available, and we do not claim that the idealized neuron models all aspects of a neocortical neuron. The principal objective of the exercise was to demonstrate that the abstract dynamical system developed in the previous chapter was capable of accounting for the qualitative dynamics of a typical neocortical column. To this end, values for the various parameters were chosen such that the resulting systems resembled *generic* neocortical columns, and the dynamics of these systems were assessed only to the extent to which they conformed with the *generic* dynamics of neocortical columns.

7.6 Summary

In order to ascertain the viability of the abstract dynamical system described in the previous chapter, we conducted simulation experiments to compare the dynamical characteristics of the

[15] The scrupulous reader will notice that the graphs in the figure exhibit divergence only after 5 sec. This, however, is an artifact of the coarseness of the recorded parameter, the total number of live spikes registered by the entire system. Divergence is immediate. However, it is discernible as a disparity in the total number of live spikes only after a while.

system, set up to model a typical neocortical column, to those of the real system.

The choice of the target system, a typical column in the neocortex, was based on several notable factors. While in theory the entire brain may be viewed as an enormous network of neurons, such an outlook is unlikely to result in useful observations, any more than finite state assumptions help understand large but finite computer systems. The neocortical column has not only been intensively investigated, but it also embodies an anatomical and functional homogeneity that confers upon it a unitary status.

The experiments revealed that the qualitative characteristics of the dynamics of the abstract system are akin to those observed in the real system. They also highlighted the fact that in the region of the phase-space corresponding to “normal operational conditions” in the neocortex, the dynamics of the system is chaotic.

Chapter 8

Local Analysis

Our objective in this chapter is to identify the local properties of trajectories in the phase-space of the abstract dynamical system formulated in Chapter 6. We pursue this goal through a measure analysis in Section 8.3 and a cross-section analysis in Section 8.4. Section 8.5 then applies the findings of these sections to the dynamics of neocortical columns. It is inferred that the dynamics of a neocortical column under normal operational conditions is almost surely *sensitive* to initial conditions, and under seizure-like conditions is almost surely *insensitive* to initial conditions.

As was noted in Chapter 2 Section 4, the definition of a differentiable manifold does not stipulate an inner product on the tangent space at a point. Since we propose to investigate aspects of the dynamics of the system that are founded on the notion of a distance measure (such as sensitive dependence on initial conditions), we first endow the phase-space with a Riemannian metric. This is accomplished in Section 8.1.

In Section 8.2, we conduct a perturbation analysis on trajectories in the phase-space of the abstract dynamical system. The nature of the Riemannian metric introduced in the previous section ensures that the analysis can be restricted to two cases: the birth of a spike and the death of a spike. The precise relationship between a perturbation before an event and the consequent perturbation after the event is derived for both cases.

In Section 8.3, the result of the perturbation analysis is utilized to demonstrate that the dynamics of the system is expansive at the birth of a spike and contractile at the death of a spike. Section 8.4 applies the same result to derive the impact of a series of births and deaths of spikes on a trajectory; the criterion for the trajectory to be sensitive to initial conditions is derived in a probabilistic framework.

Finally, in Section 8.5, we deduce the qualitative features of the dynamics of a neocortical column based on the results of Section 8.4 and anatomical and physiological parameters.

8.1 The Riemannian Metric

We remind the reader that in Chapter 6 we constructed the phase-space for the dynamical system as $\prod_{i=1}^{\mathcal{S}} {}^{i}\overline{\mathbb{L}}_{n_i}$, and endowed it with velocity fields $\mathcal{V}^1$ and $\mathcal{V}^2$. We choose the Riemannian metric in a manner such that all flows corresponding to the velocity field $\mathcal{V}^1$ on $\prod_{i=1}^{\mathcal{S}}({}^{i}\overline{\mathbb{L}}_{n_i}^{\sigma_i} \backslash {}^{i}\overline{\mathbb{L}}_{n_i}^{\sigma_i+1})$ (for any values of σ_i's) are not only measure preserving but also shape preserving. The intuitive appeal of the choice lies in the fact that under the application of such a metric, any section of a trajectory that is devoid of births and deaths of spikes turns uneventful from a measure theoretic perspective.

Since for every $\sigma_i > 1$, ${}^{i}\overline{\mathbb{L}}_{n_i}^{\sigma_i}$ corresponds to states of neuron i that feature multiple components set at $e^{ix_i^j} = 1$, it lies on the boundary of ${}^{i}\overline{\mathbb{L}}_{n_i}^{0}$. It follows from the description of ${}^{i}\overline{\mathbb{L}}_{n_i}$ in Chapter 6 that the boundary set in the neighborhood of $p_i \in ({}^{i}\overline{\mathbb{L}}_{n_i}^{\sigma_i} \backslash {}^{i}\overline{\mathbb{L}}_{n_i}^{\sigma_i+1})$ is locally diffeomorphic to an open subset of ${}^{i}\overline{\mathbb{L}}_{n_i}^{\sigma_i-1}$. Finally, the nature of the velocity fields $\mathcal{V}_i^1$ and $\mathcal{V}_i^2$ reveals that for all $p_i \in ({}^{i}\overline{\mathbb{L}}_{n_i}^{\sigma_i} \backslash {}^{i}\overline{\mathbb{L}}_{n_i}^{\sigma_i+1})$, $\mathcal{V}_i \in T({}^{i}\overline{\mathbb{L}}_{n_i}^{\sigma_i-1})$. It is therefore sufficient as well as appropriate that the Riemannian metric at $p \in \prod_{i=1}^{\mathcal{S}}({}^{i}\overline{\mathbb{L}}_{n_i}^{\sigma_i} \backslash {}^{i}\overline{\mathbb{L}}_{n_i}^{\sigma_i+1})$ be defined over $T(\prod_{i=1}^{\mathcal{S}} {}^{i}\overline{\mathbb{L}}_{n_i}^{\sigma_i-1})$, that is, as $\mathbf{\Phi} : T(\prod_{i=1}^{\mathcal{S}} {}^{i}\overline{\mathbb{L}}_{n_i}^{\sigma_i-1}) \times T(\prod_{i=1}^{\mathcal{S}} {}^{i}\overline{\mathbb{L}}_{n_i}^{\sigma_i-1}) \rightarrow \mathbb{R}$.

Let $p_i \in ({}^{i}\overline{\mathbb{L}}_{n_i}^{\sigma_i} \backslash {}^{i}\overline{\mathbb{L}}_{n_i}^{\sigma_i+1})$ denote the state of neuron i. We consider $({}^{i}\overline{\mathbb{L}}_{n_i}^{\sigma_i} \backslash {}^{i}\overline{\mathbb{L}}_{n_i}^{\sigma_i+1})$ as a subspace of ${}^{i}\overline{\mathbb{L}}_{n_i}^{\sigma_i-1}$. The imbedding $\mathcal{F}_{n_i-(\sigma_i-1)}^{n_i}$ maps ${}^{i}\overline{\mathbb{L}}_{n_i-(\sigma_i-1)}^{0}$ onto ${}^{i}\overline{\mathbb{L}}_{n_i}^{\sigma_i-1}$ in a manner such that $({}^{i}\overline{\mathbb{L}}_{n_i-(\sigma_i-1)}^{1} \backslash {}^{i}\overline{\mathbb{L}}_{n_i-(\sigma_i-1)}^{2}) \subset {}^{i}\overline{\mathbb{L}}_{n_i-(\sigma_i-1)}^{0}$ is mapped onto $({}^{i}\overline{\mathbb{L}}_{n_i}^{\sigma_i} \backslash {}^{i}\overline{\mathbb{L}}_{n_i}^{\sigma_i+1}) \subset {}^{i}\overline{\mathbb{L}}_{n_i}^{\sigma_i-1}$. The mapping $F_{n_i-(\sigma_i-1)} : T^{n_i-(\sigma_i-1)} \rightarrow {}^{i}\overline{\mathbb{L}}_{n_i-(\sigma_i-1)}^{0}$ is a local diffeomorphism at all points satisfying $e^{ix_i^1} \neq e^{ix_i^2} \neq ... \neq e^{ix_i^{n_i-(\sigma_i-1)}}$. Hence, the mapping $(\mathcal{F}_{n_i-(\sigma_i-1)}^{n_i} \circ F_{n_i-(\sigma_i-1)})$ is a local diffeomorphism at all such points. Finally, whereas the section of ${}^{i}\overline{\mathbb{L}}_{n_i}$ that is actually explored by the state dynamics of neuron i, that is, the feasible space, does contain states composed of identical components, such components are necessarily set at $e^{ix_i^j} = 1$. Consequently, if $\mathbb{W} \subset T^{n_i-(\sigma_i-1)}$ denotes the inverse image of the feasible section of $({}^{i}\overline{\mathbb{L}}_{n_i}^{\sigma_i-1} \backslash {}^{i}\overline{\mathbb{L}}_{n_i}^{\sigma_i+1})$, then the constraint $e^{ix_i^1} \neq e^{ix_i^2} \neq ... \neq e^{ix_i^{n_i-(\sigma_i-1)}}$ is satisfied throughout $\mathbb{W}$.

We are now in a position to define a C^∞-compatible basis for $T(\prod_{i=1}^{\mathcal{S}} {}^{i}\overline{\mathbb{L}}_{n_i})$ in the feasible section of $\prod_{i=1}^{\mathcal{S}}({}^{i}\overline{\mathbb{L}}_{n_i}^{\sigma_i} \backslash {}^{i}\overline{\mathbb{L}}_{n_i}^{\sigma_i+1})$, namely, the set of vectors $({}^{i}\mathcal{F}_{n_i-(\sigma_i-1)}^{n_i} \circ {}^{i}F_{n_i-(\sigma_i-1)})_\star(\partial/\partial x_i^j)$ for $i = 1, ..., \mathcal{S}$ and $j = 1, ..., n_i - (\sigma_i - 1)$. We shall, for the sake of brevity, henceforth refer to $({}^{i}\mathcal{F}_{n_i-(\sigma_i-1)}^{n_i} \circ {}^{i}F_{n_i-(\sigma_i-1)})_\star(\partial/\partial x_i^j)$ as $\mathbf{E}_i^j$. We set the Riemannian metric to $\mathbf{\Phi}(\mathbf{E}_a^b, \mathbf{E}_c^d) = 1$

if $a = c$ and $b = d$, and $\mathbf{\Phi}(\mathbf{E}_a^b, \mathbf{E}_c^d) = 0$ otherwise. Intuitively, the metric enforces that independent perturbations along any *live* spikes of neurons and exactly one *dead* spike per neuron are mutually orthogonal.

The component labels in $\mathbb{W}$ can be chosen in a manner such that $\mathbf{E}_i^1 \in T(^i\overline{\mathbb{L}}_{n_i}^{\sigma_i - 1})$ lies in $T^\perp(^i\overline{\mathbb{L}}_{n_i}^{\sigma_i} \backslash {}^i\overline{\mathbb{L}}_{n_i}^{\sigma_i+1})$, the orthogonal complement of $T(^i\overline{\mathbb{L}}_{n_i}^{\sigma_i} \backslash {}^i\overline{\mathbb{L}}_{n_i}^{\sigma_i+1})$. The feasible section of $\prod_{i=1}^{\mathcal{S}}(^i\overline{\mathbb{L}}_{n_i}^{\sigma_i} \backslash {}^i\overline{\mathbb{L}}_{n_i}^{\sigma_i+1})$, for any values of σ_i's, can now be considered a Riemannian manifold in its own right. $T(\prod_{i=1}^{\mathcal{S}}(^i\overline{\mathbb{L}}_{n_i}^{\sigma_i} \backslash {}^i\overline{\mathbb{L}}_{n_i}^{\sigma_i+1}))$ in the feasible section is spanned by the set of vectors $\langle \mathbf{E}_i^j \mid i = 1, ..., \mathcal{S}; j = 2, ..., n_i - (\sigma_i - 1)\rangle$, which forms an orthonormal basis. The feasible section of $(^i\overline{\mathbb{L}}_{n_i}^{\sigma_i} \backslash {}^i\overline{\mathbb{L}}_{n_i}^{\sigma_i+1})$ is therefore also a regular submanifold of $^i\overline{\mathbb{L}}_{n_i}^{\sigma_i - 1}$.

We now consider $\prod_{i=1}^{\mathcal{S}} {}^i\overline{\mathbb{L}}_{n_i}$ as the union of the sets $\prod_{i=1}^{\mathcal{S}}(^i\overline{\mathbb{L}}_{n_i}^{\sigma_i} \backslash {}^i\overline{\mathbb{L}}_{n_i}^{\sigma_i+1})$ for all $i = 1, ..., \mathcal{S}$ and $\sigma_i = 0, ..., n_i$, and assign it the topology *generated* by the family of all open sets in each $\prod_{i=1}^{\mathcal{S}}(^i\overline{\mathbb{L}}_{n_i}^{\sigma_i} \backslash {}^i\overline{\mathbb{L}}_{n_i}^{\sigma_i+1})$ induced by the Riemannian metric. It is clear that in the feasible section of $\prod_{i=1}^{\mathcal{S}} {}^i\overline{\mathbb{L}}_{n_i}$, this topology is identical to that presented in Chapter 6 Section 3.

$\mathcal{V}^1$ on $\prod_{i=1}^{\mathcal{S}}(^i\overline{\mathbb{L}}_{n_i}^{\sigma_i} \backslash {}^i\overline{\mathbb{L}}_{n_i}^{\sigma_i+1})$ is defined as $\sum_{i=1,j=2}^{\mathcal{S},n_i-(\sigma_i-1)}(2\pi/\Upsilon)\mathbf{E}_i^j$ in the new frame. Since the field of coordinate frames $\mathbf{E}_i^j$ for $i = 1, ..., \mathcal{S}$, $j = 2, ..., n_i - (\sigma_i - 1)$ satisfies $\nabla_{\mathbf{E}_a^b}\mathbf{E}_c^d = 0$ (∇ being the Riemannian connection) for all $a, c \in \{1, ..., \mathcal{S}\}$ and $b, d \in \{2, ..., n_i - (\sigma_i - 1)\}$, and the coefficients $(2\pi/\Upsilon)$ are constants, $\mathcal{V}^1$ is a *constant* vector field on $\prod_{i=1}^{\mathcal{S}}(^i\overline{\mathbb{L}}_{n_i}^{\sigma_i} \backslash {}^i\overline{\mathbb{L}}_{n_i}^{\sigma_i+1})$. $\mathcal{V}^1$ is therefore not only measure preserving but also shape preserving on $\prod_{i=1}^{\mathcal{S}}(^i\overline{\mathbb{L}}_{n_i}^{\sigma_i} \backslash {}^i\overline{\mathbb{L}}_{n_i}^{\sigma_i+1})$.

This leads to a substantial simplification in the analysis of the dynamics of the system. Since any trajectory $\Psi_x(t)$ in the phase-space has an associated sequence $\langle t_1, t_2, ..., t_k, t_{k+1}, ...\rangle$ of times such that for all j the segment $\{\Psi_x(t) \mid t_j < t < t_{j+1}\}$ lies strictly on $\prod_{i=1}^{\mathcal{S}}(^i\overline{\mathbb{L}}_{n_i}^{\sigma_i} \backslash {}^i\overline{\mathbb{L}}_{n_i}^{\sigma_i+1})$ for fixed values of σ_i's (segments that correspond to periods during which neither any live spike expires nor does any neuron fire), and since each such segment is volume and shape preserving, the analysis of the local properties of $\Psi_x(t)$ reduces to the analysis of a finite or countably infinite set of discrete events at times $\langle t_1, t_2, ..., t_k, t_{k+1}, ...\rangle$, each event denoting the birth and/or death of one or more spikes. Since any event involving the simultaneous birth and death of multiple spikes can be regarded as a series of mutually independent births and deaths of individual spikes,[1] the analysis can be further restricted to the birth of a spike and the death of a spike.

[1] At the time of its birth or death, a spike has no impact on any membrane potential function.

8.2 Perturbation Analysis

In the previous section, it was demonstrated that any segment of a trajectory that lies strictly on $\prod_{i=1}^{\mathcal{S}}({}^{i}\overline{\mathbb{L}}_{n_i}^{\sigma_i}\backslash {}^{i}\overline{\mathbb{L}}_{n_i}^{\sigma_i+1})$, for fixed values of σ_i's, is measure as well as shape preserving. Consequently, any perturbation on a trajectory is maintained during such an interval. We now consider what happens to a perturbation when the trajectory leaves the noted subspace either as a result of the birth of a spike or that of the death of a spike.

8.2.1 The Birth of a Spike

Let $\{\Psi_x(t) \mid t_j < t < t_{j+1}\}$ lie strictly on $\prod_{i=1}^{\mathcal{S}}({}^{i}\overline{\mathbb{L}}_{n_i}^{\sigma_i}\backslash {}^{i}\overline{\mathbb{L}}_{n_i}^{\sigma_i+1})$ for arbitrary but fixed values of σ_i's. Let the event associated with $\Psi_x(t_{j+1})$ be, without loss of generalization, the birth of a spike at neuron 1, that is, $\Psi_x(t_{j+1}) \in P_1^I$ and $\Psi_x(t_{j+1}) \notin P_i^I$ for $i = 2, ..., \mathcal{S}$. Then, $\{\Psi_x(t) \mid t_{j+1} < t < t_{j+2}\}$ lies strictly on $({}^{1}\overline{\mathbb{L}}_{n_1}^{\sigma_1-1}\backslash {}^{1}\overline{\mathbb{L}}_{n_1}^{\sigma_1}) \times \prod_{i=2}^{\mathcal{S}}({}^{i}\overline{\mathbb{L}}_{n_i}^{\sigma_i}\backslash {}^{i}\overline{\mathbb{L}}_{n_i}^{\sigma_i+1})$. Consider $p_1 = \Psi_x(t_{j+1} - t^*)$ on the segment $\{\Psi_x(t) \mid t_j < t < t_{j+1}\}$ and $p_2 = \Psi_x(t_{j+1} + t^*)$ on the segment $\{\Psi_x(t) \mid t_{j+1} < t < t_{j+2}\}$ such that $\Psi_x(t)$ for $t_{j+1} - t^* \leq t \leq t_{j+1} + t^*$ lies in a single coordinate neighborhood[2] of $\prod_{i=1}^{\mathcal{S}}({}^{i}\overline{\mathbb{L}}_{n_i}^{\sigma_i-1}\backslash {}^{i}\overline{\mathbb{L}}_{n_i}^{\sigma_i+1})$. Let p_1 be represented in local coordinates as $\langle a_1^1, ..., a_1^{n_1-(\sigma_1-1)}, a_2^1, ..., a_2^{n_2-(\sigma_2-1)}, ..., a_{\mathcal{S}}^1, ..., a_{\mathcal{S}}^{n_{\mathcal{S}}-(\sigma_{\mathcal{S}}-1)}\rangle$ where $a_i^1 = 0$ for $i = 1, ..., \mathcal{S}$, and p_2 be represented as $\langle b_1^1, ..., b_1^{n_1-(\sigma_1-1)}, b_2^1, ..., b_2^{n_2-(\sigma_2-1)}, ..., b_{\mathcal{S}}^1, ..., b_{\mathcal{S}}^{n_{\mathcal{S}}-(\sigma_{\mathcal{S}}-1)}\rangle$. Then, $b_1^1 = (2\pi/\Upsilon)t^*$, $b_i^1 = 0$ for $i = 2, ..., \mathcal{S}$, and $b_i^j = a_i^j + (2\pi/\Upsilon)2t^*$ for the remaining $i = 1, ..., \mathcal{S}$ and $j = 2, ..., n_i - (\sigma_i - 1)$.

Let $\tilde{p}_1$ on $\prod_{i=1}^{\mathcal{S}}({}^{i}\overline{\mathbb{L}}_{n_i}^{\sigma_i}\backslash {}^{i}\overline{\mathbb{L}}_{n_i}^{\sigma_i+1})$ be sufficiently near p_1 so that $\Psi_{\tilde{x}}(t)$, the trajectory through $\tilde{p}_1$, has a corresponding segment on $({}^{1}\overline{\mathbb{L}}_{n_1}^{\sigma_1-1}\backslash {}^{1}\overline{\mathbb{L}}_{n_1}^{\sigma_1}) \times \prod_{i=2}^{\mathcal{S}}({}^{i}\overline{\mathbb{L}}_{n_i}^{\sigma_i}\backslash {}^{i}\overline{\mathbb{L}}_{n_i}^{\sigma_i+1})$. Let $\tilde{p}_1$ be represented in local coordinates as $\langle \tilde{a}_1^1, ..., \tilde{a}_1^{n_1-(\sigma_1-1)}, \tilde{a}_2^1, ..., \tilde{a}_2^{n_2-(\sigma_2-1)}, ..., \tilde{a}_{\mathcal{S}}^1, ..., \tilde{a}_{\mathcal{S}}^{n_{\mathcal{S}}-(\sigma_{\mathcal{S}}-1)}\rangle$, where $\tilde{a}_i^1 = a_i^1 = 0$ for $i = 1, ..., \mathcal{S}$, and $\tilde{a}_i^j = a_i^j + \Delta x_i^j$ for $i = 1, ..., \mathcal{S}$, $j = 2, ..., n_i - (\sigma_i - 1)$. Let $\Psi_{\tilde{x}}(t)$ be parameterized in a manner such that $\tilde{p}_1 = \Psi_{\tilde{x}}(t_{j+1} - t^*)$. Let $\tilde{p}_2 = \Psi_{\tilde{x}}(t_{j+1} + t^*)$ be represented in local coordinates as $\langle \tilde{b}_1^1, ..., \tilde{b}_1^{n_1-(\sigma_1-1)}, \tilde{b}_2^1, ..., \tilde{b}_2^{n_2-(\sigma_2-1)}, ..., \tilde{b}_{\mathcal{S}}^1, ..., \tilde{b}_{\mathcal{S}}^{n_{\mathcal{S}}-(\sigma_{\mathcal{S}}-1)}\rangle$ where $\tilde{b}_1^1 = b_1^1 + \Delta y_1^1$, $\tilde{b}_i^1 = b_i^1 = 0$ for $i = 2, ..., \mathcal{S}$, and $\tilde{b}_i^j = b_i^j + \Delta y_i^j$ for the remaining $i = 1, ..., \mathcal{S}$ and $j = 2, ..., n_i - (\sigma_i - 1)$.

$\Delta y_i^j = \Delta x_i^j$ for $i = 1, ..., \mathcal{S}$ and $j = 2, ..., n_i - (\sigma_i - 1)$ since $\tilde{b}_i^j = \tilde{a}_i^j + (2\pi/\Upsilon)2t^*$ for all

[2] With the distinguished set of coordinate frames described in Section 8.1.

such values of i and j. Let Δt be such that $\Psi_{\tilde{x}}(t_{j+1}+\Delta t)$ lies on P_1^I. Then $\Delta y_1^1 = -(2\pi/\Upsilon)\Delta t$. Since both $\Psi_x(t_{j+1})$ and $\Psi_{\tilde{x}}(t_{j+1}+\Delta t)$ lie on P_1^I,

$$P_1(a_1^1, a_1^2 + \frac{2\pi}{\Upsilon}t^*, ..., a_1^{n_1-(\sigma_1-1)} + \frac{2\pi}{\Upsilon}t^*, ..., a_{\mathcal{S}}^1, a_{\mathcal{S}}^2 + \frac{2\pi}{\Upsilon}t^*, ..., a_{\mathcal{S}}^{n_{\mathcal{S}}-(\sigma_{\mathcal{S}}-1)} + \frac{2\pi}{\Upsilon}t^*) = \mathcal{T}, \quad \text{and} \tag{8.1}$$

$$P_1(a_1^1, a_1^2+\Delta x_1^2+\frac{2\pi}{\Upsilon}(t^*+\Delta t), ..., a_1^{n_1-(\sigma_1-1)}+\Delta x_1^{n_1-(\sigma_1-1)}+\frac{2\pi}{\Upsilon}(t^*+\Delta t), ..., a_{\mathcal{S}}^1, a_{\mathcal{S}}^2+\Delta x_{\mathcal{S}}^2+\frac{2\pi}{\Upsilon}(t^*+\Delta t), ..., a_{\mathcal{S}}^{n_{\mathcal{S}}-(\sigma_{\mathcal{S}}-1)}+\Delta x_{\mathcal{S}}^{n_{\mathcal{S}}-(\sigma_{\mathcal{S}}-1)}+\frac{2\pi}{\Upsilon}(t^*+\Delta t)) = \mathcal{T}. \tag{8.2}$$

$P_1(\cdot)$, being C^∞, can be expanded as a Taylor series around $\Psi_x(t_{j+1})$. Minor algebraic manipulations, and neglecting all higher order terms, then yields

$$\Delta y_1^1 = \sum_{i=1,j=2}^{\mathcal{S},n_i-(\sigma_i-1)} (\frac{\partial P_1}{\partial x_i^j} \times \Delta x_i^j) / \sum_{i=1,j=2}^{\mathcal{S},n_i-(\sigma_i-1)} \frac{\partial P_1}{\partial x_i^j} \tag{8.3}$$

All $\frac{\partial P_1}{\partial x_i^j}$'s in the expression above are evaluated at $\Psi_x(t_{j+1})$. We denote $\frac{\partial P_k}{\partial x_i^j} / \sum_{i,j} \frac{\partial P_k}{\partial x_i^j}$ by ${}^k\alpha_i^j$. Then, $\Delta y_1^1 = \sum_{i,j} {}^1\alpha_i^j \Delta x_i^j$, and for all $k = 1, ..., \mathcal{S}$ $\sum_{i,j} {}^k\alpha_i^j = 1$.

Intuitively, not only are all perturbations along the live spikes maintained, but the trajectory gains a new perturbation along the spike that just took birth. The perturbation on the new spike is given by Equation 8.3.

8.2.2 The Death of a Spike

Let $\{\Psi_x(t) \mid t_j < t < t_{j+1}\}$ lie strictly on $\prod_{i=1}^{\mathcal{S}} ({}^i\overline{\mathbb{L}}_{n_i}^{\sigma_i} \setminus {}^i\overline{\mathbb{L}}_{n_i}^{\sigma_i+1})$ for arbitrary but fixed values of σ_i's. Let the event associated with $\Psi_x(t_{j+1})$ be, without loss of generalization, the death of a spike at neuron 1. Then $\{\Psi_x(t) \mid t_{j+1} < t < t_{j+2}\}$ lies strictly on $({}^1\overline{\mathbb{L}}_{n_1}^{\sigma_1+1} \setminus {}^1\overline{\mathbb{L}}_{n_1}^{\sigma_1+2}) \times \prod_{i=2}^{\mathcal{S}} ({}^i\overline{\mathbb{L}}_{n_i}^{\sigma_i} \setminus {}^i\overline{\mathbb{L}}_{n_i}^{\sigma_i+1})$. Consider $p_1 = \Psi_x(t_{j+1} - t^*)$ on the segment $\{\Psi_x(t) \mid t_j < t < t_{j+1}\}$ and $p_2 = \Psi_x(t_{j+1} + t^*)$ on the segment $\{\Psi_x(t) \mid t_{j+1} < t < t_{j+2}\}$ such that $\Psi_x(t)$ for $t_{j+1} - t^* \leq t \leq t_{j+1} + t^*$ lies within a single coordinate neighborhood of $\prod_{i=1}^{\mathcal{S}} ({}^i\overline{\mathbb{L}}_{n_i}^{\sigma_i} \setminus {}^i\overline{\mathbb{L}}_{n_i}^{\sigma_i+2})$. Let p_1 be represented in local coordinates as $\langle a_1^1, ..., a_1^{n_1-\sigma_1}, a_2^1, ..., a_2^{n_2-\sigma_2}, ..., a_{\mathcal{S}}^1, ..., a_{\mathcal{S}}^{n_{\mathcal{S}}-\sigma_{\mathcal{S}}} \rangle$, and p_2 be represented as $\langle b_1^1, ..., b_1^{n_1-\sigma_1}, b_2^1, ..., b_2^{n_2-\sigma_2}, ..., b_{\mathcal{S}}^1, ..., b_{\mathcal{S}}^{n_{\mathcal{S}}-\sigma_{\mathcal{S}}} \rangle$. Then $b_1^1 = 0$, and $b_i^j = a_i^j + (2\pi/\Upsilon)2t^*$ for all $i = 1, ..., \mathcal{S}$ and $j = 1, ..., (n_i - \sigma_i)$ except $i = j = 1$.

Let $\tilde{p}_1 = \Psi_{\tilde{x}}(t_{j+1} - t^*)$, and $\tilde{p}_2 = \Psi_{\tilde{x}}(t_{j+1} + t^*)$ be points on a $\Psi_{\tilde{x}}(t)$ sufficiently close to $\Psi_x(t)$ so as to have corresponding segments on the noted submanifolds. Let $\tilde{p}_1$ be represented in

local coordinates as $\langle \tilde{a}_1^1, ..., \tilde{a}_1^{n_1-\sigma_1}, \tilde{a}_2^1, ..., \tilde{a}_2^{n_2-\sigma_2}, ..., \tilde{a}_{\mathcal{S}}^1, ..., \tilde{a}_{\mathcal{S}}^{n_{\mathcal{S}}-\sigma_{\mathcal{S}}} \rangle$ where $\tilde{a}_i^j = a_i^j + \Delta x_i^j$ for all $i = 1, ..., \mathcal{S}$, $j = 1, ..., (n_i - \sigma_i)$, and $\tilde{p}_2$ as $\langle \tilde{b}_1^1, ..., \tilde{b}_1^{n_1-\sigma_1}, \tilde{b}_2^1, ..., \tilde{b}_2^{n_2-\sigma_2}, ..., \tilde{b}_{\mathcal{S}}^1, ..., \tilde{b}_{\mathcal{S}}^{n_{\mathcal{S}}-\sigma_{\mathcal{S}}} \rangle$ where $\tilde{b}_i^j = b_i^j + \Delta y_i^j$ for all $i = 1, ..., \mathcal{S}$, $j = 1, ..., (n_i - \sigma_i)$. Then it follows from $\tilde{b}_1^1 = b_1^1 = 0$ and $\tilde{b}_i^j = \tilde{a}_i^j + (2\pi/\Upsilon)2t^*$ for all other i, j that $\Delta y_1^1 = 0$ and $\Delta y_i^j = \Delta x_i^j$ for all $i = 1, ..., \mathcal{S}$, $j = 1, ..., (n_i - \sigma_i)$ except $i = j = 1$.

Intuitively, the trajectory looses the perturbation along the spike that just expired. All other perturbations along the live spikes are maintained.

8.3 Measure Analysis

In this section, we demonstrate based on the results of the previous section that a trajectory is expansive at the birth of a spike and contractile at the death of a spike. In other words, we show that under the action of the dynamics, an infinitesimal section of the phase-space expands past the birth of a spike and contracts past the death of a spike. We also demonstrate that folding of phase-space,[3] a feature closely associated with chaotic dynamics, is realizable across a series of births and deaths of spikes.

8.3.1 Expansion

We demonstrate that a trajectory is expansive at the birth of a spike. We consider the adjacent segments of $\Psi_x(t)$ described in Section 8.2.1 (the birth of a spike). Let $\mathcal{C}$ denote an infinitesimal $\sum_{i=1}^{\mathcal{S}}(n_i - \sigma_i)$-dimensional hypercube spanned by vectors $\epsilon \mathbf{E}_i^j$ ($\epsilon \to 0$) for $i = 1, ..., \mathcal{S}$ and $j = 2, ..., n_i - (\sigma_i - 1)$ at any location on the segment of $\Psi_x(t)$ on $\prod_{i=1}^{\mathcal{S}}({}^i\overline{\mathbb{L}}_{n_i}^{\sigma_i} \setminus {}^i\overline{\mathbb{L}}_{n_i}^{\sigma_i+1})$. When $\mathcal{C}$ passes into $({}^1\overline{\mathbb{L}}_{n_1}^{\sigma_1-1} \setminus {}^1\overline{\mathbb{L}}_{n_1}^{\sigma_1}) \times \prod_{i=2}^{\mathcal{S}}({}^i\overline{\mathbb{L}}_{n_i}^{\sigma_i} \setminus {}^i\overline{\mathbb{L}}_{n_i}^{\sigma_i+1})$ it is transformed into the $\sum_{i=1}^{\mathcal{S}}(n_i - \sigma_i)$-dimensional parallelepiped $\mathcal{C}'$ spanned by the vectors $\epsilon(\mathbf{E}_i^j + {}^1\alpha_i^j \mathbf{E}_1^1)$ for $i = 1, ..., \mathcal{S}$ and $j = 2, ..., n_i - (\sigma_i - 1)$, where the ${}^1\alpha_i^j$'s are evaluated at the point $\Psi_x(t) \cap P_1^I$.

Vectors $\mathbf{E}_i^j$ for $i = 1, ..., \mathcal{S}$ and $j = 1, ..., n_i - (\sigma_i - 1)$ are by assumption orthonormal. Let A and A' denote the matrices associated with the vectors spanning $\mathcal{C}$ and $\mathcal{C}'$ represented as

[3] Folding refers to the phenomenon wherein a section of the phase-space, under the action of the dynamics of the system, is deformed to an extent that it appears folded. This phenomenon is predominant among systems that are expansive along at least one direction. In order for an expanded section of the phase-space to fit back into the phase-space, it is folded upon itself by the dynamics.

row coordinate vectors with respect to the above basis. A and A' are then the $(\sum_{i=1}^{\mathcal{S}} n_i - \sigma_i) \times (\sum_{i=1}^{\mathcal{S}} n_i - (\sigma_i - 1))$ matrices:

$$A = \begin{pmatrix} 0 & \epsilon & 0 & \cdots & 0 \\ 0 & 0 & \epsilon & \cdots & 0 \\ \vdots & \vdots & \vdots & \ddots & \vdots \\ 0 & 0 & 0 & \cdots & \epsilon \end{pmatrix} \quad \text{and} \quad A' = \begin{pmatrix} {}^1\alpha_1^2\epsilon & \epsilon & 0 & \cdots & 0 \\ {}^1\alpha_1^3\epsilon & 0 & \epsilon & \cdots & 0 \\ \vdots & \vdots & \vdots & \ddots & \vdots \\ {}^1\alpha_{\mathcal{S}}^{n_{\mathcal{S}}-(\sigma_{\mathcal{S}}-1)}\epsilon & 0 & 0 & \cdots & \epsilon \end{pmatrix}. \tag{8.4}$$

In A, columns corresponding to $\mathbf{E}_i^1$ for $i = 1, ..., \mathcal{S}$ are 0 vectors. All other columns contain an ϵ at an appropriate location. A' is identical to A except for the first column, which is replaced by the vector $\langle {}^1\alpha_1^2\epsilon, ..., {}^1\alpha_1^{n_1-(\sigma_1-1)}\epsilon, ..., {}^1\alpha_{\mathcal{S}}^2\epsilon, ..., {}^1\alpha_{\mathcal{S}}^{n_{\mathcal{S}}-(\sigma_{\mathcal{S}}-1)}\epsilon \rangle^T$.

The $\sum_{i=1}^{\mathcal{S}}(n_i - \sigma_i)$-dimensional measure of $\mathcal{C}$ and $\mathcal{C}'$ can now be computed as the square root of the Gram determinants[4] of the respective matrices, A and A'. They are

$$/A/ = \epsilon^{\sum_{i=1}^{\mathcal{S}} n_i - \sigma_i}, \text{ and} \tag{8.5}$$

$$/A'/ = \epsilon^{\sum_{i=1}^{\mathcal{S}} n_i - \sigma_i} \times \sqrt{1 + \sum_{i=1,j=2}^{\mathcal{S}, n_i-(\sigma_i-1)} ({}^1\alpha_i^j)^2}. \tag{8.6}$$

It follows from $\sum_{i,j} {}^1\alpha_i^j = 1$ that the volume of $\mathcal{C}'$ is strictly greater than that of $\mathcal{C}$.

8.3.2 Contraction

We demonstrate that a trajectory is contractile at the death of a spike. We consider the adjacent segments of $\Psi_x(t)$ described in Section 8.2.2 (the death of a spike). Let $\mathcal{C}$ denote an infinitesimal $\sum_{i=1}^{\mathcal{S}}(n_i - \sigma_i)$-dimensional hypercube spanned by vectors $\epsilon\mathbf{E}_i^j$ ($\epsilon \to 0$) for $i = 1, ..., \mathcal{S}$ and $j = 1, ..., (n_i - \sigma_i)$ at any location on the segment of $\Psi_x(t)$ on $\prod_{i=1}^{\mathcal{S}}({}^i\overline{\mathbb{L}}_{n_i}^{\sigma_i} \backslash {}^i\overline{\mathbb{L}}_{n_i}^{\sigma_i+1})$. When $\mathcal{C}$ passes into $({}^1\overline{\mathbb{L}}_{n_1}^{\sigma_1+1} \backslash {}^1\overline{\mathbb{L}}_{n_1}^{\sigma_1+2}) \times \prod_{i=2}^{\mathcal{S}}({}^i\overline{\mathbb{L}}_{n_i}^{\sigma_i} \backslash {}^i\overline{\mathbb{L}}_{n_i}^{\sigma_i+1})$, it is transformed into the $(\sum_{i=1}^{\mathcal{S}} n_i - \sigma_i) - 1$-dimensional hypercube $\mathcal{C}'$ spanned by the vectors $\epsilon\mathbf{E}_i^j$ for all $i = 1, ..., \mathcal{S}$ and $j = 1, ..., (n_i - \sigma_i)$ except $i = j = 1$. In other words, the $\sum_{i=1}^{\mathcal{S}}(n_i - \sigma_i)$-dimensional hypercube $\mathcal{C}$ *collapses* along $\mathbf{E}_1^1$ to produce a $(\sum_{i=1}^{\mathcal{S}} n_i - \sigma_i) - 1$-dimensional hypercube $\mathcal{C}'$. Any lower-dimensional parallelepiped inside $\mathcal{C}$ spanned by the vectors $\epsilon(\mathbf{E}_i^j + \beta_i^j\mathbf{E}_1^1)$ for $i = 1, ..., \mathcal{S}$, $j = 1, ..., (n_i - \sigma_i)$

[4]The Gram determinant of a matrix B is given by $det(B * B^T)$. The square root of the Gram determinant is also known as the modulus of B and is represented as $/B/$.

except $i = j = 1$ such that $\beta_i^j \neq 0$ for some i, j therefore experiences a contraction in volume as it passes from $\prod_{i=1}^{\mathcal{S}}({}^i\overline{\mathbb{L}}_{n_i}^{\sigma_i} \backslash {}^i\overline{\mathbb{L}}_{n_i}^{\sigma_i+1})$ into $({}^1\overline{\mathbb{L}}_{n_1}^{\sigma_1+1} \backslash {}^1\overline{\mathbb{L}}_{n_1}^{\sigma_1+2}) \times \prod_{i=2}^{\mathcal{S}}({}^i\overline{\mathbb{L}}_{n_i}^{\sigma_i} \backslash {}^i\overline{\mathbb{L}}_{n_i}^{\sigma_i+1})$.

8.3.3 Folding

We demonstrate that folding can occur across a series of births and deaths of spikes. Let $\tilde{\mathcal{C}}$ denote a $\sum_{i=1}^{\mathcal{S}}(n_i - \sigma_i)$-dimensional hypercuboid of *maximal* measure in the feasible section of $\prod_{i=1}^{\mathcal{S}}({}^i\overline{\mathbb{L}}_{n_i}^{\sigma_i} \backslash {}^i\overline{\mathbb{L}}_{n_i}^{\sigma_i+1})$ that is transformed after time $\frac{\Upsilon t}{2\pi}$ into a $\sum_{i=1}^{\mathcal{S}}(n_i - \sigma_i)$-dimensional hypersurface $\tilde{\mathcal{C}}'$ in $({}^1\overline{\mathbb{L}}_{n_1}^{\sigma_1-1} \backslash {}^1\overline{\mathbb{L}}_{n_1}^{\sigma_1}) \times \prod_{i=2}^{\mathcal{S}}({}^i\overline{\mathbb{L}}_{n_i}^{\sigma_i} \backslash {}^i\overline{\mathbb{L}}_{n_i}^{\sigma_i+1})$, past the birth of a spike at neuron 1. Let $\tilde{\mathcal{C}}$ be represented in local coordinates as $\prod_{i=1,j=2}^{\mathcal{S},n_i-(\sigma_i-1)}[a_i^j, a_i^j + \Delta_i]$, and $\tilde{\mathcal{C}}'$ be represented as $x_1^1 = h(x_1^2, ..., x_1^{n_1-(\sigma_1-1)}, x_2^2, ..., x_2^{n_2-(\sigma_2-1)}, ..., x_{\mathcal{S}}^2, ..., x_{\mathcal{S}}^{n_{\mathcal{S}}-(\sigma_{\mathcal{S}}-1)})$, where $x_i^j \in [a_i^j + t, a_i^j + \Delta_i + t]$ for $i = 1, ..., \mathcal{S}$ and $j = 2, ..., n_i - (\sigma_i - 1)$. Then the intersection of P_1^I with the hypersurface $\tilde{\mathcal{C}}$ after time $\frac{\Upsilon}{2\pi}(t-T)$, $P_1^I \cap \prod_{i=1,j=2}^{\mathcal{S},n_i-(\sigma_i-1)}[a_i^j + (t-T), a_i^j + \Delta_i + (t-T)]$, when translated by a distance T along all dimensions $(\partial/\partial x_i^j)$ for $i = 1, ..., \mathcal{S}$, $j = 2, ..., n_i - (\sigma_i - 1)$, $i = j = 1$, yields identically the hypersurface $h(\cdot) = T$ in $\tilde{\mathcal{C}}'$.[5] The shape of $\tilde{\mathcal{C}}'$ and the result of a dimensional collapse along any $\mathbf{E}_i^j$ for $i = 1, ..., \mathcal{S}$, $j = 2, ..., n_i - (\sigma_i - 1)$ on $\tilde{\mathcal{C}}'$ is therefore completely specified by the position of $\tilde{\mathcal{C}}$ in $\prod_{i=1}^{\mathcal{S}}({}^i\overline{\mathbb{L}}_{n_i}^{\sigma_i} \backslash {}^i\overline{\mathbb{L}}_{n_i}^{\sigma_i+1})$ and the nature of $P_1^I \cap \prod_{i=1}^{\mathcal{S}}({}^i\overline{\mathbb{L}}_{n_i}^{\sigma_i} \backslash {}^i\overline{\mathbb{L}}_{n_i}^{\sigma_i+1})$.

We now assume that $P_1(\cdot)$ is unimodal with respect to all variables that, at the given moment, correspond to effective spikes. Any coordinate curve of an effective variable can then have only point intersections (at most two) with $P_1^I \cap \prod_{i=1}^{\mathcal{S}}({}^i\overline{\mathbb{L}}_{n_i}^{\sigma_i} \backslash {}^i\overline{\mathbb{L}}_{n_i}^{\sigma_i+1})$. Finally, if a spike, over its finite lifetime, is effective in the generation of one or more spikes, then there exists, trivially, a last spike that it is effective on. We assume, without loss of generalization, that x_2^2 is one such spike, and x_1^1 is the final spike it is effective on.

In order for $\tilde{\mathcal{C}}'$ to be curved in such a manner that at the subsequent death of x_2^2 (irrespective of any number of intermediate births and/or deaths of spikes) it folds upon itself, there must exist a coordinate curve for x_2^2 that intersects $P_1^I \cap \tilde{\mathcal{C}}$ twice for at least one position of $\tilde{\mathcal{C}}$. This is based on the observations that (i) since x_2^2 is by assumption not effective on any intermediate births of spikes, the two intersections of such a coordinate curve with $\tilde{\mathcal{C}}'$ remain

[5] We use P_1^I and P_1^S to represent both the hypersurfaces in the phase-space and the corresponding hypersurfaces in local coordinates. The context will determine which hypersurface is being referred to.

on a coordinate curve of x_2^2 after such births, and (ii) any intermediate deaths of spikes have no impact on whether the intersections in question remain on a coordinate curve. Since $P_1(\cdot)$ is C^∞ and $P_1(\cdot)|_{x_2^2=0} = P_1(\cdot)|_{x_2^2=2\pi}$ when all other variables are held constant at any values, such coordinate curves exist for all points on $P_1^S \cap \prod_{i=1,j=2}^{\mathcal{S},n_i-(\sigma_i-1)}(0,2\pi)$. Furthermore, if $|\partial P_1/\partial x_2^2|$ at the intersection of any such coordinate curve with P_1^S, at the falling phase of $P_1(\cdot)$, is not so large as to make $\sum_{i=1,j=2}^{\mathcal{S},n_i-(\sigma_i-1)} \partial P_1/\partial x_i^j < 0$,[6] then $dP_1(\cdot)/dt \geq 0$ is satisfied by both intersections. Consequently, the coordinate curve intersects twice with the hypersurface $P_1^I \cap \prod_{i=1,j=2}^{\mathcal{S},n_i-(\sigma_i-1)}(0,2\pi)$.

The only question that remains unresolved is whether both intersections of such a coordinate curve lie on $\prod_{i=1}^{\mathcal{S}}({}^i\overline{\mathbb{L}}_{n_i}^{\sigma_i} \setminus {}^i\overline{\mathbb{L}}_{n_i}^{\sigma_i+1})$. While this question can be settled only when the specific instantiation of $P_1(\cdot)$ is known, there are two aspects of the system that have a significant impact on the answer. First, the closer $\mathcal{T}$ is to $\max\{P_1(x) \mid x \in \prod_{i=1,j=2}^{\mathcal{S},n_i-(\sigma_i-1)}(0,2\pi)\}$ and the tighter the peak of $P_1(\cdot)$ is, the greater the chances are that a coordinate curve exists in $\prod_{i=1}^{\mathcal{S}}({}^i\overline{\mathbb{L}}_{n_i}^{\sigma_i} \setminus {}^i\overline{\mathbb{L}}_{n_i}^{\sigma_i+1})$ that intersects P_1^I twice. Second, the larger Δ_i is for all $i = 1, ..., \mathcal{S}$ and $j = 2, ..., n_i - (\sigma_i - 1)$, the greater the chances are that such a coordinate curve exists. The largest Δ_i for which a $\sum_{i=1}^{\mathcal{S}}(n_i - \sigma_i)$-dimensional hypercuboid can fit into the feasible section of $\prod_{i=1}^{\mathcal{S}}({}^i\overline{\mathbb{L}}_{n_i}^{\sigma_i} \setminus {}^i\overline{\mathbb{L}}_{n_i}^{\sigma_i+1})$ is $(\frac{2\pi}{(n_i-\sigma_i)} - \frac{(n_i-\sigma_i-1)r_i}{(n_i-\sigma_i)\Upsilon})$. Clearly, folding of $\tilde{\mathcal{C}}'$ is more likely when $(n_i - \sigma_i)$ is small, that is, when the system is sparsely active.

8.4 Local Cross-Section Analysis

We are now poised to present the first of the two central results of this thesis.[7] In Section 8.2 we determined the local effects of the birth and the death of an individual spike on a trajectory through a perturbation analysis. The cumulative effect of such events on a trajectory, however, remains obscure. We address this issue in this section with regard to the dynamics of the system set up to model a typical neocortical column.

---

[6] This is generally the case for excitatory spikes in the cortex. The impact of such spikes on the potential function is given by a steep rising phase followed by a relatively gentle falling phase.

[7] The second result demonstrates that attractors in the phase-space of the dynamical system can be anisotropic, and is presented in the next chapter.

The solution is presented in several stages. First, the problem is phrased in terms of a quantifiable property of a particular matrix. A deterministic process that constructs the matrix incrementally is described in Sections 8.4.1 and 8.4.2. Next, each step in the process is reformulated as a stochastic event in Section 8.4.3. The event is analyzed, and conclusions are drawn regarding its effect on the matrix. Finally, the criterion for the trajectory to be sensitive to initial conditions is derived in Theorem 8.4.1.

8.4.1 The Deterministic Process

Our objective in this section is to determine the precise relationship between an initial perturbation on a trajectory and the corresponding final perturbation on the trajectory following several births and deaths of spikes.

We consider regular[8] trajectories that are not drawn into the trivial fixed point $\prod_{i=1}^{\mathcal{S}} {}^{i}\overline{\mathbb{L}}_{n_i}^{n_i}$ (state of quiescence). We proved that if $\langle \Delta x_1^2, ..., \Delta x_1^{n_1-(\sigma_1-1)}, ..., \Delta x_{\mathcal{S}}^2, ..., \Delta x_{\mathcal{S}}^{n_{\mathcal{S}}-(\sigma_{\mathcal{S}}-1)} \rangle^T$ and $\langle \Delta y_1^1, ..., \Delta y_1^{n_1-(\sigma_1-1)}, ..., \Delta y_{\mathcal{S}}^2, ..., \Delta y_{\mathcal{S}}^{n_{\mathcal{S}}-(\sigma_{\mathcal{S}}-1)} \rangle^T$ are perturbations on a trajectory before and after the birth of a spike at neuron 1, and $\langle \Delta x_1^1, ..., \Delta x_1^{n_1-\sigma_1}, ..., \Delta x_{\mathcal{S}}^1, ..., \Delta x_{\mathcal{S}}^{n_{\mathcal{S}}-\sigma_{\mathcal{S}}} \rangle^T$ and $\langle \Delta y_1^2, ..., \Delta y_1^{n_1-\sigma_1}, ..., \Delta y_{\mathcal{S}}^1, ..., \Delta y_{\mathcal{S}}^{n_{\mathcal{S}}-\sigma_{\mathcal{S}}} \rangle^T$ are perturbations on a trajectory before and after the death of a spike at neuron 1, then

$$\begin{pmatrix} \Delta y_1^1 \\ \Delta y_1^2 \\ \vdots \\ \Delta y_{\mathcal{S}}^{n_{\mathcal{S}}-(\sigma_{\mathcal{S}}-1)} \end{pmatrix} = \begin{pmatrix} {}^{1}\alpha_1^2 & ... & {}^{1}\alpha_{\mathcal{S}}^{n_{\mathcal{S}}-(\sigma_{\mathcal{S}}-1)} \\ 1 & 0 & 0 \\ \vdots & \ddots & \vdots \\ 0 & 0 & 1 \end{pmatrix} \begin{pmatrix} \Delta x_1^2 \\ \vdots \\ \Delta x_{\mathcal{S}}^{n_{\mathcal{S}}-(\sigma_{\mathcal{S}}-1)} \end{pmatrix} \tag{8.7}$$

$$\text{and} \quad \begin{pmatrix} \Delta y_1^2 \\ \vdots \\ \Delta y_{\mathcal{S}}^{n_{\mathcal{S}}-\sigma_{\mathcal{S}}} \end{pmatrix} = \begin{pmatrix} 0 & 1 & 0 & 0 \\ \vdots & \vdots & \ddots & \vdots \\ 0 & 0 & 0 & 1 \end{pmatrix} \begin{pmatrix} \Delta x_1^1 \\ \Delta x_1^2 \\ \vdots \\ \Delta x_{\mathcal{S}}^{n_{\mathcal{S}}-\sigma_{\mathcal{S}}} \end{pmatrix}. \tag{8.8}$$

[8] A regular trajectory is one for which the Lyapunov exponents exist. To elaborate, if v is a vector in $T(x)$ the tangent space at x, then the image of v under $D\Psi_t(x)$ is a vector in $T(\Psi_t(x))$ the tangent space at $\Psi_t(x)$. The Lyapunov exponent in the direction v is defined as $\lambda(x,v) = \lim_{t\to\infty} \frac{1}{t} \ln(\frac{\|D\Psi_t(x)[v]\|}{\|v\|})$ if such a limit exists. We note for future reference that Oseledec's multiplicative ergodic theorem (Oseledec 1968) when applied to our case affirms that any $\Psi(x,t)$ that is locally differentiable in x and satisfies $E(\ln^+ \sum_{i,j} ({}^{k}\alpha_i^j)^2) < \infty$, where $\ln^+ t$ is defined as $\max\{\ln t, 0\}$, is almost surely regular.

If we denote by A_k the matrix that corresponds to the event $\Psi_x(t_k)$, by the column vector $\Delta\mathbf{x_0}$ a perturbation just prior to the event $\Psi_x(t_1)$, and by the column vector $\Delta\mathbf{x_k}$ the corresponding perturbation just past the event $\Psi_x(t_k)$, then $\Delta\mathbf{x_k} = A_k * A_{k-1} * ... * A_1 * \Delta\mathbf{x_0}$. Alternatively, if A_0^k denotes the product $A_k * A_{k-1} * ... * A_1$, then $\Delta\mathbf{x_k} = A_0^k * \Delta\mathbf{x_0}$, where A_0^k is defined recursively as $A_0^0 = I$ (the identity matrix) and $\forall k \geq 0$, $A_0^{k+1} = A_{k+1} * A_0^k$.

Given the nature of these matrices, we deduce that

(1) If $\Psi_x(t_{k+1})$ corresponds to the birth of a spike at neuron l, then A_0^{k+1} can be generated from A_0^k by identifying rows r_i^j in A_0^k that correspond to spikes that are effective in the birth of the given spike, and introducing a new row $\sum_{i,j} {}^l\alpha_i^j r_i^j$ at an appropriate location into A_0^k, and

(2) If $\Psi_x(t_{k+1})$ corresponds to the death of a spike at neuron l, then A_0^{k+1} can be generated from A_0^k by identifying the row in A_0^k that corresponds to the given spike, and deleting it from A_0^k.

Finally, since we shall be analyzing periodic orbits and trajectories, both the initial and the final perturbations must lie on local cross-sections of the trajectory $\Psi_x(t)$. The velocity field being $\sum_{i=1,j=2}^{\mathcal{S},n_i-(\sigma_i-1)}(2\pi/\Upsilon)\mathbf{E}_i^j$, the initial perturbation must satisfy $\sum_{i=1,j=2}^{\mathcal{S},n_i-(\sigma_i-1)} \Delta x_i^j = 0$, and the final perturbation must be adjusted along the orbit (each component must be adjusted by the same quantity) to satisfy the same equation. In terms of matrix operations, this translates into $B * A_0^k * C$ where B and C (assuming A_0^k is an $(m \times n)$ matrix) are the $(m-1 \times m)$ and $(n \times n-1)$ matrices:

$$B = \begin{pmatrix} 1-\frac{1}{m} & -\frac{1}{m} & ... & -\frac{1}{m} & -\frac{1}{m} \\ -\frac{1}{m} & 1-\frac{1}{m} & ... & -\frac{1}{m} & -\frac{1}{m} \\ \vdots & \vdots & \ddots & \vdots & \vdots \\ -\frac{1}{m} & -\frac{1}{m} & ... & 1-\frac{1}{m} & -\frac{1}{m} \end{pmatrix} \text{ and } C = \begin{pmatrix} 1 & 0 & ... & 0 \\ 0 & 1 & ... & 0 \\ \vdots & \vdots & \ddots & \vdots \\ 0 & 0 & ... & 1 \\ -1 & -1 & ... & -1 \end{pmatrix}. \quad (8.9)$$

If $\Psi_x(t)$ is aperiodic, then $\Delta\mathbf{x'_k} = B * A_0^k * C * \Delta\mathbf{x'_0}$ for arbitrary value of k specifies the relation between an initial and a final perturbation, both of which lie on transverse sections of the trajectory. In this case, the sensitivity of the trajectory to initial conditions is determined by

$\|B * A_0^k * C\|_2$.[9] If $\lim_{k\to\infty} \|B * A_0^k * C\|$ is *unbounded* then the trajectory is *sensitive* to initial conditions, and if $\lim_{k\to\infty} \|B * A_0^k * C\|$ is 0 then the trajectory is *insensitive* to initial conditions.

If, on the other hand, $\Psi_x(t)$ is periodic with $\Psi_x(t_1) = \Psi_x(t_{k+1})$ (that is, a closed orbit with period $(t_{k+1} - t_1)$), then A_0^k is a square matrix and $\Delta\mathbf{x'_k} = B * A_0^k * C * \Delta\mathbf{x'_0}$ is a Poincaré map. The stability of the periodic orbit is then determined by $\rho(B * A_0^k * C)$.[10] If $\rho(B * A_0^k * C) > 1$, that is, $\lim_{r\to\infty} \|(B * A_0^k * C)^r\|$ is *unbounded* then the periodic orbit is *unstable*, and if $\rho(B * A_0^k * C) < 1$, that is, $\lim_{r\to\infty} \|(B * A_0^k * C)^r\|$ is 0 then the periodic orbit is *stable*.

It should be noted that $\lim_{k\to\infty} \|B * A_0^k * C\|$ and $\lim_{r\to\infty} \|(B * A_0^k * C)^r\|$, by virtue of the nature of their limiting values, yield identical results irrespective of the choice of the matrix norm. We use the Frobenius norm ($\|A\|_F = \sqrt{\text{Trace}(A^T * A)}$) in the upcoming analysis.

8.4.2 The Revised Process

The computation of the norms of the matrices introduced in the previous section is problematic as it requires repeated pre- and post-multiplications with matrices B and C respectively, in the case pertaining to periodic orbits.

In this section, we present a revised process that constructs a matrix $\tilde{A}_0^k$ that simplifies the computation of the spectral properties of $B * A_0^k * C$. We begin with $\tilde{A}_0^0 = I - \frac{1}{n}(\mathbf{1})$, where $(\mathbf{1})$ denotes the matrix all of whose elements are 1, and $n = \sum_{i=1}^{\mathcal{S}}(n_i - \sigma_i)$ is the number of components in the initial perturbation. We then proceed with the rest of the process (generating $\tilde{A}_0^{k+1}$ from $\tilde{A}_0^k$) unaltered. Lemma 8.4.1 relates the properties of $\tilde{A}_0^k$ to those of $B * A_0^k * C$.

Lemma 8.4.1 *Let $\tilde{A}_0^k$ be an $(n \times n)$ square matrix. Then $\lim_{r\to\infty} \|(I - \frac{1}{n}(\mathbf{1})) * (\tilde{A}_0^k)^r\| = \lim_{r\to\infty} \|\tilde{A}_0^0 * (\tilde{A}_0^k)^r\| = 0$ (is unbounded) implies that $\lim_{r\to\infty} \|(B * A_0^k * C)^r\| = 0$ (is unbounded).*

Instead, let $\tilde{A}_0^k$ be an $(m \times n)$ matrix. Then $\lim_{k\to\infty} \|(I - \frac{1}{m}(\mathbf{1})) * \tilde{A}_0^k\| = 0$ (is unbounded) implies that $\lim_{k\to\infty} \|B * A_0^k * C\| = 0$ (is unbounded).

Proof:

---

[9] $\|A\|_2$ is the *spectral norm* of the matrix A (defined as the natural matrix norm induced by the L_2 norm), that is, $\|A\|_2 = sup_{x\neq 0} \frac{\|Ax\|_2}{\|x\|_2}$.

[10] $\rho(A)$ is the *spectral radius* of the matrix A, that is, $\rho(A) = max_{1\leq i\leq n}|\lambda_i|$ where the λ_i's are the eigen values of the matrix ($Ax_i = \lambda_i x_i$).

$\tilde{A}_0^k$ is an $(n \times n)$ square matrix:

The sum of the elements of any row in $A_0^0 = I$ is 1. Since $\forall l \ \sum_{i,j} {}^l\alpha_i^j = 1$, it follows that $\forall k \geq 0$ the sum of the elements of any row in A_0^k remains 1. The sum of the elements of any row in $\tilde{A}_0^0$ being 0, the same argument proves that $\forall k \geq 0$ the sum of the elements of any row in $\tilde{A}_0^k$ is 0. Moreover, induction on k proves that $\forall k \ \tilde{A}_0^k = A_0^k - \frac{1}{n}(\mathbf{1})$.

We also note that $C*B = I - \frac{1}{n}(\mathbf{1})$, $\tilde{A}_0^k * \frac{1}{n}(\mathbf{1}) = (\mathbf{0})$, and $\frac{1}{n}(\mathbf{1}) * \frac{1}{n}(\mathbf{1}) = \frac{1}{n}(\mathbf{1})$, and conclude via induction on r that $(B*A_0^k*C)^r = B*(\tilde{A}_0^k)^r*C$. B being $\tilde{A}_0^0$ without the last row, $B*(\tilde{A}_0^k)^r$ is $\tilde{A}_0^0*(\tilde{A}_0^k)^r$ without the last row. If $\lim_{r\to\infty} \|\tilde{A}_0^0*(\tilde{A}_0^k)^r\| = 0$, then $\lim_{r\to\infty} \tilde{A}_0^0*(\tilde{A}_0^k)^r = (\mathbf{0})$. Hence, $\lim_{r\to\infty} B * (\tilde{A}_0^k)^r = (\mathbf{0})$. If, on the other hand, $\lim_{r\to\infty} \|\tilde{A}_0^0 * (\tilde{A}_0^k)^r\|$ is unbounded, then so is $\lim_{r\to\infty} \|B * (\tilde{A}_0^k)^r\|$ since $\tilde{A}_0^0 * (\tilde{A}_0^k)^r$ amounts to deleting the row mean from each row of $(\tilde{A}_0^k)^r$. Finally, the product with C does not have an impact on the unboundedness of the matrix because the sum of the elements of any row in $B * (\tilde{A}_0^k)^r$ is 0.

$\tilde{A}_0^k$ is not constrained to be a square matrix:

B is $I - \frac{1}{m}(\mathbf{1})$ with the last row eliminated. Moreover, since $\forall k \geq 0 \ \tilde{A}_0^k = A_0^k - \frac{1}{n}(\mathbf{1})$, we have $B * A_0^k = B * \tilde{A}_0^k$. The remainder of the proof follows along the lines of the previous case.

Note that by commencing the process with a slightly altered matrix we have eliminated the repeated pre- and post-multiplications with matrices B and C mentioned at the beginning of the section.

8.4.3 The Stochastic Process

In this section, we first present a stochastic counterpart for the deterministic process described above. We then argue that the stochastic reformulation is reasonable in the case where the abstract dynamical system models a typical neocortical column. Finally, analysis of the stochastic process yields the desired understanding of the local effect of a series of births and deaths of spikes on a trajectory.

The process is begun with an $(n \times n)$ matrix $\mathbb{A}$, each of whose n rows are drawn independently from a uniform distribution on $[-0.5, 0.5]^n$. Therefore, if $v_1, v_2, ..., v_n$ are the n rows of $\mathbb{A}$, then $E(v_i) = \langle 0, 0, ..., 0 \rangle$, where $E(\cdot)$ denotes the expected value. Next, the row mean $\bar{v} = (1/n) \sum_{i=1}^n v_i$ is deducted from each row of $\mathbb{A}$. This yields $\tilde{A}_0^0 * \mathbb{A}$, which we set to $\mathbb{A}_0^0$. It

is clear that $E(v_i)$ in $\mathbb{A}_0^0$ remains $\langle 0, 0, ..., 0 \rangle$. Let $\mathbb{A}_0^k$ for some k be an $(m \times n)$ matrix where m is a large but finite integer.

For the birth of a spike, $\mathbb{A}_0^{k+1}$ is generated from $\mathbb{A}_0^k$ as follows:

(1) Randomly sample the space of row vectors in $\mathbb{A}_0^k$ and choose p rows, $v_1, v_2, ..., v_p$, where p is a random number chosen from a predefined range $[P_{low}, P_{high}]$. m being large, it can safely be assumed that the rows are chosen with replacement even if they are not.

(2) Choose p independent and identically distributed (i.i.d.) random variables $X_1, X_2, ..., X_p$ from a given independent distribution. Let $x_1, x_2, ..., x_p$ be the derived random variables $x_i = X_i / \sum_{i=1}^{p} X_i$, and

(3) Set $v_{new} = \sum_{i=1}^{p} x_i v_i$, and insert the row at a random location into $\mathbb{A}_0^k$ to generate $\mathbb{A}_0^{k+1}$.

For the death of a spike, $\mathbb{A}_0^{k+1}$ is generated from $\mathbb{A}_0^k$ as follows:

(1) Randomly choose a row from the space of row vectors in $\mathbb{A}_0^k$, and

(2) Delete the row from $\mathbb{A}_0^k$ to generate $\mathbb{A}_0^{k+1}$.

In the case of a system set up to model a typical neocortical column, the deterministic process described earlier can reasonably be viewed as the stochastic process described above. First, the connectivity between neurons within a column, while having evolved to achieve a specific function, has been experimentally ascertained to fit a uniform distribution (Schüz, 1992). Therefore, when neurons in the system are spiking at comparable rates, one can reasonably assume that each spike, during its finite lifetime, is equally likely to be effective in the birth of a new spike somewhere in the system. Second, whereas v_i specifies the sensitivity of the corresponding spike to the initial set of spikes, x_i specifies the sensitivity of the spike that just originated to the spike in question. The two are therefore causally independent. Third, whereas spikes that are effective in the birth of a new spike are related spatially in the system, this does not translate into any necessary relation among the elements of the corresponding rows. Finally, the location of afferent synapses on the collaterals of neurons in a column has been shown to fit a statistical distribution (Braitenberg & Schüz, 1991). Since $X_1, ..., X_p$ (corresponding to the various $\partial P / \partial x_i^j$'s) depend on the positions of the corresponding spikes and the nature of P, they can reasonably be approximated by i.i.d. random variables.

If $\mathbb{A}_0^k = \tilde{A}_0^k * \mathbb{A}$, and $\mathbb{A}_0^{k+1}$ is generated as above, then $\mathbb{A}_0^{k+1} = \tilde{A}_0^{k+1} * \mathbb{A}$. If a row is deleted from $\mathbb{A}_0^k$ to generate $\mathbb{A}_0^{k+1}$, the act corresponds to the deletion of the corresponding row from $\tilde{A}_0^k$ to generate $\tilde{A}_0^{k+1}$. If instead, $v_1, v_2, ..., v_p$ are the rows chosen from $\mathbb{A}_0^k$ to construct v_{new}, and $u_1, u_2, ..., u_p$ are the corresponding rows in $\tilde{A}_0^k$, since $v_i = \langle u_i.c_1, u_i.c_2, ..., u_i.c_n \rangle$ (where $c_1, ..., c_n$ are the columns of $\mathbb{A}$), $\sum_{i=1}^p x_i v_i = \langle (\sum x_i u_i).c_1, (\sum x_i u_i).c_2, ..., (\sum x_i u_i).c_n \rangle$. Therefore, $\mathbb{A}_0^{k+1} = \tilde{A}_0^{k+1} * \mathbb{A}$.

The following lemma describes the statistical properties of the rows of the matrix past the act of addition and/or deletion of a row. $V(\cdot)$ denotes the variance of the rows of the matrix, that is, $V(v_i) = E((v_i - \mu).(v_i - \mu))$, and $C(\cdot)$ denotes the covariance between the rows of the matrix, that is, $C(v_i, v_j) = E((v_i - \mu).(v_j - \mu))_{i \neq j}$.

Lemma 8.4.2 *Let $E_k(v_i) = \mu$, $V_k(v_i) = \sigma^2$, and $C_k(v_i, v_j) = \xi^2$ after the kth step (the result being the $(m \times n)$ matrix $\mathbb{A}_0^k$).*

(i) If the $(k+1)$th step involves the deletion of a row (v_{del}) from the matrix, then $E_{k+1}(v_i) = \mu$, and $V_{k+1}(v_i) - C_{k+1}(v_i, v_j) = (\sigma^2 - \xi^2)$.

(ii) If, on the other hand, the $(k+1)$th step involves the addition of a row (v_{new}) to the matrix, then $E_{k+1}(v_i) = \mu$. Moreover, if $pE(x_i^2) = (1 + \Delta)$ for some $\Delta \in \mathbb{R}$ ($\Delta > -1$ necessarily), then $V_{k+1}(v_i) - C_{k+1}(v_i, v_j) = (1 + \frac{\Delta(m-1)-2}{m(m+1)})(\sigma^2 - \xi^2)$.

Proof:

(i): *Since v_{del} is chosen randomly from the population of row vectors in the matrix, we have $E(v_{del}) = E_k(v_i) = \mu$, $V(v_{del}) = V_k(v_i) = \sigma^2$, and $C(v_{del}, v_i) = C_k(v_i, v_j) = \xi^2$. Consequently, $E_{k+1}(v_i) = \mu$ and $V_{k+1}(v_i) - C_{k+1}(v_i, v_j) = (\sigma^2 - \xi^2)$.*

Before considering (ii), we note that for the derived random variables $x_1, x_2, ..., x_p$ defined earlier in the section, (a) $\forall\, i,\ pE(x_i) = 1$, *and* (b) $\forall\, i, j, i \neq j,\ pE(x_i^2) + p(p-1)E(x_i x_j) = 1$.

(a) *follows from $\sum_{i=1}^p E(X_i / \sum X_i) = 1$, and $\forall i, j\ E(X_i / \sum X_i) = E(X_j / \sum X_j)$ because of the i.i.d. nature of the X_i's.*

(b) *follows from $\sum_{i=1}^p E(X_i^2 / (\sum X_i)^2) + \sum_{i=1,j=1,i\neq j}^{p,p} E((X_i X_j)/(\sum X_i)^2) = 1$ and the fact that the X_i's being i.i.d., $\forall i, j\ E(X_i^2/(\sum X_i)^2) = E(X_j^2/(\sum X_j)^2)$ and $\forall i, j, i \neq j$ $E((X_i X_j)/(\sum X_i)^2)$ yields the same result irrespective of the values of i and j.*

(ii): $E(v_{new}) = E_k(\sum_{i=1}^{p} x_i v_i) = \sum_{i=1}^{p} E_k(x_i v_i)$. *Since the* x_i*'s are chosen* independent *of the* v_i*'s,* $E(v_{new}) = \sum_{i=1}^{p} E(x_i)E_k(v_i) = \sum_{i=1}^{p} \frac{1}{p} E_k(v_i) = \mu$. *Moreover, since* $E(v_i) = \langle 0, 0, ..., 0\rangle$ *for the initial population of row vectors, we can now conclude that* $\forall k,\ E_k(v_i) = \langle 0, 0, ..., 0\rangle$.

Since $\mu = \langle 0, 0, ..., 0\rangle$, $V(v_{new}) = E((v_{new} - \mu).(v_{new} - \mu)) = E(v_{new}.v_{new}) = E_k(\sum_{i=1}^{p} x_i v_i . \sum_{i=1}^{p} x_i v_i) = E_k(\sum_{i=1}^{p} x_i^2 (v_i.v_i)) + E_k(\sum_{i=1,j=1,i\neq j}^{p,p} x_i x_j (v_i.v_j))$. x_i *being* independent *of* v_i, $V(v_{new}) = E(x_i^2)E_k(\sum_{i=1}^{p} v_i.v_i) + E(x_i x_j)E_k(\sum_{i=1,j=1,i\neq j}^{p,p} v_i.v_j) = \frac{1+\Delta}{p} E_k(\sum_{i=1}^{p} v_i.v_i) + \frac{-\Delta}{p(p-1)} E_k(\sum_{i=1,j=1,i\neq j}^{p,p} v_i.v_j) = (1+\Delta)\sigma^2 - \Delta(\frac{1}{m}\sigma^2 + \frac{m-1}{m}\xi^2) = \sigma^2 + \Delta\frac{m-1}{m}(\sigma^2 - \xi^2)$.

Likewise, $C(v_{new}, v_i) = E(v_{new}.v_i) = p(\frac{1}{m}(\frac{1}{p}\sigma^2) + \frac{m-1}{m}(\frac{1}{p}\xi^2)) = \xi^2 + \frac{1}{m}(\sigma^2 - \xi^2)$. *The two results give rise to the recurrence relations:* $V_{k+1} = V_k + \frac{\Delta(m-1)}{m(m+1)}(V_k - C_k)$ *and* $C_{k+1} = C_k + \frac{2}{m(m+1)}(V_k - C_k)$. *Therefore,* $V_{k+1} - C_{k+1} = (1 + \frac{\Delta(m-1)-2}{m(m+1)})(V_k - C_k)$.

Finally, in the base case let $E(v_i.v_i) = \sigma_0^2$ *for* $\mathbb{A}$. $E(v_i.v_j)_{i\neq j} = 0$ *since* v_i *is chosen independent of* v_j, *and* $E(v_i) = \mu = \langle 0, 0, ..., 0\rangle$. *In the case of* $\mathbb{A}_0^0 = \tilde{A}_0^0 * \mathbb{A}$, $E(v_i.v_i) = (1 - \frac{1}{n})^2\sigma_0^2 + (\frac{n-1}{n^2})\sigma_0^2 = (1 - \frac{1}{n})\sigma_0^2$. $E(v_i.v_j)_{i\neq j} = \frac{-2}{n}(1 - \frac{1}{n})\sigma_0^2 + (\frac{n-2}{n^2})\sigma_0^2 = -\frac{1}{n}\sigma_0^2$. *Therefore,* $V_0 - C_0 = \sigma_0^2$.

Having assumed that the trajectory is not drawn into the fixed point, we note that if $\mathbb{A}_0^k$ is an $(m_k \times n)$ matrix, then $m_k \in [M_{high}, M_{low}]$ where $M_{low} \gg 0$. Moreover, $E(\|\mathbb{A}_0^k\|_F) = \sqrt{m_k V_k}$. For the sake of brevity, we shall henceforth refer to $V_k(v_i)$ and $C_k(v_i, v_j)$ for rows in $\mathbb{A}_0^k$ as $V(\mathbb{A}_0^k)$ and $C(\mathbb{A}_0^k)$, respectively.

The following theorem identifies the local properties of trajectories based on Lemma 8.4.2. In all cases, we assume a regular trajectory that is not drawn into the fixed point $\prod_{i=1}^{\mathcal{S}} {}^{i}\overline{\mathbb{L}}_{n_i}^{n_i}$. It might be claimed that without external input sustaining the dynamics of the system, an aperiodic trajectory that is not drawn into the fixed point is not realizable. We therefore consider two cases: one with and one without external input. For the case with external input, the connectivity of the neurons in the system, whether they are input neurons or interneurons, is assumed to be uniform. The number of spikes generated within the system for any given trajectory $\Psi_x(t)$ since time t_1 is denoted by $I(t)$, and the number of external spikes introduced into the system since time t_1 is denoted by $O(t)$.

Theorem 8.4.1 (Sensitivity) *Let $\Psi_x(t)$ be a regular trajectory that is not drawn into the trivial fixed point $\prod_{i=1}^{\mathcal{S}} {}^i\overline{\mathbb{L}}_{n_i}^{n_i}$.*

(1) Given a system that receives no external input, if $\Psi_x(t)$ is aperiodic, then if $\Delta > \frac{2}{M_{low}}$, $\Psi_x(t)$ is, with probability 1, sensitive to initial conditions, and if $\Delta < \frac{2}{M_{high}}$, $\Psi_x(t)$ is, with probability 1, insensitive to initial conditions.

(2) Given a system that is sustained by external input, if $\Psi_x(t)$ is aperiodic, and constants ν, c satisfy $\forall t\ |O(t) - \nu I(t)| < c$, then if $\Delta > \frac{2}{M_{low}}(1+\nu+\frac{c}{M_{low}})^2 + 2(\nu+\frac{c}{M_{low}})(1+\nu+\frac{c}{M_{low}})$, $\Psi_x(t)$ is, with probability 1, sensitive to initial conditions.

(3) Given a system that receives no external input, if $\Psi_x(t)$ is periodic with $\Psi_x(t_1) = \Psi_x(t_{k+1})$, then if $\Delta > \frac{2}{M_{low}}$, $\Psi_x(t)$ is, with probability 1, unstable, and if $\Delta < \frac{2}{M_{high}}$, $\Psi_x(t)$ is, with probability 1, stable.

Proof:

(1): *Of the k steps in the process if k_b involve birth of spikes and k_d involve death of spikes then $k_b + k_d = k$, and $|k_b - k_d|$ is bounded. Therefore, $k \to \infty$ implies $k_b \to \infty$ and $k_d \to \infty$.*

If $\Delta > 0$, then $(1 + \frac{\Delta M_{high} - 2}{M_{low}^2})^{k_b}\sigma_0^2 > V(\mathbb{A}_0^k) - C(\mathbb{A}_0^k) > (1 + \frac{\Delta M_{low} - 2}{M_{high}^2})^{k_b}\sigma_0^2$. Simple algebra demonstrates that $V((I - \frac{1}{m}(\mathbf{1})) * \mathbb{A}_0^k) = (1 - \frac{1}{m})(V(\mathbb{A}_0^k) - C(\mathbb{A}_0^k))$. It therefore follows that if $\Delta < \frac{2}{M_{high}}$, then $lim_{k\to\infty} E(\|(I - \frac{1}{m}(\mathbf{1})) * \mathbb{A}_0^k\|_F) = 0$, and since $\|A\|_F \geq 0$ for any A, $Pr(lim_{k\to\infty}\|(I - \frac{1}{m}(\mathbf{1})) * \mathbb{A}_0^k\|_F > 0) = 0$. If, on the other hand, $\Delta > \frac{2}{M_{low}}$, then $lim_{k\to\infty} E(\|(I - \frac{1}{m}(\mathbf{1})) * \mathbb{A}_0^k\|_F)$ is unbounded. Moreover, $Pr(lim_{k\to\infty}\|(I - \frac{1}{m}(\mathbf{1})) * \mathbb{A}_0^k\|_F$ is bounded$) = 0$.[11]

Since $(I - \frac{1}{m}(\mathbf{1})) * \mathbb{A}_0^k = (I - \frac{1}{m}(\mathbf{1})) * \tilde{A}_0^k * \mathbb{A}$, and $\mathbb{A}$ is, with probability 1, a bounded rank n matrix, $lim_{k\to\infty}\|(I - \frac{1}{m}(\mathbf{1})) * \mathbb{A}_0^k\| = 0$ (unbounded) $\overset{q.s}{\Leftrightarrow} lim_{k\to\infty}\|(I - \frac{1}{m}(\mathbf{1})) * \tilde{A}_0^k\| = 0$ (unbounded) . The result then follows from Lemma 8.4.1.

(2): *Since $\forall t\ |O(t) - \nu I(t)| < c$, if there are m live internal spikes at any given time, the number of live external spikes at the same time lies in the range $[\nu m - c, \nu m + c]$. If p live spikes are randomly chosen from the system and q of those are internal spikes, then $E(q) \in [\frac{pm}{(1+\nu)m+c}, \frac{pm}{(1+\nu)m-c}]$.*

[11] For it to be bounded, an infinite subsequence of events, each of which occurs with probability < 1, must take place.

We now modify the stochastic process as follows. The process is begun with $\mathbb{A}_0^0 = \mathbb{A}$. *If the* kth *step involves the introduction of an external spike into the system,* $\mathbb{A}_0^k$ *is set to* $\mathbb{A}_0^{k-1}$. *If the* kth *step involves the birth of an internal spike,* $\mathbb{A}_0^k$ *is generated from* $\mathbb{A}_0^{k-1}$ *by randomly choosing* q *rows from* $\mathbb{A}_0^{k-1}$, *choosing random variables* $x_1, x_2, .., x_p$ *as described earlier, constructing* $v_{new} = \sum_{i=1}^{q} x_i v_i$, *and inserting it at a random location into* $\mathbb{A}_0^{k-1}$.

Clearly, as in case(1), $\forall k\ E_k(v_i) = \langle 0, 0, ..., 0 \rangle$. *Simple algebra also demonstrates that at the birth of a spike* $V_k = (\frac{m}{m+1} + \frac{(1+\Delta)q}{(m+1)p} - \frac{\Delta q(q-1)}{m(m+1)p(p-1)})V_{k-1} - \frac{\Delta(m-1)q(q-1)}{m(m+1)p(p-1)}C_{k-1}$, *and* $C_k = \frac{2q}{m(m+1)p}V_{k-1} + (\frac{m-1}{m+1} + \frac{2(m-1)q}{m(m+1)p})C_{k-1}$. *Noting that* $m \geq p \geq q$ *and assuming that* $\Delta > 0$, *we arrive at* $V_k - C_k \geq (1 + \frac{\Delta(m-1)q(q-1) - 2(mp-mq+q)(p-1)}{m(m+1)p(p-1)})(V_{k-1} - C_{k-1})$.

Therefore, if $\Delta > \frac{2}{M_{low}}(1 + \nu + \frac{c}{M_{low}})^2 + 2(\nu + \frac{c}{M_{low}})(1 + \nu + \frac{c}{M_{low}})$ *it follows that* $V_k - C_k > V_{k-1} - C_{k-1}$. *Finally, based on arguments identical to those in Lemma 8.4.1, we have* $lim_{k\to\infty}\|(I - \frac{1}{m}(\mathbf{1})) * A_0^k * \mathbb{A}\|$*is unbounded* $\stackrel{a.s}{\Rightarrow} lim_{k\to\infty}\|B * A_0^k * C\|$*is unbounded.*

(3): *We modify the stochastic process so as to construct the new matrix* $(\tilde{A}_0^k)^r * \mathbb{A}$ *for arbitrary* r. *As in case (1), the process is begun with* $\mathbb{A}_0^0 = \tilde{A}_0^0 * \mathbb{A}$. *Each step in the process is then carried out in the exact same manner as in case (1). However, after every* k *steps, the row mean of the matrix is deducted from each row, that is, the row mean is deducted from each row of* $\mathbb{A}_0^{kr}$, *for* $r = 1, 2, ...$ *before the next step is performed.*

Deletion of the row mean at the end of the first passage around the periodic orbit amounts to the operation $\tilde{A}_0^0 * \mathbb{A}_0^k = \tilde{A}_0^0 * \tilde{A}_0^k * \mathbb{A}$. *It follows from a previous discussion that every subsequent addition or deletion of rows can be considered as being performed on* $\tilde{A}_0^0$. *Therefore, just prior to the deletion of the row mean after the* r*th passage around the periodic orbit, we have* $(\tilde{A}_0^k)^r * \mathbb{A}$.

Since $V(\tilde{A}_0^0 * \tilde{A}_0^{kr} * \mathbb{A}) = (1 - \frac{1}{n})(V(\tilde{A}_0^{kr} * \mathbb{A}) - C(\tilde{A}_0^{kr} * \mathbb{A}))$ *and* $C(\tilde{A}_0^0 * \tilde{A}_0^{kr} * \mathbb{A}) = -\frac{1}{n}(V(\tilde{A}_0^{kr} * \mathbb{A}) - C(\tilde{A}_0^{kr} * \mathbb{A}))$, *it follows that* $V(\tilde{A}_0^0 * \tilde{A}_0^{kr} * \mathbb{A}) - C(\tilde{A}_0^0 * \tilde{A}_0^{kr} * \mathbb{A}) = V(\tilde{A}_0^{kr} * \mathbb{A}) - C(\tilde{A}_0^{kr} * \mathbb{A})$. *The rest of the argument follows along the lines of case (1).*

Case (3) is based on the assumption that the v_i's remain independent of the x_i's in spite of the x_i's being identical each time a specific event is encountered on the periodic orbit as it is traversed repeatedly by the process. We demonstrate that the assumption is reasonable.

We illustrate the issue using an example. Figure 8.1 depicts a single traversal of a periodic

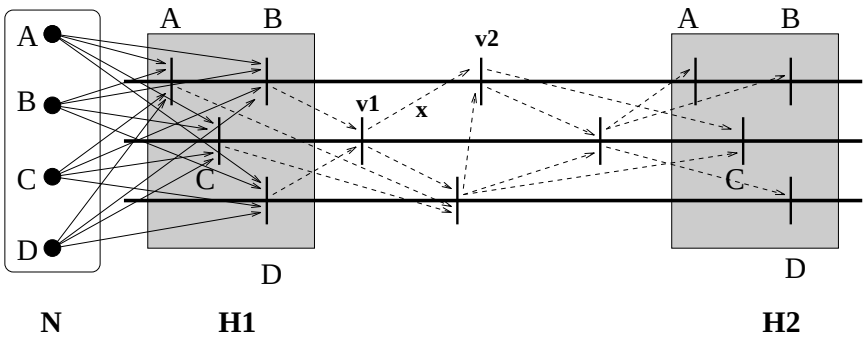

Figure 8.1: Graphical depiction of the construction of $(\tilde{A}_0^k)^n$.

orbit in a three-neuron system. The four spikes, A, B, C, and D, in region **H1** constitute the initial set of spikes (therefore, $n = 4$). Nodes in region **N**, also labeled A, B, C, and D, represent the deletion of the row mean at the end of each passage around the periodic orbit. The periodic orbit is extended to the right (**H2**) to mark the repetition of the spikes A, B, C, and D. The dotted arrows relate which spikes are effective in the birth of any given spike. We now regard the diagram as a directed graph with the additional constraint that nodes in **N** be identified with corresponding spikes in **H2**, that is, they be regarded as one and the same. Edges from nodes in **N**/**H2** to corresponding spikes in **H1** are assigned weights $(1 - \frac{1}{n})$, and to other spikes in **H1** are assigned weights $-\frac{1}{n}$. Each dotted edge is assigned weight x_i.

Let v_i correspond to any given spike i in the periodic orbit. The n $(= 4)$ elements of the row v_i (sensitivity to A, B, C, and D) after the rth passage around the periodic orbit can then be computed by identifying all paths from A in **N**/**H2** (respectively, B, C, and D for the three remaining elements) to spike i such that each path crosses **N**/**H2** r times before terminating at spike i, and setting $v_i = \sum_{\text{paths } e_1 e_2 \ldots e_q} w(e_1)w(e_2)...w(e_q)$, where $e_1...e_q$ are the edges in a path and $w(e_j)$'s their weights.

Given any spike v_i in the periodic orbit, a spike v_j that it is effective on, and the corresponding effectiveness x_i, contributions to v_i from paths that do not pass through v_j are independent of x_i.[12] Assuming that there are approximately n live spikes at any time,[13] the proportion of such paths is approximately $(1 - \frac{1}{n})^r$. The remaining paths can be partitioned into

[12]For example, in Figure 8.1 contributions to **v1** from paths that do not pass through **v2** are independent of **x**.

[13]Given that there are $\approx 10^5$ neurons in a typical column, the spiking rate of a typical neuron is $\approx 40/$ sec, and that the effects of a PSP lasts for ≈ 150 msec, $n \approx 6 \times 10^5$.

sets based on the number of times $l = 1, ..., r$, that each path passes through v_j. The assumption of independence is unbiased for each such set because $E(x_i) \sum_{j_1=1,...,j_l=1}^{p,...,p} E(x_{j_1}...x_{j_l}) = \sum_{j_1=1,...,j_l=1}^{p,...,p} E(x_i x_{j_1}...x_{j_l})$ is satisfied by the corresponding terms. The assumption of independence between the v_i's and the x_i's is therefore reasonable.

8.5 Qualitative Dynamics of Neocortical Columns

In this final section, we apply the result of Theorem 8.4.1 to characterize the dynamics of neocortical columns in the brain.

To begin, we note that the parameters of $P_k(\cdot)$, for any neuron k, can be partitioned into two sets: the set of afferent spikes into neuron k, and the set of spikes generated by neuron k. Under normal conditions, the spiking rate of a typical neuron in the neocortex is approximately 40 per second. The interspike intervals being large, $\partial P_k / \partial x_k^j \mid_{P_k(\cdot)=\mathcal{T}}$ is negligible. Consequently, at the birth of a spike at neuron k, ${}^k\alpha_k^j$ is negligible for all $j = 1, ..., n_k$.

Approximately 80% of all neurons in the neocortex are spiny (physiological experiments indicate that they are predominantly excitatory), and the rest are smooth (predominantly inhibitory) (Peters & Proskauer, 1980; Peters & Regidor, 1981; Braitenberg & Schüz, 1991; Shepherd, 1998). It therefore follows that the majority of the spikes in the system at any given time are excitatory. The impact of such spikes on $P(\cdot)$ of a typical neuron is given by a steep rising phase followed by a relatively gentle and prolonged falling phase (Bernander, Douglas & Koch, 1992). Consequently, the typical distribution of the ${}^k\alpha_i^j$'s at the birth of a spike at any neuron k comprises a few large positive elements and numerous small negative elements. We determined through numerical calculations based on mean spike rate, connectivity, and potential function data from the models presented in Chapter 7 that $E(\sum_{i,j}({}^k\alpha_i^j)^2) > 1$ under such conditions, and that $E(\sum_{i,j}({}^k\alpha_i^j)^2)$ rises as the number of small negative elements increase. The resultant values were in fact quite large and met all relevant conditions (from cases (1), (2) and (3)) in Theorem 8.4.1.

A neuronal system is considered to be operating under seizure-like conditions when most of the neurons in the system spike at intervals approaching the relative refractory period. Under such conditions, the first spike in the second set progressively assumes a significant role in the

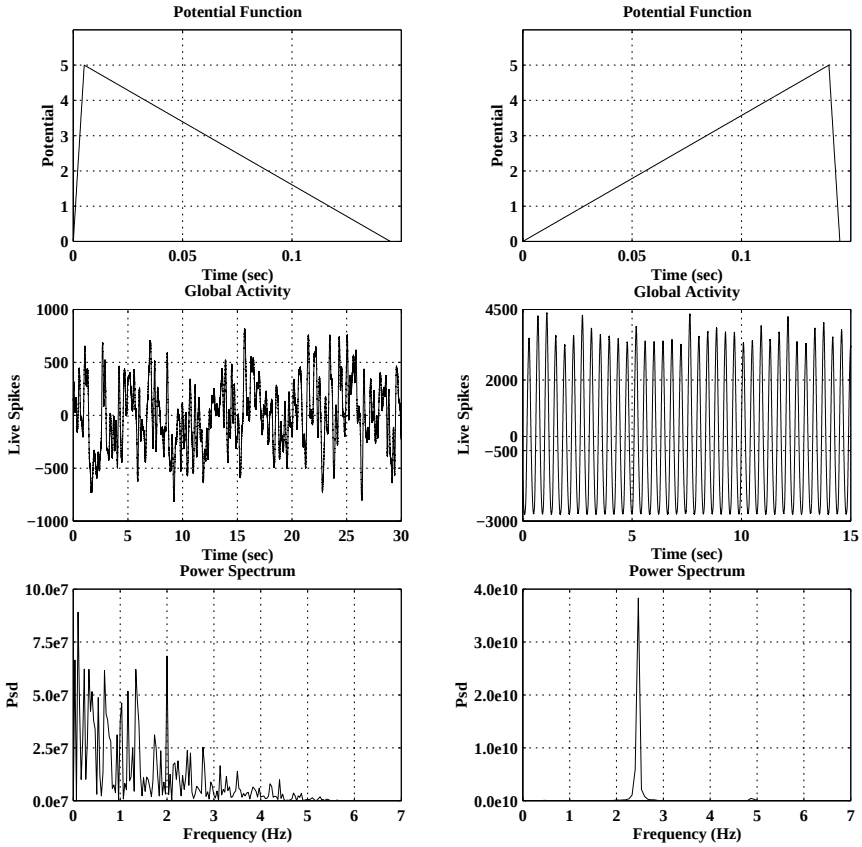

Figure 8.2: Dynamics of two systems of neurons that differ in terms of the impact of spikes on $P_i(\cdot)$.

determination of the time at which the neuron spikes next. Stated formally, if the most recent spike at neuron k is x_k^1, then at the subsequent birth of a spike at neuron k, ${}^k\alpha_k^1 = 1 - \epsilon$ and the remainder of the ${}^k\alpha_i^j$'s (that sum to ϵ) satisfy an appropriately scaled version of the distribution presented in the previous paragraph. As the system progressively approaches seizure-like conditions, ϵ drops from 1 to 0. Simple algebra shows that when ϵ is small, $E(\sum_{i,j}({}^k\alpha_i^j)^2) \approx 1 - 2\epsilon$.

In summary, as one proceeds from the region of the phase-space associated with low neuronal activity ($\epsilon \approx 1$) to the region associated with high neuronal activity ($\epsilon \approx 0$), periodic orbits go from being almost surely unstable (trajectories almost surely sensitive to initial conditions), to almost surely neutral, to almost surely stable, and back to being almost surely neutral.

We also found that under conditions of sparse activity, $E(\sum_{i,j}({}^k\alpha_i^j)^2) < 1$ if the distribution of the $\partial P_k / \partial x_i^j$'s is inverted, a state that can be realized by setting the impact of an excitatory (inhibitory) spike to have a gentle and prolonged rising (falling) phase followed by a steep and

short falling (rising) phase. Piecewise linear functions were used to fashion the potential functions in the models presented in Chapter 7, and simulation experiments were conducted. The results were consistent with the assertions of Theorem 8.4.1. Figure 8.2 presents the result of one such experiment. The columns represent two systems comprising 1000 neurons each, identical in all respects save the potential functions of the neurons. The first row depicts the effect of a typical excitatory spike on the potential function of a neuron, the second normalized time-series data pertaining to the total number of live spikes in each system, and the third results of a power spectrum analysis on each time series. While in the first case the dynamics is chaotic, in the second it is at best quasi-periodic.

8.6 Summary

In order to investigate the local properties of trajectories in the phase-space of the abstract dynamical system, we endowed the phase-space with a Riemannian metric. The metric was chosen in a manner such that sections of any given trajectory corresponding to intervals during which neither any neuron fired nor any spike expired, were both volume and shape preserving. This ensured that the local properties of trajectories could be deduced based on the analysis of two events—the birth of a spike and the death of a spike.

A measure analysis revealed that a trajectory was expansive at the birth of a spike and was contractile at the death of a spike. Analysis also revealed that folding of phase-space could occur across a series of births and deaths of spikes.

The cumulative effect of several births and deaths of spikes on a trajectory was deduced by modeling the process as a series of stochastic events. Analysis then revealed that there existed a criterion based on which one could infer whether a trajectory was sensitive or insensitive to initial conditions.

Finally, based on physiological parameters it was established that trajectories (periodic orbits) in the region of the phase-space corresponding to normal operational conditions in the neocortex were almost surely sensitive to initial conditions (unstable), and trajectories (periodic orbits) in the region of the phase-space corresponding to seizure-like conditions in the neocortex were almost surely insensitive to initial conditions (stable).

Chapter 9

Global Analysis

In the previous chapter, we investigated the local properties of trajectories in the phase-space of the abstract dynamical system. In this chapter, we explore the global structures that the dynamics of the system induces in the phase-space.

The standard approach to global analysis involves the identification of invariant sets[1] in the phase-space of the dynamical system and a subsequent investigation of their salient properties. Our approach, by comparison, is centered on the identification of the nonwandering set and an appropriate partition of it. As was demonstrated in Chapter 5, both approaches identify the same structures in the case of a dynamical system defined by a homeomorphism. The approaches however differ when the mapping is not so constrained.

This chapter is therefore organized along two themes. In the first part (Section 9.1) we elucidate the nature of the structures that are identified by our approach, in a general setting. The second part (Sections 9.2 and 9.3) then applies these results to the abstract dynamical system formulated in Chapter 6.

To elaborate, in Section 9.1 we frame the concepts of nonwandering points and basic sets in the broader context of a general mapping. These concepts, first introduced in Chapter 5 Section 3 in the context of a dynamical system defined by a homeomorphism, form the basis for the ensuing conceptual development. The need for a new construct for a dynamical system defined by a discontinuous map is demonstrated. The complex set is then defined and its nature explicated.

In Section 9.2, the abstract dynamical system formulated in Chapter 6 is transformed from a continuous dynamical system to a discrete dynamical system. The inherently discontinuous nature of the mapping is then highlighted.

---

[1] The reader should refer to Chapter 5 Section 3 for a formal definition of an invariant set.

Finally, in Section 9.3 a standard technique used to extract the nonwandering set and all basic sets from the phase-space of a discrete dynamical system is augmented to extract the basic sets, complex sets, and attractors from the phase-space of the abstract dynamical system formulated in Section 9.2.

9.1 Basic Definitions

As described in the introduction, our approach to global analysis is centered around the notion of the nonwandering set. Our objective in this section therefore is to extend all related concepts described in Chapter 5 Section 3 to dynamical systems that are defined by general mappings.

We begin by reintroducing the concepts of the nonwandering set and the basic set. In the definitions presented here, f is assumed to be a general mapping rather than a homeomorphism (unlike in the definitions in Chapter 5 Section 3). Although the shift to the broader context might seem innocuous, it has profound implications for the characterization of coherent structures in the phase-space of a dynamical system defined by a discontinuous map. $\mathbb{M}$ in the definitions denotes the phase-space of the system.

Definition 9.1.1 *A point $\mathbf{x} \in \mathbb{M}$ is labeled a* nonwandering *point of a mapping f if given any open neighborhood U of $\mathbf{x}$ and any $t_{min} > 0$ ($t_{min} \in \mathbb{Z}$), there exists a $t > t_{min}$ ($t \in \mathbb{Z}$) such that $f^t(U) \cap U \neq \emptyset$. A point that is not nonwandering is labeled* wandering *or* transient.

The set of all nonwandering points is called the *nonwandering set* and is represented by Ω.

Definition 9.1.2 *A set $\Lambda \subseteq \mathbb{M}$ is labeled a* basic set *of a mapping f if given any two points $\mathbf{x}, \mathbf{y} \in \Lambda$, any open neighborhoods U of $\mathbf{x}$ and V of $\mathbf{y}$ and any $t_{min} > 0$ ($t_{min} \in \mathbb{Z}$), there exist $t_1, t_2, t_3, t_4 > t_{min}$ ($t_1, t_2, t_3, t_4 \in \mathbb{Z}$) such that $f^{t_1}(U) \cap U \neq \emptyset$, $f^{t_2}(U) \cap V \neq \emptyset$, $f^{t_3}(V) \cap U \neq \emptyset$, and $f^{t_4}(V) \cap V \neq \emptyset$, and furthermore, Λ is a* maximal set *with regard to this property.*

It was demonstrated in Chapter 5 Section 3 that the set of all nonwandering points, Ω, is closed in $\mathbb{M}$ and that any basic set, Λ, which is necessarily a subset of Ω, is closed in $\mathbb{M}$ as well. The proofs for these statements did not exercise any constraints on f (such as it being a homeomorphism) and therefore apply to the general case defined here.

It was also proved in Chapter 5 Section 3 that under the assumption of f being a homeomorphism, membership in the same basic set defines an equivalence relation on Ω, and therefore the basic sets comprise a partition of Ω.

In the case of a general mapping f, membership in the same basic set falls short of an equivalence relation. The relation is reflexive since $\forall U, V$ open neighborhoods of $\mathbf{x}$, $U \cap V$ is an open neighborhood of $\mathbf{x}$, symmetric by definition, but not transitive since f is not a homeomorphism. Each nonwandering point is therefore a member of one or more basic sets.

This feature significantly affects the characterization of an attractor. We now define the concept of a complex set.

Definition 9.1.3 *Two basic sets Λ and Λ' are considered* coupled *if either $\Lambda \cap \Lambda' \neq \emptyset$ or there exists a finite or countably infinite sequence of basic sets $\Lambda_1, ..., \Lambda_k, ...$ such that for each i Λ_i and Λ_{i+1} are coupled, and in addition, $\Lambda \cap \overline{\bigcup_i \Lambda_i} \neq \emptyset$ and $\Lambda' \cap \overline{\bigcup_i \Lambda_i} \neq \emptyset$.*

We note immediately that this is an equivalence relation, and that it therefore partitions the set of all basic sets into equivalence classes. More significant, however, is the fact that the relation partitions Ω into disjoint sets. This follows from the observation that if, on the contrary, $\mathbf{x}$ belongs to two distinct classes, then there exist basic sets Λ and Λ', members of the respective classes, that are coupled.

Definition 9.1.4 *Each disjoint subset Ξ of Ω induced by the relation "coupled" is labeled a* complex set.

Theorem 9.1.1 *Any complex set, Ξ, (which is necessarily a subset of Ω) is closed in $\mathbb{M}$.*

Proof:

If $\mathbf{x}$ is a limit point of Ξ, then every open neighborhood of $\mathbf{x}$ contains a point in Ξ (which is necessarily a nonwandering point). Hence, $\mathbf{x}$ is a nonwandering point. Moreover, since each such point in Ξ belongs to at least one member basic set, there exist $\Lambda_1, ..., \Lambda_k, ... \subset \Xi$ such that $\mathbf{x} \in \overline{\bigcup_{i=1}^{\infty} \Lambda_i}$. Consequently, if $\mathbf{x} \in \Lambda$ then $\Lambda \cap \overline{\bigcup_{i=1}^{\infty} \Lambda_i} \neq \emptyset$ which implies that $\Lambda \subset \Xi$, and therefore $\mathbf{x} \in \Xi$. Ξ is therefore closed in $\mathbb{M}$.

Finally, an attractor is defined as in Chapter 5.

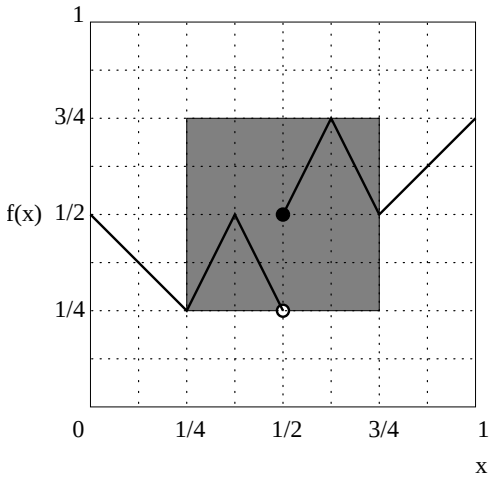

Figure 9.1: A map $f : [0,1] \rightarrow [\frac{1}{4}, \frac{3}{4}]$ that contains a chaotic attractor at $[\frac{1}{4}, \frac{3}{4}]$. The attractor is a complex set that is composed of the two basic sets $[\frac{1}{4}, \frac{1}{2}]$ and $[\frac{1}{2}, \frac{3}{4}]$.

Definition 9.1.5 *A complex set Ξ is called an* attractor *if there exists a* bounded *set U that satisfies the constraints: $\Xi \subset int(U)$ the interior[2] of U, for every complex set $\Xi' \neq \Xi$, $\overline{U} \cap \Xi' = \emptyset$, and U is positively invariant, that is, $f^t(U) \subseteq U$ for every $t \in \mathbb{Z}^+$.*

Note that an attractor that is a complex set is *anisotropic* in the sense that a trapped trajectory does not necessarily visit every basic set in the complex set, and moreover, the sequence of basic sets visited by the trajectory depends on its point of entry. In essence, the discontinuous nature of f sanctions the existence of anisotropic attractors.

In Figure 9.1 we present a simple example of an anisotropic chaotic attractor. The interval $[\frac{1}{4}, \frac{3}{4}]$ constitutes the attractor and the interval $[0,1]$ its realm of attraction. The attractor $[\frac{1}{4}, \frac{3}{4}]$ is a complex set composed of the two basic sets $[\frac{1}{4}, \frac{1}{2}]$ and $[\frac{1}{2}, \frac{3}{4}]$. The point $\frac{1}{2}$ is a member of both basic sets.

That the intervals $[0, \frac{1}{4})$ and $(\frac{3}{4}, 1]$ are comprised of wandering points follows from the fact that the function maps $[0, \frac{1}{4})$ onto $(\frac{1}{4}, \frac{1}{2}]$ and $(\frac{3}{4}, 1]$ onto $(\frac{1}{2}, \frac{3}{4}]$. Any point in these regions is therefore mapped to $[\frac{1}{4}, \frac{3}{4}]$ in a single iteration, never to return to its interval of origin.

The interval $[\frac{1}{4}, \frac{3}{4}]$, on the other hand, is comprised of nonwandering points. Note, however, that unlike in the example presented in Chapter 5, $[\frac{1}{4}, \frac{3}{4}]$ is composed of two basic sets. That the attractor is anisotropic follows from the observation that any point in $[\frac{1}{2}, 1]$ is attracted to the

[2]The interior of a set U is the set of all interior-points of U.

basic set $[\frac{1}{2}, \frac{3}{4}]$ and not the entire complex set.

9.2 Formulation of the Discrete Dynamical System

In this section, we transform the continuous dynamical system formulated in Chapter 6 into a discrete dynamical system. The transformation simplifies the upcoming analysis.

We begin by introducing an equivalence relation on all points $p \in \prod_{i=1}^{\mathcal{S}} {}^{i}\overline{\mathbb{L}}_{n_i} \setminus \bigcup_{i=1}^{\mathcal{S}} P_i^I$. For points p and q we define the relation $p \sim q$ if $p, q \in \prod_{i=1}^{\mathcal{S}} ({}^{i}\overline{\mathbb{L}}_{n_i}^{\sigma_i} \setminus {}^{i}\overline{\mathbb{L}}_{n_i}^{\sigma_i+1}) \setminus \bigcup_{i=1}^{\mathcal{S}} P_i^I$ for arbitrary but fixed values of the σ_i's, and there exists a trajectory $\Psi_x(t)$ such that $p = \Psi_x(t_1)$, $q = \Psi_x(t_2)$, and $\forall t \in [\min(t_1, t_2), \max(t_1, t_2)]$, $\Psi_x(t) \in \prod_{i=1}^{\mathcal{S}} ({}^{i}\overline{\mathbb{L}}_{n_i}^{\sigma_i} \setminus {}^{i}\overline{\mathbb{L}}_{n_i}^{\sigma_i+1})$.

We define the equivalence class of points $[p] = \{q \mid q \sim p\}$, and an associated mapping $\Theta : (\prod_{i=1}^{\mathcal{S}} {}^{i}\overline{\mathbb{L}}_{n_i} \setminus \bigcup_{i=1}^{\mathcal{S}} P_i^I)/\sim \rightarrow (\prod_{i=1}^{\mathcal{S}} {}^{i}\overline{\mathbb{L}}_{n_i} \setminus \bigcup_{i=1}^{\mathcal{S}} P_i^I)/\sim$ as $\Theta([p]) = [q]$ if there exists a trajectory $\Psi_x(t)$ such that two of its successive segments (as defined in Chapter 8) satisfy $\{\Psi_x(t) \mid t_j < t < t_{j+1}\} \subseteq [p]$ and $\{\Psi_x(t) \mid t_{j+1} < t < t_{j+2}\} \subseteq [q]$.

We operate hereafter on $(\prod_{i=1}^{\mathcal{S}} {}^{i}\overline{\mathbb{L}}_{n_i} \setminus \bigcup_{i=1}^{\mathcal{S}} P_i^I)/\sim$,[3] and forsake $\Psi(x, t)$ in favor of Θ. This concludes the reformulation of the continuous system into a discrete system.

We note immediately that Θ is only a piecewise continuous function. The analysis in the previous chapter was restricted to trajectories, $\Psi(x, t)$, that are locally continuous in x for the simple reason that all other $\Psi(x, t)$'s are, trivially, sensitive to initial conditions.

9.3 Extraction of Basic Sets, Complex Sets, and Attractors from the Phase-Space

In this final section, we demonstrate how all basic sets, complex sets, attractors, and their realms of attraction can be isolated, given the exact instantiations of P_i^I for all $i = 1, ..., \mathcal{S}$.

Figure 9.2 introduces a procedure that constructs an infinite partition of the reformulated phase-space $(\prod_{i=1}^{\mathcal{S}} {}^{i}\overline{\mathbb{L}}_{n_i} \setminus \bigcup_{i=1}^{\mathcal{S}} P_i^I)/\sim$. The procedure begins with the initial partition of the space $\{\prod_{i=1}^{\mathcal{S}} ({}^{i}\overline{\mathbb{L}}_{n_i}^{\sigma_i} \setminus {}^{i}\overline{\mathbb{L}}_{n_i}^{\sigma_i+1}) \setminus \bigcup_{i=1}^{\mathcal{S}} P_i^I/\sim \mid 0 \leq \sigma_i \leq n_i; i = 1, ..., \mathcal{S}\}$ and generates a succession of refinements. At each stage, the procedure yields a directed graph on a set of nodes, with each node corresponding to a set in the partition. We shall henceforth refer to a node in the

[3] $\prod_{i=1}^{\mathcal{S}} {}^{i}\overline{\mathbb{L}}_{n_i} \setminus \bigcup_{i=1}^{\mathcal{S}} P_i^I$ is regarded with the topology defined in Chapter 6, and $(\prod_{i=1}^{\mathcal{S}} {}^{i}\overline{\mathbb{L}}_{n_i} \setminus \bigcup_{i=1}^{\mathcal{S}} P_i^I)/\sim$ with the corresponding quotient topology.

$j := 0$ /* **Stage** 0 */
Set Initial Partition of $(\prod_{i=1}^{\mathcal{S}} {}^{i}\overline{\mathbb{L}}_{n_i} \setminus \cup_{i=1}^{\mathcal{S}} P_i^I)/\sim$
to $\{\prod_{i=1}^{\mathcal{S}} ({}^{i}\overline{\mathbb{L}}_{n_i}^{\sigma_i} \setminus {}^{i}\overline{\mathbb{L}}_{n_i}^{\sigma_i+1}) \setminus \cup_{i=1}^{\mathcal{S}} P_i^I/\sim \mid 0 \leq \sigma_i \leq n_i; i = 1, ..., \mathcal{S}\}$.
Generate initial **Directed Graph**:
(i) Queue $\mathcal{Q}_0 = \emptyset$,
(ii) Assign unique **node** to each **set** in the partition,
/* We shall henceforth refer to them as $\mathcal{N}$'s and $\mathcal{P}$'s respectively. */
(iii) $\forall a, b$ assign edge from $\mathcal{N}_a$ to $\mathcal{N}_b$ if $\exists\ [p], [q]$ s.t. $[p] \in \mathcal{P}_a$, $[q] \in \mathcal{P}_b$, and $\Theta([p]) = [q]$.
Push all **nodes** into Queue $\mathcal{Q}_0$
For (j=1 to ∞) { /* **Stages** 1 **through** ∞ */
Queue $\mathcal{Q}_j = \emptyset$
Repeat Until ($\mathcal{Q}_{j-1} = \emptyset$) {
$\mathcal{N}^{j-1}$=Pop($\mathcal{Q}_{j-1}$)
Let ${}^{I}\mathcal{N}_1^l, ..., {}^{I}\mathcal{N}_m^l$ ($l = j-1$ or j) be the nodes that receive edges **from** $\mathcal{N}^{j-1}$
Let ${}^{O}\mathcal{N}_1^l, ..., {}^{O}\mathcal{N}_n^l$ ($l = j-1$ or j) be the nodes that direct edges **to** $\mathcal{N}^{j-1}$
Let ${}^{I}\mathcal{P}_1^l, ..., {}^{I}\mathcal{P}_m^l; {}^{O}\mathcal{P}_1^l, ..., {}^{O}\mathcal{P}_n^l; \mathcal{P}^{j-1}$ be the sets in the current partition that correspond to nodes ${}^{I}\mathcal{N}_1^l, ..., {}^{I}\mathcal{N}_m^l; {}^{O}\mathcal{N}_1^l, ..., {}^{O}\mathcal{N}_n^l; \mathcal{N}^{j-1}$
Construct a finite partition of $\mathcal{P}^{j-1}$ in the following manner.
Set tentative partition of $\mathcal{P}^{j-1}$
to $\{\Theta^{-1}({}^{I}\mathcal{P}_i^l) \cap \mathcal{P}^{j-1} \mid i = 1, ..., m\} \cup \{\mathcal{P}^{j-1} \setminus \cup_{i=1}^{m} \Theta^{-1}({}^{I}\mathcal{P}_i^l)\}$.
Now construct a finite *refinement* of this tentative partition, $\{\mathcal{P}_1^j, ..., \mathcal{P}_p^j\}$,
such that $\forall i = 1, ..., p\ \mathcal{P}_i^j$ is connected, and *diam*$(\mathcal{P}_i^j) \leq \frac{1}{2}$*diam*$(\mathcal{P}^{j-1})$.
Delete $\mathcal{N}^{j-1}$ and add $\mathcal{N}_1^j, ..., \mathcal{N}_p^j$ to Graph /* Corresponding to sets $\mathcal{P}_1^j, ..., \mathcal{P}_p^j$. */
Replace all previous edges from $\mathcal{N}^{j-1}$ to ${}^{I}\mathcal{N}_1^l, ..., {}^{I}\mathcal{N}_m^l$ with new edges from $\mathcal{N}_1^j, ..., \mathcal{N}_p^j$ to ${}^{I}\mathcal{N}_1^l, ..., {}^{I}\mathcal{N}_m^l$ according to rule (iii) in Stage 0.
Replace all previous edges from ${}^{O}\mathcal{N}_1^l, ..., {}^{O}\mathcal{N}_n^l$ to $\mathcal{N}^{j-1}$ with new edges from ${}^{O}\mathcal{N}_1^l, ..., {}^{O}\mathcal{N}_n^l$ to $\mathcal{N}_1^j, ..., \mathcal{N}_p^j$ according to rule (iii) in Stage 0.
Push nodes $\mathcal{N}_1^j, ..., \mathcal{N}_p^j$ into Queue $\mathcal{Q}_j$
}
}

Figure 9.2: A procedure that constructs an infinite partition of the Phase-Space and aids in locating all nonwandering points, basic sets, complex sets, and attractors.

directed graph by $\mathcal{N}$, and the corresponding set in the partition by $\mathcal{P}$.

We note that the partition operation is well-defined since any $\mathcal{P}$ partitioned by the procedure satisfies the constraint $\Theta(\mathcal{P}) \cap \mathcal{P} = \emptyset$.

We now present a framework that will aid in the extraction of all basic sets, complex sets, and attractors from the reformulated phase-space.

Definition 9.3.1 *A node $\mathcal{N}_a^j$ from stage j is labeled a* descendant *of the node $\mathcal{N}_b^k$ from stage k if $j > k$ and the corresponding sets in the partition satisfy $\mathcal{P}_a^j \subset \mathcal{P}_b^k$.*

Let $\mathcal{N}_1^j\mathcal{N}_2^j...\mathcal{N}_n^j$ be a path in the directed graph at stage j. We define the set ${}_iP$ recursively as: ${}_1P = \mathcal{P}_n^j$ and ${}_{i+1}P = \Theta^{-1}({}_iP) \cap \mathcal{P}_{n-i}^j$.

Definition 9.3.2 *A path $\mathcal{N}_1^j\mathcal{N}_2^j...\mathcal{N}_n^j$ in the directed graph is labeled a* false *path of* primary *length p if $\forall i = 1, ..., p \quad {}_iP \neq \emptyset$ and ${}_{p+1}P = \emptyset$.*

We now make certain observations about the procedure.

1. If at stage j there is a trajectory in the phase-space that has consecutive segments in the sets $\mathcal{P}_1^j, \mathcal{P}_2^j, ..., \mathcal{P}_n^j$, then the corresponding directed graph contains the path $\mathcal{N}_1^j\mathcal{N}_2^j...\mathcal{N}_n^j$. In other words, given any trajectory in the phase-space, the corresponding path in the directed graph exists at any stage.

2. If at stage j the directed graph does not contain the path $\mathcal{N}_1^j\mathcal{N}_2^j...\mathcal{N}_n^j$, then at stage $(j+1)$ the directed graph does not contain the path $\mathcal{N}_{i_1}^{j+1}\mathcal{N}_{i_2}^{j+1}...\mathcal{N}_{i_n}^{j+1}$ for any descendant $\mathcal{N}_{i_k}^{j+1}$ of $\mathcal{N}_k^j$, $k = 1, ..., n$.

3. If at stage j, $\mathcal{N}_1^j\mathcal{N}_2^j...\mathcal{N}_n^j$ is a false path of primary length p, then at stage $(j+p-1)$ no path $\mathcal{N}_{i_1}^{j+p-1}\mathcal{N}_{i_2}^{j+p-1}...\mathcal{N}_{i_n}^{j+p-1}$ exists for any descendant $\mathcal{N}_{i_k}^{j+p-1}$ of $\mathcal{N}_k^j$, $k = 1, ..., n$.

   This follows from the observations: (i) (base case) If at stage j, $\mathcal{N}_1^j\mathcal{N}_2^j...\mathcal{N}_n^j$ is a false path of primary length 2, then at stage $(j+1)$ no path $\mathcal{N}_{i_1}^{j+1}\mathcal{N}_{i_2}^{j+1}...\mathcal{N}_{i_n}^{j+1}$ exists for any descendant $\mathcal{N}_{i_k}^{j+1}$ of $\mathcal{N}_k^j$, $k = 1, ..., n$, and (ii) (inductive case) If at stage j, $\mathcal{N}_1^j\mathcal{N}_2^j...\mathcal{N}_n^j$ is a false path of primary length p, then at stage $(j+1)$ if a path $\mathcal{N}_{i_1}^{j+1}\mathcal{N}_{i_2}^{j+1}...\mathcal{N}_{i_n}^{j+1}$ exists for any descendant $\mathcal{N}_{i_k}^{j+1}$ of $\mathcal{N}_k^j$, $k = 1, ..., n$, then the path $\mathcal{N}_{i_1}^{j+1}\mathcal{N}_{i_2}^{j+1}...\mathcal{N}_{i_{n-1}}^{j+1}$ is a false path of primary length $(p-1)$. Both observations follow from the fact that at stage $(j+1)$, $\mathcal{P}_{n-1}^j$ is partitioned in a manner such that there exist $\mathcal{P}_{i_{n-1}^1}^{j+1}, ..., \mathcal{P}_{i_{n-1}^q}^{j+1}$ that satisfy $\bigcup_{k=1}^q \mathcal{P}_{i_{n-1}^k}^{j+1} = \Theta^{-1}(\mathcal{P}_n^j) \cap \mathcal{P}_{n-1}^j$.

Definition 9.3.3 *Given any stage j, a set of nodes $\langle \mathcal{N}_k^j \rangle = \{\mathcal{N}_{i_k^l}^j \mid l = 1, ..., m_k^j\}$ is referred to as a* cluster *if $\bigcap_{l=1}^{m_k^j} \overline{\mathcal{P}_{i_k^l}^j} \neq \emptyset$.*

We now define a relation *Recurrent*$(\cdot, \cdot)$ between clusters at stage j as follows.

Definition 9.3.4 *Given any pair of clusters $\langle \mathcal{N}_a^j \rangle$ and $\langle \mathcal{N}_b^j \rangle$ at stage j, Recurrent$(\langle \mathcal{N}_a^j \rangle, \langle \mathcal{N}_b^j \rangle)$ if and only if $\exists l_a, l'_a \in \{1, ..., m_a^j\}$ and $\exists l_b, l'_b \in \{1, ..., m_b^j\}$ such that paths $\mathcal{N}^j_{i_a^{l_a}} \mathcal{N}^j_{e_1} ... \mathcal{N}^j_{e_p} \mathcal{N}^j_{i_b^{l_b}}$ and $\mathcal{N}^j_{i_b^{l'_b}} \mathcal{N}^j_{f_1} ... \mathcal{N}^j_{f_q} \mathcal{N}^j_{i_a^{l'_a}}$ exist in the directed graph where the node $\mathcal{N}_h^j$ lies on a cycle for some $h \in \{i_a^{l_a}, e_1, ..., e_p, i_b^{l_b}\}$ and some $h \in \{i_b^{l'_b}, f_1, ..., f_q, i_a^{l'_a}\}$.*

With the framework established, we are now poised to present the second of the two central results of this thesis. In the following set of theorems we identify the nonwandering set, the basic sets, and the complex sets in the reformulated phase-space of the abstract dynamical system.

The following theorem identifies all nonwandering points in $(\prod_{i=1}^{\mathcal{S}} {}^i\overline{\mathbb{L}}_{n_i} \setminus \bigcup_{i=1}^{\mathcal{S}} P_i^I)/\sim$ with the exception of the trivial fixed point at $\prod_{i=1}^{\mathcal{S}} {}^i\overline{\mathbb{L}}_{n_i}^{n_i}$. We assign the node corresponding to the set $\prod_{i=1}^{\mathcal{S}} {}^i\overline{\mathbb{L}}_{n_i}^{n_i}$ nonwandering status at the start of the process.

Theorem 9.3.1 *Let $\{\langle \mathcal{N}_k^j \rangle \mid k = 1, ..., n_j\}$ be the set of all clusters at stage j that satisfy the constraint $\forall k = 1, ..., n_j$, Recurrent$(\langle \mathcal{N}_k^j \rangle, \langle \mathcal{N}_k^j \rangle)$. Then, the set of all nonwandering points is $\Omega = \bigcap_{j=0}^{\infty} (\bigcup_{k=1,l=1}^{n_j, m_k^j} \mathcal{P}^j_{i_k^l})$.*

Proof:

$[p]$ is a nonwandering point $\Rightarrow [p] \in \bigcap_{j=0}^{\infty} (\bigcup_{k=1,l=1}^{n_j, m_k^j} \mathcal{P}^j_{i_k^l})$:

Let $[p] \in \prod_{i=1}^{\mathcal{S}} ({}^i\overline{\mathbb{L}}_{n_i}^{\sigma_i} \setminus {}^i\overline{\mathbb{L}}_{n_i}^{\sigma_i+1}) \setminus \bigcup_{i=1}^{\mathcal{S}} P_i^I / \sim$ for arbitrary but fixed values of the σ_i's. We assume, without loss of generalization, that $[p] \in \mathcal{P}_1^j$ at stage j. If $[p]$ lies in the interior of $\mathcal{P}_1^j$, an open neighborhood U of $[p]$ can be chosen such that $U \subset \mathcal{P}_1^j$. There is then a trajectory through $\mathcal{P}_1^j$ that returns to it. The unitary cluster $\{\mathcal{N}_1^j\}$ then satisfies the criterion. If, on the other hand, $[p]$ lies on the boundary of $\mathcal{P}_1^j$, there are only finitely many sets $\mathcal{P}_1^j, ..., \mathcal{P}_r^j$ in $\prod_{i=1}^{\mathcal{S}} ({}^i\overline{\mathbb{L}}_{n_i}^{\sigma_i} \setminus {}^i\overline{\mathbb{L}}_{n_i}^{\sigma_i+1}) \setminus \bigcup_{i=1}^{\mathcal{S}} P_i^I / \sim$ such that $\forall l = 1, ..., r,\ [p] \in \overline{\mathcal{P}_l^j}$.[4] We choose U such that $U \subset \bigcup_{l=1}^{r} \mathcal{P}_l^j$. Then, since $\Theta^n(U) \cap U \neq \emptyset$ for an infinite sequence of n's, $\exists l_1, l_2 \in \{1, ..., r\}$, not necessarily distinct, such that there are arbitrarily long trajectories from $\mathcal{P}_{l_1}^j$ to $\mathcal{P}_{l_2}^j$. Since the directed graph has a finite number of nodes at any stage, there exists a path from $\mathcal{N}_{l_1}^j$ to $\mathcal{N}_{l_2}^j$ such that a node on the path lies on a cycle. The cluster $\{\mathcal{N}_1^j, ..., \mathcal{N}_r^j\}$ then satisfies the criterion.

$[p]$ is a wandering point $\Rightarrow [p] \notin \bigcap_{j=0}^{\infty} (\bigcup_{k=1,l=1}^{n_j, m_k^j} \mathcal{P}^j_{i_k^l})$:

[4] Given the nature of the topology, $[p] \notin \overline{\mathcal{P}}$ for any $\mathcal{P}$ that does not lie in $\prod_{i=1}^{\mathcal{S}} ({}^i\overline{\mathbb{L}}_{n_i}^{\sigma_i} \setminus {}^i\overline{\mathbb{L}}_{n_i}^{\sigma_i+1}) \setminus \bigcup_{i=1}^{\mathcal{S}} P_i^I / \sim$.

As above, we assume $[p] \in \mathcal{P}_1^j$ at stage j. Since at each stage the diameter[5] *of each set in the partition drops by a factor of two, given any open neighborhood U of $[p]$, there exists a stage j where $(\mathcal{P}_1^j \subset U) \wedge \forall l(\overline{\mathcal{P}_1^j} \cap \overline{\mathcal{P}_l^j} \neq \emptyset \Rightarrow \mathcal{P}_l^j \subset U)$. Let $\overline{\mathcal{P}_1^j} \cap \overline{\mathcal{P}_l^j} \neq \emptyset$ for $l = 1, ..., r$. Then any cluster that contains $\mathcal{N}_1^j$ can, at best, contain $\mathcal{N}_l^j$ for some $l \in \{1, ..., r\}$. Given any such cluster, if $\exists l_1, l_2$ such that there is a path from $\mathcal{N}_{l_1}^j$ to $\mathcal{N}_{l_2}^j$ through a cycle, then the path is a false path since $\bigcup_{l=1}^r \mathcal{P}_l^j \subset U$. There is then a stage $(j+p)$ wherein all descendants of $\mathcal{N}_{l_1}^j$ and $\mathcal{N}_{l_2}^j$ do not lie on the path.*

The following corollary to Theorem 9.3.1 identifies basic sets in the reformulated phase-space of the abstract dynamical system.

Corollary 9.3.1 *Let $\{\langle \mathcal{N}_k^j \rangle \mid \ k = 1, ..., n_j\}$ for stages $j = 1, 2, ...$ be successive sets of clusters such that (i) each set maximally satisfies $\forall k_1, k_2 \in \{1, ..., n_j\}$, Recurrent$(\langle \mathcal{N}_{k_1}^j \rangle, \langle \mathcal{N}_{k_2}^j \rangle)$, and (ii) $\forall j \ \bigcup_{k=1,l=1}^{n_j, m_k^j} \mathcal{P}_{i_k^l}^j \subseteq \bigcup_{k=1,l=1}^{n_{j-1}, m_k^{j-1}} \mathcal{P}_{i_k^l}^{j-1}$. Then, $\bigcap_{j=0}^{\infty}(\bigcup_{k=1,l=1}^{n_j, m_k^j} \mathcal{P}_{i_k^l}^j)$ is a basic set. Conversely, every basic set is representable as such.*

Proof:

If $[p]_1, [p]_2 \in \bigcap_{j=0}^{\infty}(\bigcup_{k=1,l=1}^{n_j, m_k^j} \mathcal{P}_{i_k^l}^j)$ for any sequence of sets satisfying criteria (i) and (ii), then based on arguments similar to those in the previous theorem, we conclude that there exists a basic set Λ such that $[p]_1, [p]_2 \in \Lambda$. Moreover, Λ being maximal, $\bigcap_{j=0}^{\infty}(\bigcup_{k=1,l=1}^{n_j, m_k^j} \mathcal{P}_{i_k^l}^j) \subseteq \Lambda$. Finally, if there exists a $[p] \in \Lambda$ such that $[p] \notin \bigcap_{j=0}^{\infty}(\bigcup_{k=1,l=1}^{n_j, m_k^j} \mathcal{P}_{i_k^l}^j)$, then for some stage j_0 the set $\{\langle \mathcal{N}_k^{j_0} \rangle \mid \ k = 1, ..., n_{j_0}\}$ is not maximal.

Conversely, if Λ is a basic set, a sequence of sets satisfying criteria (i) and (ii) can be constructed such that $\forall [p] \in \Lambda$ and for every stage j, $[p] \in \langle \mathcal{N}_k^j \rangle$ for some cluster $\langle \mathcal{N}_k^j \rangle$ in the set. This is based on observations: (a) if $\{\langle \mathcal{N}_k^j \rangle \mid \ k = 1, ..., n_j\}$ for some stage j satisfies criterion (i), then the minimal set $\{\langle \mathcal{N}_{k'}^{j-1} \rangle \mid \forall \mathcal{N}_{i_k^l}^j \in \langle \mathcal{N}_k^j \rangle \ \exists \mathcal{N}_{i_{k'}^l}^{j-1} \in \langle \mathcal{N}_{k'}^{j-1} \rangle \ \mathcal{P}_{i_k^l}^j \subset \mathcal{P}_{i_{k'}^l}^{j-1}\}$ is Recurrent for all pairs of member clusters, and can therefore be expanded to satisfy criteria (i) and (ii), (b) if $\{\langle \mathcal{N}_k^{j_0} \rangle \mid \ k = 1, ..., n_{j_0}\}$ at some stage j_0 is a set of clusters such that $\forall [p] \in \Lambda \ \exists \langle \mathcal{N}_k^{j_0} \rangle$ where $[p] \in int(\langle \mathcal{N}_k^{j_0} \rangle)$ and vice versa, then there are only finitely many ways it can be expanded to satisfy criterion (i), and (c) there is then a stage $(j_0 + p)$ wherein all points in

[5] The diameter is defined as $\max_{\forall [p],[q]}(d([p],[q]))$ where $d(\cdot,\cdot)$ is the distance between $[p]$ and $[q]$ based on the Riemannian metric.

these additional clusters do not lie in $\bigcap_{j=0}^{j_0+p}(\bigcup_{k=1,l=1}^{n_j,m_k^j}\mathcal{P}_{i_k^l}^j)$. *In other words, an infinite sequence of sets satisfying criteria (i) and (ii) can be constructed such that* $\Lambda \subseteq \bigcap_{j=0}^{\infty}(\bigcup_{k=1,l=1}^{n_j,m_k^j}\mathcal{P}_{i_k^l}^j)$. *Finally, if* $\exists[p] \in \bigcap_{j=0}^{\infty}(\bigcup_{k=1,l=1}^{n_j,m_k^j}\mathcal{P}_{i_k^l}^j)$ *such that* $[p] \notin \Lambda$, *then arguments similar to those in the previous theorem reveal a contradiction.*

The following corollary to Theorem 9.3.1 identifies complex sets in the reformulated phase-space of the abstract dynamical system.

Corollary 9.3.2 *Let* $\{\langle\mathcal{N}_k^j\rangle \mid k = 1, ..., n_j\}$ *for stages* $j = 1, 2, ...$ *be successive sets of clusters such that (i) each set is an equivalence class of clusters generated by the transitive closure of Recurrent*$(\cdot,\cdot)$ *on the set* $\{\langle\mathcal{N}_k^j\rangle \mid$ *Recurrent*$(\langle\mathcal{N}_k^j\rangle, \langle\mathcal{N}_k^j\rangle)\}$, *and (ii)* $\forall j$ $\bigcup_{k=1,l=1}^{n_j,m_k^j}\mathcal{P}_{i_k^l}^j \subseteq \bigcup_{k=1,l=1}^{n_{j-1},m_k^{j-1}}\mathcal{P}_{i_k^l}^{j-1}$. *Then,* $\bigcap_{j=0}^{\infty}(\bigcup_{k=1,l=1}^{n_j,m_k^j}\mathcal{P}_{i_k^l}^j)$ *is a complex set. Conversely, every complex set is representable as such.*

Proof:

Λ *and* Λ' *are coupled if and only if there exists a sequence of basic sets* $\Lambda, \Lambda_1, \Lambda_2, ..., \Lambda'$ *such that each consecutive pair of basic sets shares one or more clusters at all stages. This follows from the observation that given any basic set* Λ *and its corresponding set of clusters* $\{\langle\mathcal{N}_k^j\rangle \mid k = 1, ..., n_j\}$ *for stages* $j = 1, 2, ...$, *if* $[p] \in \Lambda$, *then for every stage* j *there exists a* $\langle\mathcal{N}_{k_0}^j\rangle$ *that satisfies* $[p] \in int(\langle\mathcal{N}_{k_0}^j\rangle)$, *and in addition,* $\langle\mathcal{N}_{k_0}^j\rangle \in \{\langle\mathcal{N}_k^j\rangle \mid k = 1, ..., n_j\}$. *The remainder of the proof follows along the lines of the proof of the previous corollary.*

Having proved that the nonwandering set, the basic sets, and the complex sets in the reformulated phase-space can be identified based on the procedure described in Figure 9.2, we now demonstrate that any complex set that is also an attractor can be identified as such, as a product of the same procedure.

We first note, based on previous observations and the fact that the entire phase-space is bounded, that if $\mathcal{G}^j$ denotes the directed graph at stage j, and $\mathcal{H}^j$ is a subgraph of $\mathcal{G}^j$ such that there are no edges leading from nodes in $\mathcal{H}^j$ to nodes in $(\mathcal{G}^j \backslash \mathcal{H}^j)$, then the union of the sets corresponding to the nodes in $\mathcal{H}^j$ constitutes a bounded positively invariant set in the reformulated phase-space.

We now demonstrate that a complex set Ξ is an attractor if and only if there is a stage j_0

where no path exists from any node in the equivalence class of clusters associated with Ξ (as defined in the previous corollary) to a node in an equivalence class of clusters associated with any other complex set Ξ'.

We note that if such a stage exists, the criterion remains true for all subsequent stages. The criterion guarantees the existence of maximal subgraphs $\mathcal{H}^j$ for every $j \geq j_0$ such that (a) every cluster $\langle \mathcal{N}_k^j \rangle$ in the equivalence class associated with Ξ lies in $\mathcal{H}^j$, (b) $\mathcal{H}^j$ does not contain any node from an equivalence class of clusters associated with any other complex set Ξ', and (c) there are no edges from $\mathcal{H}^j$ to $(\mathcal{G}^j \backslash \mathcal{H}^j)$. If W^j denotes the union of the sets corresponding to the nodes in $\mathcal{H}^j$, the realm of attraction of Ξ is given by $\lim_{j \to \infty} W^j$.

If, on the contrary, at every stage j there exists a path from a node in the equivalence class associated with Ξ to a node in an equivalence class associated with some other complex set Ξ', then there is no set U such that $\Xi \subset int(U)$, $\forall \Xi' \neq \Xi \; \overline{U} \cap \Xi' = \emptyset$, and $\Theta(U) \subseteq U$. If, instead, such a U exists, since $\forall \Xi' \neq \Xi \; \overline{U} \cap \Xi' = \emptyset$, given any other complex set Ξ', there exists an open neighborhood V of Ξ' such that $U \cap V = \emptyset$. Moreover, since $\Theta(U) \subseteq U$, therefore, $\forall n \geq 0 \; \Theta^n(int(U)) \cap V = \emptyset$. This, however, is in contradiction with the existence of the noted path at every stage.

In conclusion, we recall that with regard to the dynamics of neocortical columns, we demonstrated in Chapter 8 that trajectories (periodic orbits) in the region of the phase-space corresponding to "normal operational conditions" are, with probability 1, sensitive to initial conditions (unstable). It therefore follows that attractors in this region of the phase-space are almost surely chaotic. Combined with the observation that the inherently discontinuous nature of Θ sanctions the existence of anisotropic attractors, we conclude that the dynamics of neocortical columns, under normal operational conditions, is controlled by attractors that are not only almost surely chaotic, but are also potentially anisotropic.

9.4 Summary

We began the chapter with a review of the fundamental coherent structures that exist in the phase-space of a discrete dynamical system defined by a mapping f.

In Section 9.1, we explored the implications of f not being a homeomorphism. We were

led to the realization that the phase-space of any such dynamical system contains an additional variety of coherent structures of potentially greater complexity, structures we label complex sets.

In Section 9.2, we transformed the abstract dynamical system formulated in Chapter 6 from a continuous dynamical system to a discrete dynamical system. The discontinuous nature of the mapping that defines the discrete dynamical system was then highlighted.

Finally, in Section 9.3 we introduced a procedure based on which the nonwandering set, the basic sets, the complex sets, the attractors and their realms of attraction, in the reformulated phase-space of the abstract dynamical system were identified.

Chapter 10

Conclusions and Future Research

There is general agreement in the scientific community regarding the position that the *physical states* of the brain are causally implicated in cognition and behavior. What constitutes a discrete brain state is, however, a problem far from resolved. A satisfactory resolution of this issue should at the least advance our understanding of how the brain represents and manipulates information.

10.1 Contributions of the Thesis

It has been our belief that an understanding of the nature of the coherent physical states of the brain can be achieved by analyzing, exclusively, the dynamics of the brain (or any part thereof) as constrained by its anatomy and physiology. From a dynamical systems' perspective the coherent spatiotemporal structures, if any, inherent in the dynamics of a physical system are revealed in any *attractors* that are present in its phase-space.

Our objective has therefore been to determine if there exist attractors in the dynamics of systems of neurons, and if so what their salient characteristics are. The first step in such a program is the construction of an abstract dynamical system that models systems of neurons.

We have presented in this thesis a detailed exposition of one such dynamical system. We regard the dynamical system as a significant contribution of the thesis because it has a sufficiently wide scope to be able to realistically model systems of neurons in the brain, and at the same time, it is sufficiently simple to be amenable to formal analysis.

In order to determine the viability of the model, we conducted simulation experiments on several instantiations of the system, each modeling a typical column in the neocortex to a different degree of accuracy. We found an agreeable fit between the qualitative aspects of the results and that of real data.

A significant outcome of the simulation experiments was the emergence of three distinct categories of qualitative behavior that were found to be robust across all the investigated instantiations of the system. In addition to the trivial behavior of quiescence, the class of systems displayed sustained chaotic behavior in the region of the phase-space associated with normal operational conditions in the neocortex, and intense periodic behavior in the region of the phase-space associated with seizure-like conditions in the neocortex.

The experiments also shed light on why the strictly neurophysiological perspective to the study of the brain faces profound problems. Whereas the abstract system contains a good deal of structure, such was not easily revealed in its dynamics. This is more so in the case of real neurophysiological data wherein the impression is one of an appalling lack of structure. The incongruence between data recorded at the individual or local neuronal level and at the organism's behavioral level is enormous. Bridging this gap without access to an intermediary model is a formidable task. Whereas approaching the problem via a model might be deemed weaker because acceptance of the results hinge upon the acceptance of the adequacy of the model, it is our view that given the circumstances, this is arguably the only viable approach.

Based on the evidence from the simulation experiments we surmised that coherent structures do exist in the dynamics of neocortical neuronal systems operating under normal conditions, and that they are chaotic attractors. Experimental evidence of the nature presented here, however, does not amount to a proof of existence of chaotic attractors in the said class of systems. Furthermore, the simulation experiments shed little light on the structure of the attractors.

In order to gain a deeper insight into the nature of these attractors, we conducted a formal analysis of the phase-space dynamics of the abstract system. Not only was the existence of chaos in the noted region of the phase-space confirmed, but the parameter that constituted the basis for the existence of the distinct categories of qualitative behavior was also identified.

The criterion for the dynamics of the system to be sensitive to initial conditions was deduced based on a local analysis of trajectories in the phase-space of the abstract system. An analysis of the global structures induced by the dynamics of the system in the phase-space disclosed the existence of complex sets. We concluded based on anatomical and physiological parameters that the dynamics of neocortical columns under normal operational conditions is governed by attractors that are not only almost surely chaotic but also potentially anisotropic.

10.2 Basic Implications of the Results

This thesis advances a principled proposal regarding the issue of information coding in recurrent neuronal systems (such as columns in the neocortex): that attractors in the phase-space denote the discrete computational states of such systems. While the spatial configuration of the attractors in the phase-space of certain neuronal systems might prompt the surmise of rate or population coding, such schemes are rendered epiphenomenal from this perspective.

The chaotic and potentially anisotropic nature of the attractors attains principal significance in this context. We first consider the ramifications of the attractors in question being almost surely chaotic. Recall that external input into the system is modeled by introducing additional neurons whose state descriptions match, identically, the input. Stated formally, the expanded phase-space is given by $\prod_{i=1}^{\mathcal{S}} {}^{i}\overline{\mathbb{L}}_{n_i} \times \prod_{i=\mathcal{S}+1}^{\mathcal{R}} {}^{i}\overline{\mathbb{L}}_{n_i}$, where $i = 1, ..., \mathcal{S}$ denote the neurons in the system, and $i = (\mathcal{S}+1), ..., \mathcal{R}$ denote the input neurons. Since the times at which spikes are generated at the input neurons are determined solely by the external input, the expanded phase-space does not contain hypersurfaces P_i^I for $i = (\mathcal{S}+1), ..., \mathcal{R}$. Each input corresponds to a unique trajectory $\widehat{\Psi}(t)$ in $\prod_{i=\mathcal{S}+1}^{\mathcal{R}} {}^{i}\overline{\mathbb{L}}_{n_i}$. The temporal evolution of the system upon input $\widehat{\Psi}(t)$ is given by the trajectory $\Psi(t)$ in the expanded phase-space whose projection on $\prod_{i=\mathcal{S}+1}^{\mathcal{R}} {}^{i}\overline{\mathbb{L}}_{n_i}$ is $\widehat{\Psi}(t)$.

It is based on this formulation that we demonstrated in Chapter 8 that the dynamics of a generic neocortical column under normal operational conditions, sustained by external input from the thalamus and/or other cortical columns, is sensitive to initial conditions. This implies that even if the exact input is known, it is impossible to predict, based solely on nominal knowledge of the attractor that the system currently resides in, which attractors the system will visit as its dynamics unfolds, and at what times. In other words, the dynamics of a neocortical column at the computational level can not, in general, be modeled as a deterministic automaton.

We now consider the ramifications of the fact that the attractors in question, in addition to being chaotic, are potentially anisotropic. We recall that an anisotropic attractor is an attracting complex set that is composed of multiple basic sets. Such attractors are capable of maintaining complex sequence information. The direction from which the system approaches such an attractor determines not only the subset of the constituent basic sets that the system visits, but also the

order in which they are visited. In other words, structure can be discerned in the phase-space of the neuronal system at two levels. First, there is the relationship between the attractors each of which constitutes a macro-symbolic state of the system, and within each attractor the relationship between the basic sets each of which constitutes a micro-symbolic state of the system.

10.3 Future Research

The present research has raised a number of issues that require further investigation.

In Section 4.3, we described the scope of our model of the neuron in general terms. An immediate next step would be to construct specific models (appropriate instantiations of $P(\cdot)$) of frequency-adapting regular-firing neurons, fast-spiking neurons, and intrinsically-bursting neurons, all of which are found in the neocortex (Connors & Gutnick, 1990). The construction of such models would facilitate more realistic simulations of the dynamics of columns in the neocortex.

In order to identify the salient features of the dynamics of a generic neocortical column, we modeled a regular trajectory in the phase-space of the abstract dynamical system as an i.i.d. (independent and identically distributed) stochastic process, a process that ranks amongst the simplest of stationary ergodic processes. In the ensuing analysis, the neurons in the system were assumed to spike at comparable rates, and the $\partial P_k / \partial x_i^j$'s were assumed to arise from the same distribution. An analysis based on a weaker set of assumptions would be more robust and therefore preferable.

Finally, we have just begun to understand the impact of external input on the dynamics of systems of neurons. In an alternative approach to the one presented in the previous section, one can consider an isolated system of neurons, with the input into each neuron absorbed into its membrane potential function as an additional parameter (each $P_i(\cdot)$ is now a function parameterized by the input and therefore time varying, and each $P_i(\cdot) = \mathcal{T}$ is, likewise, a hypersurface that evolves with time). From this perspective, the effect of the input plays a role that is complementary to the effect that synaptic variability has on the potential function.

While it is evident that both the input into the system as well as changes in the potential function of the neurons brought about by long-term potentiation (LTP) and depression (LTD),

can dramatically change the nature of the dynamics of a neuronal system (creating, destroying and altering the shape and location of the attractors in the phase-space), the exact nature of these changes is at present unknown.

The nature of the bounds on the number of attractors that a system can maintain, as a function of the number of neurons, their connectivity, and the nature of their potential functions, is also at present unknown. A suitable quantification would shed additional light on the dynamics of neuronal systems.

We plan to address these issues in our future work.

10.4 Epilogue

The enquiry into the nature of the mind entertains a venerable past. Over the past two thousand years, several solutions have been ventured—some have enjoyed modest success and others have suffered critical failure. While modern techniques bring new vigor to the enterprise, a reflection on the history of the endeavor should give one pause. Our sentiment at the present juncture is therefore one of cautious optimism.

Appendix A

Proofs of Theorem 6.2.1 and Theorem 6.2.2

Proof of Theorem 6.2.1

The proof of Theorem 6.2.1 follows from Theorems A.0.1 and A.0.2.

Theorem A.0.1 *All roots of* $f(z) = z^n + a_{n-1}z^{n-1} + ... + a_0$ *are distinct and lie on* $|z| = 1$ $\Leftrightarrow$ *(a)* $|a_0| = 1$, $a_i = \bar{a}_{n-i}a_0$ *for* $i = 1, ..., n-1$, *and (b)* $f'(z)$ *has all roots in* $|z| < 1$.

Proof:

(i) Distinct roots on $|z| = 1 \Rightarrow$ *(a) and (b).*

Assume w.l.o.g that $a_n = 1$. z_i *is a root of* $f(z) \Leftrightarrow z_i^* = (1/\bar{z}_i)$ *is a root of* $f^*(z)$. $|z_i| = 1$ *implies* $(1/\bar{z}_i) = z_i$. *Hence the roots of* $f(z)$ *and* $f^*(z)$ *are identical. Moreover,* $a_0 = \prod_{i=1}^{n} z_i$. *Consequently, (a) holds.*

That all roots of $f'(z)$ *lie in* $|z| < 1$ *follows from* Lucas Theorem *(Any convex polygon that contains all roots of* $f(z)$ *also contains all roots of* $f'(z)$*) and all roots of* $f(z)$ *being distinct.*

(ii) (a) and (b) $\Rightarrow$ *distinct roots on* $|z| = 1$.

That the roots of $f(z)$ *lie on* $|z| = 1$ *follows from the following theorem in (Cohn 1922).*

Lemma A.0.1 (Cohn) *Let* $g(z) = b_m z^m + b_{m-1}z^{m-1} + ... + b_0$ *satisfy the criterion* $b_{m-i} = u\bar{b}_i$ *for all* $i = 0, ..., m$. *Then* $g(z)$ *has in* $|z| < 1$ *as many roots as* $[g'(z)]^* = z^{m-1}\bar{g}'(1/z)$.

$f(z)$ *by (a) satisfies the premise, and therefore, it has in* $|z| < 1$ *as many roots as* $[f'(z)]^*$. *By (b)* $[f'(z)]^*$ *has no roots in* $|z| < 1$. *Hence,* $f(z)$ *has no roots in* $|z| < 1$. *Finally,* $|a_0| = 1$ *constraints all roots of* $f(z)$ *to lie on* $|z| = 1$. *(b) then enforces that* $f(z)$ *has no multiple roots.*

Theorem A.0.2 $\delta_1 < 0$, $\delta_2, \delta_3, ..., \delta_{n-1} > 0$ *(From Theorem 6.2.1)* $\Leftrightarrow$ *all roots of* $f'(z)$ *lie in* $|z| < 1$.

Proof:

(i) $\delta_1 < 0, \delta_2, \delta_3, ..., \delta_{n-1} > 0 \Rightarrow$ *all roots of* $f'(z)$ *lie in* $|z| < 1$.

This follows directly from the following theorem in (Marden 1948).

Lemma A.0.2 (Marden) *If for polynomial* $f(z) = a_m z^m + a_{m-1} z^{m-1} + ... + a_0$ *the sequence* $\langle f_0(z), f_1(z), ..., f_m(z) \rangle$ *is constructed as* $f_j(z) = \sum_{k=0}^{m-j} a_k^{(j)} z^k$ *where* $f_0(z) = f(z)$ *and* $f_{j+1}(z) = \bar{a}_0^{(j)} f_j(z) - a_{m-j}^{(j)} f_j^*(z)$ *for* $j = 0, ..., m-1$, *and moreover* $\delta_{j+1} = a_0^{(j+1)}$ *satisfies* $\delta_1 < 0, \delta_2, ..., \delta_m > 0$ *then* $f(z)$ *has all roots in* $|z| < 1$.

(ii) All roots of $f'(z)$ *lie in* $|z| < 1 \Rightarrow \delta_1 < 0, \delta_2, \delta_3, ..., \delta_{n-1} > 0$.

(a) $\delta_1 < 0$.

Since $f'(z) = f_0(z) = b_m z^m + ... + b_1 z + b_0$ *(here* $m = n-1$*) has all roots in* $|z| < 1$, *the modulus of the product of all roots is less than 1. Hence,* $|b_0| < |b_m|$, *and* $\delta_1 = |b_0|^2 - |b_m|^2 < 0$.

(b) $\delta_2, \delta_3, ..., \delta_{n-1} > 0$.

This follows from the following theorem in (Marden 1948).

Lemma A.0.3 (Marden) *If in Lemma A.0.2,* $f_j(z)$ *has* p_j *roots in* $|z| < 1$ *and none on* $|z| = 1$ *and if* $\delta_{j+1} \neq 0$ *then* $f_{j+1}(z)$ *has* $p_{j+1} = \frac{1}{2}\{m - j - [(m-j) - 2p_j] sgn \delta_{j+1}\}$ *roots in* $|z| < 1$ *and none on* $|z| = 1$.

$f_0(z) = f'(z)$ *has all* $n-1$ *roots in* $|z| < 1$ *and none on* $|z| = 1$. *We have shown that* $\delta_1 < 0$. *Hence,* $sgn\delta_1 = -1$. *Based on the lemma then,* $f_1(z)$ *has* $p_1 = 0$ *roots in* $|z| < 1$ *and none on* $|z| = 1$. *In other words, all roots of* $f_1(z)$ *lie in* $|z| > 1$. *Arguing as in (a), we get* $\delta_2 > 0$. *We now apply the lemma repeatedly to get* $p_2 = p_1 = 0$ *and so on, implying* $\delta_3, ..., \delta_{n-1} > 0$.

Proof of Theorem 6.2.2

The proof of Theorem 6.2.2 follows from Theorem A.0.3.

Theorem A.0.3 $x \in \overline{\mathbb{L}}_n$ *and* $x \notin \mathbb{L}_n \Leftrightarrow x$ *denotes a polynomial with all roots on* $|z| = 1$ *and at least 1 multiple root.* $x \in \overline{\mathbb{L}}_n$ *and* $x \notin \mathbb{L}_n \Rightarrow x$ *is a boundary point of* $\overline{\mathbb{L}}_n$, *that is, every open set containing* x *contains a* $y \notin \overline{\mathbb{L}}_n$.

Proof:

(i) $x \in \overline{\mathbb{L}}_n$ *and* $x \notin \mathbb{L}_n \Rightarrow$ *All roots on* $|z| = 1$ *and at least 1 multiple root.*

Since x is a limit point of $\mathbb{L}_n$, $\exists$ denumerable sequence $\langle y_1, y_2, ..., y_k, y_{k+1}, ...\rangle$, such that $\forall i\ y_i \in \mathbb{L}_n$ and $\lim_{i\to\infty} y_i = x$. We now apply the following theorem in (Coolidge 1908) to the sequence.

Lemma A.0.4 (Coolidge) *If any two given polynomials $f_1(z) = z^m + a_{m-1}z^{m-1} + ... + a_0$ and $f_2(z) = z^m + b_{m-1}z^{m-1} + ... + b_0$ are so related that $\forall i\ a_i$ is a constant, and $\forall i\ b_i$ approaches a_i, then the roots of $f_1(z)$ and $f_2(z)$, where each multiple root of order* k *is counted* k *times as* k *roots, may be put into such a one-to-one correspondence that the absolute value of the difference between each two corresponding roots approaches 0.*

Since $x \notin \mathbb{L}_n$, either the corresponding polynomial does not have all roots on $|z| = 1$, or not all roots are distinct. If the first case is true, the distance between at least one set of roots in the theorem is bounded from below thus contradicting it.

(ii) All roots on $|z| = 1$ and at least 1 multiple root $\Rightarrow x \in \overline{\mathbb{L}}_n$ and $x \notin \mathbb{L}_n$.

Trivially, we have $x \notin \mathbb{L}_n$. Let $\langle z_1, z_2, ..., z_n\rangle$ be the roots of the polynomial corresponding to x with multiple roots of order k repeated k times. Choose any $\delta > 0$ such that it satisfies $\delta < |(1/2)\min_{\forall i,j\ z_i \neq z_j}(\angle(z_i/z_j))|$. Choose $\langle \delta_1, \delta_2, ..., \delta_n\rangle$ such that $\forall i, j\ i \neq j \Rightarrow \delta_i \neq \delta_j$ and $\forall i,\ 0 < |\delta_i| < \delta$.

Now consider the sequence of ordered sets $\langle z_1 e^{i(\delta_1/2^p)}, z_2 e^{i(\delta_2/2^p)}, ..., z_n e^{i(\delta_n/2^p)}\rangle$ for $p = 0, 1, ...$ Each set comprises of distinct roots on $|z| = 1$. The sequence converges absolutely to $\langle z_1, z_2, ..., z_n\rangle$. Since coefficients are continuous functions of roots, the corresponding sequence $\langle y_1, y_2, ..., y_k, y_{k+1}, ...\rangle$ in coefficient space satisfies $\forall i\ y_i \in \mathbb{L}_n$ and $\lim_{i\to\infty} y_i = x$.

(iii) $x \in \overline{\mathbb{L}}_n$ and $x \notin \mathbb{L}_n \Rightarrow x$ is a boundary point.

$x \in \mathbb{C}^{\lfloor n/2\rfloor} \times S^1$ ($\mathbb{C}^{\lfloor n/2\rfloor - 1} \times \mathbb{M}^2$) $\Rightarrow$ *corresponding polynomial satisfies $\exists\sigma$, a permutation, such that $z_i = (1/\bar{z}_{\sigma_i})$. Let $x \in \overline{\mathbb{L}}_n$ and $x \notin \mathbb{L}_n$. Let $\langle e^{i\theta_1}, e^{i\theta_2}, ..., e^{i\theta_n}\rangle$ be the set of roots that correspond to x and w.l.o.g $\theta^* = \theta_1 = \theta_2 = ... = \theta_k$ $(k \geq 2)$. For any $\delta < 1$ consider the sequence of ordered sets $\langle((2^p - \delta)/2^p)e^{i\theta^*}, (2^p/(2^p - \delta))e^{i\theta^*}, e^{i\theta_3}, ..., e^{i\theta_n}\rangle$ for $p = 0, 1, ...$ The sequence converges absolutely to $\langle e^{i\theta_1}, e^{i\theta_2}, ..., e^{i\theta_n}\rangle$ and each set satisfies $\exists\sigma$ such that $z_i = (1/\bar{z}_{\sigma_i})$. Based on arguments identical to (ii) above the corresponding sequence $\langle y_1, y_2, ..., y_k, y_{k+1}, ...\rangle$ in coefficient space satisfies $\forall i\ y_i \notin \overline{\mathbb{L}}_n$ and $\lim_{i\to\infty} y_i = x$.*

Appendix B

The Membrane Potential Function in the Transformed Space

Assumption (iii) of Chapter 4 Section 2 makes $P(\cdot)$ C^∞ on T^n. Let $F^{-1} : \overline{\mathbb{L}}_n \rightarrow \mathbb{U} \subset T^n$ map the transformed space into the initial space, that is, $F^{-1}\langle a_{n-1}, ..., a_{\lceil n/2 \rceil}(|a_{\lceil n/2 \rceil}|); \angle a_0 \rangle = \langle x^1, ..., x^n \rangle$ for odd (even) n, such that, $0 \leq x^1 \leq x^2 \leq ... \leq x^n < 2\pi$.

Boundaries of $\mathbb{U}$ are of no concern here because (a) the range of F^{-1} could equally well be $\delta \leq x^1 \leq x^2 \leq ... \leq x^n < 2\pi + \delta$ for arbitrary δ and (b) $P(\cdot)$ is C^∞ on T^n. Let $G(\cdot)$ denote the Cartesian product of $F^{-1}(\cdot)$ with itself appropriately many times that maps the transformed space of all relevant neurons into their initial spaces. Define, tentatively, $\widetilde{P} = P \circ G$.

Since both P and F are C^∞, $\widetilde{P}$ is C^∞ wherever the *Jacobian* of F, (DF), is non-singular. The following two theorems demonstrate that (DF) is singular if and only if x^k is a multiple root for some k.

Theorem B.0.4 *$\frac{\partial x^k}{\partial a_j}$ is undefined when x^k is a multiple root, that is, $\exists a, b$ such that $x^a = x^b \Rightarrow Det(DF) = 0$.*

Proof:

$\forall j$ a_j is a symmetric function of $\langle x^1, ..., x^n \rangle$. Therefore, $\forall j$ $\frac{\partial a_j}{\partial x^a} = \frac{\partial a_j}{\partial x^b}$ when $x^a = x^b$. In other words, if $x^a = x^b$, columns 'a' and 'b' in (DF) are identical.

Theorem B.0.5 $\forall i, j$ $(i \neq j \Rightarrow x^i \neq x^j) \Rightarrow Det(DF) \neq 0$.

Proof:

We prove the theorem for cases, n is odd and n is even, separately.

(i) n is odd.

Based on the functions defining coefficients in terms of roots and simple matrix manipulations, (DF) evaluated at $\langle x^1, x^2, ..., x^n \rangle = \langle \theta_1, \theta_2, ..., \theta_n \rangle$ can be reduced to $(DF) =$

$$\begin{pmatrix} \frac{\partial \angle a_0}{\partial x_1} & \frac{\partial \angle a_0}{\partial x_2} & \cdots & \frac{\partial \angle a_0}{\partial x_n} \\ \frac{\partial \Re a_{\lceil n/2 \rceil}}{\partial x_1} & \frac{\partial \Re a_{\lceil n/2 \rceil}}{\partial x_2} & \cdots & \frac{\partial \Re a_{\lceil n/2 \rceil}}{\partial x_n} \\ \frac{\partial \Im a_{\lceil n/2 \rceil}}{\partial x_1} & \frac{\partial \Im a_{\lceil n/2 \rceil}}{\partial x_2} & \cdots & \frac{\partial \Im a_{\lceil n/2 \rceil}}{\partial x_n} \\ \vdots & \vdots & \ddots & \vdots \\ \frac{\partial \Re a_{n-1}}{\partial x_1} & \frac{\partial \Re a_{n-1}}{\partial x_2} & \cdots & \frac{\partial \Re a_{n-1}}{\partial x_n} \\ \frac{\partial \Im a_{n-1}}{\partial x_1} & \frac{\partial \Im a_{n-1}}{\partial x_2} & \cdots & \frac{\partial \Im a_{n-1}}{\partial x_n} \end{pmatrix} = \begin{pmatrix} 1 & 1 & \cdots & 1 \\ \sin(\theta_1) & \sin(\theta_2) & \cdots & \sin(\theta_n) \\ \cos(\theta_1) & \cos(\theta_2) & \cdots & \cos(\theta_n) \\ \sin(2\theta_1) & \sin(2\theta_2) & \cdots & \sin(2\theta_n) \\ \cos(2\theta_1) & \cos(2\theta_2) & \cdots & \cos(2\theta_n) \\ \vdots & \vdots & \ddots & \vdots \\ \sin(\frac{n-1}{2}\theta_1) & \sin(\frac{n-1}{2}\theta_2) & \cdots & \sin(\frac{n-1}{2}\theta_n) \\ \cos(\frac{n-1}{2}\theta_1) & \cos(\frac{n-1}{2}\theta_2) & \cdots & \cos(\frac{n-1}{2}\theta_n) \end{pmatrix}$$

We prove $Det(DF) \neq 0$ *by demonstrating that for any vector* $\vec{x}$, $\vec{x} * (DF) = 0$ *implies* $\vec{x} \equiv \langle 0, ..., 0 \rangle$. *Let* $n = 2m + 1$, *and* $f(x) = \alpha_0 + \sum_{i=1}^{m} \alpha_{2i-1} \sin ix + \alpha_{2i} \cos ix$. *For arbitrary reals* $\alpha_0, \alpha_1, ..., \alpha_{2m}$ *not all zero, we demonstrate that the* maximum *number of roots that* $f(x)$ *can have in* $[0, 2\pi)$ *is* 2m, *thus proving the claim.*

Let $g(x) = \gamma_0 + \sum_{i=1}^{m} \gamma_i \sin(ix + \beta_i)$ *such that* $g(x) \equiv f(x)$. *Since* $g(x)$ *is periodic with period* 2π, *if* $g(x)$ *has* μ *roots in* $[0, 2\pi)$ *then* $g^1(x) = g'(x)$ *has* at least μ *roots in* $[0, 2\pi)$, *and since* $g^1(x)$ *is also periodic with period* 2π, $g^2(x) = g''(x)$ *has* at least μ *roots in* $[0, 2\pi)$ *and so on.*

$g^{4k}(x) = \sum_{i=1}^{m} i^{4k} \gamma_i \sin(ix + \beta_i)$ *for* $k = 1, 2, ...$ *Hence, (a) the coefficients of* $\sin(ix + \beta_i)$ *for* $i = 1, ..., (m-1)$ *can be made negligible as compared to the coefficient of* $\sin(mx + \beta_m)$ *by increasing* k, *and (b) the magnitude of the gradients of* $i^{4k} \gamma_i \sin(ix + \beta_i)$ *for* $i = 1, ..., (m-1)$ *are also made negligible as compared to the gradient of* $m^{4k} \gamma_m \sin(mx + \beta_m)$ *near its roots. Since* $m^{4k} \gamma_m \sin(mx + \beta_m)$ *has 2m roots in* $[0, 2\pi)$, *we have* $\mu \leq 2m$.

(ii) n is even.

Let $n = 2m$. *For any* θ^*, *the mapping* $F\langle x^1, ..., x^{2m} \rangle = \langle a_{n-1}, ..., |a_{\lceil n/2 \rceil}|; \angle a_0 \rangle$ *is a* C^∞*-diffeomorphism in an open set about* $\langle \theta_1, \theta_2, ..., \theta_{2m} \rangle$ *if and only if the corresponding mapping* $F'\langle x^1, ..., x^{2m}; x^{2m+1} \rangle = \langle a_{n-1}, ..., |a_{\lceil n/2 \rceil}|; \angle a_0; x^{2m+1} \rangle$ *is a* C^∞*-diffeomorphism in an open set about* $\langle \theta_1, \theta_2, ..., \theta_{2m}, \theta^* \rangle$. *Consequently, all that needs to be shown is that for* $n = 2m$, *the mapping* $\langle a_{2m-1}, ..., |a_m|; \angle a_0; x^{2m+1} \rangle \rightarrow \langle A_{2m}, ..., A_{m+1}; \angle A_0 \rangle$ *is* C^∞ *(*A_i*'s are the coefficients of the polynomial of degree 2m+1 whose roots include the additional* $e^{i\theta^*}$*). Note that* $\forall i, j \ (i \neq j \Rightarrow \theta_i \neq \theta_j)$ *and* $\forall i = 1, ..., 2m \ \theta_i \neq \theta^*$ *is enforced by (i) above on the mapping* $\langle A_{2m}, ..., A_{m+1}; \angle A_0 \rangle \rightarrow \langle x^1, ..., x^{2m}; x^{2m+1} \rangle$.

The trivial relations between the A_i's and the a_i's immediately proves that the mapping is C^∞.

The portion of $\overline{\mathbb{L}}_n$ actually explored by the state dynamics of the neuron has multiple roots only at $e^{ix^i} = e^{ix^j} = 1$, that is, when the spikes are dead. We therefore define $\widetilde{P}(\cdot)$ as follows:

(a) If $\forall$ relevant i each $\langle x_i^1, x_i^2, ..., x_i^{n_i}\rangle$ is composed of distinct elements, then $\widetilde{P}(\cdot)$ is C^∞ as demonstrated in the preceding theorem.

(b) If $\exists$ relevant i such that $\langle x_i^1, x_i^2, ..., x_i^{n_i}\rangle$ is not composed of distinct elements, and x^* is one such multiple element (at $e^{ix^*} = 1$), then we *define*, for all m, $j_1, ..., j_{l-1}$, $k_1, ..., k_l$ (such that $\sum_{i=1}^{l} k_i = m$), and i_p^q's (not necessarily distinct, for $q = 1, ..., l$, $p = 1, ..., k_q$)

$$\frac{\partial^m P}{\partial^{k_1} x^{j_1} ... \partial^{k_{l-1}} x^{j_{l-1}} \partial^{k_l} x^*} \times \frac{\partial^{k_1} x^{j_1}}{\partial a_{i_1^1} ... \partial a_{i_{k_1}^1}} ... \frac{\partial^{k_{l-1}} x^{j_{l-1}}}{\partial a_{i_1^{l-1}} ... \partial a_{i_{k_{l-1}}^{l-1}}} \times \frac{\partial^{k_l} x^*}{\partial a_{i_1^l} ... \partial a_{i_{k_l}^l}} = 0 \quad \text{(B.1)}$$

Although $\frac{\partial^{k_l} x^*}{\partial a_{i_1^l} ... \partial a_{i_{k_l}^l}}$ is undefined in this case, imposing the additional constraint $\frac{\partial P}{\partial x^*} = 0$ over an infinitesimal interval $(e^{i\delta} > e^{ix^*} > e^{i(2\pi - \delta)})$ irrespective of the values assigned to the other variables turns $\widetilde{P}$ C^∞, since we then have $\frac{\partial^m P}{\partial^{k_1} x^{j_1} ... \partial^{k_{l-1}} x^{j_{l-1}} \partial^{k_l} x^*} = 0$ over the interval.

(c) If $\exists$ relevant i such that $\langle x_i^1, x_i^2, ..., x_i^{n_i}\rangle$ is not composed of distinct elements, but member element x^* is a distinct element, then $\frac{\partial x^*}{\partial a_j}$ can not be directly computed from $(DF)^{-1}$ since $Det(DF) = 0$. However, as is shown next, tangible value exists for $\frac{\partial x^*}{\partial a_j}$. It is also shown that $\frac{\partial x^*}{\partial a_j}$ is C^∞.

Theorem B.0.6 *Let the roots of $f(z) = z^n + a_{n-1}z^{n-1} + ... + a_0$, constrained to lie on $|z| = 1$, be $\langle e^{ix^1}, e^{ix^2}, ..., e^{ix^n}\rangle$. Let $e^{ix^a} = e^{ix^b}$ and all other roots be distinct. Let the sequence of sets $\langle y_p^1, y_p^2, ..., y_p^n\rangle$ for $p = 1, 2, ...$ be constructed such that $\forall p, q$ y_p^q is distinct, $\forall q$ $\lim_{p\to\infty} y_p^q = x^q$. Then $(DF)^{-1}$ at $\langle y_p^1, y_p^2, ..., y_p^n\rangle$ is well defined for all p and limiting values exist for $\frac{\partial x^k}{\partial a_j}$ for all $k \neq a$ or b. Moreover, $\frac{\partial x^k}{\partial a_j}$ is C^∞ for all such values of k.*

Proof:

That $(DF)^{-1}$ at $\langle y_p^1, y_p^2, ..., y_p^n\rangle$ is well defined for all p follows from the previous theorem. Just as in the previous theorem, we consider the case for odd n first. We refer to the simplified

version of (DF) evaluated at $\langle \theta_1, \theta_2, ..., \theta_n \rangle$ *given earlier. In the limit, column 'b' can be replaced by the column (*$\frac{d}{d\theta}$ *column 'a')* $\equiv \langle 0, \cos(\theta_a), -\sin(\theta_a), 2\cos(2\theta_a), -2\sin(2\theta_a), ... \rangle^T$.

We demonstrate that this matrix is invertible. Let $g(x) = \gamma_0 + \sum_{i=1}^{m} \gamma_i \sin(ix + \beta_i)$. *For arbitrary reals* $\gamma_0, \gamma_1, \beta_1, ..., \gamma_m, \beta_m$ *not all zero,* $g(x)$ *can not have* $2m$ *distinct roots and* 1 *multiple root in* $[0, 2\pi)$ *because* $g^1(x)$ *must then have at least* $2m+1$ *roots in* $[0, 2\pi)$ *and so on.*

All rows except 'a' and 'b' in $(DF)^{-1}$, *computed as* $(DF)^{-1}(DF) = I$, *therefore have finite limiting values, identical to the corresponding values in the inverse of the matrix described above. Since the elements of the matrix are* C^∞, *and its determinant (a* C^∞ *function of its elements) is non-zero, the elements of its inverse are* C^∞.

The case for even n *is treated exactly as in the previous theorem.*

References

[1] Abeles, M. (1982) Local Cortical Circuits: An Electrophysiological Study. Braitenberg V. (Ed.) Studies of Brain Function. Springer, Berlin Heidelberg New York.

[2] Abeles, M. (1990) Corticonics: Neural Circuits of the Cerebral Cortex. Cambridge Univ. Press, Cambridge.

[3] Abbott, L. F., Varela, J. A., Sen, K. and Nelson, S. B. (1997) Synaptic depression and cortical gain control. Science, 275, pp. 220-224.

[4] Adrian, E. D. (1928) The Basis of Sensation: The Action of the Sense Organs. W. W. Norton, New York.

[5] Adrian, E. D. and Bronk, D. W. (1928) The Discharge of Impulses in Motor Nerve Fibres. Part I: Impulses in Single Fibres of the Phrenic Nerve. Jour. Physiol. (London), 66, pp. 81-101.

[6] Adrian, E. D. and Zotterman, Y. (1926) The Impulses Produced by Sensory Nerve Endings. Part II: The Response of a Single End-Organ. Jour. Physiol. (London), 61, pp. 151-171.

[7] Aertsen, A. and Braitenberg, V. (Eds.) (1992) Information Processing in the Cortex: Experiments and Theory. Springer-Verlag, Berlin Heidelberg New York.

[8] Agmon, A. and Connors, B. W. (1989) Repetitive burst-firing neurons in the deep layers of mouse somatosensory cortex. Neurosci. Lett., 99, pp. 137-141.

[9] Allen, C. and Stevens, C. F. (1994) An evaluation of causes for unreliability of synaptic transmission. Proc. Nat. Acad. Sci. USA, 91, pp. 10380-10383.

[10] Amit, D. J., Gutfreund, H. and Sompolinsky, H. (1987) Information Storage in Neural Networks with Low Levels of Activity. Phys. Rev. A, 35, 5, pp. 2293-2303.

[11] Arrowsmith, D. K. and Place C. M. (1990) An introduction to Dynamical Systems. Cambridge Univ. Press, Cambridge.

[12] Babloyantz, A., Salazar, J. M. and Nicolis, C. (1985) Evidence of Chaotic Dynamics of Brain Activity During the Sleep Cycle. Phys. Lett.(A), 111, pp. 152-156.

[13] Babloyantz, A. (1990) Chaotic Dynamics in Brain Activity. Basar E. (Ed.) Chaos in Brain Function. Springer-Verlag, Berlin Heidelberg New York, pp. 42-48.

[14] Bair, W., Koch, C., Newsome, W. and Britten, K. (1994) Reliable Temporal Modulation in Cortical Spike Trains in the Awake Monkey. Proc. of the Symposium on Dynamics of Neural Processing, Washington, USA.

[15] Bair, W. and Koch, C. (1996) Temporal Precision of Spike Trains in Extrastriate Cortex of the Behaving Macaque Monkey. Neural Computation, 8, pp. 1185-1202.

[16] Barlow, H. B. (1988) The thermal limit to seeing. Nature, 334, pp. 296-297.

[17] Baylor, D. A., Lamb, T. D. and Yau, K. W. (1979) Responses of retinal rods to single photons. Jour. Physiol. (London), 288, pp. 613-634.

[18] Baylor, D. A., Nunn, B. J. and Schnapf, J. F. (1984) The photocurrent, noise, and spectral sensitivity of rods of the monkey Macaca fascicularis. Jour. Physiol. (London), 357, pp. 575-607.

[19] Banerjee, A. (2000) On the Phase-Space Dynamics of Systems of Spiking Neurons. I: Model and Experiments. Neural Computation, 13, pp. 161-193.

[20] Banerjee, A. (2000) On the Phase-Space Dynamics of Systems of Spiking Neurons. II: Formal Analysis. Neural Computation, 13, pp. 195-225.

[21] Basar, E. (Ed.) (1990) Chaos in Brain Function. Springer-Verlag, Berlin Heidelberg New York.

[22] Berger, H. (1929) Über das Elektrenkephalogramm des Menschen. Arch. f. Psychiat., 87, pp. 527-570.

[23] Bernander, O., Douglas, R. J. and Koch, C. (1992) A Model of Regular-Firing Cortical Pyramidal Neurons. CNS Memo 16, California Institute of Technology, Computational and Neural Systems Program.

[24] Bernstein, J. (1902) Untersuchungen zur Thermodynamik der bioelektrischen Ströme. Erster Theil. Pflügers Archiv gesamte Physiol. Menschen Tiere, 92, pp. 521-562.

[25] Bialek, W. and Owen, W. G. (1990) Temporal filtering in retinal bipolar cells: Elements of an optimal computation? Biophys. Jour., 58, pp. 1227-1233.

[26] Bialek, W. and Rieke, F. (1992) Reliability and Information Transmission in Spiking Neurons. Trends Neurosci., 15, pp. 428-434.

[27] Bialek, W., Rieke, F., de Ruyter van Steveninck, R. R. and Warland, D. (1991) Reading a Neural Code. Science, 252, pp. 1854-1857.

[28] Bolshakov, V. Y. and Siegelbaum, S. A. (1995) Regulation of hippocampal transmitter release during development and long-term potentiation. Science, 269, pp. 1730-1734.

[29] Boothby, W. M. (1986) An introduction to Differentiable Manifolds and Riemannian Geometry. Academic Press, New York.

[30] Bower, J. M. and Beeman, D. (1995) The book of GENESIS: Exploring realistic neural models with the GEneral NEural SImulation System. New York, Springer.

[31] Braitenberg, V. (1978) Cortical Architectonics: General and Area. Brazier M. A. B. and Petsche H. (Eds.) Architectonics of the Cerebral Cortex. Raven, New York, pp. 443-465.

[32] Braitenberg, V. and Schüz, A. (1991) Anatomy of the Cortex: Statistics and Geometry. Springer-Verlag, Berlin Heidelberg New York.

[33] Broca, P. (1861) Remarques sur le siège de la faculté du langage articulé; suivies d'une observation d'aphémie. Bulletin de la Société de l'Anatomie de Paris, 36, pp. 330-357.

[34] Brodmann, K. (1909) Vergleichende Lokalisationslehre der Grosshirnrinde in ihren Prinzipien dargestellt auf Grund des Zellenbaues. Leipzig, Barth.

[35] Bryson, A. E. and Ho, Y. C. (1969) Applied Optimal Control. Blaisdell, New York.

[36] Cajal, S. R. (1909, 1910) Histologie du système nerveux de l'homme et des vertébrés. (Translated by L. Azoulay). Paris: Maloine.

[37] del Castillo, J. and Katz, B. (1954) Quantal components of the end-plate potential. Jour. Physiol. (London), 124, pp. 560-573.

[38] Chung S. H., Raymond S. A. and Lettvin J. Y., (1970) Multiple meaning in single visual units. Brain. Behav. Evol., 3, pp. 72-101.

[39] Cohn, A. (1922) Uber die Anzahl der Wurzeln einer algebraischen Gleichung in einem Kreise. Math Zeit, 14, pp. 110-148.

[40] Connors, B. W. and Gutnick, M. J. (1990) Intrinsic firing patterns of diverse neocortical neurons. Trends Neurosci., 13, pp. 99-104.

[41] Coolidge, J. L. (1908) The continuity of the roots of an algebraic equation. Annals of Math, (series 2), 9, pp. 116-118.

[42] Cronin, J. (1987) Mathematical aspects of Hodgkin-Huxley neural theory, Cambridge Univ Press, Cambridge New York.

[43] Curtis, H. J. and Cole, K. S. (1942) Membrane resting and action potentials from the squid giant axon. Jour. Cell. Comp. Physiol., 19, pp. 135-144.

[44] Dale, H. H. (1914) The action of certain esters and ethers of choline and their relation to muscarine. Journal of Pharmacology and Experimental Therapeutics, 6, pp. 147-190.

[45] Dale, H. H. (1935) Pharmacology and nerve endings. Proc. Roy. Soc. Med., 28, pp. 319 - 322.

[46] Dear, S. P., Simmons, J. A. and Fritz, J. (1993) A possible neuronal basis for representation of acoustic scenes in the auditory cortex of the big brown bat. Nature, 364, pp. 620-623.

[47] Decharms, R. C. and Merzenich, M. M. (1996) Primary cortical representation of sounds by the coordination of action potential timing. Nature, 381, pp. 610-613.

[48] Dobrunz, L. and Stevens, C. (1997) Heterogeneity of release probability, facilitation and depletion at central synapses. Neuron, 18, pp. 995-1008.

[49] Donner, K. (1989) The absolute sensitivity of vision: Can a frog become a perfect detector of light induced and dark rod event? Phys. Scr., 39, pp. 133-140.

[50] Dreyfus, H. and Dreyfus, S. (1988) Making a Mind Versus Modeling the Brain: Artificial Intelligence Back at a Branchpoint. Graubard S. (Ed.) The Artificial Intelligence Debate, MIT Press.

[51] Eccles, J. C. (1936) Synaptic and neuromuscular transmission. ErgeUn. Physiol., 38, pp. 339 - 444.

[52] Eccles, J. C. (1937a) The discharge of impulses from ganglion cells. Jour. Physiol., 91, pp. 1 - 22.

[53] Eccles, J. C. (1937b) Synaptic and neuro-muscular transmission. Physiol. Rev., 17, pp. 339 - 444.

[54] Eccles, J. C. (1957) The Physiology of Nerve Cells. Johns Hopkins Press, Baltimore.

[55] Erb, M. and Aertsen, A. (1992) Dynamics of Activity in Biology- Oriented Neural Network Models: Stability at Low Firing Rates. Aertsen A. and Braitenberg V. (Eds.) Information Processing in the Cortex. Springer-Verlag, Berlin Heidelberg New York, pp. 201-223.

[56] Érdi, P. (1996) Levels, Models, and Brain Activities: Neurodynamics is Pluralistic (Open Peer Commentary). Behav. and Brain Sci., 19, pp. 296-297.

[57] Evarts, E. V. (1964) Temporal Patterns of Discharge of Pyramidal Tract Neurons During Sleep and Waking in the Monkey. Jour. Neurophysiol., 27, pp. 152-171.

[58] Fatt, P. and Katz, B. (1951) An Analysis of the End-plate Potential Recorded with an Intra-Cellular Electrode. Jour. Physiol. (London), 115, pp. 320-370.

[59] Fatt, P. and Katz, B. (1952) Spontaneous Subthreshold Activity at Motor Nerve Endings. Jour. Physiol. (London), 117, pp. 109-128.

[60] Fatt, P. and Katz, B. (1953) The Effect of Inhibitory Nerve Impulses on a Crustacean Nerve Fibre. Jour. Physiol. (London), 121, pp. 374-389.

[61] Fee, M. and Kleinfeld, D. (1994) Neuronal responses in rat vibrissa cortex during behavior. Soc. Neurosci. Abs., 20, 26.

[62] Fisher, S. A., Fischer, T. M. and Carew, T. J. (1997) Multiple overlapping processes underlying short-term synaptic enhancement. Trends Neurosci., 20, pp. 170-177.

[63] Fitzhugh, R. (1961) Impulses and Physiological States in Theoretical Models of Nerve Membrane. Biophys. Jour., 1, pp. 445-466.

[64] Fodor, J. A. and Pylyshyn, Z. W. (1988) Connectionism and Cognitive Architecture: A Critical Analysis. Cognition, 28, pp. 3-71.

[65] Freeman W. J. (1975) Mass Action in the Nervous System. Academic Press, New York.

[66] Freeman, W. J. (1991) Predictions on Neocortical Dynamics Derived from Studies in Paleocortex. Basar E. and Bullock T. H. (Eds.) Induced Rhythms of the Brain. Cambridge MA, Birkhaeuser Boston Inc, pp. 183-199.

[67] Fritsch, G. T. and Hitzig, E. (1870) Über die elektrische Erregbarkeit des Grosshirns. Arch. f. Anat., Physiol. und wissenschaftl. Mediz., Leipzig, 37, pp. 300-32.

[68] Gabbiani, F., Metzner, W., Wessel, R. and Koch, C. (1996) From stimulus encoding to feature extraction in weakly electric fish. Nature, 384, pp. 564-567.

[69] Goldman, D. E. (1943) Potential, Impedance, and Rectification in Membranes. Jour. Gen. Physiol., 27, pp. 37-60.

[70] Grevins, A. S. and Shaffer, R. E. (1980) A Critical Review of Electroencephalographic (EEG) Correlates of Higher Cortical Functions. CRC Critical Rev. Bioeng., 4(2), pp. 113-163.

[71] Gulyas, A. I., Miles,R., Sik, A., Toth, K., Tamamaki, N. and Freund, T. F. (1993) Hippocampal pyramidal cells excite inhibitory neurons via a single release site. Nature, 366, pp. 683-687.

[72] Hardingham, N. R. and Larkman, A. U. (1998) The reliability of excitatory synaptic transmission in slices of rat visual cortex in vitro is temperature dependent, Jour. Physiol. (London), 507, pp. 249-256

[73] Hebb, D. O. (1949) Organization of Behavior. A Neurophysiological Theory. Wiley & Sons, New York.

[74] Heidegger, M. (1927) Sein und Zeit. Niemeyer Verlag, Tübingen.

[75] Hessler, N., Shirke, A. and Malinow, R. (1993). The probability of transmitter release at a mammalian central synapse. Nature, 366, pp. 569-572.

[76] Hines, M. (1993) NEURON - A Program for Simulation of Nerve Equations. Neural Systems: Analysis and Modeling, F. Eckman(ed.), Kluwer, pp. 127-136.

[77] Hodgkin, A. L. and Huxley, A. F. (1939) Action Potentials recorded from inside a nerve fibre. Nature (London), 144, pp. 710-711.

[78] Hodgkin, A. L. and Huxley, A. F. (1952a) Currents Carried by Sodium and Pottasium Ions through the Membrane of a Giant Axon of Loligo. Jour. Physiol., 116, pp. 449-472.

[79] Hodgkin, A. L. and Huxley, A. F. (1952b) The Components of Membrane Conductance in the Giant Axon of Loligo. Jour. Physiol., 116, pp. 473-496.

[80] Hodgkin, A. L. and Huxley, A. F. (1952c) The Dual Effect of Membrane Potential on Sodium Conductance in the Giant Axon of Loligo. Jour. Physiol., 116, pp. 497-506.

[81] Hodgkin, A. L. and Huxley, A. F. (1952d) A Quantitative Description of Membrane Current and its Application to Conduction and Excitation in Nerve. Jour. Physiol., 117, pp. 500-544.

[82] Hodgkin, A. L., Huxley, A. F. and Katz, B. (1952) Measurement of Current-Voltage relations in the Membrane of the Giant Axon of Loligo. Jour. Physiol., 116, pp. 424-448.

[83] Hopfield, J. (1982) Neural Networks and Physical Systems with Emergent Collective Computational Abilities. Proc. Nat. Acad. Sci. USA, 79, pp. 2554-2558.

[84] Hornik, K. Stinhcombe, M. and White, H. (1989) Multilayer Feedforward Networks are Universal Approximators. Neural Networks, 2, pp. 359-366.

[85] Hubel, D. H. and Wiesel, T. N. (1965) Receptive Fields and Functional Architecture in Two Non-striate Visual Areas (18 and 19) of the Cat. Jour. Neurophysiol., 28, pp. 229-289.

[86] Jasper, H. H. (1981) Problems of Relating Cellular or Modular Specificity to Cognitive Functions: Importance of State Dependent Reactions. Schmitt F. O., Worden F. G., Adelman G. and Dennis S. G. (Eds.) The Organization of the Cerebral Cortex. MIT Press, Cambridge, pp. 375-393.

[87] Jones, E. G. (1994) The Neuron Doctrine. Jour. Hist. of Neurosci., 3, pp. 3-20.

[88] Kandel, E. R. (1976) Cellular Basis of Behavior, W. H. Freeman and Company, San Francisco.

[89] Katz, B. and Miledi, R. (1967) A Study of Synaptic Transmission in the Absence of Nerve Impulses. Jour. Physiol. (London), 192, pp. 407-436.

[90] Kleene, S. C. (1936a) General recursive functions of natural numbers. Math. Ann., 112, pp. 727-742.

[91] Kleene, S. C. (1936b) Lambda definability and recursiveness. Duke Math. Jour., 2, pp. 340-353.

[92] Knierem, J. J. and van Essen, D. C. (1992) Neuronal responses to static textures in area V1 of the alert Macaque monkey. Jour. Neurophysiol., 67, pp. 961-980.

[93] Koch, C. (1998) Biophysics of Computation: Information Processing in Single Neurons. Oxford University Press.

[94] Krüger, J. (1983) Simultaneous Individual Recordings from Many Cerebral Neurons: Techniques and Results. Rev. Physiol. Biochem. Pharmacol., 98, pp. 177-229.

[95] Krüger, J. (Ed.) (1991a) Neuronal Cooperativity. Springer-Verlag, Berlin Heidelberg New York.

[96] Krüger, J. (1991b) Spike Train Correlation on Slow Time Scales in Monkey Visual Cortex. Krüger J. (Ed.) Neuronal Cooperativity. Springer-Verlag, Berlin Heidelberg New York.

[97] Larkman, A. U., Jack, J. J. B. and Stratford, K. J. (1997) Quantal analysis of excitatory synapses in hippocampal CA1 in vitro during low-frequency depression. Jour. Physiol. (London), 505, pp. 443-456.

[98] Lass, Y. and Abeles, M. (1975) Transmission of information by the Axon. I: Noise and Memory in the myelinated nerve fibre of the frog. Biological Cybernetics, 19, pp. 61-67.

[99] Laurent, G. (1996) Dynamical Representation of odors by oscillating and evolving neural assemblies. Trends Neurosci., 19, pp. 489-496.

[100] Lisman, J. E. (1997) Bursts as a unit of neural information: Making unreliable synapses reliable. Trends Neurosci., 20, pp. 38-43.

[101] Loewi, O. (1921) Ueber humorale Uebertragbarkeit der Herznervenwirkung. I. Mitteilung. Pflügers Arch. Gesamte Physiol. Menschen Tiere, 189, pp. 239-242.

[102] MacGregor, R. J. and Lewis, E. R. (1977) Neural Modeling, Plenum Press, New York.

[103] Magleby, K. (1987) Short term synaptic plasticity. Edelman G. M., Gall W. E. and Cowan W. M. (Eds.) Synaptic function. Wiley, New York.

[104] Mainen, Z. F. and Sejnowski, T. J. (1995) Reliability of Spike Timing in Neocortical Neurons. Science, 268, pp. 1503-1507.

[105] Marden, M. (1948) The Number of Zeros of a Polynomial in a Circle. Proc. Nat. Acad. Sci. USA, 34, pp. 15-17.

[106] Markram, H. and Tsodyks, M. (1996) Redistribution of synaptic efficacy between neocortical pyramidal neurons. Nature, 382, pp. 807-810.

[107] Markram, H., Lübke, J., Frotscher, M., Roth, A. and Sakmann, B. (1997) Physiology and anatomy of synaptic connections between thick tufted pyramidal neurones in the developing rat neocortex. Jour. Physiol. (London), 500, pp. 409-440.

[108] McCormick, D. A., Connors, B. W., Lighthall, J. W. and Prince, D. A. (1985) Comparative electrophysiology of pyramidal and sparsely spiny stellate neurons of the neocortex. Jour. Neurophysiol., 54, pp. 782-802.

[109] McCulloch, W. S. and Pitts, W. (1943) A Logical Calculus of the Ideas Immanent in Nervous Activity. Bull. Math. Biophys, 5, pp. 115-137.

[110] Merleau-Ponty, M. (1942) La Structure du Comportement. Presses Universitaires de France, Paris.

[111] Minsky, M. and Papert, S. (1972) Perceptrons. MIT Press, Cambridge, Mass.

[112] Mountcastle, V. B. (1957) Modality and Topographic Properties of Single Neurons of Cat's Somatic Sensory Cortex. Jour. Neurophysiol., 20, pp. 408-434.

[113] Nagumo, J. S., Arimoto, S. and Yoshizawa, S. (1962) An Active Pulse Transmission Line Simulating Nerve Axon. Proc. I. R. E., 50, pp. 2061-2070.

[114] Newell, A. (1980) Physical Symbol Systems. Cognitive Science, 4, pp. 135-183.

[115] Newell, A. and Simon, H. A. (1976) Computer Science as Empirical Inquiry: Symbols and Search. Comm. of the ACM, 19, pp. 113-126.

[116] Nunez, P. L. (1989) Generation of Human EEG by a Combination of Long and Short Range Neocortical Interactions. Brain Topography, 1, pp. 199-215.

[117] Omlin, C. W. and Giles, C. L. (1996) Constructing Deterministic Finite-State Automata in Recurrent Neural Networks. Jour. Assoc. Comp. Mach, 43, pp. 937-972.

[118] Oseledec, V. I. (1968) A Multiplicative Ergodic Theorem. Ljapunov Characteristic Numbers for Dynamical Systems. Trans. Moscow Math. Soc., 19, pp. 197-231.

[119] Parker, A. J. and Hawken, M. J. (1985) Capabilities of monkey cortical cells in spacial-resolution tasks. Jour. Optical Soc. Am. A 2, pp. 1101-1114.

[120] Parker, D. B. (1985) Learning Logic. Technical Report TR-47, Center for Computational Research in Economics and Management Science, Massachusetts Institute of Technology, Cambridge, Massachusetts.

[121] Peters, A. and Proskauer, C. C. (1980) Synaptic Relationships between a Multipolar Stellate Cell and a Pyramidal Neuron in the Rat Visual Cortex: A Combined Golgi-Electron Microscope Study. Jour. Neurocytol., 9, pp. 163-183.

[122] Peters, A. and Regidor, J. (1981) A Reassessment of the Forms of Nonpyramidal Neurons in Area 17 of Cat Visual Cortex. Jour. Comp. Neurol., 203, pp. 685-716.

[123] Post, E. L. (1936) Finite combinatory processes. Formulation I. Jour. Symbolic Logic, 1, pp. 103-105.

[124] Raastad, M., Storm, J. F. and Andersen, P. (1992) Putative single quantum and single fibre excitatory postsynaptic currents show similar amplitude range and variability in rat hippocampal slices. Euro. Jour. Neurosci., 4, pp. 113-117.

[125] Rall, W. (1960) Membrane Potential Transients and Membrane Time Constants of Motoneurons, Exp. Neurol., 2, pp. 503-532.

[126] Rashevsky, N. (1938) Mathematical Biophysics. Univ of Chicago Press, Chicago, IL.

[127] Reid, R. C., Soodak R. E. and Shapley R. M. (1991) Directional selectivity and spatiotemporal structure of receptive fields of simple cells in cat striate cortex. Jour. Neurophysiol., 66, pp. 505-529.

[128] Ricciardi, L. M. (1977) Diffusion Processes and Related Topics in Biology. Springer, Berlin.

[129] Richmond, B. J., Optican, L. M. and Spitzer H. (1990) Temporal encoding of two dimensional patterns by single units in primate primary visual cortex. I: Stimulus response relations. Jour. Neurophysiol., 64, pp. 351-369.

[130] Rieke, F., Owen, W. G. and Bialek, W. (1991) Optimal filtering in the Salamander retina. J. E. Moody, S. J. Hanson and R. P. Lippman (Eds) Advances in Neural Information Processing Systems 3. Morgan Kauffman, San Mateo, CA.

[131] Roeder, K. D. (1963) Nerve Cells and Insect Behavior. Harvard University Press, Cambridge, MA.

[132] Röschke, J. and Basar, E. (1989) Correlation Dimensions in Various Parts of Cat and Human Brain in Different States. Basar E. and Bullock T. H. (Eds.) Brain Dynamics, Springer, Berlin. pp. 131-148.

[133] Rosenblatt, F. (1958) The Perceptron, a Probabilistic Model for Information Organization and Storage in the Brain. Psych. Rev., 65, pp. 386-408.

[134] Rosenmund, C., Clements, J. and Westbrook, G. (1993) Nonuniform probability of glutamate release at a hippocampal synapse. Science, 262, pp. 754-757.

[135] Rumelhart, D. D., Hinton G. E. and Williams, R. J. (1986) Learning Representations by Back-Propagating Errors. Nature, 323, pp. 533-536.

[136] Rumelhart, D. E. and McClelland, J. L. (1986) PDP Models and General Issues in Cognitive Science. Parallel Distributed Processing(I and II), MIT Press, Cambridge, Mass.

[137] Sampath, G. and Srinivasan, S. K. (1977) Stochastic Models for Spike Trains of Single Neurons. Springer, Berlin.

[138] Schikorski, T. and Stevens, C. F. (1997) Quantitative ultrastructural analysis of hippocampal excitatory synapses. Jour. Neurosci., 17, pp. 5858-5867.

[139] Schüz, A. (1992) Randomness and Constraints in the Cortical Neuropil. Aertsen A. and Braitenberg V. (Eds.) Information Processing in the Cortex. Springer-Verlag, Berlin Heidelberg New York, pp. 3-21.

[140] Shepherd, G. M. (1991) Foundations of the neuron doctrine. Oxford University Press, New York Oxford.

[141] Shepherd, G. M. (Ed.) (1998) The Synaptic Organization of the Brain. Oxford University Press, New York Oxford.

[142] Sherrington, C. S. (1906) The Integrative Action of the Nervous System. New York: Scribner.

[143] Siegelmann, H. T. and Sontag, E. D. (1992) On the Computational Power of Neural-nets. Proc. Fifth ACM Workshop on Comp. Learn. Theo.

[144] Simmons J. A. (1989) A view of the world through the bat's ear: The formation of acoustic images in Echolocation. Cognition, 33, pp. 155-199.

[145] Singer, W. and Gray C. M. (1995) Visual feature integration and the temporal correlation hypothesis. Ann. Rev. Neurosci., 18, pp. 555-586.

[146] Smale, S. (1967) Differentiable Dynamical Systems. Bull. Amer. Math. Soc., 73, pp. 747-817.

[147] Softky, W. R. and Koch, C. (1993) The Highly Irregular Firing of Cortical-cells is Inconsistent with Temporal Integration of Random EPSPs. Jour. Neurosci., 13, pp. 334-350.

[148] Stevens, C. F. and Wang, Y. (1994) Changes in reliability of synaptic function as a mechanism for plasticity. Nature, 371, pp. 704-707.

[149] Stevens, C. F. and Wang, Y. (1995) Facilitation and Depression at single central synapses. Neuron, 14, pp. 795-801.

[150] Strehler, B. L. and Lestienne, R. (1986) Evidence on precise time-coded symbols and memory of patterns in monkey cortical neuronal spike trains. Proc. Nat. Acad. Sci. USA, 83, pp. 9812-9816.

[151] Thomson, A. M., Deuchars, J. and West, D. C. (1993) Large, deep layer pyramid-pyramid single axon EPSPs in slices of rat motor cortex display paired pulse and frequency-dependent depression, mediated presynaptically and self-facilitation, mediated postsynaptically. Jour. Neurophysiol., 70, pp. 2354-2369.

[152] Tsodyks, M. and Markram, H. (1997) The neural code between neocortical pyramidal neurons depends on neurotransmitter release probability. Proc. Nat. Acad. Sci. USA, 94, pp. 719-723.

[153] Tuckwell, H. C. (1988) Introduction to Theoretical Neurobiology, Volumes I & II, Cambridge Univ Press, Cambridge New York.

[154] Turing, A. M. (1936) On Computable Numbers, with an application to the Entscheidungsproblem. Proc. Lond. Math. Soc., (2), 42, pp. 230-265.

[155] Turing, A. M. (1937) Computability and lambda-definability. Jour. Symbolic Logic, 2, pp. 153-163.

[156] Valbo, A. B. (1995) Single afferent neurons and somatic sensation in humans. M. Gazzaniga (Ed.) The Cognitive Neurosciences, MIT Press, Cambridge.

[157] Varela, J. A., Sen, K., Gibson, J., Fost, J., Abbott, L. F. and Nelson, S. B. (1997) A quantitative description of short-term plasticity at excitatory synapses in layer 2/3 of rat primary visual cortex. Jour. Neurosci., 17, pp. 7926-7940.

[158] Walsh, J. B. and Tuckwell, H. C. (1985) Determination of the Electrical Potential over Dendritic Trees by Mapping onto a Nerve Cylinder, Jour. Theoret. Neurobiol., 4, pp. 27-46.

[159] Wehr, M. and Laurent, G. (1996) Odor encoding by temporal sequences of firing in oscillating neural assemblies. Nature, 384, pp. 162-166.

[160] Werbos, P. (1974) Beyond Regression: New Tools for Prediction and Analysis in the Behavioral Sciences. Ph.D Thesis, Harvard University, Cambridge, Massachusetts.

[161] Wilson, H. R. and Cowan, J. D. (1972) Excitatory and inhibitory interaction in localized populations of model neurons. Biophys. Jour., 12, pp. 1-24.

[162] Wilson, H. R. and Cowan, J. D. (1973) A Mathematical theory of the functional dynamics of cortical and thalamic nervous tissue. Kybernetik, 13, pp. 55-80.

[163] Wright, J. J. (1997) EEG Simulation: Variation of Spectral Envelope, Pulse Synchrony and $\sim$40 Hz Oscillation. Biological Cybernetics, 76, pp. 181-194.

[164] Wright, J. J. (1990) Reticular Activation and the Dynamics of Neuronal Networks. Biological Cybernetics, 62, pp. 289-298.

[165] Zador, A. and Dobrunz, L. (1997) Dynamic synapses in the cortex. Neuron, 19, pp. 1-4.

[166] Zigmond, M. J., Bloom, F. E., Landis, S. C., Roberts, J. L. and Squire, L. R. (Eds.) (1999) Fundamental Neuroscience. Academic Press, New York.

[167] Zohary, E., Shadlen, M. N. and Newsome, W. T. (1994) Correlated neuronal discharge rate and its implications for psychophysical performance. Nature, 370, pp. 140-143.

[168] Zucker, R. (1989) Short-term synaptic plasticity. Ann. Rev. Neurosci., 12, pp. 13-31.

Vita

Arunava Banerjee

1987-91 Attended Indian Institute of Technology, Kanpur. Majored in Computer Science.

1991 *Bachelor of Technology* in Computer Science and Engineering, Indian Institute of Technology, Kanpur.

1991-2000 Graduate studies in Computer Science, Rutgers, The State University of New Jersey, New Brunswick, New Jersey.

1995 *Master of Science* in Computer Science, Rutgers, The State University of New Jersey.

1994 Banerjee, A. Initializing Neural Networks using Decision Trees. *International Workshop on Computational Learning and Natural Learning Systems*.

1994 Banerjee, A. Visual Attention and Retinal Fixation: Preprocessing Modules for Enhanced Performance in Realtime Vision. *Laboratory of Computer Science Research, Rutgers University Technical Report LCSR-TR-230*.

1995 Hirsh, H., Ellman, T., Banerjee, A., Drischel, D., Yao, H. and Zabusky, N. Reduced Model Formation for 2D Vortex Interactions Using Machine Learning. *Systematic Methods of Scientific Discovery, AAAI Symposium*.

1995 Banerjee, A., Hirsh, H. and Ellman, T. Inductive Learning of Feature Tracking Rules for Scientific Visualization. *Workshop on Machine Learning in Engineering, IJCAI*.

1998 Macskassy, S. A., Banerjee, A., Davison, B. D. and Hirsh, H. Human Performance on Clustering Web Pages: A Preliminary Study. *The Fourth International Conference on Knowledge Discovery and Data Mining*.

1998 Ellman, T., Keane, J., Banerjee A. and Armhold, G. A Transformation System for Interactive Reformulation of Design Optimization Strategies. *Research in Engineering Design*, 10, pp. 30-61.

2000 Banerjee, A. On the Phase-Space Dynamics of Systems of Spiking Neurons. I: Model and Experiments. *Neural Computation*, 13, pp. 161-193.

2000 Banerjee, A. On the Phase-Space Dynamics of Systems of Spiking Neurons. II: Formal Analysis. *Neural Computation*, 13, pp. 195-225.

2001 Banerjee, A. The Roles Played by External Input and Synaptic Modulations in the Dynamics of Neuronal Systems. Peer Commentary on Tsuda, "Towards an interpretation of dynamic neural activity in terms of chaotic dynamical systems", *Behavioral and Brain Sciences*, (to appear).

2001 *Doctor of Philosophy* in Computer Science, Rutgers, The State University of New Jersey.